

**AN INVESTIGATION INTO THE FEASIBILITY OF FOREST  
INVENTORY BY MEANS OF STEREO SATELLITE IMAGERY  
EMPLOYING DIGITAL PHOTOGRAMMETRY TECHNOLOGY**

by

HOLGER K.H. VOGT



Thesis presented in partial fulfilment of the requirements  
for the Degree of Master of Science in Forestry  
at the University of Stellenbosch

Promoter: Professor B. Bredenkamp

Co-promoter: Professor Dr. habil. C. Kätsch, Fachhochschule  
Hildesheim/Holzminde Fachbereich Forstwirtschaft  
und Umweltmanagement, Göttingen, Germany

July 2000

## **DECLARATION**

I, the undersigned, declare that the work contained in this thesis is my own original work and has not previously in its entirety, or in part, been submitted at any university for a degree.

## **AN INVESTIGATION INTO THE FEASIBILITY OF FOREST INVENTORY BY MEANS OF STEREO SATELLITE IMAGERY EMPLOYING DIGITAL PHOTOGRAMMETRY TECHNOLOGY**

### **ABSTRACT**

The aim of the study was to extract elevation information (such as tree height) from stereo satellite imagery (IRS-1C), to scrutinise the performance of the DTM (Digital Terrain Model) tools as provided by the LH (Leica/Helava) Systems' softcopy system, and subsequently to perform a feasibility study on the application of a practically viable forest inventory design.

A softcopy photogrammetry workstation (LH Systems DPW 770), IRS-1C stereo panchromatic satellite imagery, and digital aerial photography at a scale of 1:30 000 (scanned at 15 micrometers) was used. The study was conducted over various sites in the Sabie area (province of Mpumalanga) in South Africa, where extensive man made forests with pine and eucalypts are to be found. The extraction of stand parameters such as tree height was performed manually, semi-automatically, and automatically. In addition, the compartment area was determined using a GIS tool. The Digital Surface Models (DSM), representing the canopy structure of the stands, was extracted from the IRS-1C imagery and validated through a comparison of the resulting contours with the corresponding contours generated by aerial photogrammetric methods.

Due to the coarse spatial resolution of the IRS-1C imagery (5m) and the suboptimal B/H (Base/Height) ratio (0.57), only objects featuring a height exceeding 20m could be manually measured with confidence. Furthermore, only the edges of the compartments proved to be suitable for the determination of tree heights (i.e. with a sufficiently large parallax difference and image contrast).

The manual determination of tree heights in the IRS-1C imagery yielded accuracies of about 95% compared to the height values of the aerial photographs and the ground data. The application of image enhancement techniques had severe effects on the accuracy of the IRS-1C stereo model, resulting in deviations of about -57m from the 'true' value. It was observed that image matching was only a problem where features

changed their appearance (e.g. clearfelled or burnt areas) during the acquisition period of the stereo pair of the satellite imagery.

LH Systems' Adaptive Automatic Terrain Extraction (AATE) tool performed very well for the creation of digital terrain and surface models when using digital aerial photography with a high scanning rate. In contrast, the automatic creation of canopy surface models from various forest compartments did not yield any useful results when applied to IRS-1C imagery. AATE could not model the canopy structure properly. The coarse spatial resolution of the satellite imagery in conjunction with the sparse post spacing (20m) and matching errors are most likely to be responsible for this poor performance.

Two-phase sampling and the Hugershoff method were chosen for automatically derived height values to be evaluated for possible application in forest inventory. Unfortunately, neither for the determination of the regression estimator for the first method, nor for the calculation of timber volume after application of the Hugershoff method could any useful result be obtained. This is mostly due to the fact that image matching errors and blunders (resulting in tree heights of  $-885\text{m}$ ) were not properly accounted for in the terrain extraction software. However, the outcomes for the manual measurement of tree heights performed on the satellite imagery show that under optimal conditions accuracies can be achieved similar to those for the height determination in small scale aerial photographs, but at lower cost. The obtained height values can then be used for the calculation of timber volume according to Eichhorn's law.

Keywords: AATE, blunders, digital photogrammetry, DPW770, forest inventory, Hugershoff, IRS-1C, matching error, remote sensing, satellite imagery, two-phase sampling

## **'N GANGBAARHEIDSTUDIE VIR BOSINVENTARIS MET BEHULP VAN STEREO SATELLIETBEELDE MET GEBRUIK VAN SAGTEKOPIE FOTOGRAMMETRIESE TEGNOLOGIE**

### **ABSTRAK**

Die doel van hierdie studie was om elevasie inligting (soos boomhoogtes) uit stereo satellietbeelde (IRS-1C) te ontrek, en die DTM (Digitale Terrein Modelle) funksies van die LH Systems se sagtekopie sisteem te evalueer en 'n ondersoek in te stel na praktiese toepassing van die tegnologie in bosvoorraadopname.

'n Sagtekopie fotogrammetriese werkstasie (LH Systems DPW 770), IRS-1C stereo panchromatiese satellietwaarneming en digitale lugfotografie is gebruik. Die studie is uitgevoer oor verskeie areas in die Sabie omgewing (Mpumalanga, Suid-Afrika), waar daar ekstensiewe mensgemaakte woude voorkom met denne en *Eucalyptus* soorte. Die ekstraksie van opstandparameters soos boomhoogte is uitgevoer met die hand, as ook met semi-outomatiese en outomatiese metodes. Die digitale oppervlakmodelle (wat die kroondakstrukture van die opstande voorstel) was vanaf die IRS-1C beelde onttrek en gevalideer deur vergelyking van die resulterende kontoere met die korresponderende kontoere wat deur lugfotogrammetriese metodes gegenereer is. As gevolg van die growwe ruimtelike resolusie van die IRS-1C waarneming (5m) en die suboptimale B/H verhouding (0.57) kan slegs voorwerpe met 'n hoogte van meer as 20m met vertroue met die hand gemeet word. Slegs die rande van die vakke is bruikbaar vir die berekening van boomhoogtes (d.w.s. met 'n voldoende paralaksverskil en 'n sterk beeldkontras).

Boomhoogtes wat met die hand bepaal is vanaf IRS-1C beelde is 95% akkuraat in vergelyking met die hoogtewaardes verkry vanaf die lugfoto's en die veldmetings. Die toepassing van beeldverbeteringstegnieke het duidelike invloede op die akkuraatheid van die IRS-1C stereomodel met afwykings van ongeveer -57m vanaf die "werklike" waardes. Daar is ook waargeneem dat beelddooreenstemming slegs 'n probleem is waar terreinvorme se voorkoms verander het (weens afkappings of brande) gedurende die verkrygingsperiode waarin die stereo paar van die satellietbeelde verkry is.

LH Systems se Aanpassende Outomatiese Terrein Onttrekkings (*Adaptive Automatic Terrain Extraction - AATE*) instrument het goed gevaar tydens die gebruik van digitale lugfotografie met 'n hoë skanderingstempo.

In kontras hiermee het die outomatiese skepping van kroondakoppervlakmodelle van verskeie plantasievakke geen nuttige resultate gelewer wanneer dit op IRS-1C beelde toegepas is nie. Die growwe ruimtelike resoluëie van die satellietbeelde tesame met die wye paalspasiering (20m) en passingsfoute is waarskynlik vir hierdie swak resultate verantwoordelik.

Twee-fase proefneming en die Hegershoff metode was gebruik vir die bepaling van outomaties afgeleide hoogtewaardes vir evaluering van moonlike toepassing in bosvoorraadopnames. Geen bruikbare resultate kon verkry word vir die vasstelling van die regressieskatter vir die eersgenoemde metode of vir die berekening van die houtvolume volgens die Hegershoff metode nie. Dit is meestal as gevolg van beeld ooreenkomsfoute en flaters, (wat tot boomhoogtes van -885m gelei het) wat nie voldoende in ag geneem word in die terreinekstraksie sagteware nie. Die resultate vir die handgemete ('manual') boomhoogtebepaling wat uitgevoer is op die satellietbeelde (op die sagtiekopie werkstasie DPW 770), toon dat akkuraathede soortgelyk aan daardie vir hoogte bepaal op klein-skaal lugfotos onder optimale toestande verkry kan word, maar goedkoper. Die hoogtewaardes wat verkry is kan gebruik word vir die berekening van houtvolume volgens die wet van Eichhorn.

Sleutelwoorde: AATE, afstandswaarneming, bosvoorraadopnames, digitale fotogrammetrie, DPW770, flaters, Hegershoff, IRS-1C, satellietbeelde, twee-fase proefneming

'THE REAL VOYAGE OF  
DISCOVERY CONSISTS NOT IN  
SEEKING NEW LANDSCAPES,  
BUT IN HAVING NEW EYES'

Marcel Proust

## ACKNOWLEDGEMENTS

Special credit must be given to my supervisor Professor Brian Bredenkamp, who has given me the invaluable opportunity to embark on the Forest Management Unit (FMU) (space-) ship and to get involved in a great number of various research projects which have helped broaden my scope and experience. Furthermore, I owe a special thanks to my dear colleague Ben Opperman, who helped me to keep the ball rolling and provided numerous useful and critical ideas.

The author is greatly indebted to Professor Dr. Christoph Kätsch of the *Fachhochschule Hildesheim/Holzminden* in Göttingen, for his great support and furthermore for having made it possible for me to make use of the facilities and equipment (e.g. the one million Rand 'baby' Digital Photogrammetry Workstation DPW 770) at the faculty. The generous donation by the *Volkswagen Stiftung* (VW Foundation), which made the acquisition of the IRS-1C satellite imagery as well as the Digital Photogrammetry Workstation (LH DPW770) possible is greatly acknowledged. I trust the successful co-operation between the Faculty of Forestry at the *Fachhochschule Hildesheim/Holzminden* in Göttingen and the Forest Management Unit at the University of Stellenbosch will continue to bear fruit and foster many more bi-, or even multilateral projects.

Special mention should be made of the financial assistance by the Department of Water Affairs and Forestry (DWAF) during all the years of study at Stellenbosch through the support of the national forest inventory project.

Furthermore, I gratefully acknowledge that field and research data from the various forest owners (Mondi, Sappi, and Safcol) could be incorporated in this study. The kind provision of information and maps is greatly appreciated. In addition, I express my sincere thanks to the many individuals who have contributed to this thesis. They include Professor Alparslan Akça, University of Göttingen; Professor Dieter Fritsch, University of Stuttgart; Mr. Klaus Halbritter, University of Göttingen; Dr. Karsten Jacobsen, University of Hannover; Mr. D. Kaveridevi, NRSA, Hyderabad, India; Dr. Friedemann Krummheuer, *Fachhochschule Hildesheim/Holzminden*; Mr. Scott Miller, LH Systems, San Diego, USA; Mr. Lauren Peterson, EOSAT, Lanham, USA;

Professor Gordon Petrie, University of Glasgow; Professor Heinz Rüter, University of Cape Town; Dr. Leo Sayn-Wittgenstein, CCRS, Ottawa; Mrs. Andrea Sassor, *Gebrüder Wichmann*, Berlin; Mr. Martin Stöcker, *Fachhochschule Hildesheim/Holzminden* and Dr. Stewart Walker, LH Systems, San Diego, USA. Furthermore a special thanks to all the people at the *Fachhochschule Hildesheim/Holzminden*; the ERDAS support group, Atlanta, USA; the National Remote Sensing Agency (NRSA) at Hyderabad, India, and my dear colleagues at Stellenbosch, in particular the librarians and receptionists, as well as my friends from all over the world.

Special recognition is due to my family who provided many years of patient understanding and encouragement, to the Kätsch family (i.e. Christoph, Christine, Annette and Stephanie), who really made me feel at home, and to Mrs. Yeda Maria Malheiros di Oliveira, University of Oxford, for their inspiration and support.

## CONTENTS

<b>1. INTRODUCTION .....</b>	<b>1</b>
<b>2. DEFINITION OF THE TERMS ‘REMOTE SENSING’ AND ‘PHOTOGRAMMETRY’ .....</b>	<b>4</b>
<b>3. A BRIEF HISTORY OF REMOTE SENSING.....</b>	<b>6</b>
<b>4. CONCEPTS AND FOUNDATIONS OF REMOTE SENSING .....</b>	<b>8</b>
4.1 ENERGY SOURCES AND RADIATION PRINCIPLES .....	8
4.2 ENERGY INTERACTIONS IN THE ATMOSPHERE .....	9
4.3 ENERGY INTERACTIONS WITH EARTH SURFACE FEATURES .....	12
4.4 DATA ACQUISITION AND INTERPRETATION.....	17
<b>5. SOME FUNDAMENTALS OF PHOTOGRAMMETRY.....</b>	<b>21</b>
5.1 GEOMETRIC ELEMENTS OF THE AERIAL PHOTOGRAPH.....	21
5.2 THE CONCEPT OF ORIENTATION .....	22
5.3 STEREOSCOPY.....	25
5.4 GROUND CONTROL FOR AERIAL PHOTOGRAPHY AND SATELLITE IMAGERY .....	26
5.5 CHARACTERISTICS OF SATELLITE PHOTOGRAMMETRY.....	27
<b>6. REMOTE SENSING IN FORESTRY .....</b>	<b>32</b>
6.1 THE AERIAL PHOTOGRAPH IN FORESTRY .....	32
6.1.1 <i>Reconnaissance</i> .....	33
6.1.2 <i>Forest inventory</i> .....	33
6.1.2.1 Information on area from aerial photographs .....	36
6.1.2.2 Identification of tree species .....	37
6.1.2.3 The measurement of tree height and stand height.....	38
6.1.2.4 Tree counts.....	42
6.1.2.5 The measurement of the crown parameters .....	43
6.1.2.6 Tree and stand volume.....	46
6.1.2.7 The estimation of factors such as site, age, and increment.....	48
6.1.2.8 The inventory concepts.....	49
6.1.3 <i>Forest Management</i> .....	51
6.1.4 <i>Silviculture</i> .....	51
6.1.5 <i>Pest Control and Damage Assessment</i> .....	52
6.1.6 <i>Fire Control</i> .....	53
6.1.7 <i>Road location and construction</i> .....	54
6.2 SATELLITE REMOTE SENSING IN FORESTRY.....	54
6.2.1 <i>Satellite remote sensing for mapping purposes</i> .....	56
6.2.2 <i>Satellite image interpretation for mensuration purposes</i> .....	57
6.2.3 <i>Satellite remote sensing for forest disease and stress assessment</i> .....	58
6.2.4 <i>Future Applications</i> .....	58
<b>7. DIGITAL PHOTOGRAMMETRY .....</b>	<b>61</b>
7.1 BASIC ELEMENTS OF A DIGITAL PHOTOGRAMMETRY SYSTEM (DPS) .....	62
7.2 IMAGE DATA ACQUISITION AND INPUT TO A DPS .....	63
7.3 SCANNERS .....	64

7.4	DIGITAL PHOTOGRAMMETRIC WORKSTATIONS (DPWs)	66
7.5	ALGORITHMIC AND SOFTWARE ASPECTS OF DPWS	68
7.6	ANALYTICAL PLOTTERS VERSUS DIGITAL PHOTOGRAMMETRY WORKSTATIONS	70
<b>8.</b>	<b>MATERIAL AND METHODOLOGY</b>	<b>73</b>
8.1	MATERIAL	73
8.1.1	<i>The test area</i>	73
8.1.2	<i>The satellite imagery</i>	75
8.1.3	<i>Aerial photography</i>	80
8.1.4	<i>The DPW (Digital Photogrammetry Workstation) 770 by LH Systems</i>	82
8.1.5	<i>Ground data</i>	85
8.2	METHODOLOGY	87
8.2.1	<i>Workstation process flow</i>	88
8.2.2	<i>Extraction of elevation data</i>	97
8.2.2.1	Overview	97
8.2.2.2	Image matching	102
8.2.2.3	Surface fitting	105
8.2.2.4	Checking and editing	105
8.2.3	<i>Generation of DTMs from IRS-1C/D imagery</i>	106
8.2.4	<i>DTM creation – characteristics of LH Systems' DPW770</i>	108
8.2.4.1	Automatic terrain extraction	108
8.2.4.2	Interactive Terrain Edit	114
8.2.4.3	Terrain Analysis	115
8.2.5	<i>Terrain extraction from aerial photography and IRS-1C imagery</i>	116
8.2.5.1	Interior orientation	117
8.2.5.2	Triangulation	117
8.2.5.3	Rectification	120
8.2.6	<i>The extraction of inventory parameters</i>	120
8.2.6.1	Manual extraction of elevation information	125
8.2.6.2	Semi-automatic determination of elevation	128
8.2.6.3	Automatic extraction of elevation data	128
8.2.7	<i>Forest inventory concepts</i>	131
8.2.7.1	Two-Phase Sampling Using Regression Estimators	132
8.2.7.2	The Hugerhoff method	134
<b>9.</b>	<b>RESULTS AND DISCUSSION</b>	<b>137</b>
9.1	GENERAL	137
9.1.1	<i>Performance of AATE</i>	137
9.1.2	<i>Image matching</i>	139
9.1.3	<i>Image enhancement</i>	140
9.1.4	<i>Trial assessing the operator skills</i>	142
9.1.5	<i>Accuracy assessment of the IRS-1C stereo model</i>	143
9.2	DETERMINATION OF TREE HEIGHT	144
9.2.1	<i>Manual extraction of tree height and identification of tree species</i>	144
9.2.2	<i>Semi-automatic measurement</i>	146
9.2.3	<i>Automatic generation of DTMs/DSMs</i>	150
9.2.4	<i>Comparative evaluation of the described methods</i>	159
9.3	APPLICATION OF INVENTORY METHODS	163
9.3.1	<i>Two (three)-phase sampling</i>	163

9.3.2 <i>The Hugershoff method</i> .....	168
9.3.3 <i>Eichhorn's law</i> .....	172
<b>10. SUMMARY AND CONCLUSIONS</b> .....	<b>174</b>
<b>11. RECOMMENDATIONS</b> .....	<b>180</b>
<b>12. OUTLOOK</b> .....	<b>182</b>
<b>13. REFERENCES</b> .....	<b>184</b>
<b>14. APPENDICES</b> .....	<b>206</b>
<b>15. INDEX</b> .....	<b>263</b>

## LIST OF FIGURES

Figure 4.1	Typical spectral reflectance curves for vegetation, soil, and water .....	13
Figure 4.2	Reflective properties of a healthy leaf .....	14
Figure 4.3	Spectral reflectance of <i>Eucalyptus goniocalyx</i> .....	16
Figure 4.4	Solar flux .....	17
Figure 4.5	Image acquisition techniques .....	18
Figure 5.1	Topographic displacement on a photograph taken over varied terrain ....	22
Figure 5.2	Exterior orientation .....	24
Figure 5.3	Parallax displacements on overlapping vertical photographs taken over varied terrain .....	26
Figure 5.4	Orientation of the orbit-plane system relative to the inertial co-ordinate system .....	28
Figure 5.5	Relative photogrammetric accuracy vs angle of intersection .....	30
Figure 5.6	Geometry of various imaging systems .....	31
Figure 6.1	Forest inventory methods employing aerial photography and satellite imagery .....	35
Figure 7.1	Overall concept of the DPS .....	63
Figure 8.1	Location of the test site .....	73
Figure 8.2	Plantation area by species and province in South Africa .....	74
Figure 8.3	Spatial resolving capacity of different remote sensing imaging .....	76
Figure 8.4	Pan off-nadir viewing capability .....	78
Figure 8.5	Ground track of IRS-1C for southern Africa .....	79
Figure 8.6	The DPW770 by LH Systems .....	83
Figure 8.7	Workstation workflow .....	91
Figure 8.8	DTM creation – flow diagram for automatic terrain extraction on the DPW770 .....	113
Figure 8.9	Flow diagram for the extraction of forest inventory parameters from aerial photographs and satellite imagery .....	122
Figure 8.10	Example of a vertical stand profile .....	135
Figure 9.1	Contour lines of a windbreak in an aerial photograph at a 2m interval .....	137
Figure 9.2	Surface model of a pine stand .....	138
Figure 9.3	Mismatched area in an IRS-1C stereo pair .....	139
Figure 9.4	Effect of image sharpening .....	140
Figure 9.5	Contour lines of a sharpened and smoothed IRS-1C image .....	141
Figure 9.6	Distribution of tree heights for stand R33 as extracted from aerial photography .....	149
Figure 9.7	Ground fills of compartment A15 .....	150
Figure 9.8	Surface representation of compartment A15 derived from IRS-1C imagery .....	151
Figure 9.9	Vertical profile of the stand A15 as extracted from IRS-1C imagery .....	152
Figure 9.10	3-D representation of the canopy surface of compartment A15 as automatically derived from IRS-1C imagery .....	156
Figure 9.11	3-D representation of the canopy surface of compartment A15 as automatically derived from aerial photography .....	157
Figure 9.12	Surface models derived from IRS-1C and aerial photography .....	158
Figure 9.13	Linear regression showing the relationship between mean height	

aerial photography and mean height IRS-1C for compartment A15 .....	163
Figure 9.14 Linear regression showing the relationship between mean height aerial photography and mean height IRS-1C for compartment A29c.....	164
Figure 9.15 Linear regression showing the relationship between mean height ground survey and mean height aerial photography (AP) for compartment A15 .....	165
Figure 9.16 Linear regression showing the relationship between dbh ground survey and mean height aerial photography (AP) for compartment A15 .....	166
Figure 9.17 Linear regression showing the relationship between dbh ground survey and mean height aerial photography (AP) for compartment A15 .....	167
Figure 9.18 Vertical profile of compartment A15 (IRS-1C) shown as subset with 20m post spacing .....	168
Figure 9.19 Fourier transform of the IRS-1C representation of tree heights in compartment A15 .....	169
Figure 9.20 DEM of compartment A 15 .....	170
Figure 9.21 Application of high-pass rectangular filters .....	170
Figure 9.22 Resulting DEM using the inverse Fourier transform .....	171
Figure 9.23 Difference of the two DEMs.....	171
Figure 9.24 Relationship between total volume production (TVP) and mean height in <i>Pinus patula</i> .....	173

**LIST OF TABLES**

Table 3.1	Milestones in the history of remote sensing .....	6
Table 4.1	Values of albedos for various surfaces.....	12
Table 4.2	Sources of variation in multispectral response patterns of vegetation .....	15
Table 6.1	Overview of inventory parameters that can be extracted from aerial photographs .....	34
Table 6.2	Selection of launching dates of currently available and future satellite systems.....	60
Table 8.1	Specifications of the space segment of the IRS-1C/D satellites .....	76
Table 8.2	Key information on compartment characteristics .....	86
Table 8.3	Accuracies (RMSE) obtained for ground control and tie points for Aerial photography.....	118
Table 8.4	Accuracies (RMSE) obtained for ground control and tie points for IRS-1C imagery .....	119
Table 9.1	Effect of image sharpening on the elevation data.....	141
Table 9.2	Trial operator performance.....	142
Table 9.3	Accuracy assessment of the IRS-1C stereo model.....	143
Table 9.4	Manual determination of tree height in IRS-1C imagery and aerial photography .....	145
Table 9.5	Mean tree heights for the remaining stands.....	145
Table 9.6	Determination of tree height in aerial photography employing the auto correlator .....	148
Table 9.7	Tree height determination using the auto correlator .....	148
Table 9.8	Tree heights for IRS-1C imagery as extracted from automatically created surface models .....	155
Table 9.9	Tree heights for aerial photography as extracted from automatically created surface models .....	155
Table 9.10	Results of the different methods used for the extraction of tree Heights from IRS-1C.....	160
Table 9.11	Results of the different methods used for the extraction of tree Heights from aerial photographs.....	160

**LIST OF APPENDICES**

**APPENDIX 1: IRS-1C FEATURES ..... 207**

**APPENDIX 2: TERRAIN EXTRACTION / SURFACE MODELS ..... 210**

**APPENDIX 3: STEREOMODEL OF AN IRS-1C SUBSET ..... 212**

**APPENDIX 4: ACCURACY REPORT – TRIANGULATION ..... 213**

**APPENDIX 5: USEFUL INTERNET WEBSITES ON THE TOPICS OF  
REMOTE SENSING AND PHOTOGRAMMETRY ..... 217**

**APPENDIX 6: RESULTS OF THE FOURIER ANALYSIS OF  
COMPARTMENT A15 ..... 219**

**APPENDIX 7: ABSTRACT OF SOUTH AFRICAN FORESTRY  
FACTS FOR THE YEAR 1996/97 ..... 221**

**APPENDIX 8: POSITION OF FLYING STRIP : MPUMALANGA,  
SOUTH AFRICA ..... 222**

**APPENDIX 9: LAYER INFORMATION OF THE TWO IRS-1C  
SCENES ..... 223**

**APPENDIX 10: LOCATION AND DISTRIBUTION OF GROUND  
CONTROL POINTS (GCPS) IN THE TEST AREA ..... 225**

**APPENDIX 11: ELEVATION DATA FOR COMPARTMENT A15 AS  
EXTRACTED FROM IRS-1C ..... 226**

**APPENDIX 12: RESULTS OF THE REGRESSION ANALYSIS ..... 228**

**APPENDIX 13: SAMPLING DESIGNS USED IN FOREST INVENTORY .. 238**

**APPENDIX 14: IMAGE MINIFICATION ..... 249**

**APPENDIX 15: PERFORMANCE OF VARIOUS SOFTCOPY SYSTEMS 252**

**APPENDIX 16: GENERATION OF DTMS FROM NON-PHOTOGRAPHIC  
SENSORS SUCH AS SPOT, MOMS-02 AND SAR ..... 256**

**APPENDIX 17: PHOTOGRAPHS SHOWING COMPARTMENT R33  
AND A YOUNG EUCALYPT STAND ..... 262**

## GLOSSARY

AATE	Adaptive Automatic Terrain Extraction (terrain extraction tool within LH's SOCET SET software suite).
Accuracy	The statistical error of the position of a ground point, stated in ground co-ordinates.
Affine transform	A uniform stretching that carries straight lines into straight and parallel lines but may alter distances between points and angles between lines.
Anaglyphic viewing system	Simple way of creating stereo vision. One image is projected through a colour filter (such as cyan) and the other through a filter of a different colour (e.g. red). By viewing the model through eyeglasses having corresponding colour filters, the operator's left eye will see only the left image and his or her right eye will see only the right image.
Analogue photogrammetry	Optical or mechanical instruments used to reconstruct three-dimensional geometry from two overlapping images.
Analytical photogrammetry	Replacement of some expensive optical and mechanical components by substituting analogue measurement and calculation with mathematical computation.
Analytical stereoplotter(AP)	This instrument operates through the formation of a mathematical model of the terrain imaged by a stereopair. This is done by linking a comparator type viewing and measuring system to a digital computer.
Ancillary data	The data, other than remotely sensed data, that are used to aid in the classification and interpretation process.
Area based matching	An image matching technique that determines the correspondence between two images according to the similarity of their grey level values.
ASCII	American Standard Code for Information Interchange
ATE	Automatic Terrain Extraction.
B/H ratio	Description for the relationship between the base of an air-, or spaceborne image acquisition system and its altitude.

Band	A set of data file values for a specific portion of the electromagnetic spectrum of reflected light or emitted heat or some other user-defined information created by combining or enhancing the original bands.
Batch file	A text file that contains a sequence of commands.
BIL	Band interleaved by line. A form of data storage in which each record in the file contains a scan line (row) of data for one band.
BIP	Band interleaved by pixel. A form of data storage in which the values for each band are ordered within a given pixel.
Blunder	Digital photogrammetry terminology for an error, a fault, with particular reference to the deviation from an optimal solution in the triangulation process.
BMP	Bitmap. One of the numerous graphics file formats.
Breakline	A line on the ground that indicates a sudden change in terrain gradient, such as ridge or stream.
BSQ	Band sequential. A data storage format in which each band is contained in a separate file.
Bundle	The unit of photogrammetric triangulation after each point measured in an image is connected with the perspective centre by a straight light ray. There is one bundle of light rays for each image.
Calibration report	In aerial photography, the manufacturer of the camera specifies the interior orientation in the form of a report.
Check point	A ground point with a known location used to verify the quality of a triangulation solution.
CIR	Colour Infrared. A pseudocolour representation of a region of the electromagnetic spectrum corresponding to the wavelengths between about 0.78 $\mu\text{m}$ and 1 mm. Often subdivided into 'Near IR' (Infrared) (0.78 $\mu\text{m}$ to about 1.2 $\mu\text{m}$ ), 'Mid IR' (1.2 $\mu\text{m}$ to 3 $\mu\text{m}$ ) and 'Thermal IR' (3 $\mu\text{m}$ to 15 $\mu\text{m}$ ). Photographic IR (i.e. Near IR) can be detected on photographic films, whereas Mid and Thermal IR are detected using electro-optical systems.

Classification	The process of assigning the pixels of a continuous raster image to discrete categories.
Console monitor	The main computer screen used when operating the workstation. Used to display all alphanumeric windows.
Contrast stretch	The process of reassigning a range of (pixel) values to another range, usually according to a linear function.
Control point	A point on the surface of the earth that has its geodetic location known with a certain degree of accuracy. Used as input to the triangulation process.
Conjugate points	The image points in two or more images that correspond to a single ground feature.
Convolution	A technique used to enhance an image. Can be used to sharpen, smooth or detect edges in an input image. Uses a kernel matrix. The numbers in the matrix serve to weight the calculated average values toward particular pixels.
Datum	A smooth ellipsoid approximating the surface of the earth, used as standard co-ordinate reference baseline for geopositioning. A datum is specified by the parameters semimajor earth radius, eccentricity, and XYZ centre offset.
Decision rule	The procedure by which criteria are evaluated and combined to arrive at a particular evaluation, and by which evaluations are compared and acted upon.
DEM	Digital Elevation Model – used synonymously with DTM (see DTM below).
Digital Photogrammetry	Also referred to as ‘Softcopy Photogrammetry’. Photogrammetry as applied to digital images that are stored and processed on a computer.
Digitising	Any process that converts non-digital data into numeric data.
Displacement	The degree of geometric distortion for a point that is not on the nadir line.
DLT	Direct Linear Transform – a rational polynomial that may be used to approximate sensor models.

DP	Digital Photogrammetry (see above) – used interchangeably with Softcopy Photogrammetry
DPW	Digital Photogrammetric Workstation. A highly sophisticated computer environment for the manipulation, measurement and analysis of digital imagery. Represents the main component of a Digital Photogrammetry System.
DSM	Digital Surface Model. In contrast to the DTM the DSM represents the elevation information of objects (e.g. trees, buildings) above ground level.
DTM	Digital Terrain Model. A grid of elevation data points. Although the grid structure breaks up the surface into cells of uniform character, the data are considered to come from an underlying continuous surface.
Ellipsoid	An oblate spheroid used to roughly model the surface of the earth. Parameterised by eccentricity and semimajor axis.
Enhancement	The process of making an image more interpretable for a particular application.
Ephemeris data	Contained in the header of data files of satellite imagery, providing information about the recording of the data and the satellite orbit.
Epipolar line	A line formed by the intersection of the epipolar plane with a horizontal ground space plane; or one of the images used to compute the epipolar plane. To visualise stereo, the left and right images must be oriented so the epipolar line is horizontal.
Epipolar plane	For a given ground point visible in each image of a stereo pair: the plane passing through the point and the two camera stations.
ERS-1	The European Space Agency's (ESA) radar satellite launched in 1991.
Extraction cursor	The cursor overlaying imagery on the extraction monitor used for geopositioning, feature delineation, interactive terrain editing, point measurement, and other ground space pointing operations.

Extraction monitor	A stereo-capable monitor dedicated to displaying imagery. Imagery can be displayed in several modes such as stereo, split-screen, and single image.
Fast format	An image format typically used on Landsat image tapes.
Feature extraction	The process of graphically delineating and attributing features, and storing them in a feature database.
Fiducial marks	Special marks in an image which have known co-ordinates relative to the sensor frame which are used to solve for the image's interior orientation. These are typically embedded along the edge of a frame camera image. Also known as Réseau marks.
Field of view	In perspective views, an angle that defines how far the view will be generated to each side of the line of sight.
Figure of merit	A quality metric assigned to each DTM post. Numbers range in value from 0 to 255 and indicate either the source of the post (ATE, area tool, etc.), or the relative accuracy of the output of ATE.
Filtering	The process of removing spatial or spectral features for data enhancement.
Focal plane	The plane of the film or scanner used in obtaining an image.
FOM	Figure Of Merit (see above).
Fourier analysis	An image enhancement technique that was derived from signal processing, transferring values from image space into the frequency domain.
Frame	A conventional camera, or the film or imagery produced by such a camera. Includes surveying cameras, hand-held cameras, and most reconnaissance cameras.
GCP	Ground Control Point. Specific pixel in image data for which the output map co-ordinates are known. GCPs are used for computing a transformation matrix, for use in rectifying imagery.

Geocoded	Rectified or ortho-rectified (e.g. orthophoto).
Geographic co-ordinates	The co-ordinate system in which ground points are represented as latitude and longitude.
Geoid	The surface of the earth at mean sea level, idealised to pass through the continents. The geoid is not an ellipsoid, but because of the uneven distribution of mass rather an irregularly shaped surface approximating a pear.
Georeferencing	Refers to the geographic location of data represented in an image or vector file in space as defined by a known co-ordinate referencing system.
GIS	Geographic Information System. A database system for the input, storage, retrieval, analysis and display of information about the earth's surface and objects on it.
GLONASS	Global Navigation Satellite System. Russian counterpart of the NAVSTAR GPS.
GPS	A Global Positioning System calculates range (distance) to a set of simultaneously viewable satellites to determine the co-ordinates of a position according to a specified geodetic referencing system.
Ground point	An umbrella term including control points, tie points, and check points.
Ground truth	Refers to any verification of mapped data against true ground conditions.
GUI	Graphical User Interface
HRC	Hierarchical Relaxation Correlation. The algorithm used by the ATE process.
Ifov	Instantaneous Field Of View. A measure of the area viewed by a single detector on a scanning system in a given instant of time.
Image centre	The centre of the aerial photograph or satellite scene.
Image enhancement	The process of improving or altering the appearance of an image, usually to assist the operator with feature extraction.

	Image enhancement operations include convolutions, histogram equalisation, and tonal transfer curve alterations.
Image location	A directory in which pixel files are stored.
Image point	The pixel in an image that corresponds to a given ground control point. Both the image point and GCP are used during the triangulation process.
Image processing	The manipulation of digital image data, including enhancement, classification, and rectification operations.
Image pyramid	A set of overview images built from an original image. The original image is called the 1:1 image, and the other images are created by averaging every four pixels to recursively create smaller overview images, denoted as 2:1, 4:1, etc.
Image Space	The space in which the pixels in an image are located.
Interior orientation	The process of computing a transformation from film space to image space that accounts for the position and orientation of the photo when it was digitised or scanned. Requires the measurement of fiducials.
IOR	Iterative Orthophoto Refinement. A procedure to improve the accuracy of an orthophoto.
ITE	Interactive Terrain Extraction/Editing. The process of manually reviewing and correcting a DTM.
JERS-1	The Japanese radar satellite launched in 1992.
JPEG	Joint Photographic Experts Group. A graphics data format featuring image compressing techniques.
LAN	A multiband continuous image file (the name is derived from the Landsat satellite).
Landsat	A series of earth observation satellites that gather multispectral (MSS) and thematic mapper (TM) imagery.
Least squares correlation	Uses least squares estimation to derive parameters that best fit a search window to a reference window.
Least squares regression	Method used to calculate the transformation matrix from the GCPs.

LIDAR	Light Detection and Ranging.
LISS	Linear Imaging and Self Scanning Sensor.
Map projection	A method of representing the three-dimensional spherical surface of a planet on a two-dimensional map surface.
Minification	The process of generating an image pyramid from an original image.
Model	Remote sensing/photogrammetry terminus technicus referring to (1) an image and its sensor model, (2) a stereo pair of images and their sensor models.
Mosaicking	The process of piecing together images side by side, to create a larger image.
Multi-temporal	Data from two or more different dates.
Nadir	The area on the ground directly beneath a scanner's detectors.
NAVSTAR	Navigation Satellite Timing and Ranging. The American GPS consisting of 24 navigation satellites.
NDVI	Normalised Difference Vegetation Index. An index derived from reflectance measurements in the red and infrared portions of the electromagnetic spectrum to describe the relative amount of green biomass from one area to the next.
Off-nadir	Any point that is not directly beneath the scanner's detectors, but off to an angle.
OPS	Optical Sensor.
Orientation	(1) Triangulation, exterior orientation. (2) The true angles that define the viewing angle of a given frame image.
Orthophoto, Orthoimage	An image that has all distortion due to obliquity, perspective, and terrain relief removed. The process of creating an orthophoto requires an input image, an accurate sensor model for the input image, and a DTM for the image region.

Orthorectification	The process of generating an orthophoto.
Pan	Panchromatic. Single band imagery in which the band covers most of the visual spectrum. Conventional black and white photographs are panchromatic.
Parallax	Apparent displacement or difference in the apparent position, of an object, caused by the actual change of position of the point of observation.
Pass point	A tie point connecting exactly two overlapping images.
Perspective centre	(1) A point in the image co-ordinate system defined by the X and Y co-ordinates of the principal point and the focal length of the sensor. (2) After triangulation, a point on the ground co-ordinate system that defines the sensor's position relative to the ground.
Perspective scene	An artificial image created by generating a view of what a camera would see if it were located at a given point and looked in a given direction. Several perspective scenes may be viewed in rapid sequence to create an animated 'fly-through'.
Pixel	A contraction of the words 'picture element'; the smallest part of an image.
Point measurement	The process of sampling points in imagery to support a computational process such as interior orientation, image registration or triangulation.
Polygon	A closed polyline that encloses an area.
Post	A single elevation data point. A DTM is a rectangular grid of posts.
Principal point	The point in the image plane onto which the perspective centre is projected, located directly beneath the interior orientation.
Project	A collection of data files (imagery, DTM, control points, etc.) relating to a single geographic area. When a project is created, the operator specifies a co-ordinate system and datum.

Projection	Projection refers to the representation of one surface to another such as somewhat spherical Earth onto a flat medium such as paper.
Pushbroom	A scanner in which all scanning parts are fixed and scanning is accomplished by the forward motion of the scanner.
Radiometric	Concerning image appearance. Specifically, a quantitative analysis of the visual quality of a digitised image, using measures such as brightness, contrast and histogram.
Radiometric correction	The correction of variations in data that are not caused by the object or scene being scanned, such as scanner malfunction and atmospheric interference.
Radiometric resolution	The dynamic range, or number of possible data file values, in each band.
Raster data	Any data (e.g. imagery, terrain grids) which may be stored or represented as a two-dimensional array of points as opposed to vector data.
Rectification	The process of reshaping imagery to a vertical perspective by removing distortion due to camera obliquity. Rectification involves resampling.
Registration	The process discovering the correct ground location of data (terrain, feature, or imagery) whose location is initially unknown or uncertain.
Resampling	The process of reshaping an image by warping the image in a rubber sheet fashion. Resampling uses inter-, and extrapolation to determine output pixel values.
Réseau mark	See fiducial mark.
Residual	An error measure which is an indicator of the quality of the results of a process such as interior orientation or triangulation. Small residuals indicate that the solution is accurate.
Resolution	A level of precision in data. Specific types of resolution are radiometric, spatial, spectral, and temporal resolution.
RMSE	Root Mean Square Error. A measure of the variability of measurements about their true values.

Roam	The process of moving across a display so that different areas of the image appear on the display screen.
Rubber sheeting	The application of a non-linear rectification.
SAR	Synthetic Aperture Radar.
SLAR	Side-Looking Airborne Radar.
Scanner	A device used for the direct collection of raster data.
SCOP	'Stuttgart COntouring Programme'. Programme for the computation and utilisation of DTMs. Developed by the ifp (Institute for Photogrammetry) Stuttgart and Vienna and the INPHO GmbH Stuttgart.
Screen digitising	The process of drawing vector graphics on the display screen with a mouse. A displayed image can be used as a reference.
Sensor	A device that gathers energy, converts it to a digital value, and presents it in a form suitable for obtaining information about the environment.
Sensor model	For a given image, the formula that converts between ground space and image space. The sensor model embodies the sensor location, orientation, optics, and geometry.
Sensor model parameters	The variables of a sensor model formula such as camera location ( $X$ , $Y$ and $Z$ ), and camera orientation ( $\omega$ , $\phi$ , $\kappa$ ).
Shaded relief image	A thematic raster image that shows variations in elevation based on a user-specified position of the sun.
SOCET SET	Softcopy Exploitation Tools (LH Systems' digital photogrammetry software package).
Softcopy Photogrammetry	See Digital Photogrammetry above.
Spatial resolution	A measure of the smallest object that can be resolved by the sensor, or the area on the ground represented by each pixel.

Stereogram	Interpretation keys, containing information on grey scale, texture, crown density, etc., of typical forest stands are used to visually compare the features with those of unknown stands to get an estimate on timber volume.
Stereo pair	Two overlapping images used to extract terrain and feature information. The convergence angle must be large enough (usually greater than 20 degrees) to support geolocation.
Strategy	A set of parameters used to tune an algorithm to a particular dataset. For example the strategies used in ATE, where each strategy is tailored to a certain kind of topography.
Strip of images	A group of images whose footprints form a more-or-less straight line. A strip usually results from a single flight run of an aircraft. Adjacent images in the strip overlap by a certain amount (e.g. 60%).
Sun-synchronous	A term describing earth-orbiting satellites that rotate around the Earth at the same rate as the Earth rotates on its axis.
Super structure format	File format containing satellite ephemeris information.
Support data	Generally, any data accompanying an image that describes the image size, source, history, etc. Often stored as a header to the image.
Support file	An ASCII text file that contains auxiliary information about an image (sensor parameters, photo date, image size, etc.).
Swath width	In a satellite system, the total width of the area on the ground covered by the scanner.
Tie point	An image point located in two or more overlapping images and used to solve the sensor model during the triangulation process. Tie points serve to tie the individual sets of photographs into a single flight unit and to tie adjacent flights into a common network.
TIFF	Tagged Image File Format. A commonly used raster file format.
TIN	Triangulated Irregular Network. A set of DTM posts arranged in an arbitrary, nongridded pattern.

Toggle	The action of switching the mouse control between the extraction cursor and the X cursor.
Topology	Optional information stored in a feature database. Topological information describes relationships between neighbouring features such as adjacency, overlap, and intersection.
Total RMSE	The total root mean square error for an entire image. This error takes into the account the RMSE of each GCP.
Trackball	An input device, similar to a mouse, used to move the extraction cursor.
Transformation matrix	A set of coefficients which are computed from ground control points, and used in polynomial equations to convert co-ordinates from one system to another.
Triangulation	The process of calculating sensor model parameters for one or more images based on control points and tie points provided by the operator. Also called exterior orientation or image registration.
UTM	Universal Transverse Mercator.
Vector data	Geometrical data such as points, lines, and polygons.
Vitec	Visual Information Technologies Inc.
WGS	World Geodetic System (e.g. WGS84) – a spheroid.
WiFS	Wide Field Sensor.
Y parallax	The component of the horizontal distance between two ground positions, determined for the same ground point and elevation using the point position in two images, in the direction orthogonal to the epipolar direction.
Zoom	The process of expanding displayed pixels on an image so that they can be more closely studied.

## 1. INTRODUCTION

The aim of this study was to probe the potential of state-of-the-art satellite technology in forest inventory by employing digital photogrammetry technology.

The following secondary objectives were defined:

1. Extraction of inventory parameters such as tree height, canopy closure and crown diameter from the imagery (i.e. satellite scenes and aerial photography, which was used as reference) with the estimation of stand volume as a derived parameter.
2. Creation of Digital Terrain Models (DTMs) and Digital Surface Models (DSMs).
3. Comparison of the results being obtained by the application of the different terrain extraction methods (i.e. manual, semi-automatic and automatic) in terms of performance and accuracy.
4. Exploration of various forest inventory concepts for the possible integration and application of the obtained satellite information.

The proposed analysis of the satellite imagery comprises processing of these data in a digital photogrammetry environment and other image processing software packages. Some of these packages have only been introduced to the market a short while ago and have not been tested extensively on stereo satellite imagery. This is particularly true for the digital photogrammetry systems, as they have become operational only now, and some major shortfalls still exist. Recent studies have suggested that encouraging results can be obtained when automatically extracting elevation information (e.g. tree heights) from large scale aerial photographs (Stöcker, 1999; Kätsch and Stöcker, 2000). However, not a single study has been published to date on the extraction of elevation information in forested areas from stereo satellite imagery. Thus, extensive scrutiny on the performance and the achievable accuracies of the involved technologies was mandatory for the judgements as to what extent these technologies are applicable to the forestry sector. As a consequence, the presented investigation exhibits a distinct technical flavour.

The reason for this study is the Earth's booming population, her dwindling available resources, and her mercurial climate, which make for perilous decisions about land

use resource management. No policy maker and manager can hope to render sound judgement in these matters without the benefit of unbiased scientific analysis. Science, in turn, depends completely on accurate, timely observation, sometimes referred to as hard data. Remote sensing, as an equitably recent technology, has proven to be able to meet the demand of data about environmentally related issues at high quality, at fairly low cost and with an expeditious response.

A great number of studies carried out recently show very clearly that only 2.9% of the entire African continent has been mapped on a 1:25 000 scale, while cartographic maps on a 1:50 000 scale exist only for 41% of Africa. Most of these maps have become obsolete and need to be either updated or even re-created. Remote sensing technology, and the different techniques being involved, provide a highly efficient, powerful, and economical tool to generate cartographic and thematic maps, and it presents itself as an invaluable source of information about various features of our planet. For that reason, in 1992 a project was initiated by the Department of Electrical and Electronic Engineering at the University of Stellenbosch in collaboration with several other research institutions with the objective to receive remote sensing data at low cost as well as to increase engineering design opportunities for graduate students. SUNSAT (Stellenbosch University Satellite) was born.

Currently a forest cover map already exists for South Africa (Van der Zel, 1988; Thompson, 1997), however, the scale of 1:250 000 as well as the coarse ground resolution of 30m of Landsat<sup>1</sup> TM<sup>2</sup> is not able to provide a suitable source for forest inventory purposes. With these shortfalls and the improved capabilities of SUNSAT in mind, in 1994 a project funded by the Department of Water Affairs and Forest (DWAF) to investigate the application of satellite imagery received from SUNSAT in the forestry sector, particularly for a national forest inventory, was initiated. The launch of SUNSAT, originally planned for 1997, had to be deferred and took place in January 1999. Consequently, the first satellite data would be received by the middle of 1999 at the earliest. Therefore, for the purpose of this study, it was decided to make use of other satellite systems with characteristics similar to those of SUNSAT

---

<sup>1</sup> Land satellite

<sup>2</sup> Thematic Mapper

for simulation purposes. In 1996 a joint research project<sup>3</sup> in collaboration with the *Fachhochschule Hildesheim /Holzminden*<sup>4</sup> in Göttingen, Germany, was motivated. The main goal of the project was to investigate the feasibility of stereo satellite imagery for inventory purposes in plantation forestry in southern Africa. A potential test area close to the town of Sabie in the South African province of Mpumalanga was identified. The analysis of the stereo satellite imagery was carried out on a digital photogrammetry workstation DPW770<sup>5</sup> at the *Fachhochschule Hildesheim/Holzminden*. It was planned to use satellite data captured by the German MOMS-02P<sup>6</sup> sensor, which could be used to simulate the performance of SUNSAT imagery. It eventually proved to be impossible to obtain the imagery and because of the well-documented problems of the Russian Mir space station the plan had to be discarded. Another candidate, the new Indian panchromatic/multispectral scanner onboard the IRS1<sup>7</sup>-C/D twin satellite system was considered to be the most appropriate because of the high ground resolution (5m) and the stereo mode capabilities. Thanks to the generous donation of the Volkswagen Foundation one IRS-1C stereo pair of the required imagery could be acquired.

Recent studies have suggested that the estimation of woody biomass and the determination of the annual increment of forest stands can be carried out with confidence when using remote sensing information (Coops *et al.*, 1999; Ulander *et al.*, 2000). Remotely sensed images not only have the advantages of being able to quantitatively characterise stand canopies via spectral reflectance, but can also be used as a useful input into GIS and other inventory based information systems. However, in many cases expensive technology has to be employed (e.g. VHF-band Synthetic Aperture Radar) and complex and time consuming interpretation of the captured information is required. Thus, the presented study also aimed at finding low-cost and efficient solutions.

---

<sup>3</sup> “*Untersuchungen zur waldmesskundlichen Klassifikation von Plantagenwäldern im südlichen Afrika*” (Investigation into the mensurational classification of forest plantations in southern Africa)

<sup>4</sup> *Fachbereich Forstwirtschaft und Umweltmanagement*

<sup>5</sup> funded by the Volkswagen Foundation

<sup>6</sup> Modular Optoelectronic Multispectral Scanner

<sup>7</sup> Indian Research Satellite

## 2. DEFINITION OF THE TERMS 'REMOTE SENSING' AND 'PHOTOGRAMMETRY'

Remote sensing refers to a variety of techniques that have been designed for the acquisition and analysis of electromagnetic radiation, either being reflected or emitted from the Earth's surface, and detected by specific sensor systems, to provide information about the finite resources of our 'blue spaceship', the Earth. The term 'remote sensing' was coined by geographers at the US (United States) Office of Naval Research in the late 1950s, early 1960s. At the first Symposium on the Remote Sensing of Environment in Michigan in 1962, Parker (in: Howard, 1991) defined remote sensing as the collection of data about objects which are not in contact with the collecting device. Since its first official presentation, there has been a host of varying definitions concerning the contents of the field of remote sensing (see also Campbell, 1996). Despite all the differences, the central concept is the gathering of information at a distance from the object to be assessed. Nevertheless some kind of refinement appears imperative. Remote sensing is now generally accepted as: *"the science of deriving information about an object or phenomenon, by a recording device that is not in physical or intimate contact with the object or phenomenon under study"* (Thompson, 1980). Furthermore it does not only involve the collection of raw data, but also the processing (may it be in a manual or automatic manner) of these data, as well as the analysis of the imagery and the presentation of the derived information (Howard, 1991; Hildebrandt, 1996).

The term 'remote sensing' was devised to replace the traditional terms 'aerial photography' and 'aerial photointerpretation', since the new technologies also encompass the scrutiny of the electromagnetic spectrum beyond the visible portion. Although other carriers of information on the objects of interest exist, such as ultrasonic waves or magnetic fields, and objects may as well be located extra-terrestrially, many of these applications are omitted for reasons of tradition and convenience. Hence, most textbooks on this subject narrow their scope to the observation of the Earth's surface.

In contrast to the definition of the term 'remote sensing', 'photogrammetry' is basically concerned with obtaining measurements by means of photographs. The

denomination 'photogrammetry' is derived from the Greek, *photos* meaning 'light', *gramma* meaning 'something drawn or written', and *metron* meaning 'to measure' (Thompson, 1980). A more refined definition is given by the American Society of Photogrammetry (Slama, 1980), taking recent developments into account: "*Photogrammetry is the art, science, and technology of obtaining reliable information about physical objects and the environment through processes of recording, measuring, and interpreting photographic images and patterns of electromagnetic radiant energy and other phenomena*".

The recognition of photogrammetry as a specific partner to remote sensing is being reflected in the fact that many national and international institutions have recently changed their names. Some remarkable examples are the *American Society of Photogrammetry and Remote Sensing* (formerly known as *American Society of Photogrammetry*), and the *International Society of Photogrammetry and Remote Sensing* (ISPRS). The best known application of photogrammetry is the compilation of topographic maps and in surveying, but recent technological developments such as the advent of 'digital photogrammetry', are beginning to broaden the scope of applications tremendously (e.g. digital photogrammetry data being used as input into a GIS).

Photogrammetry is frequently divided into specialties according to the types of photographs or sensors used, or their various applications. For instance, *terrestrial photogrammetry* deals with photographs taken on the ground surface, whereas *close-range photogrammetry* is confined to the short distance assessment of objects in the industrial environment (e.g. foams), the medical profession (e.g. diagnostic, surgery, etc.) or even the forestry sector (determination of taper) (Dehn *et al.*, 1985; Hildebrand, 1996). Within the scope of this thesis, for practical reasons, the term 'photogrammetry' basically refers to *aerial photogrammetry*, for photographs being taken from an airborne platform, as well as to *satellite photogrammetry* (for spaceborne cameras and sensing systems).

The dedicated reader will find a detailed treatise on the subject in the *Manual of Remote Sensing* (Colwell, 1986) as well as in the *Manual of Photogrammetry* (Slama, 1980).

### 3. A BRIEF HISTORY OF REMOTE SENSING

Remote sensing and its inseparable partner, photogrammetry, have their origins reaching down to ancient cultures and philosophies. Periods of great inventions, arts, and discoveries produced genii such as Leonardo da Vinci, Albrecht Dürer, Johannes Kepler, and Isaac Newton. The results of their endeavours in optics, mechanics, geometry, and geophysics have furnished a sound foundation, on which research and even every-day-life of our modern civilisation can stand and continue to build on.

Even though photogrammetry and remote sensing in their most simple definition (i.e. the art of scribing and measuring) were practised long before the invention of the photographic process, devices were rather primitive and accomplishments fairly 'limited'. Hence, only the introduction of the camera in the nineteenth century fuelled a substantial progress in these technologies. Since then, there has been a great number of substantial advances and improvements in the civil sector, but there is little doubt that the driving force behind all big campaigns lies with the activities of the military (Cracknell and Hayes, 1988; Campbell, 1996, and others). It would seem to be a safe assumption that this is particularly true for the space programme (since 1960). However, there are indications these days, that with an increasing popularity of (applied) remotely sensed data, more and more technical know-how is either being transferred to the civilian domain or even being developed outside the military sector (in compliance with the 'open skies' policy).

An exhaustive treatise of this subject is beyond the scope of this thesis, and only a few key events are presented in the following table. More complete accounts are provided by Lillesand and Kiefer (1994), Simonett (1983) and others.

**Table 3.1** Milestones in the history of remote sensing (by analogy with Campbell, 1996)

1800	Discovery of infrared by Sir William Herschel
1839	Beginning of practice of photography (by Niepce, Talbot, Daguerre)
1846	Founding of the Zeiss Works, and Schott Glass Works (1884)
1847	Infrared spectrum shown by A.H.L. Fizeau and J.B.L. Foucault to share properties with visible light
1858-1860	First photographs from balloons (taken at Bievre, France, and Boston, USA)
1873	Theory of electromagnetic energy developed by J.D. Maxwell
1887	First aerial photograph of forest area taken close to Berlin

1903	Invention of aeroplane by the Wright brothers
1909	Photography from aeroplanes
1914-1918	World War I: aerial reconnaissance
1920-1930	Development and initial applications of aerial photography and photogrammetry
1930-1940	Development of radar in Germany; colour photography became available.
1939-1945	World War II: applications of non-visible portions of electromagnetic spectrum; training of persons in acquisition and interpretation of airphotos
1950-1960	Military research and development
1956	Colwell's research on disease detection with infrared photography
1957	Launch of the first satellite, SPUTNIK 1
1960 on	Period of very active sensor and platform development
1960-1970	First use of term "remote sensing"
	TIROS (Television Infrared Observation Satellite) weather satellite
	Skylab remote sensing observations from space
1972	Launch of LANDSAT 1
1970-1980	Rapid advances in digital image processing
1980	USSR METEOR Satellite
1980-1990	LANDSAT 4: new generation of Landsat sensors
1980s	Development of hyperspectral (high resolution) sensors
1984	Landsat 5
1986	SPOT 1
1988	IRS-1A
1990	SPOT 2
1992	JERS-1
1995	Radarsat
1995	IRS-1C
1996	MOMS-2P
1998	SPOT 4
1999	SUNSAT
1999	Ikonos 2
1999	Landsat 7
2000	Orbview 3

## **4. CONCEPTS AND FOUNDATIONS OF REMOTE SENSING**

The understanding of the factors constraining the operation of remote sensing systems is basic to the successful application thereof. Since the discussion on the principals of electromagnetic radiation is being exhaustively dealt with in many textbooks (e.g. Akça *et al.*, 1984; Baker, 1980; Barrett and Curtis, 1976; Budd, 1991; Campbell, 1996; Clarke, 1986; Colwell, 1980 and 1986; Cracknell and Hayes, 1988; Elachi, 1987; Goldsmith, 1991; Harris, 1987; Hildebrandt, 1996; Howard, 1991; Lillesand and Kiefer, 1994; Lindgren, 1985; Rees, 1990; Schanda, 1976), only a brief account of some of the relevant aspects of the physics of electromagnetic radiation will be given in this chapter; however, the specific reflective properties of tree foliage will be discussed in some detail.

### **4.1 Energy sources and radiation principles**

Although our universe is governed by a great number of different physical laws and accordingly several modes of information transfer do occur, such as acoustical energy and force fields (i.e. gravity and magnetism), only electromagnetic radiation has gained wide appreciation as a medium for environmental remote sensing. This preponderance can be explained by the fact that electromagnetic radiation can be detected fairly easily and that many of its properties (e.g. the ability of transmitting the information over long ranges without unrestorable loss) make it an ideal tool for the transfer of energy.

All material at temperatures above absolute zero ( $0^{\circ}$  K) generates electromagnetic energy. This emissive energy, being in the form of both temperature and emissivity, is governed by the object's nuclear properties, its chemical composition as well as its physical state. The radiation is generated by transformation of energy from forms such as kinetic, chemical, thermal, electrical, magnetic or nuclear. A great number of higher frequency waves such as in the infrared and the visible part of the spectrum are produced by molecular excitation followed by decay. Electromagnetic radiation is usually categorised in terms of wavelength, frequency and amplitude, whereas most remote sensing scientists, for practical reasons, focus on the measurement of the wavelength. Based on the properties of the various sensors being employed, the

electromagnetic spectrum has been arbitrarily (since the spectrum actually is a continuum) subdivided into the main spectral categories, 'Gamma- and X-rays' ( $3 \times 10^{-6} \mu\text{m}$  to  $0.1 \mu\text{m}$ ), 'ultraviolet' (up to about  $0.1 \mu\text{m}$ ), 'visible' (from  $0.4 \mu\text{m}$  to  $0.75 \mu\text{m}$ ), 'infrared' (from  $0.75 \mu\text{m}$  to  $1 \text{mm}$ ), and 'radio' (beyond  $1 \text{mm}$ , including 'microwave' ( $1 \text{mm}$  to  $1 \text{m}$ )). The properties of electromagnetic radiation have been described in form of equations and laws by scientists like Maxwell, Stefan-Boltzmann, Wien, Kirchhof, Planck and Einstein (Barrett and Curtis, 1976). Some important properties are the following:

1. The longer the wavelength involved, the lower its energy content.
2. Each radiation source emits a characteristic array of radiation waves.

The implications for remote sensing systems are that firstly, long wavelength radiation is more difficult to sense, and secondly, all emitting bodies can to some extent be identified by their spectral signature, thus presenting a sound basis for the discernment and classification of objects.

As the sun represents the most obvious, and one of the strongest source of electromagnetic radiation, it is this radiation that forms the basis for passive sensor products such as photographs and similar images. Furthermore, man-made radiation (so-called, 'active systems') such as radar or laser systems, is exploited for remote sensing. The radiation being reflected, emitted or scattered from a body generates a radiant flux density, which contains information about the physical or chemical properties of the object itself. To measure these characteristics, a collector focusing the intercepted energy (e.g. by means of a lens) is employed, followed by a detecting device, which transforms the electromagnetic energy into other forms such as heat, electric current or state change (Campbell, 1996; Lillesand and Kiefer, 1994; Rees, 1990).

#### **4.2 Energy interactions in the atmosphere**

In many respects the Earth's atmosphere can be considered a nuisance, since considerable complications arise where the atmosphere intervenes between the sensor and its target. The almost unpredictable behaviour of parts of the radiation in combination with the dynamic character of the atmosphere and its constituents make it extremely difficult to create models to account for these effects. The variation of the net effect of the atmosphere is closely related to the distance between the object

and the sensor (the so-called 'path length'), the magnitude of the energy signal being sensed, the atmospheric conditions, and the wavelengths of the radiation.

The degradation of the quality of the remotely sensed imagery is traditionally caused by the substantial influences of *attenuation* (i.e. a combination of absorption and scattering), and refraction. *Scattering* is the redirection of electromagnetic radiation by particles suspended in the atmosphere or by large molecules of atmospheric gases. The degree of scattering largely depends on the size of the particles (e.g. pollutants, water droplets), their abundance, the wavelength of the radiation, and the depth of the atmosphere. Scattering influences the direction and intensity of the radiation, the wavelength and frequency of the radiation received by the target, as well as the spectral distribution of this radiant energy. A very common form of scatter is named after the British scientist Lord J.W.S. Rayleigh, who discovered that the amount of scattering increases greatly as wavelength becomes shorter, i.e. *Rayleigh scattering* is wavelength dependent (e.g. blue light is scattered four times as much as is red light). This type of scatter occurs when atmospheric particles have diameters that are small compared with the wavelength of the radiation, and it is the cause both for the blue colour in the sky and the red colours at sunset. *Mie scattering* is caused by larger particles (water vapour, dust, etc.) present in the atmosphere. These particles have diameters that are roughly equivalent to the wavelength of the radiation. Mie scatter is also wavelength dependent and influences a broad range of wavelengths in and near the visible spectrum. A third type of scatter, the so-called *nonselective scatter*, is induced by particles such as water droplets and dust, its size being much larger than the wavelength of the scattered radiation. Radiation is scattered equally (nonselectively), hence fog and clouds appear whitish or greyish (Campbell, 1996; Cracknell and Hayes, 1988; Elachi, 1987; Rees, 1990).

*Refraction* is another source of concern to the remote sensing user community. Refraction is defined as the bending of light rays at the contact between two media of different density. It is also present in the atmosphere as light passes through atmospheric layers of varied clarity, temperature and humidity. Even in the absence of atmospheric turbulence, it is difficult to quantify the variations in density of the atmospheric layers.

*Absorption* is the process by which radiant energy is retained by a substance or body. As a consequence of this process, some part of the incident radiation is transformed into heat, and the subsequent re-emission of that energy at a longer wavelength. In the atmosphere, the absorption of radiation occurs not at its surface but in transit. Three of the atmosphere's main components, namely water vapour, carbon dioxide and ozone are particularly efficient absorbers of radiation from the sun. Ozone is known to absorb radiation in the high-energy portions of the ultraviolet spectrum, hence protecting life on Earth against serious radiation damage. Carbon dioxide effectively captivates radiation in the mid- and far infrared spectral regions, thus contributing to the so-called greenhouse effect. Finally, water vapour is omnipresent in the lower atmosphere, its contents changing greatly with time and location. This substance is several times as effective in the absorption of radiation than all other atmospheric gases combined. The wavelengths in which the atmosphere is particularly transmissive of energy are widely known as *atmospheric windows*. Source energy can be transmitted through these to and from objects on the surface of the earth, consequently determining the spectral sensitivity of the available sensors to detect and record the energy (Elachi, 1987; Rees, 1990).

*What are the major implications for remote sensing systems?*

1. The longer the path length, the more difficult it is to account for all the atmospheric influences (in the case of satellite remote sensing the radiation has to travel twice through all spheres of the atmosphere).
2. Because of the strong effect of scattering on the blue and ultraviolet regions of the spectrum, they usually are not considered useful for remote sensing.
3. Scattering directs energy from outside the sensor's field of view toward the sensor's aperture, thus decreasing the spatial detail of the imagery.
4. Scattering decreases the contrast by making dark objects brighter and bright objects darker than they would otherwise be (as influence of 'skylight').
5. Atmospheric refraction causes loss of spatial detail and distortion/displacement of ground features on the image; furthermore mirage-like apparitions can occur, deceiving the real location of the object on the earth's surface.
6. Remote sensing systems have to be designed with respect to the detectability of radiation (i.e. the atmospheric windows), not the other way round.

7. The conditions of the flying mission have to consider the above mentioned influencing factors (Campbell, 1996; Harris, 1987; Hildebrandt, 1996; Howard, 1991; Lillesand and Kiefer, 1994).

Quite a number of atmospheric correction models have been developed in the last few decades (see Hildebrandt, 1996; Kraus, 1993; Slama, 1980), but since the atmosphere is a highly dynamic system, a number of imponderables remain.

### 4.3 Energy interactions with earth surface features

Whenever electromagnetic radiation is incident on a given feature on the surface of the earth, this energy is subject to the three fundamental interactions of *reflection*, *absorption*, and *transmission*. The critical factors for *reflection* are the smoothness and orientation of the object being in the path of an electromagnetic ray. In terms of reflectance the scientific literature distinguishes two special, idealised cases, the *specular reflector*, which is perfectly smooth, and the *Lambertian reflector*, which features a 'perfect' roughness of its surface. A fairly simple method of describing the surface scattering (i.e. reflection) is commonly known as the *albedo*. It is defined as the percentage of the insolation incident upon a surface that is reflected back towards space. The following table shows albedos for a few natural surfaces.

**Table 4.1** Values of albedos for various surfaces (according to Campbell, 1996; Hildebrandt, 1996; Rees, 1990).

Type of surface	Albedo of incident visible radiation (%)
Water (naturally occurring)	1-10
Deciduous forest	17
Pine forest	14
Heather	10
Moist ploughed field	14
Fine sand	37
Dense, clean snow	86-95

Since no perfectly smooth<sup>8</sup> or rough (i.e. Lambertian reflector) surface is realised in nature, a great number of models (e.g. the facet model) have been created to explain all kinds of intermediate cases of spectral reflectance (Elachi, 1987; Rees, 1990). As

<sup>8</sup> i.e. any irregularities must be less than about  $\lambda/8$  in height; this condition is only met in certain man-made surfaces such as metal or sheets of glass

has been emphasised before, by looking at the spectral response pattern of a target, it is possible to make inferences about its properties, hence we may be able to clearly identify objects by their spectral signature (i.e. the shape of the spectral reflectance curve). An example of such a curve for green, healthy vegetation is included in Figure 4.1. Note the different reflectance minima for chlorophyll in the visible part of the spectrum and the maxima in the near infrared. In contrast, the reflectance pattern for many types of soil would have a higher intensity in the visible part and a lower intensity in the near infrared.

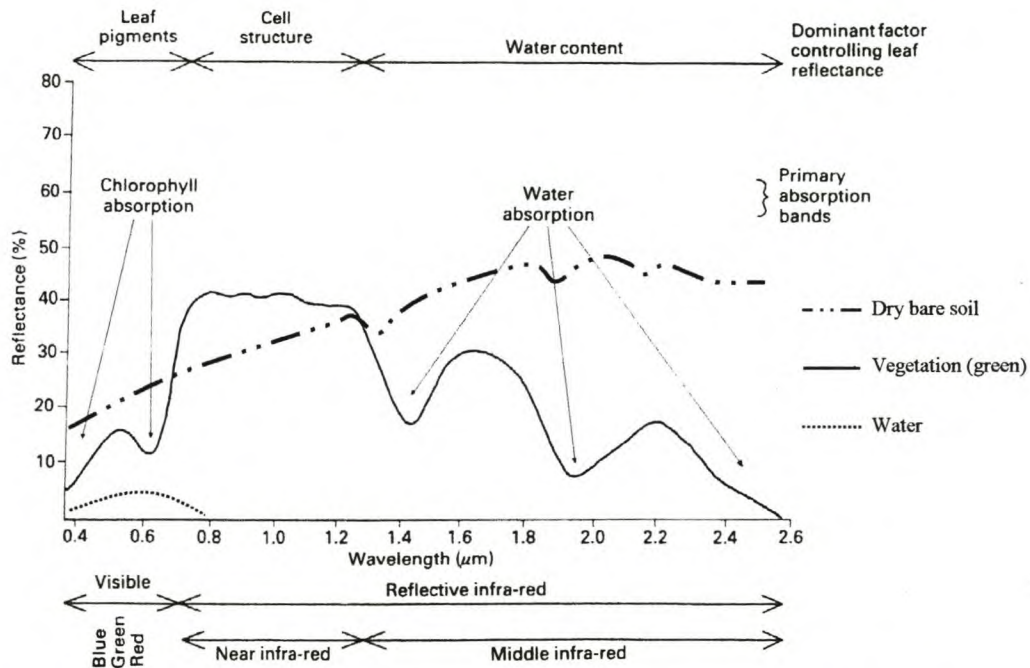


**Figure 4.1** Typical spectral reflectance curves for vegetation, soil, and water (by analogy with Goldsmith, 1991)

The various degrees of *absorption* at different wavelengths can also be extracted from the graph. As noted earlier, energy in transit may be attenuated or even completely extinguished by the process of absorption. The ability of a substance to absorb radiation is determined by its thickness and its composition. Absorption also varies with wavelength. Composition in this context refers to the internal structure of a leaf for instance, as comprising different types of tissues. The next figure presents an example of the physical composition of a deciduous leaf and its implications on the reflectance properties.

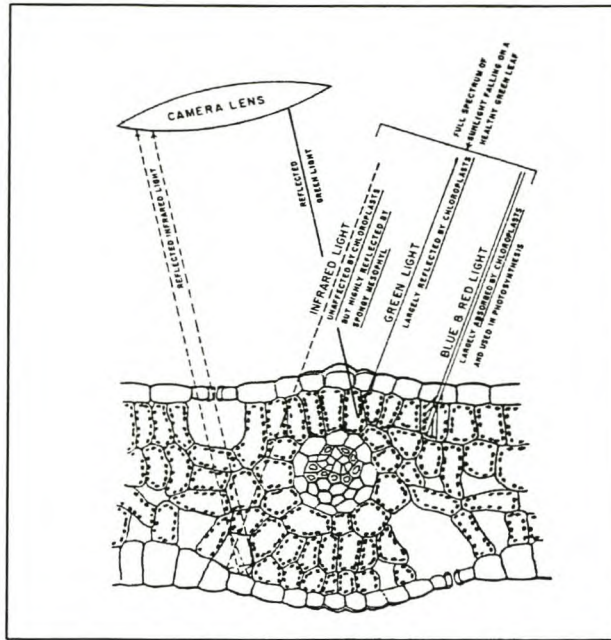


**Figure 4.2** Reflective properties of a healthy leaf (Barrett and Curtis, 1976)

The last important effect on spectral response to be dealt with is *transmission*. This occurs when radiation passes through a substance without significant attenuation. The transmittance of an object is defined as the ratio of radiation at distance  $x$  (i.e. transmitted radiation) within it to the incident radiation. This property varies greatly with wavelength, therefore a target, which is relatively transparent at a specific wavelength, may be relatively opaque at another (Elachi, 1987; Rees, 1990). So for instance, green leaves are generally opaque to visible radiation, but exhibit a high level of transmittance in the infrared (Barrett and Curtis, 1976; Goldsmith, 1991).

A lot of research has focused upon the examination of spectral properties of different objects since they form a weighty part of the whole remote sensing business. Some important sources of variation in multispectral signatures of vegetation are introduced in Table 4.2.

**Table 4.2** Sources of variation in multispectral response patterns of vegetation (in analogy with Barrett and Curtis, 1976; Hildebrandt, 1996)

<p><i>Illumination conditions</i>  Illumination geometry (sun angle, cloud distribution)  Spectral distribution of radiation</p> <p><i>Site environmental conditions</i>  Meteorologic  Hydrologic  Geomorphologic</p> <p><i>Reflective and emissive properties</i>  Spatial properties (geometrical form, pattern and distribution)  Spectral properties (e.g. reflectance, colour)  Thermal properties (temperature, emittance)</p> <p><i>Plant conditions</i>  Maturity  Physical condition (nutrient level, disease, etc.)  Variety</p> <p><i>Atmospheric conditions</i>  Water vapour, aerosols, etc.</p> <p><i>Viewing conditions</i>  Observation geometry (see also Hildebrandt, 1996)  Time of observation (seasonal effects)  Altitude</p> <p><i>Multichannel sensor parameters</i>  Electronic noise, drift  Accuracy and precision of measurements</p>
--

In many instances the spectral separability between vegetated and non-vegetated surfaces, as well as between the different appearances of vegetation is crucial to a great number of applications in remote sensing and its related fields. As mentioned at an earlier stage the structure of the leaf and its chemical composition play a major role in its spectral behaviour. In case of the near infrared energy the structure of the different types of tissue (mesophyll and palisade tissue) is responsible for the reflectance (about 60%) of this part of the electromagnetic spectrum. This property proves to be very useful in facilitating the discernment between vegetated and non-vegetated surfaces. As a plant matures, or is exposed to different kinds of stress (drought, insect attacks, etc.), the spectral characteristics of the leaf may change both in the visible and near and mid infrared regions, as being exploited by different vegetation indices. The reflectance in the near infrared is controlled by the cell structure, whereas the response pattern in the mid-infrared is governed by the water

content of the leaf. This behaviour has made the use of the infrared sensors particularly valuable for the observation of the changes of the condition of the plant. Not only the intraspecific differences between different species may be reflected in the spectral response pattern, but also phenological aspects (growth, flowering, senescence, and dormancy) can cause a substantial deviation from the 'normal' spectral behaviour. Such behaviour in the case of *Eucalyptus goniocalyx* is shown in the following graph.

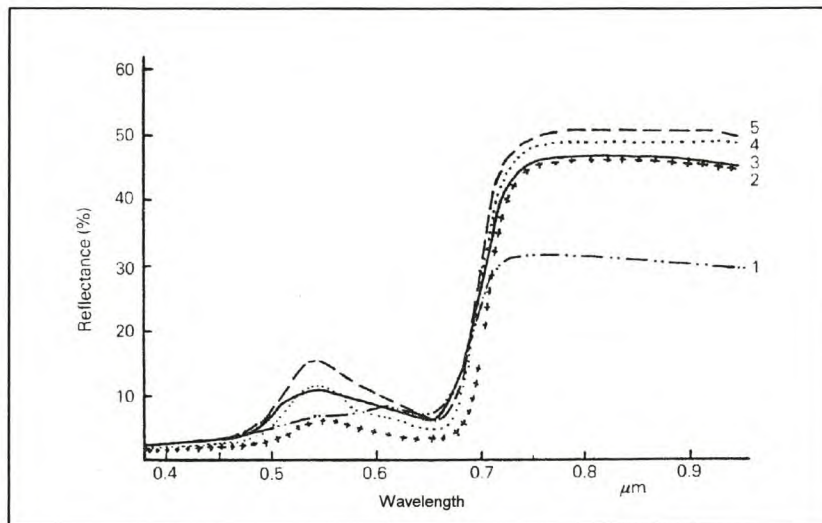


**Figure 4.3** Spectral reflectance of *Eucalyptus goniocalyx*. The curves show the changes of spectral reflectance with the increasing leafage: 1: young orange-red tinted expanding leaf; 2: old full green healthy leaf, which will shortly be shed; 3: mature leaf; 4: mature leaf, slightly younger than 3; 5: recently fully expanded light green leaf (Howard, 1991)

Another relevant aspect to consider is the study of the reflective properties of *vegetation canopies*. Plant surfaces are composed of many separate leaves, differing in size, shape, orientation, and coverage. Thus the many layers of leaves form a combination of reflectance and shadow, with a varying amount of spectral response from the underlying soil. In general it holds to be true that the reflectance of a canopy is lower than values assessed for individual leaves. However, numerous studies have shown that the relative decrease in the near infrared region is much lower than that in the visible, being a result of retransmittance of the near infrared portion of the spectrum. Detailed accounts on the spectral behaviour of vegetation canopies can be found in Hildebrandt (1996), Howard (1991), and Campbell (1996).

The solar flux, and how little energy (between 8-15%) entering from the outer atmosphere actually is available for the detection of spectral response from targets on the ground is shown as Figure 4.4.

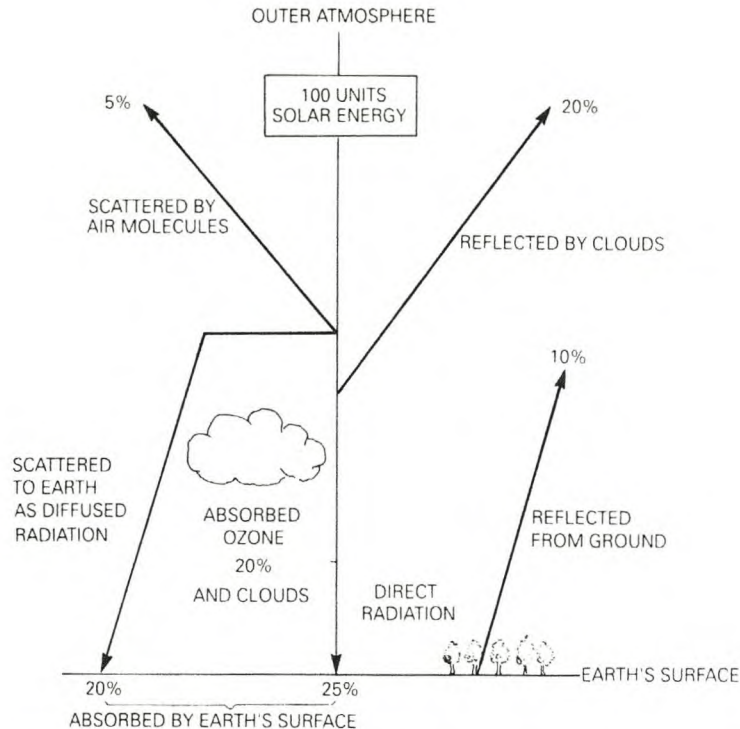


**Figure 4.4** Solar flux. One hundred units of solar energy is assumed to enter the outer atmosphere at a rate of  $2 \text{ cal cm}^{-2} \text{ min}^{-1}$  (Howard, 1991)

These figures help to understand that the detection of the various forms of electromagnetic radiation inevitably reflects a lot of limitations and constraints on the available technologies in terms of spatial, spectral and radiometric resolution.

#### 4.4 Data acquisition and interpretation

The *detection* of electromagnetic radiation can be in the form of photographs (using light-sensitive film), or electronically by generating an electrical signal. Although some substantial improvements on film material have been achieved (e.g. sensitivity, grain size, spectral consistency) in the last few years, electronic sensors offer the advantages of a greater spectral sensitivity, superior calibration, electronic transmittability and providing the information in computer readable format. Electronic sensors commonly consist of either single detectors or an array of detector elements, being generally referred to as *charge coupled detectors* (CCDs). In the

following figure various kinds of image acquisition techniques are presented. The most advanced technology are the so-called *pushbroom* imaging devices (b, and d), featuring superior image geometry, reduced noise factors, and no moving mechanical parts being involved. The more ‘old-fashioned’ techniques are called *whiskbroom* imagers, characterised as mechanical scanners.

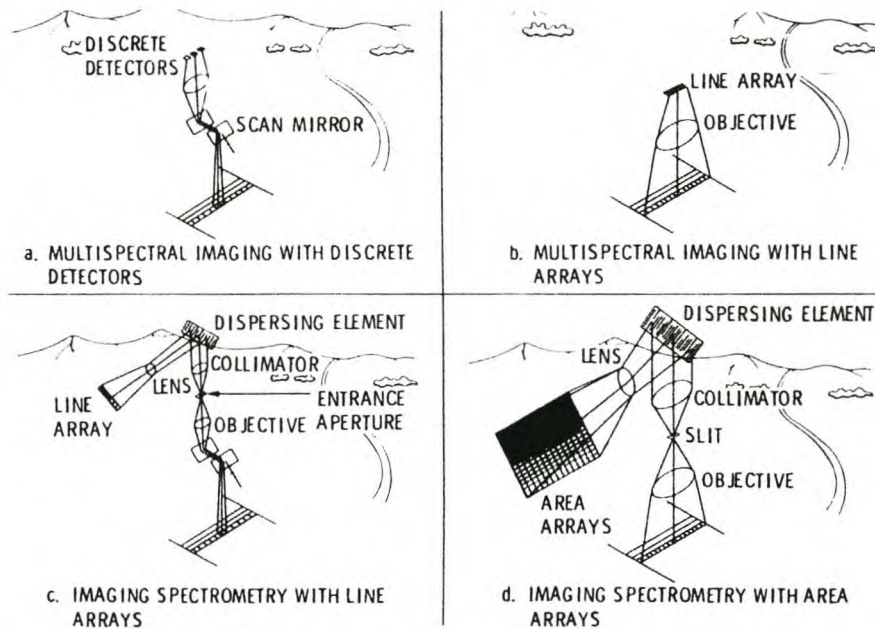


**Figure 4.5** Image acquisition techniques. (a) Whiskbroom imager with discrete detector elements (e.g. Landsat TM), (b) pushbroom imaging system with line detector arrays (e.g. SPOT and IRS-1C/D), (c) whiskbroom imaging spectroscopy with line detector arrays (e.g. AVIRIS), (d) pushbroom imaging spectroscopy with area detector arrays (e.g. AIS) (Dwivedi, 1990)

Some of the new spaceborne imaging systems even have stereo image acquisition capabilities (e.g. on board IRS-1C/D, IKONOS 1, SPOT). Video cameras, as well as microwave (i.e. radar) and laser (e.g. LIDAR) imagers are becoming more and more popular these days.

Film acts as both the detecting and *recording* medium. In contrast, electronic sensor signals are stored on magnetic tapes on board the air-, or spaceborne platform in a digital format, or directly transmitted to the ground receiving station (and subsequently recorded on tape, CD, optical disk, etc.). Yet, these signals may be converted to an image by means of a film recorder (as a so-called ‘hardcopy’), or simply be displayed on a screen (as a ‘softcopy’) for visual interpretation and assessment (Hildebrandt, 1996; Lillesand and Kiefer, 1994).

Photographs and images contain semantic, thematic, and spatial (i.e. measurable) information that can be extracted and rendered. The *visual interpretation* of any kind of imagery (i.e. in an analogue or digital format) is based on the faculty of the human brain to recognise objects and put them in context to each other. In many instances this process is accomplished within a fraction of a second resulting in the creation of useful information. The interpretation operation conventionally considers the following basic characteristics:

- Shape (referring to the general form, configuration, or outline of individual objects).
- Size (as to be considered with respect to the image scale).
- Pattern (as relating to the spatial arrangement of objects).
- Tone (i.e. the brightness or colour of objects).
- Shadows (the shape of shadows affords an impression of the profile view of objects).
- Site (topographic or geographic locations are particularly important aids in the interpretation of vegetation types).
- Association (as being related to the occurrence of features in relation to others; sometimes referred to as 'topology').

The interpretation process can often be facilitated through the use of so-called *interpretation keys* (see Hildebrandt, 1996, Howard 1991; and Lötsch and Haller, 1964, for interpretation keys in forestry). However, *spectral and textural characteristics* of features are not always fully assessed in visual interpretation tasks, because of the brain's limited ability to discern tonal values. In these cases it is preferable to employ *digital* (i.e. computer-assisted) analysis techniques. The image itself (either a digital original or a scanned analogue image) is composed of a two-dimensional array of discrete pixels (i.e. picture elements), with a value for brightness (as measured electronically) being assigned to each element. The output values of the sensor signal are recorded and stored in binary coding scales as for instance in an 8-bit or 10-bit format, representing intensity values from 0 to 255 (i.e. 256 grey levels) and 0 to 1023, respectively. The initial stages of image restoration (i.e. radiometric and geometric correction) and image enhancement (e.g. application of edge and smooth filters, zooming and rotating, Fourier transfer, etc.) are subsequently followed by a classification process, in which the intensity values of the image pixels are allocated

to distinct clusters and then visualised, thus being transformed into information. A host of various classification algorithms (e.g. supervised classification, maximum-likelihood, minimum-distance classifiers, etc.) for a great variety of applications have been designed to date. Nonetheless, since computer programmes are restricted in their ability to evaluate spatial patterns, visual and numerical techniques are complementary in nature (Campbell, 1996; Goldsmith, 1991; Howard, 1991).

## 5. SOME FUNDAMENTALS OF PHOTOGRAMMETRY

Photogrammetry is used to reconstruct or restituate spatial objects from photographs and imagery, and to perform measurements thereof. The procedures involved are based on a wide spectrum of mathematical principles and methods, and since many textbooks have been written on these subjects, this chapter is devoted primarily to a few selected topics in order to impart a better understanding of the possible implications for the analysis of the photographs. Thorough treatments on photogrammetry are given by Hildebrandt (1996), Akça *et al.* (1984), Konecny and Lehmann (1984), Kraus (1993), Lillesand and Kiefer (1994), Moffitt (1959), Slama (1980), Spurr (1960), Thompson (1980), Wolf (1974), Wong (1980) and many others.

### 5.1 Geometric elements of the aerial photograph

Photographs taken from either an air-, or spaceborne platform represent a perspective of the area underneath the craft. A fundamental characteristic of this photograph is that each image point on the (two-dimensional) photograph corresponds to a unique point in the (three-dimensional) object space. In many cases we deal with photographs, which are taken nearly vertically, that means that in the ideal case the camera axis is plumb. The view of the aerial camera is said to be perspective, thus implying that the images of objects on the ground are displaced radially outwards on the photograph. The most relevant properties of such a vertical photograph are shown in Figure 5.1. In this figure, the datum plane has been set at the average terrain elevation. Since terrain points above the datum plane are nearer to the camera, they are displaced radially outwards (from  $A$  to  $a$ ), and points beneath the datum are therefore shifted radially inwards (from  $B$  to  $b$ ) towards the principal point ( $o$ ). Because  $A'$ ,  $B'$  and  $C$  lie at the same elevation, the image line  $a'b'c$  is true to scale in orientation and length. When introducing terrain displacement, not just orientation and length are distorted but also angles as shown in Figure 5.1(b). Thus, the distorted angle  $acb$  will occur on the photograph. Due to the radial nature of terrain displacement, only angles about the origin ( $o$ ) will not be distorted. The points  $o$ ,  $O$  (the so-called ground nadir), and  $O'$  feature zero distortion. Ground co-ordinates for

points at different elevations can then be determined from photo co-ordinates by employing the method of similar triangles (Lillesand and Kiefer, 1994).

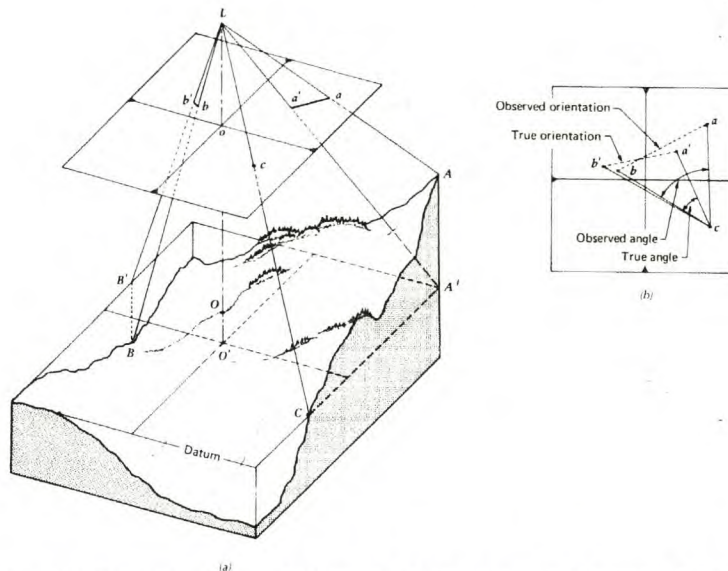


**Figure 5.1** Topographic displacement on a photograph taken over varied terrain: (a) displacement of terrain points; (b) distortion of horizontal angles measured on photograph (Lillesand and Kiefer, 1994)

The property of displacement can even be used to determine heights, though not very accurately, of objects on the ground, such as trees. Unfortunately, these co-ordinates will contain systematic errors from various sources. These errors are:

1. Failure of fiducial axes to intersect at the principal point.
2. Shrinkage or expansion of photographic materials.
3. Lens distortion.
4. Atmospheric refraction distortions.
5. Earth curvature distortions (Hildebrandt, 1996; Akça *et al.*, 1984).

These influencing factors will be addressed in subsequent chapters.

## 5.2 The concept of orientation

As mentioned earlier, stereo photographs and images are subject to various internal and external influences effecting the geometry of the stereomodel. In order to perform measurements and accurately extract features from these photographs/images, the reconstruction of the geometry and its registration to the ground (i.e. co-ordinate system) are indispensable requisites. The construction of a

model of the stereoscopic overlap area of imagery/photography basically comprises a number of processes known by the generic term *orientation*.

The first of these processes, *interior orientation*, includes preparations necessary to re-create the geometry of the projected rays to duplicate the geometry of each photograph/image. The perspective geometry of the camera/imager plays a key role in this process, with the following parameters to be taken into account: (1) the calibrated focal length; (2) the position of the principal point in the image plane; and (3) the distortion characteristics of the lens system. When calibrated cameras are used (e.g. the Zeiss RMK TOP, or KFA 1000), calibration reports of the specific camera are available for each flying mission. In a computer-assisted environment (i.e. analytical plotter as well as softcopy systems), the above-mentioned parameters are used to compute the geometry of the camera, with reference to the location of the fiducial marks (i.e. four or eight marks which are permanently mounted in the camera housing, being visible on the frame of the photograph; their purpose is to define the location of the principal point).

*Relative orientation* is the determination of the relative position and attitude of the photographs/images in a stereoscopic pair with respect to each other. The main purpose of this kind of orientation is to orient the photographs so that each corresponding pair of rays from the images intersects in space. Since relative orientation does not use ground control points, the triangulation solution will not be linked to the ground, so products (e.g. DTMs) being generated from the imagery will not be accurate in an absolute sense. Hence, relative orientation can be considered a prerequisite for performing absolute orientation. A very popular method is to define the location of six tying points (the so-called 'Gruber' points) in the overlap area of the imagery, subsequently calculating their values necessary for rotating and tilting the images. With a perfect relative orientation, y-, and x-parallaxes (the latter one referring to the parallax in flight direction) can be eliminated during this process to obtain a perfect stereoscopic view (Kraus, 1993; Wong, 1980).

After relative orientation is achieved, the stereo model must be scaled, translated and levelled with regard to a ground reference co-ordinate system. This process is referred to as *absolute orientation*. The co-ordinate transformation from ground space

to image space includes the parameters scale ( $\lambda$ ), translation ( $X$ ,  $Y$ , and  $Z$ ), and rotation (about the  $x$ -,  $y$ -, and  $z$ -axes).

The *exterior orientation* (known by other names such as triangulation, image registration, geopositioning, resection, aerial triangulation) of a camera is defined by the geographical position of the exposure centre and the direction of the optical axes. The purpose of exterior orientation is to update the sensor model (i.e. a mathematical formula which models the relationship between ground space and image space) of the photographs (for further information on the various sensor modelling approaches see McGlone, 1996). The geographical position of the exposure centre is defined by its co-ordinates in a three-dimensional rectangular co-ordinate system, and the direction of the optical axis is specified by three rotation angles (either  $\omega$ ,  $\phi$ , and  $\kappa$  or tilt, swing and azimuth). The primary inputs to triangulation are *ground control points* and *tie points* (found in the overlap region of the imagery with ground space location being unknown). The relationship between photographic/image co-ordinates of the image points and the ground co-ordinates of the corresponding object points is used to mathematically transform the image locations into real world locations. The location of points in object space as well as the three rotation axes are shown in Figure 5.2.

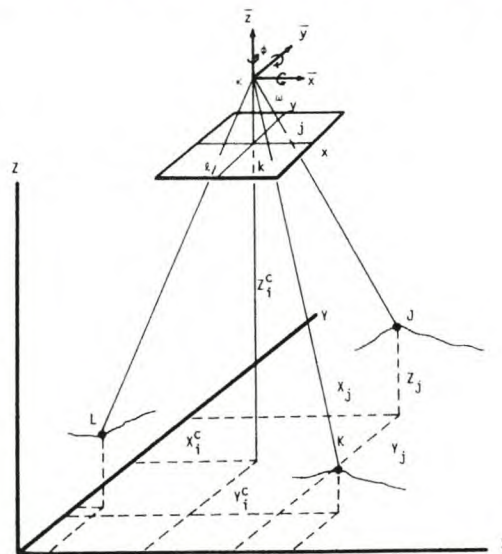


**Figure 5.2** Exterior orientation. The location of any point  $j$  in the object space can be defined by its three co-ordinates  $X_j$ ,  $Y_j$ , and  $Z_j$ . The position of the exposure centre of a photograph can be defined by its co-ordinates  $X_j^c$ ,  $Y_j^c$ , and  $Z_j^c$ . The direction of the optical axis may be described by the rotation angles  $\omega$  ( $\phi$ ), and  $\kappa$  about the  $x$ -,  $y$ -, and  $z$ -axis of the photo co-ordinate system (Wong, 1980)

With absolute orientation it is possible to remove most of the effects of the errors in the relative orientation.

### 5.3 Stereoscopy

Stereoscopy deals with the use of images to create a three-dimensional visual model with characteristics analogous to those of real features using true binocular vision (Laprade, 1980). Some of the primary applications are the estimation of slopes, the accurate measurement of height differences (e.g. to determine tree heights, or to create DTMs), and of course the recognition of the form of a three-dimensional feature. It has been shown that in general it is possible to reconstitute the same geometrical conditions in an image/photograph as it existed the very moment it was taken. Accurate three-dimensional measurements of objects in image space can only be taken by creating such a perfect stereoscopic model. For this purpose the faculty of the human eye-brain-system to perceive the depth and size of objects is exploited. In order to be able to mimic true binocular vision, the requirements concerning the binocular cues of convergence accommodation, retinal disparity, and focusing accommodation have to be met. Although a great number of stereoscopic analogue systems have been developed (e.g. stereoscopes, vectographs, anaglyph and flicker systems), the objective of perfectly true binocular vision is only partially obtained due to design limitations (Kraus, 1993).

In three-dimensional space perception, the most significant characteristic, the angular disparity, is produced by the apparent displacement of the position of an object in relation to a reference point, also referred to as *parallax*. The nature of parallax on overlapping vertical photographs, indicating the principal point as reference point is illustrated in Figure 5.3. Note that the position of the recorded objects ( $A, B$ ) in relation to each principal point ( $o, o'$ ) will vary due to a shift in the point of observation or camera station in the aircraft. Note further that the parallax displacements occur only parallel to the line of flight, which in most cases corresponds to the fiducial X-axis. The parallax of point  $A$  for instance is expressed as

$$p_a = x_a - x'_a$$

Where  $p_a$  is the parallax of point  $A$ ,  $x_a$  is the measured X co-ordinate of image  $a$  on the left photograph of the stereopair, and  $x'_a$  is the X co-ordinate of image  $a'$  on the right photograph.

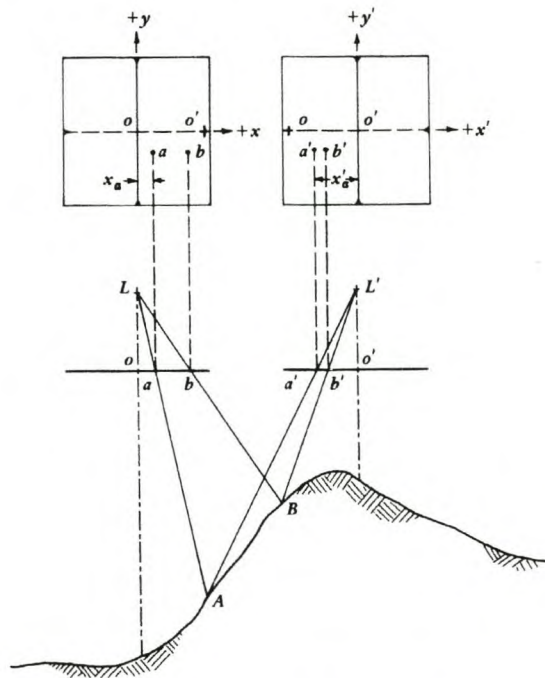


**Figure 5.3** Parallax displacements on overlapping vertical photographs taken over varied terrain (Lillesand and Kiefer, 1994)

The direct measurement of the height of an object (e.g. a tree, a building, etc.) can be achieved by applying the formula

$$h = H (\Delta p) / p + \Delta p$$

where  $p$  is the parallax of a particular point,  $h$  the height of the object, and  $\Delta p$  the parallax difference (in this case:  $ab + a'b'$ ) (Hildebrandt, 1996; Lillesand and Kiefer, 1994). Employing the principle illustrated above, a number of devices have been designed to accurately measure image parallax. The most successful devices (e.g. parallax bar, stereoplotters) are based on the principle of the floating mark, where half marks appear to float at a specific level in the stereomodel when fused together visually.

#### 5.4 Ground control for aerial photography and satellite imagery

For most photogrammetric operations accurate ground reference data are essential. Great care has to be taken in the acquisition of the horizontal and/or vertical positions of identifiable points (i.e. on the photograph/image as well as on the ground itself),

since the collection is expensive and the fidelity of the geometric model of the photograph/image is dependent on the accuracy of the position of the ground control points. Artificial control points depicting various shapes and made from different kinds of material are established on the ground prior to flying (for further information see Combs, 1980, and Hildebrandt, 1996). Often, control points are selected and surveyed after the flying mission to ensure better recognition on the photograph. 'Natural' features, such as road intersections, and corners of buildings are often used in such cases. The positions of these points are traditionally determined by employing maps, terrestrial methods (e.g. theodolite), and aerotriangulation. In order to minimise the cost and effort to obtain the co-ordinates, research has been active in developing and establishing more efficient means such as the employment of GPS (Global Positioning Systems). By means of satellite navigation technology it is possible to achieve sub-meter accuracy in real time. A number of recent studies even suggest that GPS technology has already advanced to such an extent that the acquisition of ground control will become obsolete in the near future. Differential GPS equipment on board of airborne platforms, being linked to the photographic devices and the instrument panel in the cockpit, gather highly accurate positional information for the time of exposure and whenever needed to ensure optimal performance of the flying mission (Ackermann, 1996; Günther and Klemp-Höpfner, 1994; Kilian *et al.*, 1996; Škaloud *et al.*, 1996; Tang *et al.*, 1997; Welch and Remillard, 1996).

### **5.5 Characteristics of satellite photogrammetry**

Remote sensing is characterised by the fact that the nature of the object being imaged is of major importance, whereas in satellite photogrammetry the main focus is geometry. The emphasis in this chapter therefore will be on the photogrammetric issues of imagery acquired from space.

What has been stressed before with regard to the characteristics of aerial photography applies to satellite photogrammetry in many respects. However, there are a few fundamental differences that have to be considered. The most important factors concern:

1. The influence of the atmosphere on the quality of the imagery.

2. The inherent problems related to the geometry of the satellite orbit.
3. The internal geometry of the imaging system (Light, 1980).

The *atmosphere* substantially influences the quantity (e.g. the effects of attenuation) and the quality (e.g. the effects of refraction, and change in spectral composition of the reflected radiation) of the radiation. Looking at satellite imaging systems, it is important to realise that the atmospheric influences are much more eminent, since the solar radiation has to travel twice the whole distance through the atmosphere to reach the detecting device. Therefore, the application of atmospheric models in conjunction with proper ground truthing is crucial for the assessment of features on the ground (Slama, 1980).

Platforms in space orbit the Earth at a minimum altitude of about 200 km, with the result that geometry becomes more complex than for aerial photography. The diagram shown in Figure 5.4 illustrates a satellite's orbit in relation to the Earth's surface.

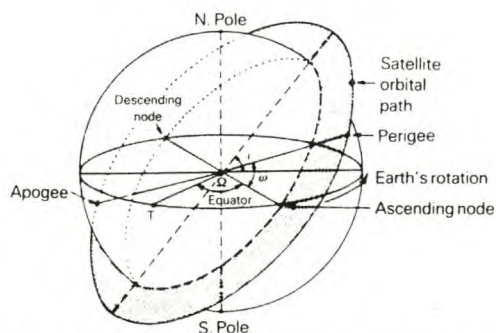


**Figure 5.4** Orientation of the orbit-plane system relative to the inertial co-ordinate system (NRSA, 1995)

Since there is no atmospheric turbulence in space, the operating conditions are relatively stable. However, other factors, such as the laws of gravitation determining the orbit, cause deviations from a perfectly circular geometry (e.g. orbits becoming elliptical, and the introduction of perturbed motions). By employing modern computer technology, the orbital characteristics (ephemeris) can be modelled mathematically with good accuracy. On-board control systems (e.g. stellar cameras, GPS) ensure angular stability for pitch ( $y$ -tilt), roll ( $x$ -tilt) and yaw (swing) to guarantee vertical, or almost vertical geometry of the imager at the time of exposure. Altitudinal control (e.g. by means of laser altimeters) in the nadir line is vital for the preservation of the image scale, and also necessary to control the satellite's velocity

due to geoidal variations resulting from the Earth not being a perfect sphere and the ellipsoidal orbit of the satellite. Another factor influencing the geometry is that the Earth exhibits a rotating motion. Without orbital control, the sub-satellite track would not retrace its track, and furthermore the sub-satellite track would describe a wave-shaped path.

Errors caused by the Earth's curvature can be significant when working at very small scales. With increasing flying altitudes, relief displacements are reduced, but in return the displacement due to the Earth's curvature increases. Consequently, employing a spaceborne sensor with a limited overall field of view, a nearly orthographic projection can be obtained. The resulting image, representing approximately correct planimetric form, is suitable for many mapping applications without a need to perform further geometric corrections. For small-scale imagery the error in elevation due to the curvature can be calculated fairly easily by applying a simple formula based on the characteristics of radial displacement (Light, 1980).

A three-dimensional satellite photogrammetry imaging system designed for mapping must be able to provide three kinds of information, namely content (as referred to cultural and natural features represented on the map), horizontal location (i.e. the reference graticule, datum), and elevation (e.g. spot heights, contour lines, profiles).

*Map content* is mainly determined by scale and photographic resolution. Since map scale is given in many cases, the required resolution has to be calculated. As a rule of thumb the following formula can be used to estimate the minimum resolution at which objects are photographically identifiable:

$$Rg = 5 \times 10^{-5} Sm$$

where

$Rg$  = required ground resolution (in metres)

$Sm$  = map scale number (Light, 1980).

Ground control points generally provide the co-ordinate system for the *horizontal location* of objects. If such control does not exist, orbital tracking data coupled with precise information on the attitude of the satellite, and the time of exposure, can provide an accurate means of determining absolute horizontal location.

*Elevations* are traditionally obtained by means of image parallax, which largely depends on the image scale and the sensor's geometric configuration. In conjunction with these determining factors the so-called *Base to Height (B/H) ratio* is assigned a key role. A *B/H* ratio being much less than 1.0 is considered to significantly degrade the capability of a system to determine elevations from stereoscopic image pairs. Figure 5.5 shows the *B/H* ratio and convergence angle (*A*) both as vital contributing factors towards the reduction of the error (denoted as  $\sigma_h = \frac{H}{B} \cdot \frac{H}{f} \cdot m_x \cdot \sqrt{2}$ ) in measuring relative heights. When using photographs *N* and *N + 1* the error will be much larger; using photographs *N + 1* and *N + 7* considerably reduces the error as a function of a larger *B/H* ratio.

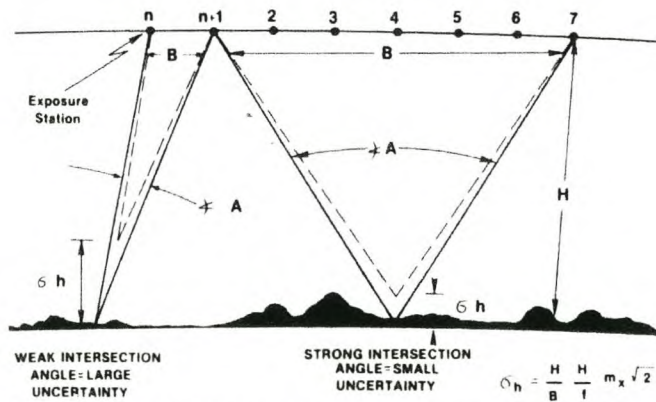


**Figure 5.5** Relative photogrammetric accuracy vs angle of intersection. *H* indicates the flying height above ground, and *f* the focal length; *m<sub>x</sub>* in the formula stands for 'precision of measuring an image point' (Light, 1980)

Another factor deserving special consideration is the geometry of the imaging scanner (see also chapter 7.2). The figure below illustrates the geometry of various imager systems.

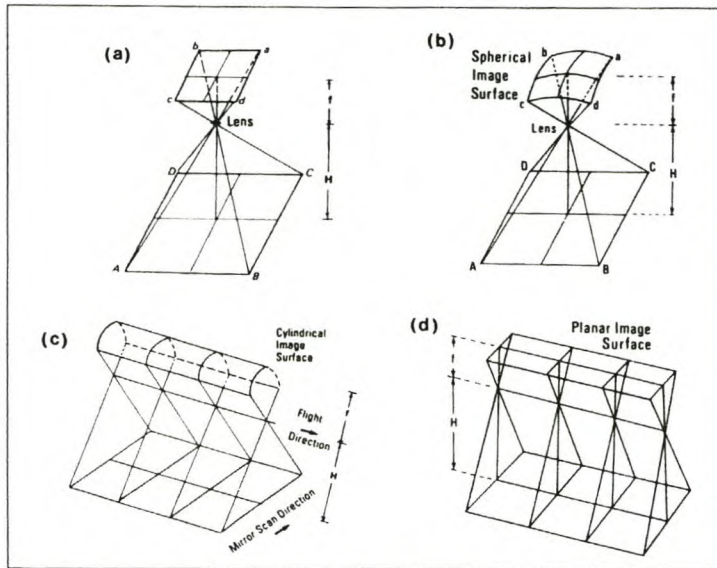


**Figure 5.6** Geometry of various imaging systems. (a) photographic or video camera; (b) video frame scanner; (c) optical-mechanical scanner; (d) pushbroom scanner. A, B, C, and D indicate points on the ground, whereas a, b, c, and d denote corresponding points in image space;  $f$  specifies the focal length of the imaging system, and  $H$  the flying height above ground (Petrie, 1995)

Optical-mechanical scanners and pushbroom scanners produce a single continuous strip image sequentially through the forward motion of the imaging platform. Strictly speaking, each line of the scanner image features its own individual central projection, orientation, and tilt. In contrast, frame-type imagery (as produced by aerial or space cameras) is taken from a single exposure station, therefore producing a single central projection. Consequently different photogrammetric procedures have to be applied for scanner imagery to those which are employed for frame imagery.

## **6. REMOTE SENSING IN FORESTRY**

Although many people are aware of the changes in our natural environment and the increasing pressure of mankind on the limited resources of our planet, only those professionally involved in forestry issues seem to realise the rapid deterioration of the world's forested areas. Recent estimates reveal that about 200 million people live in the forests of the world, and more than 2000 million people depend on wood as a source for domestic energy (Howard, 1991). According to the latest UN<sup>9</sup> reports the world's population increases by 27 people every ten seconds, the experts dire predictions are 11 billion people by the year 2050 (Swerdlow, 1998). The strain being imposed by the burgeoning world population on the forestry sector is indisputable. The impacts we are facing already result in deforestation, soil erosion, damage caused by pollution, declining soil fertility, desertification, and the like. Since these effects do not seem likely to decrease in the foreseeable future, decisions to be taken today to alleviate this burden must be based on sufficient background information. In this scenario, remote sensing has the role of an emerging discipline, providing essential tools of trade to many people from different disciplines being involved in the decision making process.

In the forestry sector, as in others, aerial photographs are used directly as a substitute for planimetric and topographic maps; even information on the forest stock can be derived with ease and high accuracy. With the advent of satellite remote sensing in association with the rapid developments in digital image processing, new, exciting applications in forestry have materialised.

### **6.1 The aerial photograph in forestry**

Forestry is mainly concerned with the management of forests for wood, but in addition, the forested landscape's dedication extends to the supply of forage, water, wildlife, and recreation. Because the principal raw product from forests is wood (timber), forestry is especially occupied with timber management, maintenance and improvement of existing forest stands and fire control. Forests of one type or another cover nearly a third of the world's land area, amounting to about 4 321 million ha

---

<sup>9</sup> United Nations

(FAO, 1985; Mather, 1992). They are distributed unevenly and their resource value varies widely. For the last couple of decades air photo interpretation has proven to provide a feasible means of monitoring many of the world's forest conditions.

Since the first attempts of aerial photo interpretation for forestry purposes in 1887, the extraction of information on forest stocks has undergone many fundamental changes in terms of improvement of accuracy, efficiency, and quality. Reflecting this development, the following sections will briefly deal with the application of aerial photograph interpretation to tree species identification, the measurement of different tree and stand parameters, timber cruising, and the assessment of disease and insect infestations as well as abiotic damages.

#### 6.1.1 Reconnaissance

The aerial photograph is particularly useful for the reconnaissance of the large, almost inaccessible virgin forests in tropical countries. A problem of major importance in tropical forests is the location of merchantable timber. Here the photo-interpreter meets difficulties, as it is seldom possible to identify individual species. It may be possible to identify certain species, which are found in rich as well as poor forest types. Therefore information and intimate knowledge about local or regional conditions and forest type characteristics is of great importance. Topographic features may also be very helpful. A number of studies suggest that the productivity of forest-types on slopes will usually be different from those found in the valleys (Hildebrandt, 1996; Lillesand and Kiefer, 1994). Field observations play an important role in the identification and classification process, where the prevailing forest types are identified and correlated with relief or soil features. These field observations are then compared with observations from the photographs, and stereograms are prepared for future reference (Lötsch and Haller, 1964).

#### 6.1.2 Forest inventory

The main object of forest inventory is the assessment of the volume and the increment of the growing stock and yield within certain forest areas. Consequently the information related to areas is of importance. The information related to single trees

is as a rule summed up to obtain mean values for forest areas. Many single-tree-related parameters can be transformed to information related to areas, and even "invisible" or concealed parameters can be derived from the visible ones because of their correlation. Table 6.1 demonstrates a selection of the most important dendrometrical parameters that can be extracted from aerial photos; it also shows some of the accuracies that can be achieved.

**Table 6.1** Overview of inventory parameters that can be extracted from aerial photographs (Kätsch, 1991)

Dendrometrical parameters	on aerial photograph			measurable by means of	
	identifiable	can be estimated	countable	simple technology	digital technology
<b>Tree height</b>	++	+ (2-3 m)		++ (1-1.5 m)	(0.5 m)
<b>No. of crowns</b>	++		++	+	
<b>Crown parameters:</b>					
<b>Crown width</b>	+			+	(10 %)
<b>Canopy area</b>	++			+	(5 %)
<b>Surface area</b>	+			+	(4 %)
<b>Crown length</b>	+			+	(3 %)
<b>Crown volume</b>				+	(5 %)
<b>Crown density</b>	++	+ (0.2)		++ (0.1)	(0.1)
<b>Age:</b>					
<b>Natural age class</b>		++ (6 classes)			
<b>Age classes</b>		+ (40 yrs.)			
<b>Growing space profile</b>					++

+ = good

++ = very good

Since remotely sensed imagery provides a synoptic view of our planet's multiform face, it is perfectly suited to serve as a base for the generation of thematic maps. Depending on the scale and the quality of the data, features such as road networks, drainage lines, artificial and natural boundaries, topography and the like can be extracted with ease and high accuracy. Almost all forest maps, and the resulting management plans, render information obtained from some kind of remote sensing device. By employing state-of-the-art technology, new maps and updates can be generated efficiently and at low cost. Even a simple, uncorrected aerial photograph can serve foresters in the field as a very valuable means for orientation and provides feedback on the effects of actions taken.

For the last couple of decades a plethora of inventory methods based on remote sensing techniques have been developed and applied successfully. Determined

mainly by the scale and the purpose of the inventory, remote sensing data can either be utilised as a source for ancillary information or even represent a stand-alone source. The overview in Figure 6.1 gives account of some of the most relevant area based inventory schemes, whereas methods 1 and 2 are more suited for inventories on a local and regional scale, methods 3 and 4 for large scale such as provinces and countries, and 5 for monitoring and inventory tasks referring to continents or even the entire globe.

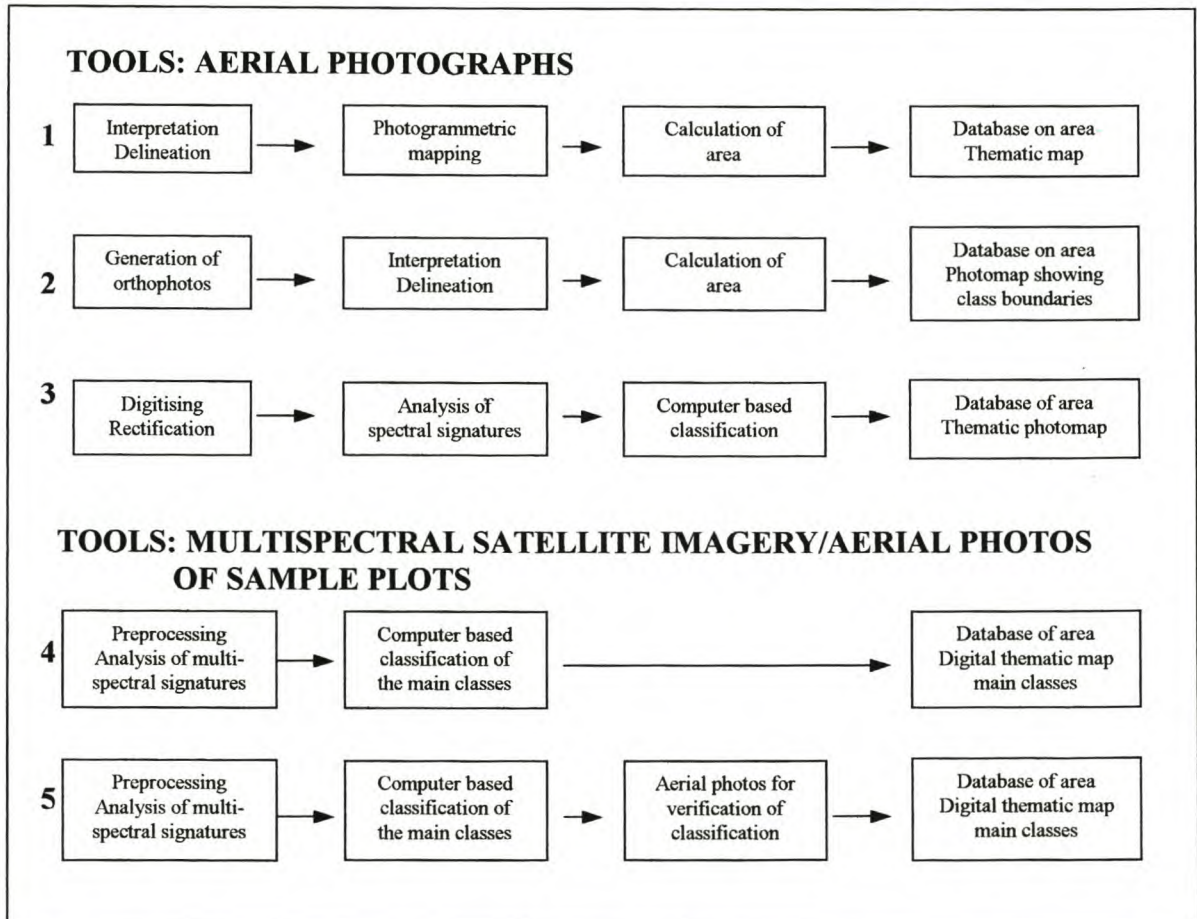


**Figure 6.1** Forest inventory methods employing aerial photography and multispectral satellite imagery (Hildebrand, 1996)

Forest inventories on a small scale (e.g. countrywide) are destined to contribute to forest policy and statistics, and therefore focus on the acquisition of information concerning timber volume, tree species, increment of the stock, structure of ownership, spread of diseases, etc. Inventories on a regional or even local level require much more detailed and accurate information, with the consequence of being more expensive and time-consuming than the previous scheme.

A great number of concepts such as sampling techniques, stratification, etc. have been devised to increase the efficiency and accuracy of the gathering of data. These are exhaustively dealt with in textbooks by Akça *et al.* (1984), Hildebrandt (1996), and Howard (1991) (see also Appendix 13). In the following paragraphs only a few inventory designs will be presented when applicable.

#### 6.1.2.1 Information on area from aerial photographs

The most important information which can be obtained from aerial photographs for purposes of forest inventory are the locations of area categories, such as forest types, cutting classes, age classes, species classes, etc. Areas can only be estimated accurately from aerial photographs provided that the terrain is flat, or if further information on terrain (e.g. Digital Terrain Model (DTM), Digital Elevation Model (DEM)) is provided. The photo-scale can be calculated by measuring the distance between two corresponding points on a photograph and on an accurate map.

Photographs are unsuitable for direct planimetric area determinations if the differences of ground elevations in relation to datum plane exceed three percent of the flying height. Area computations must be adjusted for scale differences in hilly countries, otherwise hill top areas will be overestimated and valley bottoms underestimated. Various instruments are in use to measure areas: polar planimeter, photoelectric planimeter, transacts, grids, glass scales, electronic co-ordinate digitizer, grids (e.g. dot grids), analytical and digital photogrammetric stereoplotters. Sophisticated devices like the analytical plotter, or digital photogrammetry workstations take these displacements into account by creating highly accurate stereo models in image space. The position of every single feature as well as the required areas are computed automatically. With these high precision instruments it is fairly easy to generate DTMs which can be superimposed on the aerial photographs and therefore serve as a basis for the creation of orthophotos. These photos being true in area can then be imported into GIS and digital image processing software packages for further analysis.

### 6.1.2.2 Identification of tree species

The aerial photography interpretation process for the identification of tree species is generally more complex than for agricultural crop identification, since a given area of forestland is often occupied by a complex mixture of many tree species. The identification of tree species plays an important role in many forest inventories because of the different utilisation value of the various species and because of the various specific requirements with respect to climate, soil, plant association as well as silvicultural treatment. Foresters may also be interested in the species composition of the forest understory, which is often blocked from view on aerial photos by the crowns of the large trees in the area.

The recognition of tree species serves a dual purpose in forest inventory: (i) the subdivision of an assessment area into different strata such as forest types, and (ii) the allocation of estimated standing volumes, or factors which contribute to the volume such as height, crown diameter and number of trees, to tree species or groups of tree species. The main factors for an accurate identification as well as interpretation of tree species are considered the *spatial characteristics* of the object (tree), its *spectral signature*, and an intimate knowledge about the preferences concerning soil and climate. Genetic variations, differences in age, varying site and growing conditions, as well as particular effects of damages and diseases cause a natural variability of the crown features and the spectral reflection characteristics. On the other hand there are many similarities between the different tree species. As a minimum requirement for a positive identification of a tree specie a 90% probability of a correct interpretation is widely accepted (Hildebrandt, 1996).

Tree species can be identified on aerial photographs through the process of elimination. The following eight pictorial elements are used within the identification process (Lötsch and Haller, 1964; Hildebrandt, 1996):

1. shape,
2. size,
3. tone (colour),
4. texture (as a result of the coarseness of the crown or canopy),
5. shadow (providing a profile image of trees),

6. pattern (repetition),
7. location (position, site), association.

The accurate interpretation of tree species and other features on aerial photographs requires very special skills, like competence and knowledge, the faculty of association of ideas and to a certain extent even imagination. A great many studies have shown that in a number of cases visual interpretation is often superior to the digital image processing and interpretation (Howard, 1991; Rosenholm, 1993).

Under specific circumstances, species identification can be an art more than a science. Intensive field training is indispensable to familiarise the interpreter with the local conditions. A local *interpretation key* for species identification can be produced in the course of such training. All interpretation keys unavoidably are generalisations, because they cannot describe the whole variety of variations of the different features. In the end it will be the interpreter's final, subjective decision. In essence the following additional factors have to be taken into account:

- the seasonal phenology of the vegetation,
- the different site conditions,
- the genetic variation,
- the knowledge about the requirements of the different species, and
- the information about the influences on the texture, time and tone, as well as on the brightness of the photograph at exposure (Hildebrandt, 1996).

In the recent history several methods for the semi-automated or fully automatic identification of tree species have been devised (Hänel *et al.*, 1987; Meyer *et al.* 1996). So for instance, a study carried out by Meyer *et al.* (1996) yielded an accuracy of 80% when looking at the classification of mixed forest areas in Switzerland employing CIR photography.

### 6.1.2.3 The measurement of tree height and stand height

Manifold ways of obtaining the desired tree/stand height exist:

- By measuring the heights of single trees (as whole population or just as samples) in order to gain mean or dominant height; various weighting factors can be applied (Hildebrandt, 1996; Nielsen, 1971; Van Laar, 1963 and 1964).
- By generating vertical stand profiles; Hegershoff contrived this method to determine the growing space, and subsequently the volume of the stock. A detailed description is to be found in Akça (1983), Hegershoff (1933 and 1939) and Van Laar and Akça (1997).
- By establishing a correlation between stand height and the (multi-)spectral reflectance values of the stock (Hildebrandt, 1996).
- By analysing Digital Surface Models (Carson *et al.*, 1996; Carson *et al.*, 1997).

The presented schemes yield more or less the same accuracies, as mentioned above, yet at different degrees of efficiency.

The height of trees plays an important role in the estimation of volumes in the stratification and in the classification of sites.

There are four methods to determine tree heights in aerial photography:

1. the measurement of the length of the tree shadows,
2. the measurement of parallax difference on stereoscopic pairs of aerial photographs (in an analogue or digital environment),
3. the measurement of the topographic displacement, and
4. the ocular estimation of the height.

### **Shadow method**

The basic formula for the determination of the tree height is as follows:

$$h = l \frac{1}{RF} \tan \alpha$$

where  $l$  = the measured length of shadow on the photograph;

$RF$  = the representative fraction (scale);

$\alpha$  = the angle of the elevation of the sun;

$h$  = tree height.

The time of exposure and the approximate geographical position of the locality must be known for the calculation of the inclination of the sun (see also Van Laar, 1963, 1964). The shadow method has certain limitations. For example, shadow length can

only be measured accurately along the edges of the stand, and slopes, which shorten or lengthen the shadows, are an additional source of bias (Hildebrandt, 1996; Lötsch and Haller, 1964). Because of inherent disadvantages, this approach has not gained wide acceptance.

### **Parallax differences on stereoscopic pairs**

As has been described in previous sections (5.1, 5.3), photogrammetric height measurements are based on the principle of the measurement of the difference between the horizontal parallaxes for the top and bottom point of the object ( $\Delta px = px_1 - px_2$ ). The parallax can either be determined by fairly simple means (e.g. parallax bar, parallax wedge), or more accurately in a sophisticated analogue, analytical or digital environment (analytical plotter, softplotter).

The formula for the calculation of the height of an object (e.g. tree) is:

$$h = \frac{h_0 \times \Delta px}{px_0 + \Delta px}$$

where  $h$  = height of the object

$h_0$  = the altitude of the platform above ground (base of the object)

$px_0$  = the absolute x-parallax

$\Delta px$  = the parallax difference

Aerial photos taken at scales from 1:5 000 to 1:15 000 can yield measurement accuracies of about 1.5m employing basic instruments, whereas on a stereoplotter, it is possible to obtain heights being close to the values of terrestrial assessments, i.e. an error of 3-5% (Akça, 1983; Akça *et al.*, 1984; Hildebrandt, 1996).

### **Topographic displacement**

The topographic displacement of the top of the tree in respect to the base is

$$d = \frac{r \times h}{H}$$

where  $d$  = topographic displacement

$r$  = distance from the top of the tree to the principal point

$h$  = tree height

$H$  = flying height

After measuring the parameters  $d$  and  $r$ , the tree height can be calculated when flying height is given. Unfortunately the displacement cannot be determined accurately,

since it is limited to perpendicular image geometry, flat terrain, and a minimum of displacement (i.e. objects in the centre of the image cannot be measured). Consequently the standard error of estimate is high (Akça *et al.*, 1984; Lötsch and Haller, 1964).

### **Ocular estimation**

The height class of a tree (such as 2m -, 3m -, etc. classes) is estimated by comparing the height with the height of one or more trees which have been measured in the neighbourhood. Ocular estimation is often used in cases where the forest floor is obscured and it is not possible to measure a tree height accurately. This method is the least accurate of all the methods presented. However, an experienced interpreter is able to estimate tree heights fairly accurately.

The different structures and shapes of the tree crowns, the seasonal phenology concerning foliage, the visibility of the forest floor (undergrowth, floor vegetation) and wind sway result in specific conditions for the determination of height measurements. For instance the extremely small terminal bud of many coniferous trees can't be accurately identified using the floating mark of the measurement instrument. In the cases of flat-topped or wide-spreading crowns it is very difficult for the interpreter to define the top of the tree. The most serious measurement problems occur in connection with the measurement of the base of the tree, which is usually concealed by the tree crown. The measurement therefore has to take place on a visible part of the forest floor. Sometimes the entire area of a stand is covered with a thick layer of grass, moss, fern or some other weed. In these cases it is very useful to get some information about those local conditions.

For inventory purposes the appraisal of average *stand heights* is of even greater importance than the determination of the height of a single tree.

According to Van Laar and Akça (1997) the stand height is required:

- To determine the site index of a stand.
- To calculate the stand volume.
- To predict the future growth from stand characteristics.

- To present a target variable in provenance, progeny and species trials, as well as silvicultural experiments.

In practice only a fraction of all visible trees, for instance the dominant and co-dominant ones, is measured to obtain the mean. However, studies have shown that with respect to average heights accuracies of 96-97% can be achieved with analytical plotters. The photogrammetrically acquired heights seem to correspond very well to the actual mean heights (with an underestimation of about 3%), contrary to the widespread belief of these being equivalent to the dominant height (Akça, 1983; Akça *et al.*, 1984).

#### 6.1.2.4 Tree counts

The number of trees counted per unit area on aerial photographs can be used for the estimation of timber volume. A great number of studies have shown that the actual timber volume of the understory contributes very little to the total timber volume of the stand (about <3% in Middle European forests). Consequently there is even a much higher correlation between the volume of the trees being visible on the photograph and the total volume than in regard to the real number of trees in the stand (Hildebrandt, 1996). Correlation coefficients of better than 0.8 have been documented, yielding volume estimates with an error of  $\leq 15\%$  (Kätsch, 1991).

Trees are usually counted fully, by means of a sampling technique (e.g. dot grid), or using a digital pattern recognition tool. In many cases the number of trees is underestimated, because the crowns of small trees are not resolved. Therefore only the dominant and co-dominant trees are being represented in the count. The precision of the estimate might also be affected by the thinning regime. In heavily thinned stands in which the small trees have been removed, the recovery will be greater than in unthinned stands.

Depending on the structure of the forest, tree counts can differ up to 35% from the actual number of trees. Accurate tree counts are almost impossible with respect to naturally reproduced young stands, afforested areas with weed dominating, as well as very dense young stands, thick bush forests, many types of the rainforests, mangrove and bamboo forests (Howard, 1991; Lötsch and Haller, 1964).

#### 6.1.2.5 The measurement of the crown parameters

In addition to the measurement of tree heights, the determination of parameters such as crown diameter and crown closure makes a substantial contribution to the proper estimation of timber volume. There is no shortage of evidence that many of these parameters are closely correlated to each other (e.g. diameter breast height (dbh) and crown diameter), and thus can be used as auxiliary variables when no direct measurement of the target variable (e.g. dbh) is possible (Kätsch, 1991; Shiver and Borders, 1996; Van Laar and Akça, 1997).

The determination of all crown parameters is subject to a number of limitations. Firstly, the quality of the image is of major importance. Secondly, rather banally, only the visible trees can be measured: only such trees belonging to the upper canopy (i.e. Kraft's classes 1 and 2) can be seen; it is possible that parts of a crown are hidden by neighbouring trees or are invisible for other reasons. However, under optimal conditions the difference between the features on the aerial photograph and the terrestrially gathered information can be considered rather insignificant. It can be foreseen that with the advent of high-resolution satellite imagery and its superior image geometry, a few of these problems will cease to exist.

In general the task of measuring *crown diameters* is no different from performing other distance measurements on photos. For instance micrometer wedges and dot wedges are used for this purpose. The micrometer wedge consists of two calibrated converging lines, which are superimposed on the tree crown. The dot or circle gauge consists of a row of dots or circles of different sizes. The gauge is shifted close to the tree crown until that circle, which corresponds closest to the area of the crown, is adjacent to the crown. The measured values are in terms of instrument scale units at photo scale. These values must then be converted to crown diameter in meters or feet. Results with an error of about 10% can be achieved.

The proportion of the ground area covered by tree crowns is a suitable measure of *stand density*. It is therefore an essential guide in estimation the volume from aerial photographs. It seems logical to include in crown closure estimates only those trees that are believed to contribute to the volume. In fact, most of the stand aerial volume

tables prescribe that only the dominant and co-dominant trees are included in this characteristic. In closed even-aged stands (e.g. plantations) all trees with visible crowns contribute to the volume. In uneven-aged stands it is much more difficult to decide which trees should be included. A good solution is to fix a minimum height below which trees are not regarded as belonging to the crown cover (Lötsch and Haller, 1964).

In many cases the estimation of the *crown closure* percentage from aerial photographs is much more accurate than the one being performed during a cruise on the ground. An objective check of aerial photograph measurements of crown closure by terrestrial measurements is extremely difficult. The measurement and mapping of the irregular crown shapes is far too laborious and will remain restricted to scientific work (Koukoulas and Blackburn, 1997).

A number of influences effect a bias in crown closure estimates. Shadows as well as the displacement of the crowns are possible sources of bias.

The crown closure/width can be determined in eight different ways:

1. by dot sampling techniques,
2. by crown density scales,
3. by crown wedges,
4. by crown closure template,
5. by particle site analysator,
6. by airphoto counting-wedge,
7. by ocular estimation, and
8. by computer-based approach (digital automatic crown dissection, wavelets).

The *dot sampling* technique utilises a transparent overlay with a mesh of small and evenly distributed dots. The relation of number of dots, which fall on dominant trees, to the total number of dots within the stand gives the crown closure in percent. Accuracies with an error of below 10% are reported (Kätsch, 1991). *Crown density scales* have been widely used in the USA and Canada for many decades because of its simple and practical design. The stand-density can be determined by comparing the photograph with a scale, representing densities ranging from 5 to 95%. The U.S. Forest Service has used *crown wedges* for many years. Two diverging lines being printed on a transparency are superimposed on the photograph. The wedge has to be shifted so that the tree crown fits perfectly between the two lines. The reading of the

crown width has then to be multiplied by the scale of the photograph. A reading accuracy of 0.001 inches has been reported by Lötsch and Haller (1964). The *crown closure template* was designed by the ITC<sup>10</sup>, Enschede. This estimation aid consists of circles of different sizes, of which the areas of the corresponding sectors represent fractions of areas of known size. The *particle size analyser* is an opto-electronic device equipped with an adjustable aperture and was originally designed for the measurement of small particles in emulsions, medical (clinical) dissects, and for microscopic sections of minerals. The *airphoto counting-wedge* is based on the principle of the Bitterlich method, which is described exhaustively by Hildebrandt (1996).

The *ocular estimation* of the crown closure on the ground usually gives smaller values than the estimation on aerial photographs. The observer on the ground tends to overrate the small spaces between the crowns which are a normal feature even of fully stocked stands, while these small openings are not visible on the aerial photograph.

In a digital, *computer-based* environment, crown diameters can be measured with ease using the measuring tool of a GIS-, digital image processing-, or a digital photogrammetry software package. A rather new development is the digital automatic crown detector. This computer technology analyses the grey-density matrix of scanned aerial photographs. By means of digital image processing software (thresholding) it is possible to detect and delineate tree crowns automatically (Hänel *et al.*, 1987).

The whole theory about wavelets has been in fashion with the community of physicists for a few years now. A great number of successful applications has evolved around this new, fascinating concept. It is based on the fact that it is possible to explain the characteristics of a signal by breaking it up into a combination of sine and cosine waves. A transformation function is then used to convert an image (i.e. signal) from the spatial domain into a frequency domain. The Fourier transforms are typically used for the removal of image noise (e.g. striping, spots), or vibration by identifying periodicities. This technique can also be used as another form of pattern/feature recognition. An encouraging application in forestry employing *Fourier*

---

<sup>10</sup> International Training Centre

(i.e. a special case of wavelet theory) analysis has been described by Krummheuer (1998). The diameter of beech crowns could be extracted and determined accurately by analysing a specific periodic structure of the grey values of CIR aerial photography. A slightly different approach of extracting features is to make use of the physical properties of light. Based on an analogue technology, the structure of electromagnetic radiation is analysed employing the *Fourier* technique. According to its authors, this recent, revolutionary development is deemed far more efficient than the digital approach (Bains and Mullins, 1998).

In general, all crown parameters can be measured with much greater ease and accuracy within a more sophisticated, digital environment. This in particular concerns the assessment of the circumference, the area and the length (volume) of the tree crown. The latter represents an important factor for the determination of increment. Numerous studies suggest a strong correlation between the crown surface area and the basal area increment. Furthermore the same seems to be true for the relationship between crown diameter (width) and tree volume (Akça *et al.*, 1984; Kätsch, 1991). The relationship between crown width and dbh are dependent on the tree species, the site quality, the tree age, and the stand density (Hildebrandt, 1996).

#### 6.1.2.6 Tree and stand volume

The timber volume of single trees cannot be determined from aerial photography as such, but can be derived from parameters that can be either measured or estimated. The accuracy of the estimation of the timber volume is largely determined by the scale of the photo, the accuracy of the parameters acquired from the image, and of course by their relationship with the volume (Hildebrandt, 1996; Lötsch and Haller, 1964; Sayn-Wittgenstein and Aldred, 1967).

The most popular methods in obtaining tree and stand volume in this context are:

1. the generation of *stereograms*; interpretation keys, containing information on grey scale, texture, crown density, etc., of typical stands are used to visually compare the features with those of unknown stands to get an estimate on volume; however, sampling of terrestrial data is essential;

2. the creation of *aerial photo volume tables*; these exploit the relationship between photogrammetric parameters (e.g. tree height, crown width) and the volume for single trees;
3. *aerial photo stand volume tables*; these are similar to tables, but use the mean height of the stand as an entry (Hildebrandt, 1996);
4. *common volume tables*; the photogrammetrically obtained tree height and the crown density are converted and used as entries;
5. *vertical stand profiles*; the calculated growing space of trees is applied to determine stand volume (Hugershoff, 1939);
6. *regression estimators*; this very promising and successful methodology is based on the implementation of regression models, where auxiliary variables (e.g. tree height, crown diameter) are used to estimate the subject variable (e.g. dbh); achievable standard errors range from  $\pm 10-15\%$  for single stands to a magnitude of  $\pm 1-5\%$  for huge forested areas (Akça, 1983; Howard, 1991; Kättsch, 1991; Wolff, 1992).

In terrestrial inventories the volume of the growing stock of a forest area is obtained by measuring suitable variables on single trees, such as dbh, basal area and tree height. The tree volume can be calculated in many different ways then, e.g. using the simple formula:

$$V = h \times BA \times f$$

where

$V$  = volume of tree

$h$  = tree height

$BA$  = basal area

$f$  = form factor.

A similar procedure can be adopted on the aerial photograph. The tree height can be measured on the aerial photograph. The measurement of the crown diameter replaces the measurement of the invisible diameter at breast height (dbh), since in many instances there is a very close correlation between these two parameters (Hildebrandt, 1996; Kättsch, 1991). The larger the amount of foliage, the more can the tree be expected to assimilate, and the more will its timber volume increase in time. For the determination of the tree volume, the dbh can be derived by means of regression of the crown diameters, or the crown diameter gets directly correlated to the volume of

the tree (in either case in relation to the tree height). In many instances the correlation coefficients are between 0.5 and 0.8. The relationship between dbh and crown diameter (denoted as D in the formulae below) is presented in the following examples for commercial tree species in Central Europe (Hildebrandt 1996):

Spruce           $dbh = -33.6 + 26.6 D - 2.5 D^2$

Fir                 $dbh = -5.2 + 6.8 D$

Pine              $dbh = -3.5 + 8.1 D + 0.31 D^2$

Beech             $dbh = -6.4 + 8.7D - 0.4 D^2$ .

The volume of single trees is less accurately estimated from photographs than from terrestrial measurement. According to Lötsch and Haller (1964) the photo-volume regressions have standard deviations which are up to four times larger than those of terrestrial volume regressions. On the other hand, investigations carried out by Hildebrandt (1996) have shown that the error of estimation ranges from about  $\pm 8-12\%$ , average (Central European) conditions assumed. The error is thus quite similar to terrestrial sampling techniques or estimations employing the Bitterlich method.

#### 6.1.2.7 The estimation of factors such as site, age, and increment

Generally, site quality, diameter increment, age, timber quality, etc. cannot be interpreted on aerial photographs with sufficient accuracy for purposes of forest inventory. Nevertheless the correlation between landform, site, soil and forest type is often close and has been used for preliminary stratification and for purposes of land use planning (Lötsch and Haller, 1964). Sometimes the soil formation or even the series may be identified by means of certain characteristic pictorial features, especially in connection with the information that can be extracted from a DTM.

Close relationships between the crown diameter, the amount of foliage, and the increment (concerning height as well as diameter) have been reported by Akça *et al.* (1993), Hildebrandt (1996), and many more. Stem form and cull cannot be measured directly on aerial photographs. This is a serious disadvantage, especially in the tropics. Usually the information from aerial photographs has to be combined with ground information to attain useful results.

The age of a specific stand can be estimated by means of a regression equation with photogrammetrically determined stand height and crown width as predictors. However, because of the intrinsic imponderables, a stand is usually assigned to either 20-year age classes or natural development stages.

#### 6.1.2.8 The inventory concepts

In a great number of cases too little or uncritical attention is paid and insufficient time devoted to the selection of efficient and suitable design concepts, and following the beaten track does not necessarily result in satisfactory and correct outcomes. A host of textbooks and scientific papers have been published on this subject in the last few decades (see for instance Akça *et al.*, 1984; Akça *et al.*, 1993; Avery and Burkhart, 1988; Cochran, 1977; Hildebrandt, 1996; Holopainen and Lukkarinen, 1994; Howard, 1991; Kätsch, 1991; Kramer and Akça, 1996; Lötsch and Haller, 1964; Shiver and Borders, 1996; Van Laar and Akça, 1997), and therefore only the more promising inventory schemes are presented in the following section (see also Appendix 13 for more information).

Traditionally the initial phase of an inventory consists in the classification and delineation of the entire forest area (e.g. different forest types, discrimination of tree species, etc.) as well as the ground control thereof (“ground truthing”). The next step is to decide about the sampling design (depending on the size and shape of the area), such as stratification (see also Holopainen and Wang, 1998), partial delineation, transect method, randomised or systematic sampling, etc. It has become quite customary to use transparencies with different sampling designs imprinted as overlays for the aerial photographs, some of the designs even take the terrain displacement (scale variation) into account. In many instances systematic sampling techniques are being given preference because of the less cumbersome application in the field. Nonetheless, one has to take into account that this procedure is implemented at the expense of statistical correctness and fidelity. With the advent of sophisticated and efficient positioning systems (e.g. *Differential Global Positioning System (DGPS)*) for orientation on the ground this shortcoming can be overcome (Næsset, 1999).

The most popular and successful inventory designs for the last few decades have been the concepts of *multistage sampling* and *multiphase sampling*. In multistage sampling, the sampling units are selected in hierarchical order, in which the population is partitioned into primary units, which in turn are subdivided into secondary, tertiary units, etc. An important characteristic of this method is that the selection of the sampling units for each stage is performed in a random manner. A different, highly successful inventory concept is called two- or multiphase sampling, employing regression estimators. The first approach is to measure all independent variables, such as tree height, crown diameter, and crown percentage, of all the sample plots on the aerial photograph. Subsequently, a much smaller sub-sample of the sample plots is taken for the terrestrial measurement of the timber volume (as the dependant variable). Finally, the stand volume is computed by multiple regression analysis, using the independent and dependant variables to establish a correlation between the terrestrially gathered parameters and the ones being extracted from the photography. Correlation coefficients of between 0.766 and 0.964 have been reported by Hildebrandt (1996) in conjunction with European pilot studies. This sampling method is widely used for regional and small-scale timber volume estimation because of its efficiency and accuracy. Multiphase (double) sampling using regression estimators can only be economically justified if the following ratio holds:

$$\frac{\text{cost per terrestrial sample } (c_t)}{\text{cost per sample on aerial photograph } (c_i)} \geq \frac{(1 + \sqrt{1 - r^2})^2}{r^2}$$

where:  $r$  = correlation coefficient.

Numerous studies have shown that in many cases the ratio between  $c_t$  and  $c_i$  ranges from 10:1 to 30:1 (Akça, 1993). A recent investigation conducted by Kätsch (1991) yielded a ratio of 2.5:1. However, it is clear that the use of aerial photographs in the forestry sector can make a substantial contribution to the economization of a forest inventory. It is reckoned that the savings amount to 30 to 40% of the total costs of a terrestrial method (Hildebrandt, 1996). Many well-proven statistical techniques used in forest inventory are highly efficient and cost-effective, and often those designed for the use of aerial photography are equally applicable to satellite imagery (Howard, 1991; Van Laar and Akça, 1997).

### 6.1.3 Forest Management

The aerial photograph is a very useful tool in the everyday management of forests, with many possible utilisations, some of which are of particular interest.

The contribution of airphoto interpretation to the identification of tree species, for forest inventory, the estimation of site quality, etc., can be fairly substantial. However, the forest management applications of airphoto interpretation extend far beyond the margin of these activities. Additional applications include such tasks as forest land appraisal (see also forest inventory), timber harvest planning, monitoring of logging and reforestation, planning and assessing applications of herbicides and fertiliser in forest stands, assessing plant vigour and health in forest nurseries, mapping forest fuels to assess fire potential, and planning fire suppression activities. Furthermore the assessment of potential slope failures and erosion, planning of forest roads, inventory of forest recreation resources, census of wildlife and evaluation of wildlife habitat, monitoring vegetation regrowth in fire lanes and power lines, and of course forest damage assessment (Hildebrandt, 1996; Lillesand and Kiefer, 1994; Lötsch and Haller, 1964).

Once again, the success of virtually all of the above mentioned applications is conditional on the existence of high quality reference data to aid in the aerial photo interpretation process. The use of aerial photographs and “conventional” ground methods of observation and measurement are typically closely intertwined.

### 6.1.4 Silviculture

The aerial photograph may be used to determine the necessity to perform thinnings, to record the history of forests and stands (i.e. documentation purpose), to control changes with composition of selection forests, to make and update stand maps, etc. Reforestations can be planned (e.g. a selection of tree species in correspondence with different site qualities or morphological variations), and monitored more accurately and efficiently.

### 6.1.5 Pest Control and Damage Assessment

Forests, as either natural or anthropogenic ecosystems, are exposed to all kinds of biotic or abiotic impacts as well as human interference. In well-managed forests some of the major tasks and activities to limit these impacts and interferences are for example (Hildebrandt, 1996):

- prophylactic measures (e.g. silviculture, forest engineering) for lessening the risks (prevention),
- the continuous monitoring of the forest area,
- the elimination of the cause of the damage (fire, pests, etc.) if possible, and the limitation thereof (counter measures),
- the assessment of the nature and extent of the damage,
- the appraisal of the implications of the damages,
- the planning and performance of the activities for restoration and sanctification.

Airphoto interpretation has been used in many instances to survey forest and urban tree damage as caused by disease and insect infestations. A variety of film types and scales have been utilised for this purpose. Although panchromatic photographs have often been used, the most successful surveys have typically employed medium or large-scale colour and colour infrared (CIR) photographs. Damage due to tree disease caused by bacteria, fungus, virus, and other agents that have been detected using airphoto interpretation are ash dieback, Douglas fir root rot, Dutch elm disease and oak wilt. Other types of forest damage include those resulting from air pollution (e.g. ozone, sulphur dioxide and “smog”), animals (e.g. beaver, deer, porcupine and baboon), fire, frost, snow, moisture stress, soil salinity, nutrient imbalance and storm (Hildebrandt, 1996; Lillesand and Kiefer, 1994).

Differences in vigour as well as disease or stress related changes of the leaf-structure and colour can only be accurately detected and interpreted on colour and in particular on CIR photographs. The reorganisation of the cell structure in the leaves induces a decrease of the reflectance in the infrared part of the spectrum. The recently detected so-called “blue-shift” indicates a very similar physical change in the foliage. This

pre-visual detection of damage symptoms caused by an indisposition of the tree has been reported by a great number of scientists, but there is still a great deal of research to be done to achieve an overall acceptance. Some of the following crown features can be detected:

- dead skeleton-like trees, being clearly visible,
- dead parts of the crown or very big branches,
- broken tree tops (caused by snow or storm),
- crown deformations (as an effect of e.g. climatic factors, air pollution, fire and animal damage),
- loss of foliage,
- change in colour of the foliage (e.g. chlorosis), for instance caused by nutrient deficiency, uptake of toxic substances, decay of chlorophyll, insect infestations, etc.,
- presence of parasitic or symbiotic plants in the tree crowns (e.g. lichens, mistletoe, liana) (Hildebrandt, 1996).

In many instances the cause for a particular condition or health status cannot be determined or inferred without corresponding information from ground control. The loss of foliage in particular as well as its change in colour is very often fairly unspecified.

A very well studied phenomenon in central Europe is the forest damage caused by air pollution, the so-called "forest decline". CIR photography has proven to be the superior tool to assess the magnitude and quality of this occurrence.

#### 6.1.6 Fire Control

In America, but increasingly in other countries as well (e.g. Switzerland, Australia, France, Greece, Spain etc.), the aerial photograph has become an important and efficient implement in forest fire control. Topographic features and the occurrence of fuel, which are related to the rate of spread of fires and the difficulty of control, can be identified on aerial photographs. This is useful information for planning suppression activities. For example the accessibility of potentially imperilled areas can be easily determined, as well as the planning concerning the logistics involved. The water

regime of an entire area can be assessed; even the capacity of dams and other kinds of water reservoirs are measurable by means of photogrammetric techniques.

#### 6.1.7 Road location and construction

Because aerial photographs made it possible to measure slopes (even automatically) and to recognise soil features, they can be used advantageously for a reconnaissance of road location and for road construction. Photogrammetric procedures have been most widely adopted by the American and Canadian forest services (van Laar, 1964). The possible and most feasible routes for forest roads are selected on the photograph, plotted with high-order stereoscopic plotting instruments, and checked by ground inspection. By the employment of analytical plotters, different routes can be devised and simulated: it is even possible to detect obstacles and to calculate the corresponding cut and fill.

### 6.2 Satellite remote sensing in forestry

Past studies have suggested that sound knowledge about the reflectance characteristics of objects could be of great value in understanding the physical, chemical, and the spatial properties of features on our planet. These characteristics can be assessed remotely, and the techniques hold considerable promise for the inventory and monitoring of natural resources (Goldsmith, 1991; McCloy, 1990; Simonett, 1976). However, a significant lack of information concerning the full potential of this recent technology has resulted in a lack of appreciation of the many possible applications in various domains.

More than 40 years ago, on October 4<sup>th</sup> 1957, the first controlled satellite, named Sputnik I, was launched by the former USSR. This launch can be considered the dawn of a development, which saw the launch of a further several hundred satellites, designed for a great variety of purposes. Although the interpretation of aerial photographs has been a well-established and recognised technique in forestry and in many of its related fields for nearly a century, it was only in the sixties that it became possible to integrate various sensor systems (i.e. metric cameras, multispectral sensors, radar, laser systems) into spaceborne platforms.

Since the introduction of the first earth resource satellites in the early seventies of this century, the analysis of remotely sensed data from space has become a prevalent and well established process in the forestry sector. The launch of Landsat<sup>11</sup> 1 (formerly known as ERTS<sup>12</sup> 1) with its multispectral sensing capacity sparked off the motivation for a host of research projects with forestry applications. In this respect, one of the most intrepid operations was performed to gather primary information about the nation-wide forest cover of Brazil (the so-called Brazilian Forest Cover Mapping Project), with particular interest in the distinctly vulnerable rain forests of the Amazon region. Subsequently, Landsat data served as an additional source of information for landscape inventory, land use classification, as well as an aid in connection with multi-phase and multi-stage forest inventories in Europe and North America. In the mid-seventies Landsat data were successfully employed to generate an informative set of hardcopy satellite images for the whole of Southern Africa.

A new era of the application of remotely sensed data dawned with a much more sophisticated generation of earth observation satellites. The substantially improved geometric resolution, as well as the introduction of sensors capable of detecting far- and thermal infrared radiation (e.g. on board SPOT<sup>13</sup> and Landsat), instigated a new impetus to practical applications. Despite these advances, the fairly coarse ground resolution still imposes some limitations on the classification of imagery. In practice, this can result in misclassifications using computer-assisted techniques. Therefore, a sound knowledge of the reflective properties of natural surfaces seems indispensable.

Another new technology revolutionised the entire field of remote sensing in the early 80s, when the first prototypes of the Synthetic Aperture Radar (SAR) proved to be a viable option for the monitoring and assessment of the resources of our planet. Howard (1991) describes successful applications with respect to tropical forest cover (i.e. deforestation) and forested wetland systems. The paramount properties of microwave sensors are that they operate independently of sun illumination and are insensitive to weather conditions or cloud cover.

---

<sup>11</sup> Land satellite

<sup>12</sup> Earth Resources Technological Satellite

<sup>13</sup> Système pour l'Observation de la Terre

### 6.2.1 Satellite remote sensing for mapping purposes

Modern digital classification procedures enable the user to automatically categorise pixels (i.e. picture elements) in an image into spectrally separable classes, so for instance into different themes, land cover or forest types. An example of such an application in South Africa is the above-mentioned successful mapping of forest areas, where four different classes, namely *PINE*, *GUM*, *WATTLE* and *INDIGENOUS FOREST* could be determined with considerable accuracy. Similar studies using Landsat imagery indicated the successful discrimination of age classes and tree species of coniferous and deciduous forest areas in Southern Germany. Field verification yielded a final mapping accuracy of between 70% and 85% (at the 95% confidence limit) for the six distinct classes (Kätsch and Vogt, 1999). Schardt (1990) reported an incredible accuracy ranging from 92% to 100% when looking at the discernment of a variety of tree species in southern Germany. An achievable overall accuracy of 80-90% for computer-assisted analysis in forestry is mentioned by Howard (1991). He further gives account of a new approach of improving the performance of classification procedures by introducing the analysis of texture (“Difference and not similarity is the criterion”).

Undeterred by the fact that semi-automatic or automatic digital image interpretation has become common practice, Rosenholm (1993), and Rydén (1997) have proven that even ‘simple’ visual interpretation of satellite imagery is able to yield excellent results. The advantage of visual analysis is that it can be intimately associated with fieldwork and local knowledge, and furthermore does not require sophisticated equipment.

Notwithstanding the fact that the sensor systems of many environmental satellites feature a very coarse spatial resolution (in the case of NOAA<sup>14</sup> it is 1.1km x 1.1km), the high temporal resolution (i.e. frequent coverage) and the low cost of imagery per surface area make it a very useful tool for zonal and global monitoring and mapping. By exploiting the wide range of spectral sensitivity and applying techniques such as

---

<sup>14</sup> National Oceanic and Atmospheric Administration

band ratioing and vegetation indices, data acquired by environmental satellites are highly suitable for land use classification, the estimation of biomass (e.g. Leaf Area Index, Net Primary Production, etc.), the detection of environmental impacts and the like. Examples of successful applications are to be found in Howard (1991), Hildebrandt (1996), Kättsch and Vogt (1999).

### 6.2.2 Satellite image interpretation for mensuration purposes

Remote sensing, particularly aerial photography, has traditionally and successfully dealt with the physical properties of vegetation canopies. However, the coarse ground resolution as well as the absence of stereoscopic imaging capabilities of spaceborne sensing systems have imposed substantial constraints on the feasibility of the satellite technology for the last few decades. The launch of the current generation of satellites on the other hand gives rise to the hope that most of these limitations will soon be overcome.

In many of these cases the user will find a well-defined relationship between the values of the reflected radiation (used as an auxiliary variable) and stand related parameters such as timber volume and the degree of canopy closure. This has been corroborated by the observation that, for instance, the parameter timber volume and the spectral reflectance intensity of Landsat TM's infrared band (channel 4) are highly correlated.

Since 1992 Landsat data have been successfully implemented in the Finnish National Forest Inventory. Designed as a "Multi Source National Forest Inventory", essential parameters like the average timber volume, the proportion of saw timber, as well as the percentage of other products are being inferred fairly accurately with the aid of satellite data in conjunction with terrestrial information (Kilkki and Päivinen, 1987; Tomppo, 1993). Numerous studies testify that the difference in accuracy between the estimates being derived from the satellite images and the ground truthing itself is virtually insignificant. So, for instance, the application of the Finnish inventory system on forest areas in Germany yielded accuracies of 96-99% for the estimation of timber volume (Tomppo and Pekkarinen, 1997). Some further accounts are given by Akça *et al.* (1984), Hildebrandt (1996), and Howard (1991).

### 6.2.3 Satellite remote sensing for forest disease and stress assessment

The sensor's ability to detect physically (e.g. insect attacks) and non-physically (e.g. acid rain) induced stress is crucial to the monitoring of spread patterns and the development of predictive models. In particular, the early detection of stress engendered symptoms (so-called 'red' and 'blue shift') has become a cogent prerequisite for effective forest management. The successful application of infrared imagery has stimulated the development and implementation of an array of practices. The occurrence of "*neuartige Waldschäden*" (the so-called "forest decline") in Central Europe in the early eighties, which disastrously damaged vast forest areas, prompted numerous institutions to utilise colour infrared (CIR) aerial photography as the main medium for disease and stress detection. On account of its eminent success in damage assessment, CIR has been employed as standard procedure ever since. Even multi-temporal Landsat TM and SPOT images have proven to be very valuable for this particular purpose and the topic has received adequate attention in the literature (Hildebrandt, 1996; Howard, 1991).

### 6.2.4 Future applications

As has been previously stressed, the applications of remotely sensed data in forestry have been subject to a number of limitations due to the paucity of fine spatial resolution of the sensor systems. Although the potential of this technology has not yet been exploited to its full extent, in many respects satellite derived imagery is being pushed into the background when it comes to tasks where high spatial accuracy is required (Hildebrandt, 1996; Howard, 1991). In these cases first priority is being given to the use of aerial photographs. However, remote sensing techniques hold considerable promise for the mapping of forests at a small scale and can serve as high quality ancillary information for the purpose of forest inventories.

In comparison with traditional aerial photography, high-resolution satellite imagery has the following advantages (Goldsmith, 1991; Hildebrandt, 1996; Lillesand and Kiefer, 1994):

1. The frequency of data collection (i.e. revisitation rate).

2. Global availability of remote sensing data.
3. Data from remote sensing platforms are commonly in a form suitable for computer processing, particularly in terms of digital analysis and classification.
4. Data is gathered at relatively low cost: According to American reports (Corbley, 1996), the costs are to the magnitude of about \$33.00 /km<sup>2</sup>, hence only 40% to 60% of the total costs of equivalent aerial photographs (about \$55.00 to \$110.00 /km<sup>2</sup>).

The satellite remote sensing business is in a continual state of flux since new satellites are being launched and new designs for sensors are being advanced at a rapid pace. In only two and a half decades the painstaking technology of Earth observation has progressed from experimental and limited to quasi-operational and global. Furthermore, the emergence of the concept of studying the earth as a system rather than observing its components has led to a better understanding of all ecological processes operating on our planet and their interdependence.

Since their first appearance about 30 years ago, methodologies of remote sensing have deservedly gained a well-established position in the observation and monitoring of environmentally related features. In particular, the supreme characteristic of acquiring synoptic detailed information with a single image, and the capability to select certain regions of the electromagnetic spectrum while considering a specific thematic focal point, has contributed to its great success as a mapping tool in forestry and environmental planning.

The portrayed technical development will certainly open up new markets in satellite remote sensing, which have traditionally been dominated by small-scale aerial photographs. Similar geometrical resolutions, and multispectral and stereo capabilities in conjunction with the benefits of computer aided digital analysis, will make it possible for satellite imagery to be applied in forest and landscape inventory even on a high intensity level. Wherever and whenever detailed information on the structures of landscape is required, these new systems will be the appropriate tool to provide these data.

A selection of new sensor platforms, which are currently operational or are to be launched in the near future, is shown as Table 6.2.

**Table 6.2** Selection of launching dates of currently available and future satellite systems

Satellite	Country	Year of (intended) launch	Type of sensor	Spatial resolution	Stereo capability
ERS 2	Europe (ESA)	1995	SAR	25.0m	
Radarsat	Canada	1995	SAR	28.0x25.0m – 10.0x9.0m	
IRS-1C	India	1995	PAN/MSS	5.8m/23.5-188.3m	Yes
MOMS-2P <sup>1</sup>	Germany	1996	PAN/MSS	4.5m/13.5m	Yes
CTA Clark	USA	1996	PAN/MSS	3.0m/15.0m	
Early bird I <sup>2</sup>	USA	1997	PAN/MSS	3.0m/15.0m	
SPOT 4	France	1998	PAN/MSS	10.0m/20.0m	Yes
Kitsat 3	South Korea	1999	MSS	15.0m	Yes
SUNSAT	South Africa	1999	MSS	15.0m	Yes
IKONOS 2	USA	1999	PAN/MSS	1.0m/4.0m	Yes
Landsat 7	USA	1999	PAN/MSS	15.0m/30-60m	
Orbview 3	USA	2000	PAN/MSS	1.0m/4.0m	
Orbview 4	USA	2000	PAN/MSS/ Hyperspectral	1.0m/4.0m 8.0m	
Quickbird	USA	2000	PAN/MSS	0.8m/3.3m	Yes
SPOT 5	France	2002	PAN/MSS	5.0m/10.0m	Yes

<sup>1</sup> The sensor is currently not active due to technical problems on the MIR spacestation

<sup>2</sup> The satellite was lost during the initial phase

## 7. DIGITAL PHOTOGRAMMETRY

As always when new technologies and methods develop, there is no unified terminology, let alone an overall accepted definition of *Digital Photogrammetric Systems* (DPSs). According to Kraus (1993) *digital photogrammetry* is deeply embedded into computer vision (sometimes referred to as 'pattern recognition' or 'image understanding'). The main characteristic of this technology is that "...the illumination in the image plane of the camera is not recorded photographically, but by electronic means; there then follow computerised techniques which simulate human vision and recognition". *Analogue photogrammetry* by contrast begins with photographs (printouts denoted as being 'hardcopies') and continues with optical-mechanical instruments. *Analytical photogrammetry* is the much more advanced successor, which has been the mainstay of photogrammetry for the last few decades. This also deals with photographs, but continues with computerised instruments. A widely accepted definition of the term Digital Photogrammetric System is given by the ISPRS (International Society for Photogrammetry and Remote Sensing) as "hardware and software to derive photogrammetric products from digital images using manual and automatic techniques" (Dowman, 1991). A slightly more comprehensive definition of a DPS is "the hardware and software for deriving input data for Geographic Information Systems (GIS) as well as for Computer Aided Design (CAD) systems and other photogrammetric products from digital imagery using manual and automatic techniques" (Heipke, 1995).

Digital photogrammetry (the term 'softcopy photogrammetry' is used interchangeably) has been the buzzword in the photogrammetric community for the last two decades, and has sparked off some extensive research in this field. This fairly recent technology is often attributed to terms such as 'paradigm shift', 'evolutionary earthquake' (Boniface, 1996), or even 'revolution' (Leberl, 1991). However, there is evidence that there has been a substantial period of transition from the traditional, well-established analytical systems to the introduction of the first commercially available softcopy system, the Kern DSP1, in 1988 (Petrie, 1997b). Highly sophisticated computer-assisted analytical plotters like the Kern DSR-15, the Leica SD 3000, the Wild BC 3, or the Zeiss P1, all manufactured in the 1980's, feature

components typical for softplotter systems such as graphics stereo superimposition and correlation systems (e.g. for point transfer, and near-automatic inner, relative and absolute orientation) (Petrie, 1997b).

A *Digital Photogrammetric Workstation* (DPW) represents the main component of a DPS. A wide diversity of opinion about the functionality and the degree of automation DPWs should exhibit has dominated the discussion in the photogrammetry community since the first appearance of a softcopy system. However, a few essential characteristics can be specified:

1. A DPW handles digital images (from all kinds of sources).
2. It provides user interaction.
3. A DPW uses photogrammetric functions.
4. A significant amount of automation is implicit.
5. The environment is fully digital.
6. All expensive high-precision mechanical components have become redundant (Dowman, 1991; Gülich, 1996; Mayr and Reinhardt, 1996; Petrie, 1997b).

The development of DPWs have been largely influenced by factors such as the drive for automation due to high labour cost, the availability of digital imagery from various sensor systems (e.g. multispectral scanners, laser altimeters, radar), the need for real time operations in quality control and robotics, the inherent stability of a digital system, and the availability of low-cost computer components. Furthermore, the need for integration of information from different sources (e.g. GIS, CAD, and GPS) has become another primary concern. Currently, softcopy systems can be considered operational. Yet, because of the immense costs involved in the procurement of a softcopy system, the economic and analytic advantages over traditional systems (e.g. analytical plotters) have to be demonstrated in order to provide a wide acceptance of this new technology.

### **7.1 Basic elements of a Digital Photogrammetry System (DPS)**

The major characteristics are as follows:

- (i) the system combines computer hardware and software to allow photogrammetric operations to be performed on digital image data;

- (ii) the digital image data consist of arrays of pixels (picture elements) of fixed size and shape; each pixel is assigned a specific brightness value;
- (iii) the imaging sensor can take the form of a digital camera, a pushbroom or whiskbroom scanner, a laser or radar system;
- (iv) digital image data are often derived from frame images on photographic film; these are converted into digital form employing high precision scanners;
- (v) the core of a DPS is the DPW on which the mathematically based photogrammetric operations are executed to generate data for input to CAD, GIS, digital mapping;
- (vi) these operations are performed either manually or interactively, or using automated or semi-automated methods (e.g. triangulation, DTMs, orthophotos);
- (vii) final output (either as hardcopy or softcopy) may take the form of vector maps, DTM/DSM (Digital Terrain Model/Digital Surface Model) data, or image maps.

An overall impression of the main components of a DPS is shown in Figure 7.1.

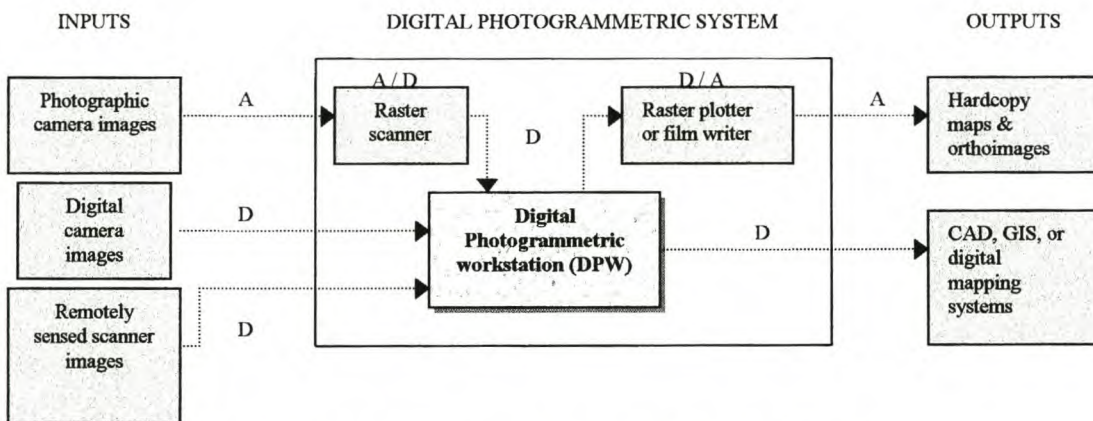


**Figure 7.1** Overall concept of the DPS; A (analogue) and D (digital) indicate the data format (Petrie, 1997b)

## 7.2 Image data acquisition and input to a DPS

There is a vast range of digital data formats from various sensor systems that has to be handled and stored in a DPS. Despite the advances in the development of *digital metric and video cameras*, systems able to accomplish the functionality of aerial mapping cameras are not on the horizon, and most concepts are far from mature (Hildebrandt, 1996; Leberl, 1996; Lillesand and Kiefer, 1994, Mayr and Reinhardt,

1996). Only special systems employed in close-range photogrammetry (e.g. the Rollei RSC) would be able to meet the requirements with respect to resolution (about 3.0 million pixels per image as a reasonable equivalent) and spectral sensitivity, but still feature many operational limitations. A typical video or CCD areal array generating black-and-white images features an image area of 512 x 512 pixels, requiring 0.25Mb of storage, and with more sophisticated cameras with an area of 2 000 x 2 000 pixels taking up a storing space of 4Mb. In this respect it should be noted, that for every twofold improvement in resolution, there is a fourfold increase in the data storage required.

The requirements concerning the data storage capacity are noticeably larger when looking at *pushbroom scanners* commonly used in satellite remote sensing. For instance, the SPOT HRV pan sensor creates images with 6 000 x 6 000 pixels (i.e. requiring 36Mb of storage). For a three-band false colour image acquired by SPOT XS, 27Mb of digital data needs to be stored. However, by far the greatest source of imagery is still photography taken by *aerial frame cameras*. The latest cameras equipped with forward-motion compensation and high-resolution film (e.g. the Zeiss RMK TOP) give a resolution on the original negative of 60 lines per millimetre (l/mm), corresponding to a pixel size of 8.5 $\mu$ m. Being scanned at rate of 2 500dpi<sup>15</sup> (i.e. 10 $\mu$ m), the data volume will be 529Mb for a monochrome image, the figures to be doubled for a stereopair, and multiplied by another three times for colour imagery (amounting to about 3.2Gb for stereo colour imagery). Even though sophisticated data compression techniques are used to lessen the burden of large data volumes, mapping agencies commonly exhibit storage capacities of about 100Gb in order to be able to handle and store huge blocks of aerial imagery (Kubic and Harvey, 1996; Schiewe, 1998; Shah, 1996; Toth, 1996; Zeng and Ze, 1996).

### 7.3 Scanners

One of the key elements in digital photogrammetry is the scanning process, since the quality of the original photography has to be transformed from the analogue into the digital environment with as little loss of information as possible (Grabmeier *et al.*, 1996; Kölbl, 1996; Petrie, 1997b). The scanners currently available on the market

---

<sup>15</sup> Dots per inch

usually employ one of the four main technologies for use with transparent (positives and negatives) film images:

1. Drum scanners. This type is being used extensively in the graphic arts world, but unfortunately only high performance systems are able to meet the requirements with respect to resolution, geometric accuracy and radiometric range for photogrammetric purposes.
2. Flatbed scanners. They are equipped with a photo head or CCD linear array. An example for such a commonly used system is the Zeiss/Intergraph series.
3. A 1D scanning linear array of CCDs, which scans the photograph in a single sweep (e.g. the XL Vision Ortho Vision 950).
4. A CCD areal array, allowing a patch-by-patch scanning process of the photograph (e.g. used in the Leica/Helava series and in Rollei and Topcon scanners).

Consensus has been achieved on the fact that a photogrammetric scanner should feature the same accuracies as a mainstream analytical plotter (Boniface, 1996; Chapuis, 1995; Hildebrandt, 1996; Kölbl, 1996; Petrie, 1997b; Walker and Petrie, 1996). This implies a requirement for linear measuring resolutions of 1 to 2 $\mu$ m and accuracies (RMSE<sup>16</sup>) of 2 to 5 $\mu$ m, with a minimum pixel size of 8 to 10 $\mu$ m (2 500 dpi). It usually takes between 5 to 20 minutes for a scan of a single black-and-white 23cm x 23cm image with a resolution of about 10 $\mu$ m. The scanning process often includes the automatic measurement of the fiducial marks for inner orientation. Radiometrically satisfactory data should be provided in 8 (i.e. 256 grey levels) or 10 bit (i.e. 1,024 levels) greyscale, and 24bit for colour imagery. Most of the new scanning systems are able to handle negative roll film (e.g. the Leica/Helava DSW 300), or even large formats (23cm x 46cm) as being used by the U.S. military mapping and reconnaissance agencies. Numerous low-cost solutions, that have been developed for the desktop publishing industry, have resolutions of about 40 to 80 $\mu$ m, a restricted 4 or 6bit grey level range, too small page formats, and poor geometric accuracy, and are therefore not suitable for serious photogrammetric tasks.

---

<sup>16</sup> Root Mean Square Error

#### 7.4 Digital Photogrammetric Workstations (DPWs)

As mentioned before there is still considerable confusion concerning the design of a DPW, and many authors have presented their ideas on conceptual and structural issues (Boniface, 1996; Dowman, 1991; Dowman *et al.*, 1992; Graham *et al.*, 1997; Güllich, 1996; Heipke, 1995; Leberl, 1991; Mayr, 1997; Miller *et al.*, 1992; Nolette *et al.*, 1992; Petrie, 1997b; Walker and Petrie, 1996). However, a few common major design features can be identified. They comprise:

1. A powerful CPU and an exceptionally large RAM to handle large volumes of image data.
2. Additional processing capability in form of a graphics accelerator (e.g. VITec) or an array processor for rapid refresh rates in stereo viewing.
3. High-capacity hard disk and backup storage devices, and network access.
4. Very fast data transfer (i.e. buses) rates between the RAM, the video memory and the main storage system.
5. A high-resolution colour display monitor with stereo-viewing capability.
6. A convenient 3D measuring device (e.g. the P-cursor by Zeiss, or the 3D-mouse by LH Systems) (Boniface, 1996; Dowman, 1991; Petrie, 1997b; Walker and Petrie, 1996).

The mainstream photogrammetric system suppliers traditionally use Unix-based top performance graphics workstations, containing either the Sparc processors as used in Sun Sparc Station and Sun Ultra workstation, or the MIPS processors to be found in the Silicon Graphics Indy and Indigo workstations. Quite a number of PC-based DPWs have been introduced recently (e.g. Intergraph's Image Station, and LH Systems' SOCET SET), the high performance systems running on Windows NT software, and being equipped with twin Intel Pentium processors. A minimum RAM capacity of 64Mb is common for DPWs, however, experience has shown that 128Mb and more RAM is advisable. Hard disks should feature multi-gigabyte capacity, supplemented by CD-ROM drives. For archiving and backup of data compact tape drives (with DAT or Exabyte cartridges) or optical disk drives can be employed. A high-resolution monitor with a minimum resolution of 1 024 x 1 024 pixels is compulsory with a DPW, with a monitor size of at least 21-inch (Intergraph's Image Station Z uses a 28-inch screen). High refresh rates (typically 100 or 120Hz) of the monitor screen are necessary to obviate flickering of the stereo model.

Stereo viewing is a vital element of a DPW for measuring ground control points, map revision, feature extraction, and editing elevation data. Five methods are currently in use:

1. The first approach uses two flat screen monitors, the stereo images being viewed using a mirror-stereoscope or an optical train.
2. With the second method the left and right images are displayed side by side on a single monitor (the so-called split screen method), employing a mirror stereoscope for viewing (examples are the Kern DSP1 and Leica's DVP).
3. Another system, a real low-cost solution, makes use of the anaglyph technique; unfortunately the use is limited to monochrome images.
4. A very common stereo-viewing system alternates the right and left component images on a single monitor at high speed. Viewing is performed through spectacles equipped with alternating shutters synchronised with the alternating images on the monitor (e.g. the CrystalEyes system).
5. The last method also uses alternating corresponding images displayed on a single monitor, but each image has a different polarisation pattern induced by an electronic prism mounted in front of the monitor. Users view the images by means of 'passive' spectacles, featuring corresponding polarising filters (e.g. the NuVision system).

Almost all DPWs feature two monitors, one for displaying the imagery, the second one for the display of system information, commands, etc. Superimposition of vector data over the stereoscopic image has become a standard feature of most DPWs (Miller *et al.*, 1992; Petrie, 1997b; Walker and Petrie, 1996).

According to the products, which can be derived, and the overall performance, DPWs currently available can be categorised as follows:

1. High-end systems are based on graphics workstations running under Unix, and feature the ability to generate the complete range of photogrammetric tasks (e.g. Leica/Helava (DPW 770), Intergraph (ImageStation), Zeiss (PHODIS), Vision International, VirtuoZo, and Matra).
2. DPWs running on powerful PCs usually under MS Windows. In general the functionalities are limited, but the systems are less expensive than these being offered by the mainstream suppliers in category (1). Examples for manufacturers

of the PC based systems are Topcon, ISM, KLT, DVP Geomatics, LH Systems and Intergraph.

3. Systems tuned to only one function, but offered at an economical price (Vexcel Imaging (triangulation), ISM (orthophoto), and Vision International (orthophoto)).
4. Photogrammetric modules offered by certain remote sensing suppliers, allowing the creation of orthophotos, DTMs and perspective scenes (for instance ERDAS (Orthomax), PCI (EASI/PACE) and MicroImages (TNTmips)).
5. Low price solutions with limited functionality, but still offering a wide selection from the DPW spectrum (DVP, R-WEL, and VTA) (Petrie, 1997b; Scherz and Schmidt, 1997; Walker and Petrie, 1996).

The prices range from about US\$ 1 000 for add-on modules and about US\$ 200 000 for fully-fledged systems based on high performance workstations.

### 7.5 Algorithmic and software aspects of DPWs

Almost all available DPWs are capable of emulating analytical plotters, therefore the fundamental operations are very similar. They use a common basis of projective geometry and identical mathematical models. While all systems are expected to be able to handle aerial photography, a great many also include facilities to manipulate *satellite images* such as SPOT, IRS-1C/D, JERS-1, with packages for Ikonos 2, Quickbird and OrbView (see also Table 6.2) in the pipeline. Furthermore, most systems offer an enormous variety of different map projections and co-ordinate systems, and even user defined datums, for example, are made allowance for.

Typically, *orientation* procedures are compulsory in all DPWs, and a few systems even have impressive automated functions (e.g. Zeiss PHODIS) (further information can be found in Drewniok and Rohr, 1997; Friedman, 1980; Heipke, 1996a; Leberl, 1991; Morgado and Dowman, 1997; Petrie, 1997b). Inner orientation is fairly simple and straightforward, whereas exterior orientation procedures can vary. Some orientation philosophies are based on bundle adjustment strategies, others still use the classical sequential relative and absolute orientation. Even though automatic or semi-automatic modules are provided, absolute orientation almost always requires operator interaction to identify ground control points.

Highly automated *triangulation* as a more recent development marks the actual strength of high performance DPWs (Boniface, 1996; Dam and Walker, 1996; Dowman, 1991; Graham *et al.*, 1997; Gülich, 1996; Haumann, 1995; Heipke, 1995; Honkavaara and Høgholen, 1996; Kersten and O'Sullivan, 1996; Kersten and Stallmann, 1995; Krupnik and Schenk, 1997; Leberl, 1991; Mayr, 1997; Miller *et al.*, 1992; Nolette *et al.*, 1992; Petrie, 1997b; Schenk, 1996; Tang *et al.*, 1997; Walker and Petrie, 1996). In particular, if image matching (area or feature-based) is applied to the transfer of tie points and control points, productivity can be increased to a large extent. Current versions of block adjustment software can use airborne kinematic GPS measurements of the exposure stations to adjust values of co-ordinates of the triangulation points, thus adding substantial efficiency to the entire triangulation procedure (Ackermann, 1996b; Connors and Perry, 1996; Kletzli, 1996; Kraus, 1993; Lucas and Lapine, 1996; Mader, 1996; Welch and Remillard, 1996).

Most often DPWs feature some kind of software for the compilation of maps. Third-party software packages that were developed originally to support stereoplotting instruments in the acquisition of photogrammetric data (*feature extraction*) are assigned to that particular use. Examples for such packages are ATLAS from KLT, CADMAP from Zeiss, DGN/CAPTURE from DAT/EM, and PRO 600 (based on Bentley's MicroStation) from Leica. These packages offer feature coding and input of attribute data, and after having captured the vector data, these can be transferred to CAD, GIS, or digital mapping systems. Currently no general-purpose, universally accepted automatic feature extraction method is available, since the reconstruction of surfaces in particular is an ill-posed problem. Therefore, operator interaction is still required for many operations. Although extensive research has been carried out in this field for many years, the automated process of feature extraction is far from being operational (Petrie, 1997b; Schenk and Toth, 1992; Walker and Petrie, 1996). At this stage, only the extraction of buildings and roads can be handled with considerable ease.

By far the best reasons for travelling the softcopy route is for the purpose of the automatic generation of digital elevation data (DTM, DSM, TIN, contour lines, etc.) and digital orthoimages (Dowman, 1991; Heipke, 1995; Leberl, 1991; Mayr, 1997; Miller *et al.*, 1992; Petrie, 1997b; Walker and Petrie, 1996). The production of the

latter is fairly straightforward and the methods applied are very successful. With the advent of in-flight GPS, most systems have mosaicking capabilities, and allow virtually seamless orthoimage products to be accomplished. These digital orthophotographs can subsequently act as an image backdrop in a GIS, or can stand in as a substitute for a map (Manzer, 1996). In the case of automatic DEM operations, failures do occur, in particular when dealing with ill-defined structures, poor contrast, discontinuities and little texture. Hence, the provision of interactive editing facilities is a crucial requisite for the successful implementation of the entire process. A more detailed account on this subject is provided in sections 8.1.4, 8.2.2 and 8.2.4 .

The final products obtained as a result of the manipulation of imagery within a softcopy environment can be in either in form of a softcopy (used as input into other software systems) or various hardcopy products. Hardcopy outputs can be produced by devices such as electrostatic plotters, inkjet plotters, and thermal and laser plotters. Where the full preservation of the intrinsic resolution of original imagery is paramount, sophisticated film plotters come into play. Not only can large formats be handled by such devices, but resolutions of higher than 4 000dpi can be achieved. Traditional outputs would then be orthophotographs and orthoimages (Petrie, 1997b; Walker and Petrie, 1996).

## **7.6 Analytical plotters versus Digital Photogrammetry Workstations**

The predecessor of softcopy photogrammetry systems, the analytical plotter (AP), was invented in 1958. Yet it took well into the 1980's for computer-driven measurements from film images to become established in modern photogrammetric operations. Today, of the reckoned 3500 to 5000 stereo systems in operation worldwide, at least 1500 are analytical (Leberl, 1996).

Since the advent of softcopy photogrammetry about 15 years ago, this technology has been developing steadily. Despite the advantages of softcopy systems over the analytical counterpart, APs are still being sold in very large numbers (Petrie, 1997b). For the last decade there has been a very controversial debate on the virtues of digital against analytical photogrammetry. Based on the work of Droesen and Van Deventer (1996), Gülich (1996), Heipke (1995), Kaiser and Miller (1996), Kraus (1997), Leberl

(1991 and 1996), Lue (1996), Petrie (1995 and 1997b), Schenk and Toth (1992), Schenk (1994), Tang *et al.* (1997), Trinder and Donnelly (1996), Walker (1995), and Walker and Petrie (1996) the following strengths and weaknesses of digital systems can be identified.

Merits:

- No repetition of interior or exterior orientation.
- More functions and more products (e.g. orthophotos).
- Models are ready to use immediately on completion of triangulation.
- No calibration or wear and tear; the DPW eliminates all the expensive high-precision mechanical components of the analytical plotter (e.g. photo stages, carriages); furthermore in a softcopy environment no high-quality optical components of the AP are required.
- Softcopy photogrammetry benefits largely from innovations in computer technology (e.g. in computer vision for animated 3-D visualisation).
- Easy hardware maintenance.
- Colour, stereo superimposition at no additional cost.
- Focus on extensive automation in interior orientation, triangulation, DTM generation, orthophotos, mosaics and feature extraction.
- End-to-end (i.e. digital data capturing to product output) workflow, providing greater simplicity.
- Easy exchange of data from other technology systems such as GIS, CAD, GPS.
- Direct use of a large variety of digitally captured primary information (e.g. digital cameras, spaceborne multispectral sensors, radar, Lidar).
- Very high efficiency and speed due to automation of certain processes (e.g. DTM generation).
- No limits on magnification for stereo perception.
- Manual collection of terrain data generally faster than in an AP; furthermore manual collection can be assisted with image matching techniques.

The demerits include:

- Additional cost of scanner.
- To achieve image quality of AP, extremely high scanning rates have to be used (i.e. requires very high disk storage capacity).
- Less smooth image roaming than APs.

- Zooming limited to fixed levels (image pyramids).
- Ergonomics less well thought through.
- Very large data volumes.
- Greater computer literacy required.
- More complex software, less easy to use than APs.
- Lack of standards, particularly concerning image formats and quality control.
- Most software packages still have limited capability for quality control.

Undoubtedly the most significant benefit and potential of the fully digital systems lies in the automation of processes such as orientation, triangulation and feature extraction (Heipke, 1996a; Kraus, 1997; Leberl, 1991 and 1996; Petrie, 1997b; Walker and Petrie, 1996). However, the softcopy systems still bear an extremely costly price tag and require intensive operator training as well as continuous maintenance, thus still having to prove their merit to the user community.

The dedicated reader will find more information about the South African forestry industry in the pamphlet published by the Forest Owners Association (provided as Appendix 7). A detailed description of the particular stands under scrutiny is provided in section 8.1.5.

### 8.1.2 The satellite imagery

The imagery acquired by the IRS-1C/D satellites represents one of the highest resolution Earth information products available on the commercial market today. The IRS mission is part of the Indian space programme (initiated in the late 70's), whose major focus has been to accelerate the country's economic development by improving management of land and water resources. IRS-1C was launched in December 1995. It was followed up IRS-1D in September 1997 in order to provide imagery at a higher revisit rate. Besides the supremacy of its ground resolution, the twin pair features stereo capability for the Pan<sup>17</sup> imagery. Various studies have clearly demonstrated the potential of this new satellite generation for the surveillance and monitoring of the vast resources of our planet. Mapping and assessment of different kinds of land uses, with forest resources in particular, have proven that IRS-1C/D multispectral imagery can be used for the extraction of features, adequate to a scale of up to 1:25 000, and in combination with high resolution Pan imagery even to a scale of 1:10 000 (Armenakis and Savopol, 1998; Jacobsen *et al.*, 1998; Meinel *et al.*, 1998; Rao *et al.*, 1996; Rosenholm and Åkerman, 1998; Roy *et al.*, 1996;).

One of the most striking advantages of IRS-1C/D over other satellite systems such as SPOT is the higher resolution and scene size. An impression of the spatial resolution of various remote sensing media is shown in the following figure.

---

<sup>17</sup> Panchromatic

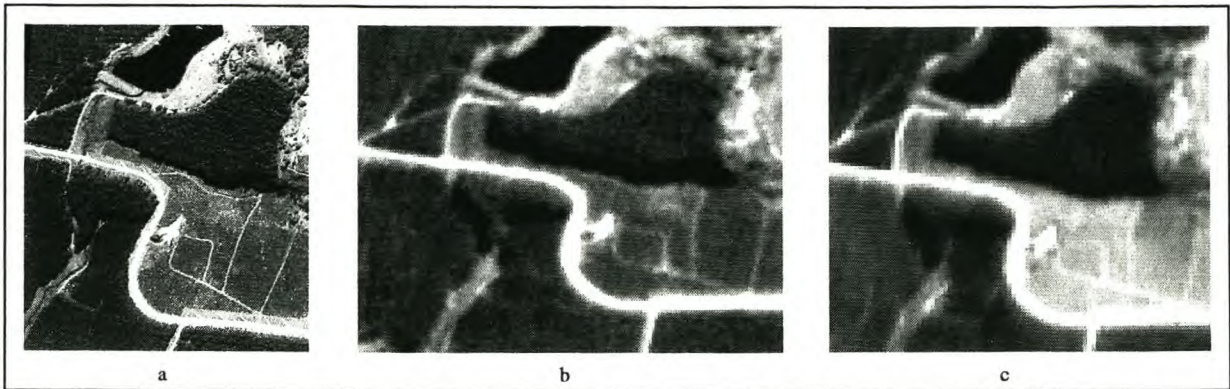


**Figure 8.3** Spatial resolving capacity of different remote sensing imaging systems; (a) aerial photography (resolution of about 30cm); (b) IRS-1C PAN (5m); (c) SPOT PAN (10m). The images show part of the test area close to Sabie, with the Klipkraal dam on the top.

Furthermore, the imagery from all three sensors on IRS-1C/D (Pan, LISS-III<sup>18</sup>, and WiFS<sup>19</sup>) are all received at every pass and simultaneously, implying that for instance merged 5 metre colour images can be obtained from Pan and LISS-III from virtually all passes. Further details on the space segment of the IRS-1C/D system (NRSA, 1995, 1997) are provided in Table 8.1.

**Table 8.1** Specifications of the space segment of the IRS-1C/D satellites (NRSA, 1995 and 1997)

ORBIT	:	Polar, sun synchronous, 817km altitude
REPETIVITY <sup>20</sup>	:	341 orbits / 24 days
REVISIT CAPABILITY <sup>21</sup>	:	5 days
MISSION LIFE	:	3 years
<u>PAYLOADS</u>		
TYPE	:	Optical sensors (CCD) linear array (4096 elements)
SENSORS / BANDS	:	Pan 0.50-0.75 $\mu$ m
		LISS-III Band 2 0.52-0.59 $\mu$ m
		Band 3 0.62-0.68 $\mu$ m
		Band 4 0.77-0.86 $\mu$ m
		Band 5 1.55-1.70 $\mu$ m
		WiFS Band 3 0.62-0.68 $\mu$ m
		Band 4 0.77-0.86 $\mu$ m
SPATIAL RESOLUTION	:	Pan 5.8m
		LISS-III 23.5m for B2,B3,B4 ; 70.5m for B5
		WiFS 188.3m
SWATH	:	Pan 70km (nadir); 90km (at maximum look angle); steering range $\pm$ 26 degrees
		LISS-III 141km for B2,B3,B4; 148km for B5
ENCODING	:	Pan – 6 bits; LISS-III – 7 bits; WiFS – 7 bits
ONBOARD TAPE RECORDER / CAPACITY	:	62Gb (24 minutes)
POINTING ACCURACY	:	roll $\pm$ 0.15 degrees; pitch $\pm$ 0.15 degrees; yaw $\pm$ 0.2 degrees
DRIFT	:	$3 \times 10^{-4}$ deg/sec

<sup>18</sup> Linear Imaging and Self Scanning Sensor

<sup>19</sup> Wide Field Sensor

<sup>20</sup> Elapse of time between two passes over the same area

<sup>21</sup> Due to the camera's tilting capacity, a given area can be viewed more than once within one cycle

All three sensors employ pushbroom technology, and are as such well suited for precise geometric correction. The best-known of these sensors, the IRS Pan, features a scene size of 70km x 70km, being viewed by three CCD-line sensors, hence a full scene is being delivered as three separate files with 4 096 x 14 798 pixels (each 23.5 km wide). Due to the satellite's construction, the three sub-scenes do not match perfectly and seamlessly. Geometric problems such as the non-parallelism of the sensors, the shift in image plane, or the difference in focal lengths therefore need to be properly addressed. Several successful approaches at rectifying these discrepancies have been described for instance by Jacobsen *et al.* (1998), Rosenholm and Åkerman (1998); Savopol and Armenakis (1998). Other, more general effects on the geometric fidelity of the imagery are largely caused by the deviations of orbit and attitude parameters. Orbit perturbations are responsible for deviations from the ideal sun-synchronous orbit. Atmospheric drag leads to a loss of altitude, the asphericity of the Earth results in variations in altitude as well as velocity of the satellite and luni-solar gravitational attraction causes variation in the inclination of the orbit, thus affecting ground track patterns. Similarly, due to internal and external torque acting on the satellite, its attitude slowly drifts, inducing track deviations of the image. Even though it is rather difficult to accurately model the true motion of the satellite, within certain limits the critical parameters can be controlled by the attitude and orbit control system (e.g. magnetic torquers, sun and star sensors, yaw sensors and gyros). The correction of all these deviations from the optimal trajectory and the consideration of other factors such as the rotation of the Earth or the calibration of the sensors, are reflected in the variability of the various products being available. These products range from hard-, to softcopies of the imagery, from uncorrected (raw) to highly specialised data, black and white and false colour composites, which are supplied on different types of media and in a great number of formats (e.g. BSQ, fast format, BMP, LAN, etc.), and from full scenes to sub-scenes. In all instances some kind of radiometric or geometric correction is applied. Radiometric corrections account for factors such as the non-uniform response of the detectors, the failure of a specific element, or image to image variations. Geometric distortions can be either scene related (e.g. Earth rotation effect), sensor related (e.g. off-nadir pointing induced distortions, or sensor focal plane geometry), spacecraft related (e.g. altitude, attitude and velocity variations), or be related to measurement or calibration errors. These

corrections are traditionally performed through a dynamic model using a few ground control points, by which an image to ground mapping is finally achieved.

The oblique viewing capability of the PAN sensor can be used to acquire stereo imagery. The stereo coverage is obtained by recording the same area from one of the neighbouring tracks after the sensor orientation has changed for an across track angle (up to  $\pm 26$  degrees) in the opposite direction. The revisit periods due to Pan's steerability is demonstrated in Figure 8.4. A path with three adjacent paths on either side from the equator is shown, furthermore the tilt angle with which the central path can be viewed

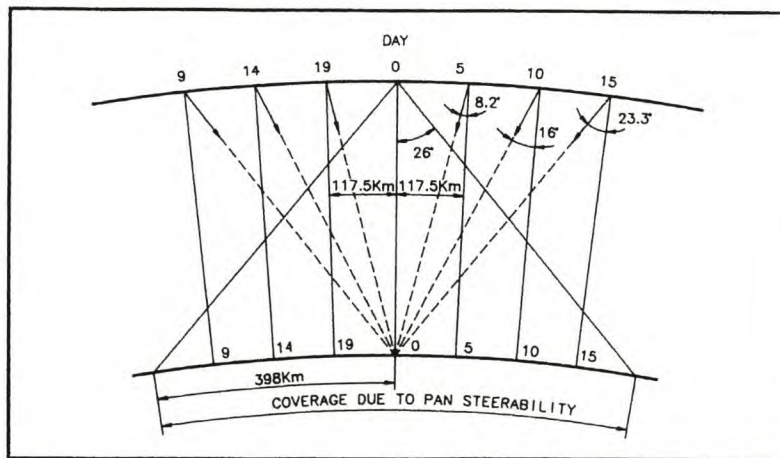


**Figure 8.4** Pan off-nadir viewing capability (NRSA, 1995)

from adjacent paths and also the day number on which the adjacent paths occur relative to the central path. The Pan camera can see only three paths on either side at equator, and as the satellite travels away from the equator, the paths apparently become closer to each other, hence more paths can be viewed at high altitudes. Since the total swath of the Pan detectors is only 70km, the steerability of the camera can be used to close the gap between any two orbits (the distance between adjacent traces is 117.5km). The across track configuration has been designed to increase the ground coverage, acquire stereo imagery, and allow revisit periods about 4 to 5 times shorter than the repeatability cycle.

Two sub-scenes (23.5km x 23.5km each) covering the test area for this project were acquired. The coverage pattern of IRS-1C for southern Africa is shown in Figure 8.5.

procedures as part of the modelling process. The pixel data of the imagery is recorded in a Band Sequential (BSQ) format, resulting in a required storage space of 19.7Mb for each image.

### 8.1.3 Aerial photography

Because most photogrammetric operations involve some kind of reference data, aerial photography was chosen to serve as an indispensable subsidiary means for the assessment of the IRS-1C imagery. Furthermore, the use of different input media was expected to allow certain inferences on the overall performance of the softcopy system used as well as on its suitability for specific applications.

The Forest Management Unit was fortunate enough to be able to acquire a set of black and white aerial photographs of the test area taken on 21/06/1997, shortly before the evaluation in the field was implemented. The flying mission was executed by the AOC (Aircraft Operating Company) based at Johannesburg, by order of one of the forest owners (Sappi Forests Ltd.). The mission yielded a set of photographs consisting of 41 single exposures, however for practical reasons only a small subset was selected in correspondence with the coverage of the satellite imagery. Appendix 8 demonstrates the position of the flying strip, indicated by the number of each photograph, with an IRS-1C scene used as backdrop.

The photography features the traditional *overlap* (i.e. in flight direction) of about 60%, which is necessary for extending horizontal and vertical control by photogrammetric methods. The *sidelap* between the flight lines amounts to about 20% and is requisite for proper coverage of the ground. A Zeiss RMK A15/23 camera with a focal length of 152.72mm was used for the acquisition of the photography. The average flying height of about 5740m above ground in conjunction with the focal length of the camera results in a photographic scale of about 1:30 000 with reference to the vertical datum. This scale can be considered sufficient for most interpretation and inventory tasks, though small features such as tips of young trees may not be identifiable (Akça, 1984; Hildebrandt, 1996; Howard, 1991). The entire set of photographs exhibits excellent quality in terms of contrast, crispness, and resolving power, and despite the adverse timing of the mission (09:00), the lengths of the

shadows have no significantly degrading effect on the discernibility of features. Moreover, the spirit level as shown on the instrument panel indicates that, as is desirable in general, the image geometry is near to perpendicular, implying that very little additional distortion of objects on the photographs was to be encountered.

In order to be used as input into a softcopy system, the analogue information of the aerial photography had to be transformed into a digital format. This process of digitisation is traditionally performed by means of scanners (for more information see also chapter 7.3). High scanner accuracy (as is for mainstream analytical plotters) is obligatory if the quality of the hardcopy is to be preserved and the introduction of geometric errors is to be avoided. To date, unfortunately only a very limited number of photogrammetric scanners are designed for additional use with hardcopies, therefore the second best choice, a high quality drum scanner (Linotype TC3000/10), as being employed in the graphic arts world, was used. After having run a few trials at various scan rates (with a rate of 1 250dpi<sup>24</sup> the achievable accuracy and the identification of features decreased considerably), the aerial photographs were finally scanned at a rate of 2 500 dpi, being equivalent to a resolution of 10µm. This rate also reflects the recommendations to be found in the dedicated literature (e.g. Kölbel *et al.*, 1996; Leberl, 1996; Petrie, 1997). Top performance photogrammetric scanners are able to produce pixel sizes of about 3µm (e.g. the Lenzar Lenzpro 2000/20001), however it has to be taken into account that the maximum attainable resolution of a film/camera system (including compensation for forward motion) ranges between 108 lp/mm (line pairs per millimetre) for panchromatic (black & white) photographs and 119lp/mm for colour photography (Hildebrandt, 1996; Kraus, 1993). Under normal conditions resolutions of about 50lp/mm can be achieved, corresponding to a digitising interval of 7µm. Pixel sizes smaller than this value cannot be achieved today with an acceptable effort. With a decrease in pixel size, the so-called *signal-to-noise-ratio* (as a measure for the quality of the sensor) also decreases to a magnitude of about 1, meaning that the noise is as large as the image information or signal (Kraus, 1993). Since the volume of data captured during the digitising process is very large, in many instances a compromise between the required resolution of the scanned image and the available storage capacity has to be established. In the existing case of

---

<sup>24</sup> dots per inch

an usual format of an aerial photograph of 23cm x 23cm, a pixel size of 10 $\mu$ m x 10 $\mu$ m and its representation by 256 grey levels, a disk space of about 560Mb was occupied, whereas a single colour image featuring similar characteristics would require a space three times as much. For storing the entire flight strip, 2.24Gb of data had to be managed. The scanned photography was stored on 4 CD-ROMS using a TIF (tagged interchange file) format.

#### 8.1.4 The DPW (Digital Photogrammetry Workstation) 770 by LH Systems

Some of the commercially available Digital Photogrammetry Systems have a long pedigree. They evolved more than a decade ago from individual pioneering systems devised by research groups in certain European universities and the specialised systems designed for military intelligence and mapping agencies in the United States. The system used for the analysis of the IRS-1C imagery in this study is based on high performance hardware and software originally developed for the Defence Mapping Agency (in the USA) with expertise from Dr. Uki Helava, the 'father' of the analytical plotter. The successor of Helava Associates, Inc., Marconi Integrated Systems, San Diego, USA, continues to supply military systems. A subsidiary formed an alliance with other partners in 1998, now called Leica Helava (LH) Systems. This company supplies systems to the commercial market through Leica and Zeiss. The latest release of this company, the DPW 770, represents a system at the top end of the performance and price scale and is commonly hosted by either a SUN Sparc or a Sun Ultra workstation, controlled by a Unix operating system. The configuration used for the IRS-1C project consisted of a SUN Ultra1 Creator 3D with a 64bit Ultra Sparc processor and a capacity of 384Mb RAM. A 9Gb harddrive storage space was required to handle the amount of imagery for the project. Two high resolution colour monitors are part of the system; one of them used for displaying system information, commands, etc., and the other (sometimes referred to as 'extraction monitor') for the display of the stereo image employing the NuVision screen system. The extraction monitor features a refresh rate of 112Hz, thus avoiding flickering and strain of the user's eyes. The set-up of the DPW770 featuring a SUN Sparc workstation and a NuVision stereo viewing system is shown in Figure 8.6.



**Figure 8.6** The DPW770 by LH Systems. A trackball is used for measurements (picture courtesy of LH Systems)

As an integral part of the DPW, the photogrammetry software being called SOCET SET (**Softcopy Exploitation Tools**) was launched in 1990 as a commercial version of specialist software used in the government sector. Being developed and distributed by LH (Leica/Helava) Systems, it has become the world's most popular digital photogrammetry suite with more than 1000 licences sold worldwide. For this project the latest version of SOCET SET, the 4.0.9 was used. Like its less sophisticated predecessors, it is based on a modular structure, and includes some third party packages for map compilation and DTM generation. The package is very user-friendly thanks to X-Windows and Motif interfaces, and the open architecture can be exploited for the integration of specifically tailored software written in C or C++ to meet the customer's particular demands. Some possible applications are:

- Processing of aerial photography, close range imagery and satellite data.
- Import and export of a wide range of popular formats of imagery (e.g. TIFF, ASCII, DXF, LAN, IMG, etc.), orientation parameters, block adjustment data, DTMs and vector map data.
- Automated triangulation.
- Digital Terrain and Surface Models (DTMs/DSMs).
- Line of sight analysis.
- Orthophotos, mosaics and image maps.
- Perspective scenes, walk-throughs and fly-throughs.
- Compilation with a wide variety of Leica and third party mapping and GIS packages.

Apart from the CORE<sup>25</sup> module, which provides basic photogrammetric functionality such as image import and export, the creation of image pyramids, project management, image enhancement, and orientation and triangulation, SOCET SET consists of a large number of optional modules:

- STEREO – stereoscopic viewing
- LANDSAT – Landsat imagery
- JERS – JERS-1 optical band
- ORTHO – orthophotos
- RADARSAT – Radarsat imagery
- IRS-1C – IRS-1C panchromatic imagery
- SPOT – SPOT level 1A and 1B panchromatic and multispectral imagery
- HATS – Helava Automated Triangulation System for block set up, automated generation and measurement of tie points, GPS import, block adjustment and blunder detection
- TERRAIN – automated DTM generation with interactive editing; now including Adaptive Automatic Terrain Extraction (AATE); generation of grid and TIN models (ATLAS by KLT Associates, Inc.)
- FEATURE – compilation with user defined attributes; semi-automated feature extraction
- PRO600 – compilation with Bentley Systems MicroStation95; option of Terrasolid
- MOSAIC – mosaicking from multiple images
- CONVERT – utility to transform orientation parameters between SOCET SET and various analytical plotters
- MAP – generation and output of mixed raster and vector images
- CLOSE-R – close range photogrammetry
- PSP – perspective scenes, walk-throughs and fly-throughs
- POSTSCRIPT – output SOCET SET raster images in PostScript
- EasyCopy/EasyConvert
- DEVKIT/TOOLKIT – libraries for developers.

---

<sup>25</sup> core module of SOCET SET

On-line links to GIS packages exist for Unisys System 9 and Clemessy GeoCity. Currently work is in progress such that SOCET SET's feature extraction module will be able to read and write ARC/INFO coverage files directly. Furthermore, developments are underway to accommodate future users of Ikonos2 and Quickbird imagery (Scott Miller<sup>26</sup>, personal communication, 1999).

#### 8.1.5 Ground data

As previously indicated, the employment of reference data (often referred to as 'ground truth') is vital for most remote sensing activities. The acquisition of these reference data traditionally involves collecting measurements or observations about the features that are being remotely sensed. In many instances, these data stem from field checks on the identity, extent, and condition of the object to be assessed. Ground truth can serve the following purposes:

1. To aid in the analysis and interpretation of remotely sensed data.
2. To calibrate a sensor.
3. To verify information extracted from imagery acquired by a space-, or airborne sensor (Hildebrandt, 1996; Lillesand and Kiefer, 1994).

The collection of reference data has to be performed in accordance with the principles of statistical sampling design.

The gathering of field data in the test area for this study referred to the more important forest inventory parameters such as tree height, dbh (diameter breast height), basal area, stand density, canopy closure, age, and ancillary information such as slope and aspect. For practical reasons, i.e. because of the simplicity of its implementation in the field, a systematic grid with a spacing of 50 metres between each sampling plot was chosen. The starting point for the determination of the first sampling plot was that of a single random character, therefore producing unbiased estimates of the population mean and variance for a random forest (Cochran, 1977; Shiver and Borders, 1996). The different inventory parameters were determined on a minimum of ten trees tallied, using angle count sampling, per sampling plot (for angle count

---

<sup>26</sup>Executive Vice President (Development) at LH Systems, San Diego

sampling see also Bitterlich, 1984). To obtain measurements of the various inventory parameters, the following instruments were used:

1. Forestor Vertex Digital Hypsometer (for tree height).
2. Measuring tape (for vertical distances).
3. Callipers (for dbh  $\geq$  7cm).
4. Kramer's dendrometer (for estimation of basal area per hectare).
5. Suunto clinometer (for slope).
6. Suunto bussole/compass (for bearing).

The crown density was determined by means of ocular estimation.

The measurements yielded the following results, being presented as average values for each stand:

**Table 8.2** Key information on compartment characteristics

Compartment	Species	Planting date	Mean height in metres <sup>1</sup>	Mean dbh in centimetres <sup>2</sup>	Mean basal area m <sup>2</sup> /ha	Stems/ha	Volume m <sup>3</sup> /ha
A 15	<i>E<sup>3</sup>. grandis</i>	01/1985	40.01	34.39	26.92	289.7	392.38
A 29c	<i>E. grandis</i>	02/1977	43.88	38.48	22.53	196.9	362.23
A 61/ 62	<i>E. grandis</i>	1983/84	41.49	31.66	23.73	310.5	376.43
R 19d/e	<i>P<sup>4</sup>. elliotii</i>	1970/71	28.32	42.15	21.70	156.6	236.73
R 33	<i>P. elliotii</i>	1931	43.38	70.80	-	127.0	855.72
R 40a	<i>P. elliotii</i>	01/1973	28.22	35.22	22.58	233.4	248.42
A 16a	<i>P. patula</i>	11/1989	13.34	16.81	16.90	784.3	86.77

<sup>1</sup> The mean heights are based on the calculation of the arithmetic mean for each compartment

<sup>2</sup> Mean dbh was calculated using the quadratic mean of the dbh

<sup>3</sup> *Eucalyptus*

<sup>4</sup> *Pinus*

A Safcol's Frankfort plantation

R Mondi's Klipkraal plantation

Mean height was calculated as the arithmetic mean of the heights of the tallied trees, although mean height is commonly defined as the height of the tree with mean basal area. The proposed method can be justified by the fact that firstly the dbh cannot be measured directly on either the satellite imagery or the aerial photography and secondly that the sampling size was very small. In addition, when employing the angle count method, the trees with a high dbh are more likely to be tallied than smaller trees. It is these taller trees which are the co-dominant and dominant trees that can be detected on aerial photographs.

The stand volumes were subsequently calculated in accordance with the formulae to be found in the South African Forestry Handbook (Bredenkamp, 1994), using the

mean height and dbh as input parameters. The equations used are based on the Schumacher and Hall model, written as:

$$\log_{10} V = b_0 + b_1 \log_{10} (D+d) + b_2 \log_{10} H$$

where: V = stem volume (m<sup>3</sup>, underbark), usually to 75mm tip diameter

D = breast height diameter (cm, overbark)

d = correction factor

H = tree height (m) (Bredenkamp, 1994).

Coefficients for the estimation of volume using the Schumacher and Hall model:

	b <sub>0</sub>	b <sub>1</sub>	d	b <sub>2</sub>
<i>Eucalyptus grandis</i> (general, 75mm top)	-4.2328	1.7154	-2	1.1070
<i>Pinus elliotii</i>	-4.6370	1.9306	0	1.1567
<i>Pinus patula</i>	-5.8497	2.4396	8	1.3254 (Bredenkamp, 1994).

Ground truthing was carried out in the period from August until September 1997, thus closely corresponding to the time of the flying mission. Even though the satellite imagery was acquired one year later, the height and diameter increment were not expected to have a major impact on the results, since the increment would not be adequately reflected in the vertical accuracy of the stereo model.

## 8.2 Methodology

The methodology section consists of the following ‘themes’:

1. A general description of the workstation (DPW 770) process flow. This particular section dwells on issues such as the import and orientation of imagery and photography, and the triangulation and rectification process. All these processes are crucial for the proper further analysis of the imagery (section 8.2.1).
2. The extraction of elevation information (such as tree height) in the softcopy environment. In this subsequent, fairly broad section information on the automatic generation of digital surface models (DSMs) and digital terrain

models (DTMs) is provided. Background information on the procedures of image matching, surface fitting and checking and editing of the extracted elevation data is given (section 8.2.2). General problems associated with the generation of DTMs from IRS-1C imagery are portrayed in section 8.2.3. Special attention is paid to aspects such as the automatic terrain extraction, the terrain editing and the terrain analysis in the SOCET SET environment (section 8.2.4).

3. A detailed account on the processes of import, orientation, triangulation and rectification of the aerial photography and satellite imagery used in this study can be found in chapter 8.2.5.
4. Chapter 8.2.6 deals with the actual extraction of the forest inventory parameters such as tree/stand height and compartment area from the aerial photographs and IRS-1C images. Issues such as the overall performance of the automatic terrain extraction algorithms, the fidelity of the stereo model of the imagery and the operator skills for the manual determination of the tree heights are addressed. The manual, semi-automatic and automatic determination of tree/stand height as employed in this study is described in detail.
5. In chapter 8.2.7 an account is given on the way in which the extracted inventory parameters can be used to determine timber volume. The emphasis is put on two forest inventory concepts, namely the two (three)-phase sampling using regression estimators and the Hegershoff method.

### 8.2.1 Workstation process flow

The following section describes general matters prior to the extraction of inventory parameters from aerial photography and satellite imagery. The reader being familiar with the DPW770 system is kindly requested to skip this section and proceed to chapter 8.2.2. The entire process flow from data input to the final product for the extraction of terrain features is presented in Figure 8.7 on page 91. More detailed information can be found in the SOCET SET user's manual provided by LH Systems (1998) and in a publication by Chapuis (1995).

A large number of different data files are usually created during workstation operation. These encompass terrain files, image files, and feature and ground point files. In order to organise these files in a manageable fashion, they are allocated and arranged in a suitable manner, as so-called *projects*. The data that are extracted from a set of imagery are stored in the project directory that contains that set of imagery. When creating a project, the co-ordinate system as well as a datum has to be specified. The key constraint imposed by projects is that all data stored in a given project must conform to the parameters of that specific project. Data in a different co-ordinate system have to be converted before entering into a project. SOCET SET supports a great variety of different co-ordinate systems such as UTM (Universal Transverse Mercator), Geographic (specified as longitude/latitude), and Grid/State Plane. The choice amongst various datums is even greater. Two distinct datums are required to establish a co-ordinate system for measurements on the Earth's surface: a horizontal datum as being represented by a smooth ellipsoid (e.g. WGS84, or Clarke1880), and a vertical datum using either the ellipsoid or the Mean Sea Level (MSL) Geoid as reference.

The *import* and *export* of data in a DPW environment traditionally concerns the transfer of information in the form of image files, ground point files, image point files, terrain files, and feature files (also known as vector files). The most common interchange data formats supported by SOCET SET include formats such as:

- Sensor support data: frame (conventional camera), SPOT (BIL, BSQ), Landsat, JERS, IRS-1C (BSQ, super structure), generic polynomial, map projections and orthophoto.
- Image (pixel files): Sun raster, plain raster, TIFF, Tiled (VITec<sup>27</sup>), Helava scanner, and JPEG.
- Terrain: ASCII, DEM (7.5 minute UTM type), and Intergraph DGN post.
- Vector/feature: DXF, ARC-INFO, and Intergraph DGN feature.

---

<sup>27</sup> Visual Information Technologies Inc.

## OVERVIEW OF WORKSTATION PROCESS FLOW

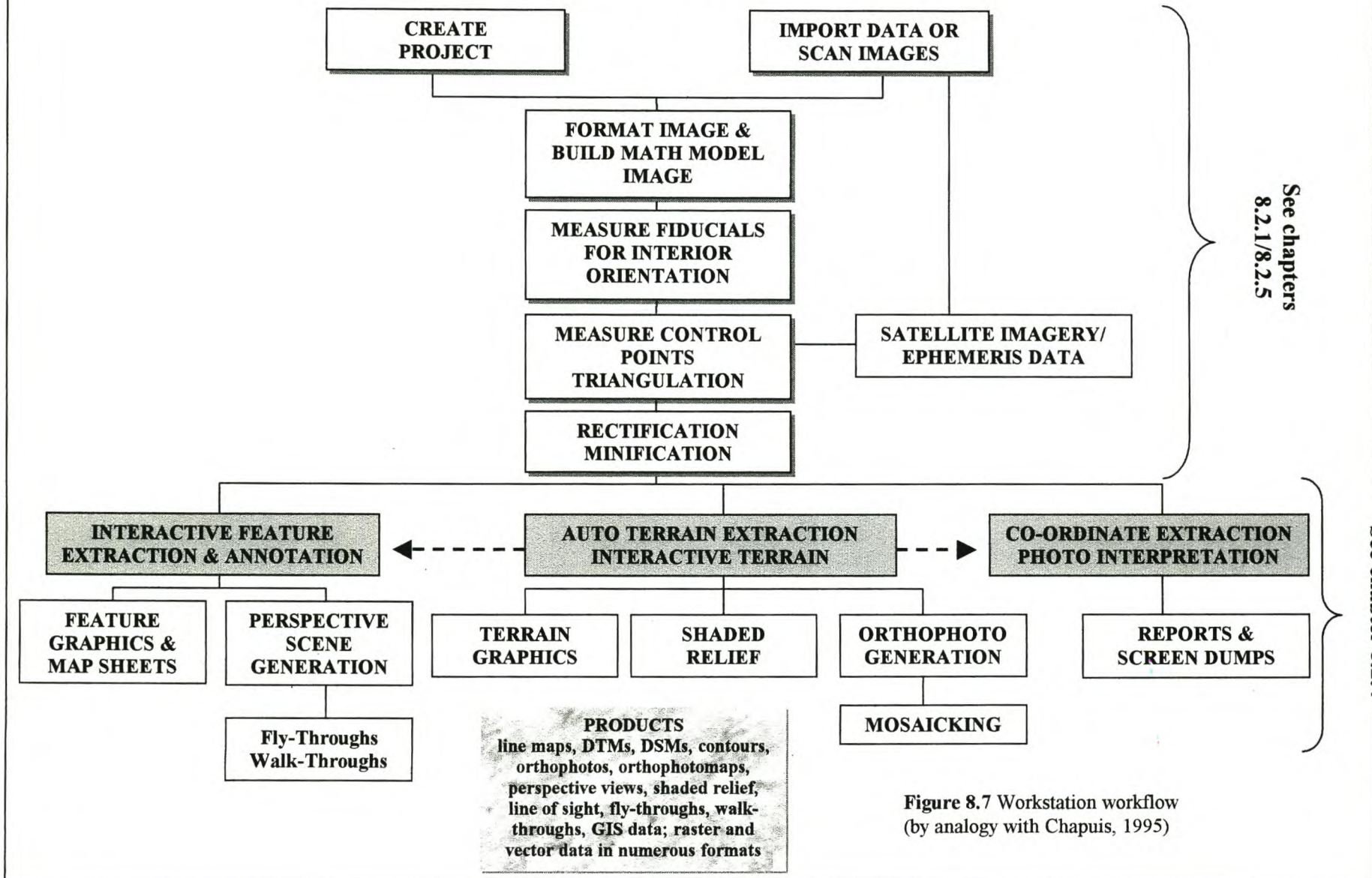


Figure 8.7 Workstation workflow (by analogy with Chapuis, 1995)

Image data can be handled as 8-bit greyscale or colour rasters or as 24-bit colour images. Unfortunately the SOCET SET software package does not allow the display of pseudocolour images.

Aerial photography is commonly referred to as *frame photography* when taken by a frame or panoramic camera. A frame camera is a conventional camera with simple projective geometry, and a frame image therefore is a digitised (i.e. scanned) version of such a frame photograph. Importing imagery represents one of the initial steps in a process flow after creating a project. Subsequently the frame import is typically followed by interior orientation, triangulation, and then finally by feature extraction or terrain extraction. The inputs to frame import not only include the raster image files, but even more importantly the image support data, thus containing the frame math model parameters. The latter can consist of triangulation information (camera position, attitude, focal length), scanned photo data (image dimensions and photo-to-image transformation data), camera calibration data (camera fiducial co-ordinates, lens distortion data, principal point offset), and very specific (e.g. ALBANY) triangulation results. All these may be provided in file formats or may be entered by keyboard. One of the key inputs to the frame import process is camera orientation. This is generally expressed as the angles omega, phi and kappa (see also previous chapter on interior orientation), defining a transformation from ground space into film space, or by entering the angles roll, pitch, and heading as sequential rotations. The orientation angles may be provided in the camera calibration file and/or other documentation accompanying the aerial photography. If this information is not supplied, there are opportunities to either have these angles computed by SOCET SET during the triangulation process or estimating the angles for pitch, roll and heading. These approaches, particularly the latter, are known to yield less accurate results than using the data from the flight report.

SOCET SET provides an option for accounting for atmospheric refraction. As being stressed in previous chapters, atmospheric refraction results in radial displacement of image points in a photograph (image). In phototriangulation, the effect of refraction is minimised by correct scaling of the initial model or by a corresponding change in the focal length of the projectors. A great number of models have been developed in the last few decades to compensate for the effects of this phenomenon (Baker, 1980;

Hildebrandt, 1996; Light, 1980; Lillesand and Kiefer, 1994). No specific information on this issue was available from the designer of the photogrammetric software. In order to be able to fully exploit the refraction models, accurate information on the location of the camera is required. This was unobtainable for the flying mission of this project, since the employment of highly sophisticated instrumentation such as kinematic GPS was unrealisable due to cost constraints. However, most of the influencing atmospheric effects could be eliminated, or at least attenuated, by use of highly accurate ground position data (ground control) within the triangulation procedure.

The import of IRS-1C/D imagery within the SOCET SET environment is straightforward and similar to import of SPOT imagery. It is important to notice that when creating a project that will include IRS images, the geodetic datum must be based on an earth-centred ellipsoid such as WGS 84. For this specific project the ellipsoid WGS 84 was chosen for the satellite as well as the aerial imagery, as the majority of modern maps and GPSs use this as a reference basis. The photogrammetry software package accommodates users of IRS panchromatic and LISS colour sensors, with the exception of band 5 of the LISS and the entire spectrum of the WiFS bands. Furthermore, only IRS' 'super structure format' is supported, since the other so-called 'fast format' does not contain any ephemeris information. The pixel data of IRS imagery is traditionally recorded in the formats BIL (band interleaved by line) and BSQ (band sequential), thus only BSQ is sustained. Of the four pre-processing levels being available for IRS imagery, the import options are limited to the levels '0-Raw' (i.e. raw, uncorrected data), '1-Browse' (imagery which contains radiometric and geometric corrections only for earth rotation) and '2-Standard' (imagery that has been radiometrically and geometrically corrected). Two panchromatic IRS-1C sub-scenes of the level '1-Browse' were acquired for this project. The entire area of the subframe was used for the analysis. However, SOCET SET also allows for importing just a portion of the image. During the importing process generally both the image and support (i.e. ephemeris) data are extracted and stored in subsequent files on the harddisk. Interior orientation is not required with IRS images, since the sensor is a digital camera, resulting in a known, fixed relationship between each image pixel and the sensor lens.

After having formatted the imagery and having built a mathematical model, *image enhancement* techniques can be applied for better visualisation of the imagery. For this purpose convolution filters, histogram operations, rotation tools, tonal transfer curve editors and the like are at the operator's disposal.

The *orientation* of digital metric images can be directly compared with the numerical orientation of metric images in an analogue format. However, the result of the orientation process of digital metric images goes beyond the mere determination of the six elements of outer orientation (i.e. the object co-ordinates of the camera position (X, Y, Z) and the three rotations of the photograph) of a metric photograph (Kraus, 1993). One of the first operations in most systems is orientation, often preceded by the creation of image pyramids. High levels of automation exist for interior and relative orientation (i.e. image control only using tie points, no ground control). *Interior orientation* creates a transformation from film space to digitised image space. The determination of the three parameters, namely the image co-ordinates of the principal point and the principal distance, are resulting values that are used in the subsequent computational procedure for the definition of the central projection of the photograph. Interior orientation is required for all images that have been created by scanning film, in contrast to non-film-based imagery such as SPOT and IRS-1C, where the ephemeris information from the header is exploited to create a proper model of the sensor geometry. In cases where highly sophisticated devices for scanning the photographs were used, the interior orientation information is provided with the digitised image. The image restitution begins with the determination of the individual fiducial (Réseau) marks of the digitised photograph. After having entered all the required information such as the number of the fiducial marks and their corresponding co-ordinates as being provided by the camera calibration report, the marks can then be measured either manually or automatically. Considering the latter, a correlation method commonly employed in feature extraction (image matching) is applied, where a specific search matrix is used to detect the target (i.e. the mark). SOCET SET provides three different types for transforming the obtained parameters from camera space to image space (e.g. affine transformation). The resulting root mean square error of the residuals, as given in pixels, ideally should not exceed a value of more than one pixel (LH Systems, 1998).

Interior orientation is usually followed by the so-called *triangulation*, also known as geopositioning, resection, and image registration. The purpose of this procedure is to register images to the ground and other images, therefore combining exterior and relative orientation. With triangulation the sensor models of the images are updated. The primary input are ground control points and tie points. Ground control points are identifiable objects in the image with known co-ordinates, whereas tie points are points found in the overlap region of two or more images for which no knowledge of ground location space exists. SOCET SET has been designed to handle imagery stemming from a variety of sources, so for example the software can orient a SPOT image simultaneously with a frame camera image. Furthermore, large blocks of frame images (as resulting in a bundle adjustment) and even imagery without initial support data are feasible options. The specific software module dealing with triangulation, called HATS (Helava Automated Triangulation System), automates the tedious procedure of selecting and measuring the image co-ordinates of pass points, tie points, and control points. Unacceptable tie points are automatically flagged and displayed for remeasurement without the operator's intervention. HATS uses and integrates existing support information from previous procedures (e.g. interior orientation, ground point control files), yet requiring further input information such as sensor type, forward/side lap of the imagery, aircraft altitude, and mean ground elevation. A point measurement strategy file (i.e. automatic or interactive) has to be selected in order to guide the hierarchical matching algorithm for the determination of conjugate tie and ground control points. A tie point pattern file, offering various options, is used to control the placement and number of tie points, which are needed for relative orientation. The recommended number of tie points is six (also referred to as 'Gruber points'), nevertheless a higher number will increase the accuracy of the resulting model (Hildebrandt, 1996; Jacobsen, 1998a and 1998b; LH Systems, 1998). Traditionally, a tie point pattern focussing on the edges of the overlap area yields sufficient accuracy, thus a design using evenly distributed tie point clusters seem to work very well for the HATS suite (Andrea Sassor, pers. comm.<sup>28</sup>, 1998). Tie points and ground control points can be used in combination for performing absolute

---

<sup>28</sup> Service assistant, Gebr. Wichmann, Berlin

orientation or either of these for single image absolute orientation (GCPs) or relative orientation (tie points).

Automatic point measurement measures the image co-ordinates of tie points in overlapping images and also transfers measurements of tie points and GCPs to other overlapping images (i.e. a strip). In cases where the matching algorithm fails, the interactive phase will automatically display the images that require remeasurement. After the successful performance of measurements, HATS can be prompted to compute the sensor model parameters. Blunders are automatically detected and invoke the operator for interactive editing. An accuracy and statistics report, providing detailed information on the resulting residuals of image co-ordinates of all points (tie points and GCPs), is a useful aid in deciding what points are to be remeasured, weights to be altered, or even excluded from further processing at all. Using the interactive point measurement tool, this procedure can be run repeatedly, until a satisfactory solution is found. In addition, an automatic parallax removal (i.e. Y-parallax) capability is available in this module to facilitate genuine stereo vision. The key indicator of the quality of the solution is represented by the root mean square of the image pixels. As a rule of thumb, these values should not be greater than 0.5 pixels (LH Systems, 1998). When accepting the solution, HATS will then update the residuals in the ground point and tie (image) point file, update the sensor model parameters in each image support file, and create a solution accuracy quality report for the project directory.

Triangulation may be followed by epipolar or relative to North *rectification*, for convenience in viewing and in later computational processes (e.g. for better correlation results in automatic terrain extraction), and the generation of another *image pyramid* (see also Appendix 14 for image minification). The process continues with the generation of products such as maps, DTMs, and orthophotos. A mapping tool (PRO 600), based on Bentley's Microstation, and an on-line GIS solution have been integrated into SOCET SET for the user's convenience (Chapuis, 1995; LH Systems, 1998).

The procedure for extracting terrain data is explicitly dealt with in the subsequent chapter.

## 8.2.2 Extraction of elevation data

The extraction of elevation information, whether it be performed in an automatic or manual manner, represents the vital core of this investigation. The following sections provide an overview on the key issues when extracting elevation information in a softcopy environment. Processes such as image matching, image minification, surface fitting and the inherent structure of automatic terrain extraction software (ATE, AATE) are being dealt with. The problems in terms of system performance (i.e. sensor modelling and DTM generation) and the design of the various sensor devices that are likely to be encountered when using IRS-1C imagery are described. The reader with prior knowledge is kindly requested to proceed to section 8.2.3.

### 8.2.2.1 Overview

Data conversion is a major cost of GIS, and one of the driving forces behind digital photogrammetric systems has been to provide a cost-effective and efficient solution for input of geographical data into GIS databases. Most GIS applications rely on the availability of accurate and timely digital terrain data (Bernhardsen, 1992, Bill and Fritsch, 1996, and Maguire *et al.*, 1991). Such data, in the majority being provided as DTMs or DEMs (the terms DTM and DEM are used interchangeably since the procedures of their generation as well as the quality are identical), can be either stand-alone products or be used for generating secondary products such as orthophotos. Digital photogrammetry systems provide an ideal environment for the generation of digital terrain products, as one of the indisputable advantages of this technology over traditional stereo plotters is the ability to automatically generate DTM. In this context the term 'automatic' is quite misleading since one would expect the computer to perform the same task that is usually assigned to an operator. Instead, human intervention is still necessary to some degree and will not become obsolete in the foreseeable future.

DTMs are traditionally used as input for:

- Contour generation.
- Generation of TINs.

- Calculation of slope.
- Calculation of aspect.
- Visualisation / perspective scenes (virtual reality).
- Verification/creation of orthophotos.
- Image draping (e.g. for flight simulation).
- Feature extraction.
- Texture analysis.
- Shadow analysis (line of sight, visual impact analysis).

The input of accurate elevation information is mandatory for a variety of applications such as:

- Hydrological modelling.
- Geological applications.
- Natural disaster management (e.g. avalanche modelling).
- Fire simulation / management.
- Modelling electromagnetic propagation.
- Civil engineering (road construction, etc.).
- Forest management.
- Military (e.g. warfare simulations and performance of ‘intelligent’ missiles).

Another possible useful application of elevation data is reported by Catlow (1986), who used DEM information in its primary form to correct radiometric and geometric effects in satellite imagery due to terrain variation over the image area. In addition, elevation data may be exploited for the modification of classification algorithms, simply by deriving from and subsequently incorporating ‘*a priori* knowledge’ into the dataset.

DTM data can be obtained from a variety of different sources. The extraction from aerial photogrammetry certainly still represents the major source, and using digitised contour lines from topographic maps is another popular option. Tachometric ground surveys still provide the most accurate co-ordinate measurements, but since being very cost-intensive, this method is becoming gradually replaced by modern satellite navigation systems such as NAVSTAR<sup>29</sup> and GLONASS<sup>30</sup>. Once captured, digital

---

<sup>29</sup> Navigation Satellite Timing and Ranging

terrain data can be further processed with specific DTM software packages such as ARC/TIN, HIFI, Intergraph Modeller, SCOP, Orthomax or SOCET SET'S DTM module.

DTM creation, surface reconstruction and feature extraction (object recognition) share a great number of problems. For that reason many software packages offer solutions for all three components, featuring a great variety of algorithms and approaches. Useful accounts are given by Bernhardsen (1992), Bill and Fritsch (1996), Busch (1996), Eckstein (1996), Förstner (1993), Grün and Li (1996), Heitzinger and Kager (1998), Heitzinger and Pfeifer (1996), Jamet (1996), Leberl (1996), Leberl *et al.* (1996), Maguire *et al.* (1991), McKeon *et al.* (1996), Rottensteiner (1996), Sagerer *et al.* (1996), Schenk and Toth (1991), Smit *et al.* (1996), Taylor (1991), Vohra and Dowman (1996), Wild and Krzystek (1996), Wrobel and Krauth (1996), Zhang and Kirby (1997), and Zheng (1993).

The observed points and breaklines, as measured manually, serve as input to the computational part of the DTM generation. In the process, various kinds of interpolation procedures such as polynomial, collocation, or spline are used to produce a regular grid. In order to achieve DTMs of high quality, an appropriate data acquisition (i.e. dense and qualified data) method is imperative. As a rule of thumb, the derived grid spacing should be two to three times denser than the original observations. In that fashion, the curvature of the terrain can be accounted for to a higher level. Numerous studies have confirmed that errors of the DTM increase almost linearly with the point distance for a given terrain (Ackermann, 1996a). In this respect rugged terrain in particular has a severe impact on the degree of fidelity of an interpolated DTM surface representing the real terrain. In addition to common criteria such as completeness, reliability, consistency and uniformity of the accuracy distribution within the DTM, the appropriate morphological description of the terrain by breaklines, peaks, etc. contributes to the quality of the DTM to a large extent. Although no generally accepted specifications about the accuracy of DTMs exist, for practical reasons it has become common for a DTM grid to be such that the vertical accuracy would correspond to about 1/20th of the linear grid size for smooth terrain

---

<sup>30</sup> Global Navigation Satellite System

and about 1/10th for rougher conditions (Ackermann, 1996a; Ackermann and Eslami Rad, 1996).

Manual data acquisition with analytical plotters usually comprises the extraction of between 2 000 and 10 000 points per stereo model. For a trained operator this task translates to an input of 1.5 to 8 working hours (i.e. about 2 to 3 seconds per point) (Ackermann, 1996). The scenario is very much different for DTM system automation within a softcopy environment. Compared to conventional systems, even interactive data acquisition performed by an operator is much faster, since softcopy systems use image matching algorithms for the determination of elevation. Depending on the desired density of the resulting grid, 10 000 to 4 000 000 data points are typically extracted from a stereo model. The automatic determination of up to 20 000 elevation points per minute is reported by LH Systems (1998) when carrying out the terrain extraction on a high performance hardware system (e.g. Sun Ultra, or Silicon Graphics Indigo). Such a terrain extraction session (with 2 000 000 data points), including automatic feature extraction, feature matching and grid derivation would then require about 15 to 20 minutes. However, automated DTM generation requires considerable additional interactive checking and editing which can range from about 1.5 hours for moderate terrain to about 4 hours per stereo pair for mountainous scenes. These figures comprise the manual capturing of breaklines and the correction of terrain points (Ackermann, 1996a). With the advent of more user-friendly and highly efficient editing tools, time consuming operator input can be kept to a minimum. Automatic terrain extraction employing digital photogrammetry systems has become operational and has proven to be economic in most cases. In addition, automated systems can measure many more points than can be done manually and has the potential to considerably improve the reliability and accuracy of the DTM. Due to high data redundancy, automatically derived DTMs has a very high accuracy potential. Accuracies of better than 1/10 000th of the flying height have been empirically confirmed (Ackermann, 1996a; Warner *et al.*, 1997).

When building terrain databases, the following problems can be identified for conventional analytical photogrammetry. This technology:

- Is costly, both in equipment and labour.
- Requires specialised equipment.

- Is excessively prone to human error.
- Is labour intensive and has slow production rates (i.e. low productivity).
- Requires extensive operator training (Allen and Shears, 1995).

Digitising contours or spot heights from hardcopy maps to create a surface:

- Involves an element of 'guesswork' since interpolation techniques can only speculate intermediate height values.
- Is likely to compound errors since map contours, if photogrammetrically derived, generally only have an accuracy of about half the vertical interval.
- May not be up-to-date when using outdated map material.
- Is labour intensive and time consuming.

Existing off-the-shelf terrain products:

- Provide fixed resolution for height data, which may be not appropriate for many applications.
- Give no control over accuracy and quality of DTM/DEM if such information is missing.
- May not be up-to-date.
- May not exist for specific geographical areas (Allen and Shears, 1995).

Most of these impediments can be surmounted by implementing digital softcopy technology. Digital systems not only exploit a greater range of imagery, but the performance in terms of collecting elevation points is about 2 400 times higher than achievable by an experienced mechanical system operator (Allen and Shears, 1995; Shears and Allan, 1996).

For the automatic generation of DEMs from a digital stereomodel the following three tasks have to be accomplished:

1. Find conjugate points (image matching).
2. Interpolate and densify the surface (surface fitting).
3. Check and edit the DEM (quality control).

The first two tasks usually do not necessitate any human interaction, whereas task three is truly interactive (Ackermann, 1996a; Baltsavias *et al.*, 1996; Jensen, 1996; Leberl, 1996; Maune, 1996; Schenk, 1996). A detailed description of the three essential tasks is provided below.

### 8.2.2.2 Image matching

The key issue of softcopy photogrammetry is to establish correspondence between individual points in two images, commonly referred to as image matching. In general, matching techniques are commonly applied in computer vision, pattern recognition and surface reconstruction. Finding conjugate points in two different images is particularly necessary for the creation of accurate stereo models (e.g. by using tie points) and the derivation of data thereof such as DTMs. The complexity of the matching task and the appropriate strategy will depend on several factors:

1. Is the task to match entities in the image domain (i.e. 'iconic'), or to match an image with abstract models 'symbolic' (e.g. change detection, or object recognition)?
2. Do the entities to be matched represent 2-D or 3-D information?
3. To what extent does the scene content vary (i.e. from natural terrain to highly structured urban environments)?
4. What constraints do exist from prior knowledge (e.g. camera geometry) (Nevatia, 1996)?

According to Zhang and Miller (1997) the following problems associated with the matching process can be identified:

1. Photometric (radiometric) problems: e.g. resolution, reflectance, illumination, exposure parameter differences, sensor noise, sensor radiometric calibration differences.
2. Geometric problems: Such as relief displacement, projective deformation, scale variation, base/height ratio.
3. Textural problems: Featureless surface (e.g. very homogenous forest stands, repetitive texture, thin objects, ambiguous levels such as tree top and ground below the tops).

Considering all the above dilemmas, the only system capable of overcoming these matching difficulties seems to be the human vision system. However, a few image matching techniques have proven to render very usable results. There are five major approaches: Intensity-based methods, edge-based methods, hybrid methods, symbolic and global matching.

### 1. Intensity (area) -based methods:

These methods match the conjugates of a point along conjugate epipolar lines and are based on the assumption that scene points have the same intensity in each image and that there is significant variation in image intensity in both images. A large number of image matching algorithms have been devised to match two signals (i.e. grey levels) by calculating the sum of squared differences or determining the correlation over a certain window. To overcome the matching difficulties such as the signal variation and the variation of the disparity within the window, window sizes must be adaptively selected. Unfortunately, these two factors present conflicting requirements since a large window tends to increase the signal variation, whereas at the same time it tends to include points of different disparity. Despite this conflict, this matching method is the preferred method in photogrammetry, since in this environment it works more accurately than feature-based matching (Tseng *et al.*, 1997). More sophisticated software packages offer an area-based image correlation technique which incorporates the assessment of a set of parameters such as terrain type, signal power, flying height, X and Y parallax, and image noise level. Sub-pixel accuracy in correlation can be achieved through the use of least squares matching techniques or by interpolation within the correlation function.

### 2. Edge (feature) -based methods:

Feature-based matching is predominantly applied in computer vision and feature extraction. Correspondence between image points is established by matching image intensity patterns along conjugate epipolar lines. They detect edges or other features and subsequently seek matches between these features' intersections with conjugate epipolar lines. This approach is based on the assumption that enough features exist, hence it does not hold for very homogenous, poorly textured images. On the other hand a very common problem, referred to as image noise, can be eliminated more successfully than in employing the area-based strategy, since image noise has less effect on edges than on image intensities (Zhang and Miller, 1997). According to Schenk (1996), edge operators are noise sensitive, since taking differences (i.e. edges) amplifies noise. Image-to-image registration by matching area features has been significantly improved by using Fourier descriptors in conjunction with neural networks (Tseng *et al.*, 1997). Feasibility studies of the edge detection technique are

provided for instance by Alwan and Naji (1996), Lo (1996), Maas (1996), and Tyukavkin and Beklemishev (1995).

### 3. Hybrid methods:

A combination of the previously mentioned methods, exploiting intensity value, intensity edge, variance value, variance edge, and first and second derivative values of image points to perform a correct match is known as hybrid methods. A variation of this method is presented by R  ther and Van der Merwe (1996), where the local structure of the features as well as the spatial relationships between the feature and its neighbours are taken into account in a two-stage approach.

### 4. Symbolic matching:

This matching technique refers to methods that compare symbolic descriptions (as referring to grey levels or derived features) of images and measure the similarity by a cost function. Symbolic matching is not strictly based on geometric similarity properties, rather on the comparison of topological characteristics.

### 5. Global matching:

Instead of matching local areas or features separately, this matching technique attempts to match all pairs of homologous image points or features within a simultaneous framework (Gr  n, 1985).

Many new techniques try to overcome the shortcomings of the suggested methods. Problems such as the presence of extreme scale variations within the matching process (due to foreshortening in the stereo pair), or the lack of accurate orientation information have been addressed and promising solutions (such as the employment of wavelet pyramids) have been presented (Agouris and Stefanidis, 1996; Pan, 1996; R  ther and Van der Vlugt, 1996; Vosselman, 1995). However, a great number of these approaches are far from being feasible at the present stage and require further scrutiny. A good survey of these issues and approaches is given by Ebner *et al.* (1993) and Heipke (1996b).

### 8.2.2.3 Surface fitting

Since matching is not always successful (dissimilarities in corresponding images are caused by different illumination, divergent recording of sloping terrain, i.e. geometric differences, etc.), there would be holes in the DEM even if all pixels were selected. The most commonly used remedy for that kind of problem is to interpolate values for the required 3-D points. In conjunction with this a host of methods have been developed which can be categorised according to criteria such as goodness of fit, extent of support (local versus global methods) or class of mathematical model (weighted average, polynomials, spline, etc.) (Schenk, 1996). Another method for surface fitting employs approximation algorithms, and some new approaches hinge on techniques which are commonly used in a GIS environment, such as the creation of Thiessen polygons or the employment of Fuzzy logic (Eastman, 1997).

### 8.2.2.4 Checking and editing

Although many softcopy systems provide internal quality check tools, the intervention of the human operator is still indispensable at the final stage of the generation process of the DEM. The quality control is traditionally implemented in an interactive environment where the DEM is first visualised and then edited if necessary. A quick assessment of the DEM can be performed by displaying the digital terrain data as a frame model or as a shaded relief model using an artificial light source. For the detection of subtle mistakes, however, it has proven successful to get a true 3-D display of the DEM superimposed on the imagery. A successful method to perform the quality control by iteratively refining the DEM employing orthophotos has been described by Norvelle (1992 and 1996). This technique can be applied for both generating and editing DEMs.

A completely different approach for the refinement of DEMs has been proposed by Piechullek and Heipke (1996). In their so-called 'Shape from Shading' (SFS) they exploit the fact that surface patches are imaged with different brightness in the images where the grey values of these patches are directly related to surface inclination. SFS performs very well in areas with poor image texture. However, correct results can only be produced when the reflectance properties of the surfaces are modelled

properly. Despite all advancements in computer technology, quality control remains a tedious and challenging process (Norvelle, 1996; Schenk, 1996).

### 8.2.3 Generation of DTMs from IRS-1C/D imagery

The deficiency in ground resolution of the SPOT imagery has resulted in much interest shown in the application of IRS-1C/D imagery that has 5m (resampled) ground pixel size. The panchromatic images of the Indian satellite pair currently provide the highest spatial resolution of the operational civilian cartographic space sensors usable for 3-D mapping. The results from numerous studies evaluating the mapping qualities of IRS-1 images show that this sensor system has the potential to outperform SPOT images and may even meet the cartographic requirements for 1:10 000 scale land use/analysis (Gopala Krishna *et al.*, 1996; Rao *et al.*, 1996; Srivastava *et al.*, 1996). In contrast, Jacobsen (1998b), and Jacobsen *et al.* (1998) found the information content and the pixel size of IRS-1C Pan imagery only able to produce satisfactory results at the 1:50 000 map scale. This conclusion has been supported by Armenakis and Savopol (1998) and Light (1980), who showed that an observer's eye cannot resolve better than 5-10lines/mm, thus translating into a minimum ground pixel size of 2.5 to 5m at the 1:50 000 scale. Meinel *et al.* (1998) and Jacobsen *et al.* (1998) suggest a workable scale of 1:25 000 for general data updating. High accuracies were achieved for the classification of various forest types for forestry applications in India (Roy *et al.*, 1996; Tiwari, 1994). It was found that forest biomass can be estimated with confidence, at an acceptable level of accuracy (Tiwari, 1994).

Stereo imagery acquired by IRS-1C/D has been on the commercial market virtually since the launch of the platforms in 1995 and 1997 respectively. Initially the radiometric and to some extent the geometric quality left a lot to be desired. After a number of modifications and improvements stereo pairs with considerable fidelity have reportedly only been available as from the beginning of 1998. This may have contributed to the fact that so few studies concentrating on the evaluation of IRS stereo imagery have been carried out so far. In addition, as far as is known, not a single paper exists to date giving adequate attention to forestry applications other than

for mapping purposes as part of a land use/cover project. In these cases stereo satellite imagery was only used for the reason that it facilitates the identification of features.

One of the biggest problems encountered when trying to fuse the three CCD sensors into one whole scene (i.e. 70km x 84km) seems to be geometrically related, since the sensors may have a different focal length, may not be parallel to each other, or be orthogonal against the optical axis, or there may even be a shift in the image plane. However, certain efficient and reliable methods and algorithms as described by Cheng and Toutin (1998), Jacobsen (1998a), Rosenholm and Åkerman (1998), Savopol and Armenakis (1998), and Srivastava and Alurkar (1996), have been devised to overcome this deficiency successfully. In conjunction with the modelling of the sensor geometry, Cheng and Toutin (1998) suggest that preference be given to the super structure format of IRS-1C data, since the fast format as provided by EOSAT does not contain any ephemeris and attitude information. The quality of ground control as well as the number of ground control and check points apparently determine the fidelity of the resulting geometry to a great extent. A planimetric accuracy (i.e. identification of control/check points) in the range of between 0.5 and 1 pixel can be realistically expected and has been confirmed by Armenakis and Savopol (1998), Cheng and Toutin (1998), Jacobsen (1998a), Rosenholm and Åkerman (1998), and Savopol and Armenakis (1998). The pointing accuracy has been found to lie between 0.2 and 0.7 pixels (Jacobsen 1998a). In terms of vertical accuracy, different results have been obtained. The proper determination of elevation points largely depends on the area (i.e. terrain) and almost more importantly on the base to height relation (B/H ratio). As a consequence, no fixed rules seem to exist for the required standard deviation. With an underlying B/H ratio of about 0.8 to 1.0, height accuracies of about 8 to 10m have been achieved, therefore translating to accuracies similar to those of SPOT (Jacobsen, 1998a; Jacobsen, 1998b; Jacobsen *et al.*, 1998; Savopol and Armenakis, 1998). A very weak value of about 20m was obtained in the test conducted by Savopol and Armenakis (1998), but this outlier is due to the poor B/H ratio of 0.087.

Many authors have complained about the lack of contrast in the PAN imagery. This is caused by the 6-bit quantisation, thus translating into 64 different grey values. In

many cases the radiometric resolution could be substantially improved by scaling it to 8 bit levels. It is thus not just the pixel size of an image which represents an important criterion for the successful evaluation, but it is also the spectral information provided. Another factor likely to become a real problem resulting in the degradation of the quality of a stereo imagery is the time delay between the separate image acquisitions. This can cause difficulties in cross identification of control/check points and failure of the image matching process. This dilemma is very common to SPOT stereo imagery, too. There seems to be no real remedy for this and only by changing to imagery acquired in an along-track mode could this be solved.

#### 8.2.4 DTM creation – characteristics of LH Systems' DPW770

##### 8.2.4.1 Automatic terrain extraction

The LH Systems' software package SOCET SET provides two different modules for the automatic creation of digital terrain data, namely the Adaptive Automatic Terrain Extraction (AATE) and the non-adaptive version thereof (ATE). There is also a variety of options for the operator to perform manual extraction of terrain information in the traditional way. The non-adaptive ATE method requires that terrain type does not change within each subregion of the 3D model, so that a unique set of correlation parameters can be implemented. There are quite a number of strategies (i.e. a given combination of parameters) for the user to choose from, ranging from flat to steep terrain, and prioritising from high-speed extraction to high-accuracy (i.e. low-speed) extraction and a combination thereof. A strategy has to be selected that is best suited to the imagery and its topography. To cater for different terrain types in an image scene, the various strategies can be combined and applied to the specific area where a certain terrain dominates. The DTM file that is created will always be rectangular, even though a polygon option is available, as posts (i.e. elevation values) outside the polygon will be marked with a value of "outside boundary" and will not be considered as valid posts by any applications. For both methods the DTM boundary has to be defined, furthermore the new DTM's post spacing needs to be specified. AATE can work on multiple stereo (multispectral) imagery simultaneously, whereas ATE can extract information only from one image pair at a time. Non-adaptive ATE process

normally utilises a Hierarchical Relaxation Correlation algorithm for locating conjugate data points in the stereo imagery and calculating elevation offsets based on the positional difference of these points (LH Systems, 1998; Zhang and Miller, 1997).

In contrast to the non-adaptive ATE the new AATE does not require the setting of correlation parameters and the creation of subregions owing to its adaptivity. AATE's inference engine consists of three components: A rulekit knowledge system, a set of inference rules, and an application interface. For AATE, the inference engine generates a set of image correlation parameters by a set of rules based on a group of facts. The latter is derived from the terrain type, signal power, flying height, and X and Y parallax. The (static) set of rules governs the rulekit knowledge system to produce a set of parameters for image correlation. As AATE progresses, new and more facts are derived and a more suitable set of parameters for image correlation are generated until an optimal solution is yielded. The set of rules being used by the inference engine generates image correlation parameters such as window size, search distance and correlation coefficient acceptance threshold values. One of the most crucial components in this context is the choice of the right window size as this determines the quality of the match of conjugate points. Window size and signal power (as measured by the variation of the signal within the window) are two conflicting parameters in image correlation, since a larger window tends to increase signal power, but at the same time tends to include pixels of different X and Y parallax and therefore unduly correlates the signals of corresponding pixels. Consequently, a window size must be adaptively generated depending on the variation of X and Y parallax and signal power to ensure the calculation of reliable and accurate X parallax (elevation value) at each point. The variation of X and Y parallax is the combination of the terrain factors slope and elevation variation, and image geometry. As a rule of thumb one can say that the larger the slope of the terrain and the elevation variation, the larger the variation in parallax (i.e. X and/or Y). In flat areas therefore one would expect small signal power, and hence the window size would be increased. Alternatively the window size should be decreased in areas of large terrain slope and elevation variation. As AATE progresses from the top of the image pyramid to the bottom, the terrain parameters are extracted and integrated into the model. The search distance in the X direction has to be adaptively generated too, since a distance being too large increases the probability of yielding a false image correlation. The

correlation coefficient peak as well as the amount of data processing are directly proportional to search distance. Search distances, which are too large, are at the expense of computing time, but on the other hand the correct X parallax cannot be computed accurately with a too small search distance. The variation in X and Y parallax are computed as AATE percolates the image hierarchy.

AATE exploits multiple images and selects the optimal pairs for image correlation for different areas by deciding on the images where the algorithm (AATE) can best “see” the terrain. The best image pair is a function of terrain slope, orientation, and sensor geometry, and features the least image relief distortions and obscurities. Furthermore, AATE can be used to generate a single DTM covering a specific area of the flight mission, i.e. the entire photogrammetric project. For this purpose AATE automatically determines the boundary of the DTM for a selected set of overlapping images. The whole process can be performed in batch mode (LH Systems, 1998; Zhang and Miller, 1997).

Inherent to all photogrammetric models is a number of systematic and random errors due to variety of sources such as lens distortion, ground control, tie points, film deformation and atmospheric refraction. For atmospheric correction in particular it is impossible to create an accurate mathematical model since the atmosphere is subject to highly dynamic processes. For this reason a residual Y parallax of one to two pixels is very common in a typical photogrammetric project. Searching in two dimensions to compensate for the Y parallax is not a practical solution, since firstly the epipolar constraint is not adequately used and, secondly, the computation effort is dramatically increased. AATE uses a dynamic Y parallax sampling algorithm that works as follows:

- Partition the terrain or image into small blocks;
- For every block, sample a number of reliable residual Y parallax points by searching in two dimensions;
- Use residual Y parallax from step two to compensate all image correlations within a block (Zhang and Miller, 1997).

The Y parallax gets accounted for while AATE progresses ‘on the fly’ (LH Systems, 1998; Zhang and Miller, 1997).

Image noise is not a problem out of the ordinary in digital photogrammetry. As image correlation is very sensitive to this kind of infidelity, the success rate of the correlation may drop substantially. Accordingly the accuracy of the DTM may degrade because interpolation methods are employed to fill in the missing points when the algorithm rejects a match. AATE uses a typical convolution filter to reduce image noise.

Test results demonstrate the superiority of AATE over the previous non-adaptive ATE with substantially higher image correlation success rates (Bacher, 1998). According to Zhang and Miller (1997) the DEM accuracy showed an improvement of 15 to 35% on the average. However, the new AATE algorithm, like other commonly applied image matching techniques, failed in situations where shadows and very poor signal characteristics occurred on the imagery.

The following steps have to be performed for the terrain extraction using (A)ATE (see Figure 8.8 on page 114 for graphical representation of this workflow) :

1. Import stereo pair(s).
2. Solve sensor models of the stereo pair(s) by running interior orientation and triangulation.
3. Pairwise rectify the images.
4. Minify the imagery.
5. Create DTM file.
6. Merge geomorphic features into the DTM (optional) (LH Systems, 1998).

After importing the stereo pair(s) and performing interior orientation and triangulation, the imagery has to be rectified. Subsequently a minification procedure is necessary to allow for quick zooming and to support the matching process (for image minification see Appendix 14). A digital terrain model can now be created and a feature database containing geomorphic features (such as drains, breaklines, lakes, and ridges) be integrated.

(A)ATE automatically creates a terrain grid from stereo imagery. The terrain grid is usually stored in the project co-ordinate system but can be transformed into various other co-ordinate systems and projections within the SOCET SET environment. The (Adaptive) Automatic Terrain Extraction module determines elevations by measuring

the X parallax in the rectified images. The algorithm, which is used iteratively, begins with the small minification level image and sparse post spacing, increasing the post density for each minification level until the original scale of 1:1 is reached. SOCET SET's (A) ATE Statistics Window provides a user-friendly tool where information about the status of the terrain extraction correlation algorithm is retrievable while (A)ATE is running. Once completed, the elevation as well as the accuracy of every post is stored in the output DTM file. On the average 70% to 95% of the posts generated by (A)ATE do not require any further editing by the operator (LH Systems, 1998). For those posts that do not meet the requirements concerning certain accuracy limits, the Interactive Terrain Editing tools can be used for review and adjustment.

SOCET SET provides the capability to display DTM data on the monitors. Display parameters such as DTM representation (mesh, contours, profile, etc.), post spacing (every n-th post), and colour-coding technique can be selected. Furthermore overlays of other terrain data can be incorporated into the display.

## TERRAIN EXTRACTION WORKFLOW

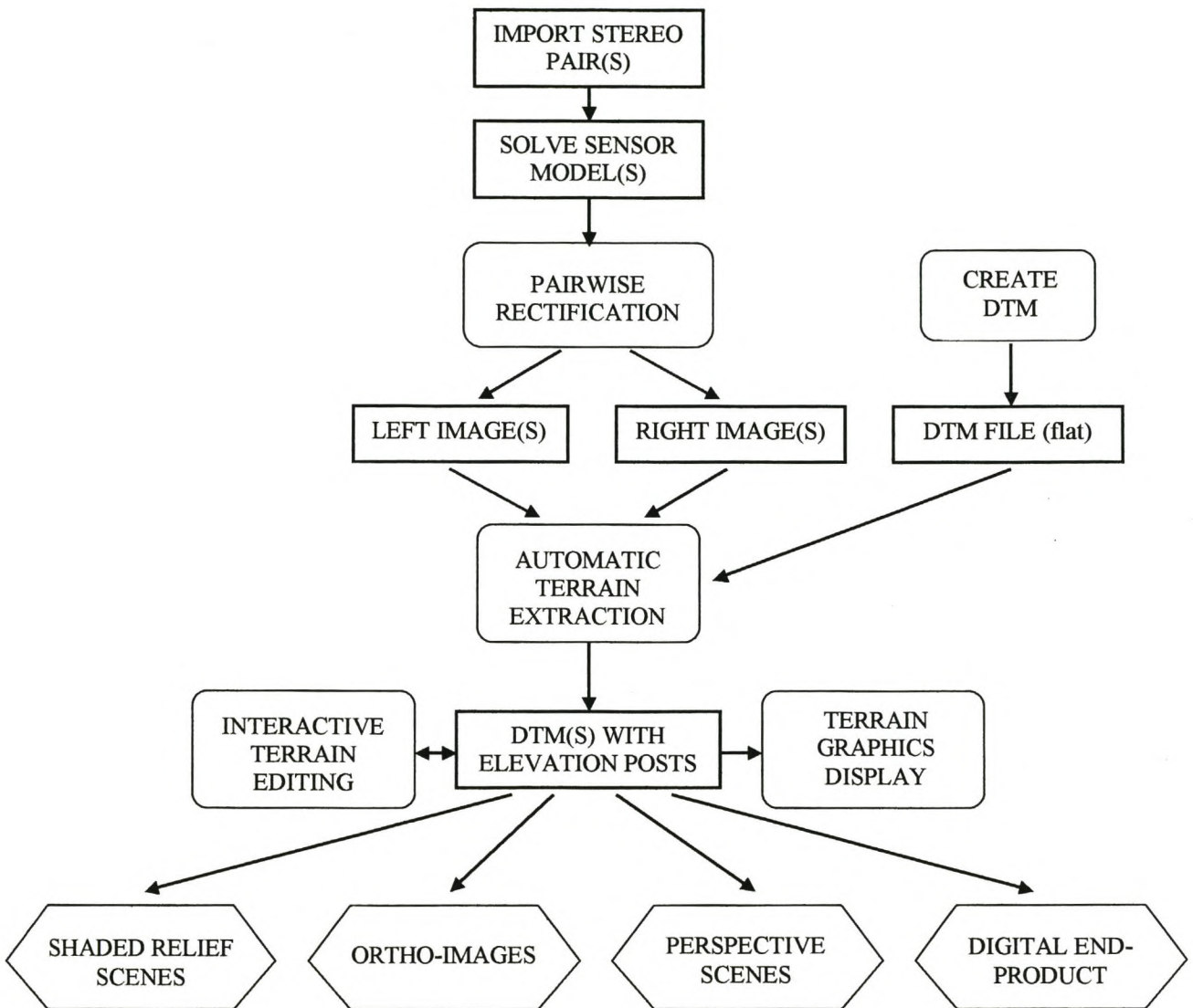


**Figure 8.8** DTM creation – flow diagram for automatic terrain extraction on the DPW770 (LH Systems, 1998)

#### 8.2.4.2 Interactive Terrain Edit

SOCET SET's Interactive Terrain Edit (ITE) module is used to interactively review and edit DTM data. ITE contains tools that will remove buildings, trees, hedges, and other artefacts. In addition, DTMs can be smoothed, forest canopies can be removed and lakes be filled. Traditionally ITE is applied in the following circumstances:

1. To display a DTM graphically (as dots, a mesh, contours, with or without imagery).
2. After (A)ATE has been performed for review of DTM. Edit tools permit the filling of regions obscured by cloud cover, enhance ridges, and in general edit areas that ATE was unable to correctly correlate.
3. New DTM in large-scale urban imagery, to account for buildings.
4. Review imported DTM from other systems.
5. Converting DTM to vector format
6. Image Map Overlays, where DTM overlays can be etched into image maps.
7. Before performing (A)ATE, to provide better results in specific cases (e.g. mountain ridges). (A)ATE will not override the edits that will be made.

Terrain data can be interactively edited with tools such as the *post-*, the *area-*, and the *geomorphic editor*. The *area editor* changes all posts within an area delineated by a polygon. It is used for filling lakes, smoothing, planefill (e.g. for the creation of virtual forest floors), interpolation, etc. The area edit tool offers a suite of statistical filters (e.g. 3x3, 5x5 convolution) and interpolation algorithms (e.g. 1<sup>st</sup> order, 2<sup>nd</sup> order, bilinear) for removing noise from elevation data, for filling planes and eliminating artefacts (such as buildings). A specific tool has been designed for filtering out objects such as trees, hedges, and houses, where the height and the width of the object to be eliminated has to be entered. The *geomorphic editor* represents a very powerful means for the adjustment of terrain profiles. It forces DTMs to conform to linear features like ridges and drainage lines, and for this purpose resets elevation points within the DTM, based on their distance from the delineation. DTM points that are further away than the specified distance will not be affected. The *post editor* has been designed for detailed editing operations. With a click of a button a particular post can be grabbed and arrow buttons allow the cursor to be moved

between posts. The user can then adjust the elevation of the post by moving the trackball. Crucial information for editing such as elevation and Figure Of Merit (FOM) is displayed for guidance. The FOM provides a numerical value as assigned by the terrain extraction process. It may either indicate a questionable automatic measurement, a successful or good performance, or the type of editing that was employed. Examples for FOM definitions are 'low\_signal\_power', 'low\_correlation', or 'large\_diff\_signal\_power' (LH Systems, 1998).

A new technique, described by Norvelle (1996) can be used to correct the digital elevation data obtained employing digital correlation methods on terrain stereo images. The strategy provided by SOCET SET, referred to as IOR (Iterative Orthophoto Refinement), generates an orthophoto from each of the input images given a DTM and exterior orientation parameters for a stereo pair. Any positional difference in conjugate points between the two orthophotos is assumed to be caused by error in the input elevation data. Subsequently, elevation corrections are calculated and applied to refine the original DTM. New orthophotos can then be generated from the updated DTM and the process repeated in an iterative fashion until no measurable mismatches exist. Feasibility studies have shown that the IOR method can be more accurate and up to 10 times faster than conventional correlation on original stereo imagery followed by manual or interactive editing. Under normal circumstances, only two to three iterations are necessary to obtain a correct DTM (Norvelle, 1992 and 1996).

#### 8.2.4.3 Terrain Analysis

After successful terrain extraction, the resulting DTM may be re-registered in cases when better ground control was later received or an imported DTM has to be shifted to conform to ground truth. The DTM registration tool then warps the DTM so it aligns correctly with the region's topography (LH Systems, 1998).

Correctly extracted terrain data may be subject to further analyses since various kinds of information can be derived from elevation points. For this purpose SOCET SET provides an export/import option, where DTM format conversions for several

interchange formats, including DEM, ASCII, DTED, and Intergraph DGN Post are supported. Moreover, the software allows the user to specifically define a DTM output file format.

Most of the previously mentioned procedures and tasks such as the generation of TINs and contours, the visualisation of perspective scenes, feature extraction and shadow analysis carried out with SOCET SET, can be treated with confidence. SOCET SET provides a couple of useful features for better visualisation and further manipulation of the terrain data. So for instance by using the 'terrain analysis module' two different products from DTMs can be created. This would be either a visibility analysis mask for gaining viewshed information, or a shaded relief image by shading output image pixels according to the sun intensity reflected off of the terrain slope of a particular geographic area. In addition, the 'line of sight' tools allow the user to evaluate potential placements of objects that are sensitive to line-of-sight obstructions (e.g. antennas, power plants, etc.), and with the 'perspective scenes' tool photo-realistic three-dimensional scenes from user-specified viewpoints can be achieved. The 'feature extraction module' is very useful for the creation and storage of a database of three-dimensional point, line, and polygon objects including rivers, roads, buildings, lakes, and ridgelines. The information extracted from the imagery is stored as vector data and is either manipulated further in SOCET SET's add-on GIS module or exported for the use in specific GIS packages (LH Systems, 1998).

#### 8.2.5 Terrain extraction from aerial photography and IRS-1C imagery

In order to provide a better understanding of possible error resources and various influences governing the determination of elevation data, a few key procedures preceding terrain extraction are briefly reviewed. The descriptions are supplemented by flow charts (Figure 8.8 on page 114; Figure 8.7 on page 91 for more general information) depicting the process of extracting terrain data. Although standard procedures for the extraction of terrain information have been in place for a few years, the complicated structure of forest areas as well as the imponderables inherent to the IRS-1C imagery made it necessary to develop and adapt methodologies while

proceeding with the terrain and surface extraction. Thus, some overlap of the methodology section with the results section is to be expected.

#### 8.2.5.1 Interior orientation

Only film-based imagery has to be subjected to interior orientation (Kraus, 1993; LH Systems, 1998). The aerial photography of the test area was digitised by a non-photogrammetric scanner and some minor errors in terms of geometric fidelity were to be expected (see also chapter 8.1.3). An average RMSE of 1.6 pixels for the entire set of aerial photographs was calculated, and this translates into a ground distance of 54cm. A rule of thumb is that results better than one pixel are required, and the above value is thus too high. However, as the intended usage of the photography was the comparison with IRS-1C imagery, the result was considered to be acceptable (Andrea Sassor<sup>31</sup>, pers. comm. 1998). Since no adverse effects such as shrinkage or swelling of the photography could be identified, it was assumed that the presented residual error is directly related to the scanning process.

#### 8.2.5.2 Triangulation

This is the most crucial part of the sensor modelling process, since the accuracy of the resulting model determines whether the subsequent procedures such as terrain extraction, or the generation of orthophotos will succeed or fail. The results of the triangulation process performed by SOCET SET are shown in Table 8.3. More detailed information is provided in Appendix 4, presented as a 'Solution Accuracy Quality Report'.

---

<sup>31</sup> Service and support assistant, Gebr. Wichmann, Berlin

**Table 8.3** Accuracies (RMSE) obtained for ground control and tie points for aerial photography

RMSE control points:			
Image ID	X (m)	Y (m)	Z (m)
529	1.168	1.900	0.814
530	0.982	1.573	0.869
531	0.676	2.095	0.863
532	0.491	2.526	0.059
Average for ground control (all 4 photographs)	0.902	2.061	0.753

Fourteen corresponding ground control points (e.g. road intersections, corners of buildings) were identified on the satellite imagery, aerial photography and the topographical map and then measured in the field using a highly (i.e. sub-meter) accurate real-time DGPS<sup>32</sup> (Trimble Pathfinder XRS). The points had to be well distributed over the entire test area (see also Appendix 10). However, for the triangulation procedure only eight of the fourteen measured ground control points were used for the calculation. Two of these eight points yielded very poor residuals and were subsequently discarded, whereas the remaining points could not be unambiguously identified on some photographs or were located beyond the overlapping area of the strip. Clearly, the requirement of achieving a RMSE better than 0.5 pixel (i.e. 0.15m in this particular case) is not met. However, as the aerial imagery served as a mere comparison medium to evaluate the performance of IRS-1C imagery in this study, the results were considered acceptable. The high RMSE values in the Y-direction can be attributed to a sub-optimal performance of the drumscanner for this direction.

The results of the triangulation process for the satellite imagery are shown in the following table 8.4.

---

<sup>32</sup> Differential Global Positioning System

**Table 8.4** Accuracies (RMSE) obtained for ground control and tie points for IRS-1C imagery

RMSE control points:			
Image ID	X (m)	Y (m)	Z (m)
Scene 1	5.834	6.068	2.521
Scene 2	5.834	6.068	2.521
Average for ground control (both scenes)	5.834	6.068	2.521

The RMSE values are identical for both scenes, since the same ground control and tie points were used in the overlap area of scene 1 and scene 2. The situation was totally different for the solution for the aerial photography. Because of the block structure of the set of photographs different ground control and tie points were used for each aerial photograph (see also bundle block adjustment in chapter 8.2.1 on page 95). The solution accuracy report presented as Appendix 4 indicates good results for the IRS-1C imagery in ground space in general, in particular for the height (Z) value (ranging from -4.26m to 4.69m). These outcomes compare well with the results achieved by Jacobsen (1998a and 1998b), and outperform the reported height accuracy by a factor of about three (8.7m). This is quite surprising, as the B/H ratio of the imagery exploited in this study (i.e. 0.57) was much poorer than in above mentioned investigation (i.e. 0.8). After having implemented the sensor model (see also chapter 8.2.5.2 for results) the optimism about the remarkably good results was dampened. Elevation errors of up to 12m occurred when looking at the ground control and check points. A possible reason for this might be the algorithm structure intrinsic to the triangulation software. The simultaneous solution in SOCET SET is a fully weighted bundle adjustment programme. If ground control is used with a high accuracy (0.5m as in this case) and the measurement is performed in imagery with a coarse resolution (i.e. 5m here), and thus the image co-ordinate accuracy is 0.5 pixels, then the residual error is forced into the image space. Hence, even though the ground residuals are small, it is likely to have a one or two pixel residual in image space. Combining this with a poor B/H ratio of IRS-1C, there is a good chance of getting a large Z problem in the magnitude of about two pixels (Scott Miller<sup>33</sup>, personal communication, 1998).

<sup>33</sup>Executive Vice President (Development) LH Systems, San Diego

### 8.2.5.3 Rectification

Rectification has the benefit of enabling stereo visualisation and furthermore permits ATE to correlate the imagery much better and thus yield higher quality DTM data. The procedure was carried out on the IRS-1C imagery as well as the aerial photography. The imagery was rotated relative to North, using a bilinear interpolation method for the resampling procedure.

### 8.2.6 The extraction of forest inventory parameters

The first attempts to introduce aerial photographs as a remote sensing tool in forestry were made in 1887 (Van Laar and Akça, 1997). Since then, the methods for extracting forest inventory parameters such as tree height, crown closure, crown diameter and stand area have been gradually improved. Subsequent technical development (e.g. analytical plotters, softcopy systems) and computational advances (e.g. regression statistics) have contributed very little to change the fact that most inventory parameters can only be determined when these are visually detectable and measurable. These limitations become rather apparent when dealing with satellite imagery. Unfortunately, the appearance of high resolution satellite imagery has not yet managed to present an effective remedy for this situation. The limited spatial resolution remains one of the major shortfalls, resulting in problems when it comes to identify and measure single objects, particularly those with a complicated and diverse structure such as trees. This condition is also applicable to the high resolution IRS-1C imagery, where only very big solitary trees or at least groups of smaller trees can be discerned. The picture presented as Figure 8.3 on page 76 conveys a very good indication of the implications of limited ground resolution. In some part of the IRS-1C imagery, forest stands appear as big greyish blobs. Mere visual inspection will not permit any deductions about the inherent forest structure. It was therefore decided to extract only the stand height from the satellite imagery and use the area of the stand as ancillary information for the calculation of the timber volume. The situation was very much different for the exploitation of the aerial photography compared to the IRS-1C images. The flow diagram for the extraction of certain forest inventory parameters from aerial photographs and the IRS-1C imagery is shown in Figure 8.9 on page 122.

Although taken at a fairly small scale, i.e. at 1: 30 000, single trees could be identified on the aerial photography. Subsequently the measurements of their heights could be used to calculate the stand (mean) height. No further parameters, except the area, were evaluated from the aerial photographs, as the focus of this investigation was to investigate the potential of high resolution satellite imagery for forest inventory purposes. Thus, the aerial photography was employed only as a reference tool. Finally, the information as obtained from the extraction of the spaceborne and airborne imagery, as well as the results of the terrestrial inventory were critically assessed and compared to each other in terms of validity and accuracy.

As mentioned before the adaptive automatic terrain extraction (AATE) algorithm was given preference for the creation of the surface and terrain models. A number of studies (Bacher, 1998; Kätsch and Stöcker, 2000) and own trials have indicated that the AATE strategy appears to be best suited for the tasks to be carried out.

Although the terrain extraction essentially centred on the determination of the stand/tree height, further information was sought about the actual generation of the elevation models. Some of the questions concerning the procedure were:

1. What is the overall performance of AATE when dealing with a big variety of objects in terms of size and structure?
2. Furthermore, what kind of error and what magnitude are to be expected in conjunction with image matching failures, and what are the implications thereof?
3. What kind of degradation does the sensor model (i.e. decrease of elevation accuracy) suffer when applying image enhancement techniques such as contrast stretch and image sharpening/smoothing?
4. To what extent do the skills and the experience of the operator effect the outcomes when elevation data is manually extracted?
5. What is the fidelity of the stereo model created from the IRS-1C scenes compared to the (presumably) much more accurate model of the aerial photography used as reference?

# EXTRACTION OF FOREST INVENTORY PARAMETERS IN A SOFTCOPY ENVIRONMENT

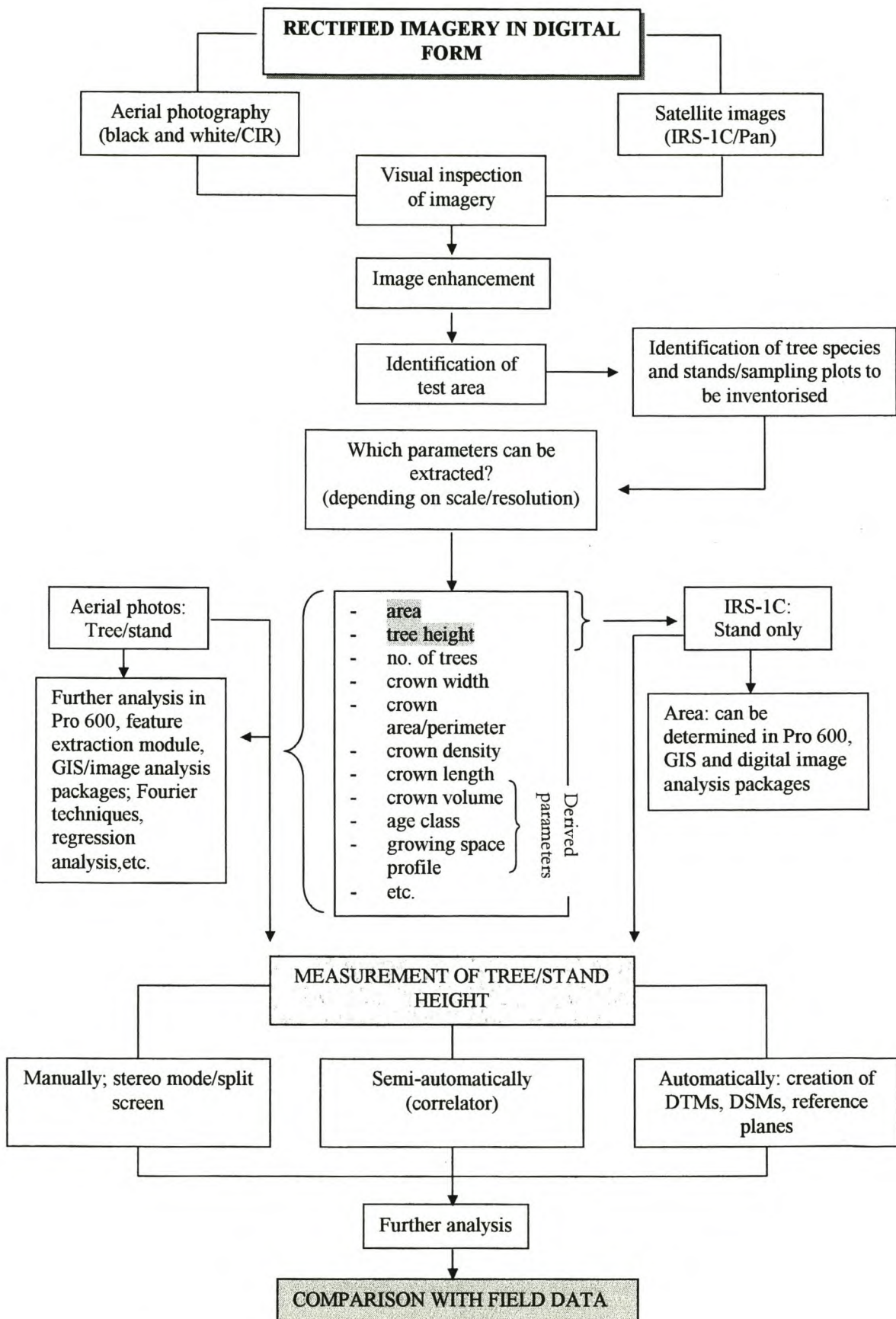


**Figure 8.9** Flow diagram for the extraction of forest inventory parameters from aerial photographs and satellite imagery

Although automatic terrain extraction methods (as a key component of digital photogrammetry software) have been in use for some years now, surprisingly little information is currently available on the performance of these procedures with application to forested areas. To the author's knowledge, only two studies dealing with this specific issue have been published so far (i.e. Carson *et al.*, 1996; 1997), even though concentrating only on the exploitation of digitised aerial photographs. Ergo, not a single publication is in existence on the analysis of stereo IRS-1C or SPOT imagery in this respect. Thus, prior to the automatic determination of tree heights in the test area, the scrutiny of the AATE module for the decision on a suitable strategy was indispensable.

With regard to the first and second question (on page 121), AATE was used to generate contour lines, which were subsequently superimposed on the stereo imagery. By visual inspection it was then possible to assess to what degree certain objects and features such as trees, buildings, and gorges in the imagery (i.e. satellite imagery and aerial photography) had been properly represented in the terrain model. In addition, the contour lines of a digitised topographical map (sheet 2530BB Sabie, scale 1:50 000) were used to get an impression on how well the model matches with the map features. Moreover, the resulting DTMs as created by AATE were inspected visually for image matching errors and blunders, as these were to be expected due to the time gap between the acquisition of the two IRS-1C scenes (e.g. clearfelled and burned areas). The statistics of the terrain models as reflected in the FOMs were assessed and the interpolation process for the 'bad' points verified.

The application of image enhancement techniques has become a standard tool not just in an image processing context. For the user's convenience, simple procedures such as the manipulation of contrast and brightness are now executable in many software packages dealing with display of graphics. Looking at the processing of images one has to be particularly aware of the fact that any kind of manipulation (such as contrast stretching), unless used only for the sheer convenience of display, will change the original pixel value of each image point. The resulting effects are not always conducive to a proper analysis of the imagery, since they consequently might be quite deceptive. It is known to remote sensing specialists that image enhancement has the potential to improve or degrade procedures such as image classification substantially.

It can be safely assumed that this is not just true when working in a two-dimensional (X, Y) but also for a three-dimensional (X, Y, Z) image space. Therefore it was crucial to look into this matter more deeply, especially taking into consideration that many IRS-1C users perform some kind of image enhancement to remedy its radiometric deficiencies.

In order to evaluate the effects of the image enhancement techniques, posed as question 3 above (page 121), identical ground points were measured on the enhanced and the original IRS-1C image. These ground points were then checked for deviations from the elevation information in the image that had not been manipulated. Contour lines, as generated by AATE from the original and the enhanced image, were superimposed on the original stereo model for comparison. This process was then followed by visual inspection to find out whether the image enhancement had any effect on the shape on the contour lines and how well these represented the true characteristics of the terrain.

The skills and experience of the person executing the height measurement play an important role in the quality of the extracted information (Akça *et al.*, 1984; Hildebrandt, 1996; Howard, 1991; Lillesand and Kiefer, 1994). Operators enjoying dissimilar degrees of skill and experience interpret parts of the model in different ways. Some persons might encounter problems with the proper positioning of the floating mark on the ground level in difficult terrain, others with the identification of certain objects (e.g. tree tops). Consequently, the bias induced by such variation can be substantial (Theodossiou and Dowman, 1990). In particular with the small parallax differences and the coarse pixels of the IRS-1C imagery in mind, it was interesting to see what the outcomes of a trial would be in terms of accuracy and consistency. For this purpose three persons with different levels of experience and skill were asked to perform manual height measurements in the satellite imagery, similar to the procedure of extracting elevation data in an analytical plotter. The three operators had to repeatedly measure the intersection of a forest road, the edge of a well-textured forest stand as well as the edge of a stand featuring a low image texture in the IRS stereo model. One of the test persons (denoted as No.2) was well experienced in the operation of analytical plotters, with a sound general background in photogrammetry. Test person No.1 had undergone thorough training on a softcopy

system, but showed little experience with analytical plotters. The project operator (denoted as test person No.3) himself had gained some experience in handling analytical and basic photogrammetry systems, featuring an in-depth exposure to digital photogrammetry technology. The zooming level of the IRS imagery was kept constant, while the colour and shape of the extraction cursor could be changed for the operator's convenience. The reading of the elevation data was carried out by an independent observer, so not to provoke any bias on the operator's part.

As indicated before (see question 5 on page 121), accuracy assessments for the ground space may yield results much different to the ones obtained in image space. In order to get an impression about the authenticity of the satellite stereo model in image space, eight checkpoints were used and cross-checked with the values of the corresponding points in the aerial photography.

Three different modi supported by SOCET SET, namely manual, semi-automatic, and automatic (AATE) were applied for the subsequent extraction of terrain data. This was to render information on the performance, efficiency, and accuracy of the various solutions.

#### 8.2.6.1 Manual extraction of elevation information

The manual determination of object heights is very much the same as in a non-digital environment (e.g. analogue plotter or mirror stereoscope with parallax bar), where a floating mark has to be positioned at the top and the base of the selected feature. The reading of the resulting parallax difference gets converted into real world geographical units such as meters and represents the real height of the object.

After the successful completion of the test phase (see above for operator trial), the heights of seven selected forest stands were determined by the project operator and one of either evaluator. The extraction of the height information on the aerial photography was carried out by the project operator only.

In brief the following comparisons were carried out:

1. Average tree height for each corresponding sampling plot on the IRS-1C imagery and the aerial photographs (for compartments A29c and A15 only because of the time consuming procedure).
2. The calculated mean height for each individual compartment in the satellite imagery and aerial photography.
3. Calculated mean height for each sampling plot in aerial photographs and for each plot on the ground (for compartment A15 only because of the time consuming procedure).
4. Calculated mean height for each compartment in the aerial photographs and for each stand on the ground.
5. The calculated mean height for each individual stand in the satellite imagery and the corresponding information obtained from the terrestrial survey.

Tree heights were measured on the IRS-1C imagery in a random manner (i.e. by drawing random numbers and then allocating these to points on a regular grid superimposed on the area where it was possible to carry out height measurements), since the proper identification of the terrestrial sample plots was not possible on the satellite scene. In this respect it was more important to find a location with a distinct parallax difference, rather than try to reproduce the sampling grid of the ground survey. The determined mean tree heights for each plot/stand as extracted from the aerial photography were used as reference. For comparison between the determined height on each measuring point in the IRS-1C imagery and the aerial photographs the following method was applied. For practical purposes ten (visible) trees nearest to the corresponding location of the measuring point on the satellite imagery were measured in the aerial photographs. Subsequently the arithmetic mean height was calculated for each particular measuring point in the aerial photography and set against the single value obtained from the IRS-1C image. Due to the inherent characteristic of the satellite imagery (i.e. coarseness) an averaging effect on the elevation information (e.g. tree height) could be expected.

The suggested procedure for the height determination for each individual sampling plot on the aerial photography was to identify the ground locations of the sampling

plots in the photographs and then perform the measurements on ten trees nearest to the plot centre (for bias in estimation of tree height see also Hildebrandt, 1996; Howard, 1991; Van Laar and Akça, 1997). SOCET provides a tool where the operator can manually enter the co-ordinates for a specific point and the cursor then moves to the designated location. Another tool enables the user to measure horizontal distances (e.g. distance from tree to plot centre). The calculated arithmetic mean of the heights was then set against the information as obtained on the ground. Because of the time consuming character of this procedure it was only applied to one compartment.

At least eight measurements were carried out for each compartment on the satellite imagery (only in areas with sufficient parallax difference) and more than 15 on the aerial photographs to obtain the stand height. The common procedure was to superimpose a dot grid onto the imagery/photography with numbers assigned to each dot. Subsequently random numbers were drawn and the height of the tree closest to the designated dot on the grid was measured. Stand height was calculated as the arithmetic mean of all individual measurements. The results were then set against the mean heights obtained from the ground samples. The mean heights for the terrestrial sample (per sampling point) were obtained by taking the arithmetic mean of the heights of a minimum of ten trees being tallied in the angle count sample sweep. Since thicker and thus higher trees are more likely to be counted using the angle count method, the results of the calculation of mean height would correspond much better to the measurement on the satellite imagery and aerial photography. The overall mean height per compartment was determined by calculating the arithmetic mean height of all individual height measurements (see also chapter 8.5).

The delineation of the stand boundaries, as to achieve the stand area, was performed using the PRO600 CAD add-on module in SOCET SET. This process was very similar to on-screen digitising, which has become a standard tool of many GIS and digital image processing packages. Once the designated areas are delineated the area gets calculated automatically by the software.

### 8.2.6.2 Semi-automatic determination of elevation

All forest areas were assessed again on the satellite imagery and aerial photography in a second phase, this time making use of the auto correlator option as catered for by SOCET SET. This technique employs a specific image matching algorithm (i.e. area-based matching), which allows the operator to efficiently and most accurately determine the position and elevation of selected features, provided that the image matching process does not fail. In the latter case, the operator has to intervene and guide the computer to the correct location of the conjugate point. The auto correlator was chosen to assist in the correct identification of the treetops, which were either obscured by shadow or difficult to determine visually. For the determination of the tree/stand heights the same procedures as described above were applied.

### 8.2.6.3 Automatic extraction of elevation data

The generation of surface models of tree canopies is not new to the user community. These models, usually created by means of an analytical plotter, provide information on the inherent structure of a forest stand such as texture (roughness) and tree height (Beleit, 1994; Hildebrandt, 1996; Van Laar and Akça, 1997). In order to achieve a realistic representation of the canopy, the construction of a fairly dense grid of elevation points (i.e. 1m to 2m distance between grid points) is essential. This task has become easy and straightforward with the advent of new systems amalgamating the strength of computer technology and photogrammetry. However, knowledge of the underlying structure and performance of the algorithms used for the automatic extraction of the elevation parameters seems mandatory.

The surface of a tree canopy is characterised by a marked discontinuum of elevation, thus an automatic measurement tool must be designed to handle sudden and abrupt changes within short distances. In comparison, a rocky and rugged surface of a steep mountain cannot be a greater challenge. Although SOCET SET provides a variety of strategies to accommodate various terrain types, only the adaptive method AATE appeared to be suitable for accurately modelling a highly dynamic canopy relief. With non-adaptive ATE it is possible to alter the parameters in the specific strategy files, so for instance the threshold for the correlation parameters can be set to different

values (Scott Miller<sup>34</sup>, pers. comm., 1998). By contrast, the adaptive terrain extraction (AATE) is much more complex and complicated in its structure as the algorithm uses an inference engine to generate a set of image correlation parameters. Since detailed information on the structure of the algorithm is not available to customers (also referred to as ‘black-box’ systems), any alterations of the structure are not recommended. Thus, the user simply has to rely on the accurate performance of this module. With this in mind, the sole possible way of assessing the accuracy of the system is to perform a comparative study, using information such as elevation data from other sources. However, a number of studies have demonstrated the supreme qualities of AATE when automatically extracting elevation data from aerial photography, even in difficult terrain such as forested areas (Bacher, 1998; Carson *et al.*, 1996; Carson *et al.*, 1997; Kätsch and Stöcker, 2000; Stöcker, 1999). Nevertheless, a few minor problems remain to be solved, particularly concerning boundaries shared with flat, open areas and dense forests (Bacher, 1998). In light of all presented facts, in particular because of the lack of adaptability of the ATE strategies, priority was given to AATE in the investigation described here.

In order to achieve a numerical profile of the stand heights, a DTM representing the ground level (i.e. forest floor) as reference base, as well as a corresponding digital surface model (DSM) of the tree canopy had to be created. To distinguish the canopy model from the actual terrain model (DTM), the term ‘Digital Surface Model’ (DSM) was chosen for the former. The process of determining the stand/tree height can be subdivided into the following steps:

- Select the specific stand and create a reference plane (DTM).
- Generate a surface model of the canopy (DSM), using the same boundaries as in step 1.
- Verify the accuracy and quality of the models and edit interactively if necessary.
- Export the obtained elevation data of both models and calculate the elevation differences (i.e. tree/stand height).

The designers of the AATE software recommend as a rule of thumb to use a post spacing for the DTM and DSM of about 5 to 10 pixels (LH Systems, 1998).

---

<sup>34</sup>Executive Vice President (Development), LH Systems, San Diego

However, in a few specific cases selection of a denser spacing can achieve a better representation of the surface (Andrea Sassor<sup>35</sup>; Scott Miller<sup>36</sup>, pers. comm., 1999). In this case 2m was chosen for the aerial photography and 20m for the satellite imagery to achieve the densest possible post spacing.

The initial task was to create a reference plane for each stand. This is the most tricky part of the process, as the incorrect definition of the reference plane can lead to substantial errors in the final calculation of the stand height. Since no sufficiently accurate information from other sources could be exploited, the only option was to manipulate the data from existing stereo models of the imagery. A method based on the calculation of a regression level suggested by Akça (1989) and others (Van Laar and Akça, 1997; Stöcker, 1999; Wolff, 1992) did not yield accurate enough results. Due to the high stand density, no gaps within the stand could be identified for subsequent use in the calculation process. Fortunately, SOCET SET provides a specific option in the Interactive Terrain Edit (ITE) tool, which permits the changing of posts within a determined area such as for filling lakes, planefill, interpolation, etc. The boundaries of the stands were then delineated on ground level by a polygon and filled with posts by smoothly interpolating from the perimeter delineation. In this case the 2<sup>nd</sup> order polynomial produced the best results. The outcomes of the IRS-1C planefills were later compared with those obtained from the aerial photographs, whereas in turn these were evaluated against the contour lines of a topographic map. Despite the small scale of the map, one could get a fairly good idea about the characteristics of the topography of the test area.

The adaptive automatic terrain tool (AATE) was then used for the generation of a surface model based on the above-mentioned post spacings and the perimeter delineation as performed in the planefill operation. The intermediate products, in the form of meshes, contour lines, and regular dot grids (indicating the corresponding FOMs) then had to be superimposed on the stereo imagery to check for blunders and accuracy. In the process, the display of the FOMs revealed very useful information about the correlation and interpolation results of each elevation post. For example

---

<sup>35</sup> Service assistant, Gebr. Wichmann, Berlin

<sup>36</sup> Executive Vice President (Development), LH Systems, San Diego

elevation points were indicated as 'LOW\_SIGNAL\_POWER' when the signal power for the right or left image patch in the correlator did not meet AATE's power cut-off threshold, or a very good correlation was indicated by a value of 95. Unfortunately the software does not permit the simple subtraction of values from different elevation models. As a result tree height cannot be determined in batch mode. The terrain data had therefore to be imported into a spreadsheet software package (e.g. MS Excel was used in this case) for further manipulation. Once the co-ordinates of each elevation point had been transformed from radians into the project units (i.e. longitude, latitude, with WGS 84 as reference ellipsoid), the difference of the elevations representing the canopy surface and the corresponding ground points, thus indicating tree height (if the top of the tree was marked by a post), could be calculated. Finally the surface model of each stand was graphically displayed and could be viewed from various perspectives to check for fidelity.

Since the obtained elevation information using AATE showed some unexpected and unusual characteristics (e.g. sudden drop of the elevation value), some methodology had to be developed while proceeding with the further analysis of the terrain data. For this reason, some overlap of the "Results" section with the section dealing with "Methods" can be expected.

#### 8.2.7 Forest inventory concepts

The primary objective of forest inventory is the estimation of volume of standing timber in a forest. In the process of obtaining reliable volume estimates, certain parameters such as tree height and crown diameter have to be estimated through accurate and cost-effective sampling methods. Two well-established methods, namely the 'two-phase sampling' and the 'Hugershoff method', which have been applied successfully in the remote sensing and photogrammetry user community, were investigated. More information on sampling designs used in forest inventory can be found in Appendix 13.

### 8.2.7.1 Two-Phase Sampling Using Regression Estimators

Two-phase sampling has found beneficial applications in forest inventories since aerial photography are available to obtain quick and inexpensive estimates of the auxiliary variable (e.g. tree height, crown diameter). In the first phase, a large number of image plots have to be established either in a random fashion or by generating a systematic grid. In the course of the process, a relatively easily determinable auxiliary variable ( $x_i$ ), which is known to be well-correlated with the variable of interest ( $y_i$ ), is measured in each sampling unit, i.e. the image plots. In the second phase, a random subsample (from which both variables  $x_i$  and  $y_i$  were determined) is drawn from the main sample and measured on the ground. The second phase data are used to construct a regression equation between the target variable (e.g. dbh) and the auxiliary variable (e.g. tree height). Subsequently, by substituting the first phase data in the regression equation, an estimate of the variable of interest can be obtained.

The estimation process for two-phase sampling with regression is identical to the process for regular regression estimation. Thus, the resulting equation is:

$$\bar{y}_{\text{dstr}} = \bar{y} + b(\bar{x}' - \bar{x})$$

where:  $\bar{y}_{\text{dstr}}$  = mean of variable of interest for double (i.e. two-phase) sampling with linear regression

$\bar{y}$  = mean of variable of interest from second-phase sample

$b$  = slope of the regression

$\bar{x}'$  = mean of auxiliary variable from first-phase sample

$\bar{x}$  = mean of auxiliary variable from second-phase sample (Shiver and Borders, 1996).

It is important to point out that the described sampling method is successful and efficient only if the auxiliary variables and the subject variable are closely correlated. One of the major prerequisites for the success is that the sampling plots on the ground can be unambiguously identified in the imagery. If this requirement cannot be met, the two-phase sampling will not be more cost-efficient than simple random sampling.

Detailed accounts on two-phase sampling using regression estimators can be found in Akça *et al.* (1993), Avery and Burkhart (1988), Cochran (1977), De Gier and Stellingwerf (1994), Hildebrandt (1996), Kättsch (1991a), Kättsch (1991b), Kättsch and Van Laar (1994), Lötsch and Haller (1964), Shiver and Borders (1996), Van Laar and Akça (1997), and Wolff (1992).

The only auxiliary variable that could be measured on the satellite imagery was the tree (stand) height. For the determination of the regression estimator, a correlation between the terrestrially obtained mean heights per sample plot and the heights as determined for the imagery (i.e. aerial photography and IRS-1C scenes) was established. If the correlation between the different heights (i.e. for height ground data height against aerial photography and height aerial photography against height IRS-1C) were satisfactory (i.e. high  $R^2$ ), then this relationship could be exploited to resolve the regression equation for the mean *dbh* used as variable of interest (i.e. correlation between tree height as determined in IRS-1C imagery and *dbh* from terrestrial sample). However, a high correlation between *dbh* ground survey and height aerial photography had to be a prerequisite for further calculations. If this condition was met, the results would then be used as input for the calculation of tree and stand volume (formulae as proposed in Chapter 8.1.5).

The identification of the ground sampling plots on the aerial photography was not too difficult after a correction for the terrain (i.e. slope) was established. The manipulated ground co-ordinates were then entered for the extraction cursor of the digital photogrammetry workstation to be automatically driven to the specified location. Unfortunately, in many cases, the existing shadows due to the low sun angle hampered an accurate measurement of the tree heights. The tops of the trees were either obscured or simply too small. However, the auto correlator option of the SOCET SET software was a valuable aid in finding reliable locations of treetops.

With the IRS-1C imagery these problems were negligible. Due to the inherent coarse resolution, it was absolutely impossible to resolve single trees. In order to be able to perform height measurements in the satellite imagery, priority had to be given to the existence of sufficient parallax difference within the selected stands. Due to the coarse spatial (i.e. in planimetry and elevation) resolution of the imagery, it was only

close to the edges of the specific stands that parallax differences big enough could be encountered. As a result, it was decided to confine the evaluation to the particular areas of the imagery where edges could be detected. Fortunately, when dealing with rather homogenous objects such as plantations, the height variability of the trees can be assumed to be fairly small (Howard, 1991; Van Laar and Akça, 1997). The edges of the compartments, where the measurements could be carried out, can be considered as strata. Within these strata the points for the actual height measurement to be performed were selected randomly (using random numbers and a dot grid). The number of measurements was limited by the size of the edge. The ground sample plots nearest to these image plots would then have to be used for the establishment of the correlation. However, for practical reasons, sampling plots on the aerial photography (with ten trees visually selected closest to the centre of the plot) were used as reference instead of ground sampling plots, since most of the latter were not situated close enough to the edge of the compartment. Because of the averaging effect of the coarse IRS-1C resolution, one measurement on the satellite imagery was considered corresponding to the average tree height per sampling plot (i.e. the average of 10 trees) on the aerial photography (see also chapter 8.2.6).

Since data from two different remote sensing media (i.e. aerial photography and IRS-1C imagery) were used to estimate dbh ground survey, the two-phase sampling (using only one remote sensing medium) is in fact to be considered a three-phase sampling.

#### 8.2.7.2 The Hugershoff method

For forest inventory purposes as well as for assessments in growth and yield, the determination of the mean height of a forest stand is much more important than the height of a single tree. The mean stand height can be estimated by either measuring a number of single trees or by evaluating the vertical stand profile. The measurement of such profiles was devised and introduced by the German engineer Hugershoff and his colleague Neumann already in the late 1920s (Akça, 1983; Hugershoff, 1933; Hugershoff, 1939; Lötsch and Haller, 1964; Van Laar and Akça, 1997). The method has gained very little interest in the user community because of the laborious capturing of the required data when using analog instruments. However, with the

advent of modern analytical and digital photogrammetry systems, the construction of such profiles is substantially facilitated.

The suggested method is based on the principle of linear taxation, which allows the quick and efficient determination of tree heights and the number of the individual trees in the stand (Hugershoff, 1933). In this context it is important to mention that the profile touches the ground at several points so that the surface level can be determined (Lötsch and Haller, 1964).

A number of studies have indicated that the mean height of the vertical stand profile, calculated as the area of the profile divided by its length, does not yield a reliable estimate of the mean height of the stand. In addition, it has been shown that the greater the roughness of a canopy surface, the smaller the mean height of the profile is in comparison with the mean height of the stand. The relationship between the various height estimates in a vertical stand profile is shown in the following figure.

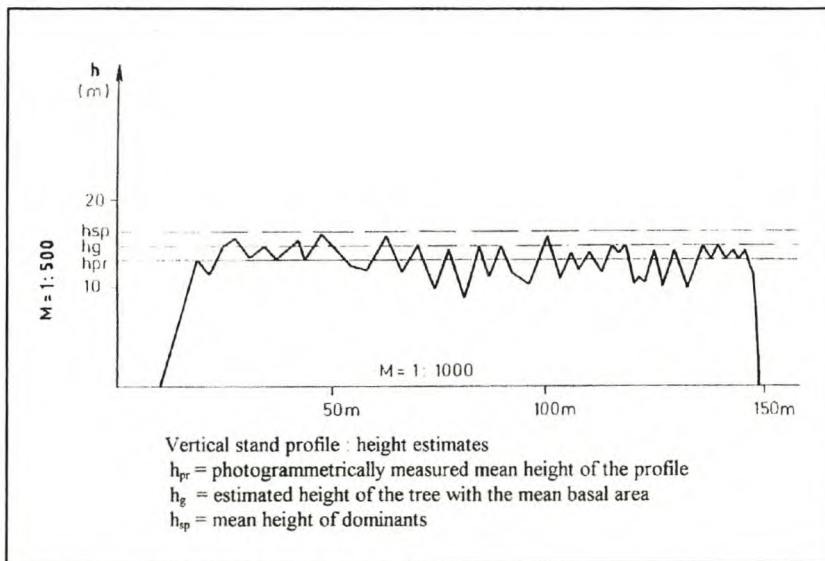


**Figure 8.10** Example of a vertical stand profile: It is shown that the height estimates using the photogrammetrical profile method are unlike the estimates for the tree with mean basal area (Van Laar and Akça, 1997)

The mean height of the profile averages the area beneath the curve, whereas the mean height of the stand is represented by the height of the tree with the mean basal area. Nevertheless, more accurate results can be obtained from a fitted regression equation with profile height or profile area as the predictor and true stand height as the target

variable (Van Laar and Akça, 1997; Prof. A. Akça<sup>37</sup>, personal communication, 1998; 1999).

The method as proposed by Hugershoff and Neumann can be used to estimate the growing stock of a stand. The growing space is obtained as follows:

$$R = a \times D$$

Where  $R$  = growing space of the stand,  $a$  = area of the profile and  $D$  = distance between profiles. Subsequently, the growing stock of a specific stand is a result of the multiplication of the calculated growing space and the stocking index (as retrieved from conventional yield tables or determined in ground surveys). This method produces satisfactory results in even-aged dense forest stands. Hugershoff (1933; 1939) reports accuracies of between 93-95% compared to terrestrially obtained timber volumes.

This method works best when choosing a high density for the measurements in conjunction with the measuring points coinciding with a tree top, therefore representing the real height of a tree (Prof. A. Akça<sup>38</sup>, personal communication, 1998). Despite the fact that the IRS-1C imagery features a fairly coarse ground resolution, thus implying that no single trees can be identified, precisely this coarseness might be an advantage because of its inherent levelling character. The procedure was to first obtain a graphical display of the extracted elevation data (i.e. tree heights) and then to transform this information into the frequency domain using a Fourier transform to check for consistency, frequency and possible noise (i.e. errors). The idea was then to employ regression equations for the calculation of the profile height to serve as input for the estimation of the growing stock.

---

<sup>37</sup> Head of the Department of Remote Sensing, Faculty of Forestry, University of Göttingen

<sup>38</sup> Head of the Department of Remote Sensing, Faculty of Forestry, University of Göttingen

the neighbouring pine stand. In this context it was a reasonable assumption that this kind of performance might have been an indication for the lack of flexibility of the terrain extraction algorithm. The portrayed phenomenon also applies to areas which had been clearfelled, so special care had to be taken when constructing terrain models from parts of the image that were most likely to be effected by this kind of blunder. Matching errors in aerial photography were found to be less severe due to the finer ground resolution, allowing for higher adaptability of the matching algorithm.

### 9.1.3 Image enhancement

The IRS-1C satellite imagery as used for this investigation rendered an overall good but not optimal contrast (see also Appendix 9 for image histograms). Although a few small white spots occurred in the scenes, indicating a failure of the sensor system, no action in terms of radiometric manipulation was taken as the flaws were located outside the actual test area. However it was interesting to see what happened to the elevation values once image enhancement was applied to the stereo model of the imagery.

A split image of the same area (as shown in Figure 9.3) is presented in Figure 9.4, indicating the original image on the left-hand side and the sharpened image on the right. At a first glance the texture seemed to have improved (i.e. it looks more ‘crisp’) on the right image, however owing to the coarsening character of the sharp filter some detail was lost.

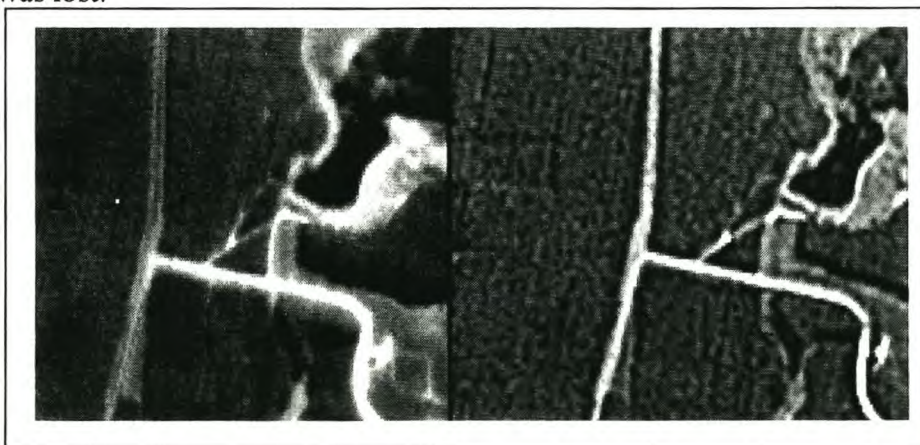


**Figure 9.4** Effect of image sharpening (original image on the left, enhanced image on the right): the image on the right appears much more crisp, thus at the expense of detail; a sensor failure in the left image (indicated as a white dot on the left) was eliminated through filtering (right image – the pixel value of the neighbouring elements was used for interpolation)

conditions required temporary image manipulation such as the adjustment of contrast (e.g. performing a histogram equalisation or a Gaussian contrast stretch).

#### 9.1.4 Trial assessing the operator skills

Due to the limited 3-D impression caused by the B/H ratio and the resolution, it was rather challenging and a predicament for all test persons to find a suitable zooming level. When zooming in to a certain convenient level, it was easier to identify objects and find locations more accurately. Unfortunately as a result the spatial perception of the model was degraded to such an extent that the height measurements could not be executed with sufficient confidence. Finally a zooming level to accommodate the various aspects could be agreed upon. The results of the accuracy assessment are disclosed in the following Table 9.2. For each of the three selected features ten measurements had to be taken. After each measurement, the test person had to move to the next feature, in order to avoid any bias. Furthermore, the readings were documented by an independent person, so the trial was performed without any prior knowledge of the elevations to the three operators.

**Table 9.2** Trial operator performance. The different test persons achieved different results (i.e. elevations) for the same objects to be measured.

Test person	Forest road				Well-textured stand				Stand with low texture			
	Range	Mean	St.dev	Correlator*	Range	Mean	St.dev	Correlator	Range	Mean	St.dev	Correlator
1	965-983	973.2	6.09	990.8	1002-1029	1016.4	7.24	1036.9	1003-1067	1032.8	20.33	988.6
2	970-980	976.9	3.09	991.2	996-1004	1000.3	2.85	973.5	1011-1019	1017.8	2.38	987.7
3	962-981	973.5	7.21	991.7	958-981	970.6	7.46	1022.3	960-979	970.1	6.66	994.7

all values in metres  
 \* values achieved by using SOCET SET's automatic correlator

The resulting values suggest that in general manual measurements can be carried out with confidence and consistency. However, the standard deviations indicate clearly that adequate training and experience (as was with No.2) are a definite advantage. Furthermore there seems to be no real difference between the outcomes for well-textured features and the ones low in texture. On closer inspection it seems more likely that in this case the intensity of the edge of the stand (that is where most of the measurements were taken) had much greater leverage than the factor texture. It can be further concluded that the number of measurements can be limited to between 8

and 10 per stand to achieve fairly accurate results. Apparently the correlator (i.e. automatic matching) values do differ slightly from the manually obtained outcomes. This fact should not be considered alarming, as the actual proper determination of the height (i.e. relative determination) of an object is much more important than the absolute determination of an elevation point.

#### 9.1.5 Accuracy assessment of the IRS-1C stereo model

With reference to section 8.2.5.2 the outcomes for the elevation accuracy in ground space (on average 2.521m) looked very promising. Unfortunately, as can be seen in table 9.3, these values are not reflected throughout the image space.

All measurements were carried out with the aid of the image auto correlator to obtain unbiased values. In general, the fidelity of the model can be considered very satisfactory as indicated by the average of the differences in elevation. A trend of the IRS-1C values to underestimate the heights also seems apparent, thus with no consistency. However, the maximum errors reveal that an infidelity in the magnitude of up to two pixels (i.e.  $\pm 12\text{m}$ ) has to be allowed for, and taken into consideration when conducting absolute elevation determinations.

**Table 9.3** Accuracy assessment of the IRS-1C stereo model in comparison with the stereo model created for the aerial photography

Check point ID	Elevation (m) IRS-1C	Elevation (m) aerial photography	Difference (m)
1	1291	1293	-2
2	1337	1342	-5
3	1270	1275	-5
4	1317	1322	-5
5	1341	1339	2
6	1355	1349	6
7	1408	1420	-12
8	1243	1244	-1
9	1246	1258	-12
10	1401	1400	1
<b>Mean</b>			<b>-3.3</b>
<b>St. deviation</b>			<b>5.77</b>

## 9.2 Determination of tree height

The determination of tree/stand height has proven to be a key factor for the estimation of timber volume and site quality (Bredenkamp, 1994; Bruce and Schumacher, 1963). Errors in the measurement of the height can therefore result in a gross over-, or underestimation of timber volume and site quality. Thus, great care has to be taken in the proper extraction of this specific parameter.

### 9.2.1 Manual extraction of tree height and identification of tree species

At this stage, given the prevailing limited ground resolution, the identification of a specific tree species in a satellite image is virtually impossible. Nevertheless, the texture of a mature stand is able to convey some indication as eucalyptus stands appear slightly more bright and rough than pine plantations. Young and very dense plantations present themselves as grey, homogenous blotches in the image. Thus, any attempt to accurately recognise a certain specie is mere speculation and ancillary information is required. In contrast, patches of indigenous forest are fairly easy to identify because of their inherent characteristics as being very heterogeneous in structure (i.e. high texture) and occupying steep, inaccessible terrain.

The results of the manual determination of tree height are presented in Tables 9.4 and 9.5. Two of the initially selected test stands could not be measured with confidence owing to the extremely small parallax difference. This phenomenon is very common for young stands (i.e. low height) and can be further caused by the adverse tilt angles of the satellite sensor. Only trees exceeding a height of about 20m could be measured properly. Hence, the height values of compartments No. A44 and A16a were not considered to be representative. In addition, no results were available for compartments A62 and A44 to compare with the outcomes for IRS-1C, as they were located beyond the boundaries of the photography. In the following table only the values for the compartments A15 and A29c are presented in detail, the remaining measurements are indicated as means.

**Table 9.4** Manual determination of tree height in IRS-1C imagery and aerial photography

Compartment	Plot no.	Tree height IRS-1C (m)	Tree height AP* (m)	Difference (m)	Difference (%)	Area IRS-1C (ha)	Area ground survey (ha)
A29c	1	42	43.2	-1.2	-2.78		
	2	38	42.7	-4.7	-11.00		
	3	40	43.4	-3.4	-7.83		
	4	35	42.2	-7.2	-17.06		
	5	40	43.7	-3.7	-8.47		
	6	46	46.1	-0.1	-0.22		
	7	45	45.3	-0.3	-0.66		
	8	48	47.9	0.1	0.21		
	9	38	43.0	5.0	11.63		
Mean		41.33	44.17	-1.72	-4.02	21.9	23
St.dev.		4.27	1.87	3.52			
Difference in mean height between IRS-1C and AP				<b>-2.84</b>	<b>-6.43%</b>	Difference between the two area measurements	<b>-1.1 (-4.78%)</b>
AP* = aerial photograph							
Difference in % = difference in % from AP							
Compartment	Plot no.	Tree height IRS-1C (m)	Tree height AP* (m)	Difference (m)	Difference (%)	Area IRS-1C (ha)	Area ground survey (ha)
A15	1	30	33.8	-3.8	-11.24		
	2	37	37.5	-0.5	-1.33		
	3	37	37.4	-0.8	-2.14		
	4	39	39.8	-0.8	-2.01		
	5	42	42.7	-0.7	-1.64		
	6	42	43.5	-1.5	-3.45		
	7	38	38.6	-0.6	-1.55		
	8	40	40.4	-0.4	-0.99		
Mean		38.13	39.21	-1.14	-3.04	18.2	19.2
St.dev.		3.83	2.92	1.13			
Difference in mean height between IRS-1C and AP				<b>-1.08</b>	<b>-2.75%</b>	Difference between the two area measurements	<b>-1.0 (-5.2%)</b>

**Table 9.5** Mean tree heights for the remaining stands

Compartment	# of measurements	Tree height IRS-1C (m)	Tree height AP* (m)	Difference (m)	Difference (%)	Area IRS-1C (ha)	Area ground survey (ha)	Difference in area (ha)
A44a	2	33.00	-	-	-	19.8	20.9	-1.1
A62	9	41.11	-	-	-	32.5	34.4	-1.9
A16a	6	21.83	14.28	<b>7.55</b>	52.87	13.7	14.3	-0.6
R40a	11	29.00	28.20	<b>0.80</b>	2.84	16.7	17.3	-0.6
R19d/e	6	29.50	24.30	<b>5.20</b>	21.40	*	10.0	-
R33	12	35.08	40.16	<b>-5.08</b>	-12.65	*	-	-
					Difference in % from AP			
* no clear definition of area possible								
- = no information available								

Considering the fact that the determination of elevation from IRS-1C imagery has an inherent error potential of one to two pixels (i.e. 6 to 12m), the yielded results in general are excellent. The results reveal that the stand height could be determined

with an accuracy of about 90 to 97% compared to the heights derived from the aerial photography. Furthermore, it can be observed that the values obtained from the extraction from the satellite imagery tend to underestimate the heights from the aerial photography.

The stands A15 and A29 presented themselves in the best conditions (as opposed to stand R19d/e) for measurements of elevation in the IRS-1C scenes, as illumination was perfect, contrast good and shaping of the stand edges splendid. The results for compartment A16a are very poor. The trees of this compartment only feature an average height of about 20m, thus the parallax difference in the stereo model was very small and therefore difficult to determine. The measured values for stand R33 are slightly better than for compartment A16a. Since no severe difficulties in the determination of the stand height for R33 were encountered in the satellite imagery, at this stage only the comparison to the values of the terrestrial assessment could help find an explanation for this outcome.

In general, the means of the heights are almost able to match the accuracies that can be achieved from height determinations using aerial photography. As has been reported by Hildebrandt (1996) and Van Laar and Akça (1997), the achievable accuracy ranges from  $\pm 3\%$  to  $\pm 4\%$  for medium scale aerial photography (1:10 000 to 1:15 000), when employing analogue stereo plotters. However, these results have to be seen in perspective i.e. that aerial photographs were used as reference source, thus presumably introducing some additional error inherent to this medium. Shadowing effects caused by the trees and the terrain, and also the coarse ground resolution of the satellite imagery, might be responsible for the deviation of the values as obtained for the area. In a few cases the boundaries of particular stands were not clearly visible, thus any attempt at proper delineation was doomed to fail. Nevertheless, the outcomes (i.e. an underestimate of about 3-10%) seem acceptable, if the accuracy requirements for the terrestrial surveys are relaxed.

### 9.2.2 Semi-automatic measurement

The handling of the auto correlator proved to be extremely difficult within the coarse environment of the satellite imagery. No useful results could be obtained in terms of

elevation determination, since the visual inspection would not allow the verification of the measurements. Therefore, the IRS-1C imagery had to be excluded from further investigation in this specific trial. In contrast, the correlation tool happened to be a valuable aid for the identification of treetops in the aerial photography, since the small scale (i.e. 1:30 000) and additionally the shadows of the trees were obstacles to be surmounted. In a number of cases the treetops were obscured by shadow, nevertheless, the correlator managed to find sufficient information to perform a correlation (in consequence leading to an elevation measurement). The operator's task was then to scan only a small section of the obscured area and find the maximum elevation for this specific tree (i.e. treetop). So, instead of basing the measurements on guesswork, the mensuration could be carried out with the confidence of achieving useful and fairly accurate results. However, even an intelligent tool like the auto correlator is fallible, and resulted in a few total mismatches. Due to its inherent matching algorithm, the correlator searched for similar grey value patterns. In a few cases, as caused by the different acquisition angle of the photographs and the different appearance of terrain, the pixel values of a treetop in the left image were very similar to a shadow on the ground representative of a totally different tree. Thus, the floating mark of the computer had to be guided to an area with a high probability for finding a conjugate point to match the same feature. After several attempts, the intervention of the operator proved to be rewarding in all instances.

The results of the height measurements for stand A15 (*Eucalyptus grandis*) are given in detail in Table 9.6. The outcomes for the other stands (trees to be measured were selected in a random manner due to time constraints) are only provided as mean heights as represented in Table 9.7. Stand A15 is a very dense hardwood stand, so ground sight was scarce. Fortunately the terrain proved to be fairly homogenous, so extraction lines within and forest roads outside the stand could be used as substitute for the measurement of the tree base. For determining of the distance of trees in relation to the sample plot centre, SOCET SET's measuring tool was put into operation.

**Table 9.6** Determination of tree height in aerial photography employing the auto correlator

Compartment	Plot no.	Tree height AP* (m)	Tree height ground survey (m)	Difference (m)	Difference (%)	Area AP* (ha)	Area ground survey (ha)
<b>A15</b>	1	40.0	41.0	-1.0	-2.44		
	2	39.8	41.3	-1.5	-3.63		
	3	40.4	40.7	-0.3	-0.74		
	4	39.4	42.3	-2.9	-6.86		
	5	43.5	50.0	-6.5	-13.00		
	6	42.7	42.8	-0.1	-0.23		
	7	37.4	37.0	0.4	1.08		
	8	36.1	36.5	-0.4	-1.10		
	9	35.4	36.0	-0.6	-1.67		
	10	37.5	37.5	0	0		
	11	35.3	35.5	-0.2	-0.56		
	12	37.4	38.5	-0.9	-2.86		
	13	38.4	41.0	-2.6	-6.34		
Mean		38.72	40.01	-1.28	-2.95	18.6	19.2
St.dev.		2.57	3.91	1.85	3.84		
Difference in mean height between AP and ground survey				<b>-1.29m</b>	<b>-3.22%</b>	Difference between the two area measurements	
						<b>-0.6 ha (-3.1%)</b>	
AP* = aerial photograph							
Difference in % = difference in % from ground survey							

**Table 9.7** Tree height determination using the auto correlator

Compartment	Number of measurements (random)	Tree height AP (m)	Tree height ground survey (m)	Difference (m)	Difference (%)	Area AP (ha)	Area ground survey (ha)	Difference in area
A15	26	38.27	40.01	-1.74	-4.35	18.8	19.2	-2.08
A29c	17	44.91	43.88	1.03	2.35	22.6	23.0	-1.74
A16a	17	13.94	13.34	0.6	4.50	13.9	14.3	-2.80
R40a	17	27.69	28.22	-0.53	-1.88	16.8	17.3	-2.89
R19d/e	19	24.47	28.32	-3.85	-13.59	*	10.0	-
R33	45	40.55	43.38	-2.83	-6.52	*	-	-
* no clear definition of area possible					Difference in % from ground survey			
- = no information available								

The results for the stand heights using random sampling are slightly worse than these for stand A15. However, they seem acceptable and converge with observations from other investigations (e.g. Hildebrandt, 1996; Van Laar and Akça, 1997). The very poor performance of the measurements for stand R19d/e can possibly be attributed to the bad weather conditions (i.e. rain, mist) during the ground survey. A survey performed by the staff of Mondi yielded an average height of 24.3m for R19d (measured in 1993) and 26.4m for R19e (measured in 1998), so the real height would be to the order of ca. 26m for compartment R19d/e at the time the ground survey was

carried out. Thus the height error for the aerial photography would not be -13.59% as obtained, but about -5.5 % to -6.0%. The trend of underestimating tree heights as measured in aerial photographs is substantiated by the results as obtained in this study. However, this has to be seen in a certain perspective. According to Hildebrandt (1996) deciduous trees can be measured more accurately than coniferous trees. This might be particularly true for old broadleafed trees with big crowns, but eucalyptus trees which have been growing in plantation conditions, show crown shapes similar to those of conifers (i.e. pines). Although one of the two investigated eucalyptus stands (i.e. A29c) showed an overestimate of the height to some extent, the sampling size is simply too small to draw any general conclusions.

The results for the determination of stand areas (i.e. an underestimate of between 2% and 3%) are tolerable, especially when taking in account that some borders could not be clearly identified because of shadows and concealment by trees) and therefore not delineated accurately. Nevertheless, the delineation tool provided by the SOCET SET/PRO 600 software is much more efficient, user friendly, and in many cases more accurate than employing methods using grid counts and planimeters for instance.

The height distribution within compartment R33 is presented in Figure 9.6.

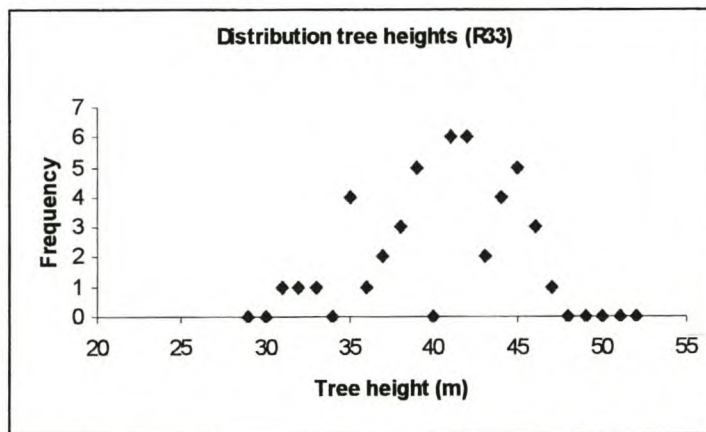


**Figure 9.6** Distribution of tree heights for stand R33 as extracted from aerial photography

Despite the limited sample size, a more or less normal distribution of the tree heights can be observed.

The top of the figure (containing contour lines) suggests that due to the coarse resolution of the satellite imagery the AATE algorithm is not flexible enough to create a proper shape of the stand edges. Instead of correctly moulding the sharp rise of the edge (as could be seen with the contours created using the aerial photography in Figure 9.1) the algorithm forms a smooth transition from the first measurement (i.e. the ground outside the stand) until the top of the canopy is reached. This retarding effect can also be observed in the mesh model when looking at a section at the bottom of the image (i.e. the depression, as indicated in magenta). For some reason (most probably a matching error) this blunder had a high leverage so that the error was carried through, deep into the stand. However, a visual inspection of the IRS-1C subset and the aerial photograph did not give any indication of big openings in the canopy or the existence of broad forest roads, which could justify such a response from the terrain extraction algorithm. Since no visual explanation could be found for this phenomenon, no editing of the surface model was carried out. In order to get information on the possible reasons for the demonstrated flaw it was necessary to assess the underlying elevation data. An illustration of the vertical profile of the elevation data (i.e. a 2D representation of 3D data) of compartment A15 is shown in Figure 9.9. The height information was obtained through forming the difference of corresponding elevation points (i.e. same co-ordinates) between the surface model and the reference plane (see also Appendix 11).

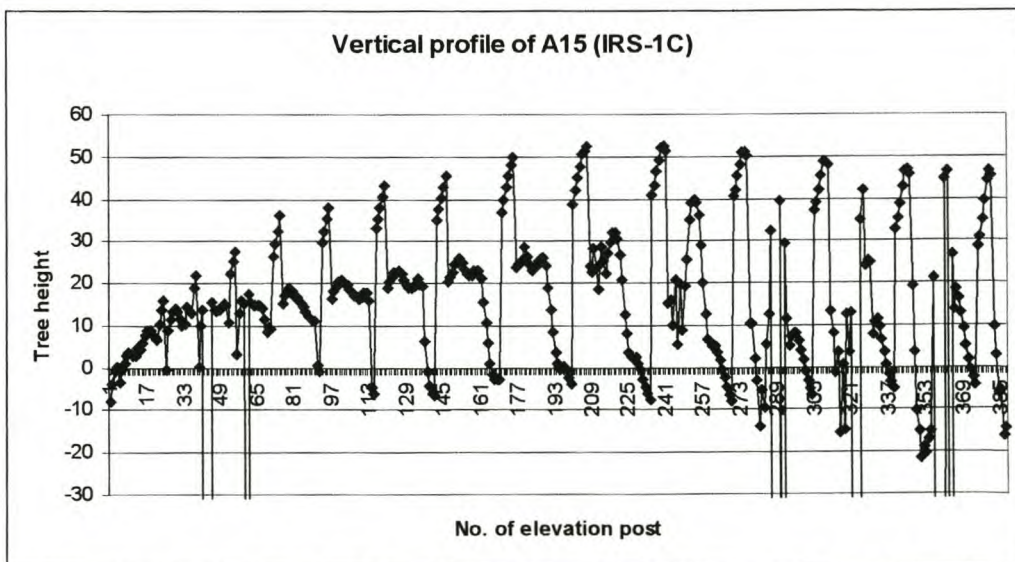


**Figure 9.9** Vertical profile of the stand A15 as extracted form IRS-1C imagery (only 400 of the 715 measuring points are shown)

The following trends can be extracted from the graph presented as Figure 9.9:

1. It takes the automatic terrain extraction a good while to rise to a presumably realistic tree height (i.e. only as about from point no.50, which is located a fair distance from the edge); this characteristic is already evident in the provided pictures, showing that the stand edges do not get modelled properly.
2. Due to the coarseness of the satellite imagery and the resulting sparse post spacing, only the heights of a small number of trees are measured, as the chances of hitting a treetop are relatively slim.
3. The great number of extreme outliers (i.e. errors) is of concern. They range from  $-800\text{m}$  to  $-886\text{m}$  but are displayed to  $-30\text{m}$  only.
4. The forest floor seems to be adequately represented by the reference plane, as only a fraction of the total values are located beneath the zero line.
5. A certain repetitive pattern is apparent. This suggests that an underlying trend probably exists (for further assessment see section 9.3.2).
6. A closer look at the structure of the elevation data reveals that the extracted elevation information seems to be closely correlated with the shape of a specific stand. It was discovered that a great number of very low elevation values were to be found along the edges of a compartment (see for example Figure 9.12). Thus, the ratio of the circumference of a specific compartment to its area plays an important role in the evaluation of the tree heights.

The implications of the observations are that the extracted height information can only be used after putting some effort into the elimination of grave errors and manipulation of the remaining data to result in reasonable and realistic outcomes. Reasonable and possible solutions to the presented problems are:

1. Ignore the values close to the edges of a stand since they contribute nothing to the creation of an accurate model.
2. Accordingly exclude the outliers (i.e. values greater than  $-800\text{m}$ ) from any further assessment.
3. Truncate the remaining data in such a way that firstly the retarding effect of the algorithm close to the stand edges gets accounted for, and secondly acceptable (i.e. realistic) stand heights are achievable.
4. Perform a Fourier transform on the data for the identification of certain data patterns and furthermore check for inconsistencies (i.e. noise) in the data. The

corresponding data analysis is being dealt with in chapter 9.3.2 (The Hegershoff method).

Based on the before mentioned findings it was decided to discard the extreme outliers and the values representing elevation close to the stand edges for further assessment of the elevation data (i.e. the calculation of tree heights). Because of the enormous leverage of these values, any useful calculation of the tree heights would have been seriously compromised.

For practical reasons it was decided to assess the data in the following three different manners in order to achieve a result close to the corresponding terrestrial data:

1. Identify the maximum value for each elevation profile line (i.e. including edge effect) and calculate the mean height of the stand. It is assumed that the maximum value per vertical profile represents a hit, i.e. the top of a tree.
2. Considering the maximum values of all profile lines, consolidate a cut-off value representing 50% of the overall maximum tree height and truncate all values below for the profile lines; subsequently calculate mean for stand.
3. Truncate each side of the resulting distribution from procedure 2. for 25% (i.e. equivalent to the calculation of the interquartile range) and calculate mean for stand.

The results of these calculations are submitted in the following tables. However, in two cases (compartments A16 and R33) as mentioned below it was discovered that the AATE algorithm was unable to model the surface of the stands properly. The values of compartment A16 were not taken into further consideration, since the low average height of the trees (calculated as 13.34m for the ground survey) precluded any useful assessment. The visual inspection of the automatically obtained elevation data for A16 as extracted from the IRS-1C imagery showed that the tree heights did not exceed a value of about 4.5m. In addition, no further appraisal of compartment R33 was undertaken due to its very poor circumference/area ratio and the small size of the stand. These two factors resulted in automatically derived height values of about 3.5m, which is not being representative of the tree heights in the compartment.

**Table 9.8** Tree heights for IRS-1C imagery as extracted from automatically created surface models

Compartment	$h_t$ (m)	$h_t$ (%)	$h_{aut1}$ (m)	$h_{aut1}$ (%)	$h_{aut2}$ (m)	$h_{aut2}$ (%)	$h_{aut3}$ (m)	$h_{aut3}$ (%)
A15	40.01	100	32.32	80.78	41.69	104.2	48.61	121.49
R19d/e	28.32	100	14.13	49.89	19.62	69.28	21.3	75.21
R40a	28.22	100	20.25	71.76	28.60	101.35	25.34	89.79
A62	41.49	100	47.56	114.63	49.86	120.17	48.18	116.12

$h_t$  = terrestrial measurement (ground survey)  
 $h_{aut1}$  = mean height of all profile lines (see 1. on previous page)  
 $h_{aut2}$  = mean height using cut-off value (see 2. on previous page)  
 $h_{aut3}$  = mean height using truncation (see 3. on previous page)

The results for the extraction of elevation data from aerial photography using the same post spacing as for IRS-1C (i.e. 20m) are given below.

**Table 9.9** Tree heights for aerial photography as extracted from automatically created surface models

Compartment	$h_t$ (m)	$h_t$ (%)	$h_{aut1}$ (m)	$h_{aut1}$ (%)	$h_{aut2}$ (m)	$h_{aut2}$ (%)	$h_{aut3}$ (m)	$h_{aut3}$ (%)
A15	40.01	100	38.50	96.23	44.35	110.85	50.52	126.17
R19d/e	28.32	100	21.99	77.65	24.15	85.28	25.58	90.32
R40a	28.22	100	23.35	82.39	26.00	92.13	25.48	90.29
R33	43.38	100	27.14	62.56	39.24	90.46	42.43	97.81

$h_t$  = terrestrial measurement (ground survey)  
 $h_{aut1}$  = mean height of all profile lines (see 1. on previous page)  
 $h_{aut2}$  = mean height using cut-off value (see 2. on previous page)  
 $h_{aut3}$  = mean height using truncation (see 3. on previous page)

The following observations can be made:

- With respect to the IRS-1C imagery, in most cases the option  $h_{aut1}$ <sup>41</sup> yields inferior results compared to the other options.
- Concerning the categories  $h_{aut2}$ <sup>42</sup> and  $h_{aut3}$ <sup>43</sup> no clear trend can be distinguished - in some cases  $h_{aut2}$  performs better than  $h_{aut3}$ , and the other way round.
- Regarding the results obtained from the aerial photographs, no trend can be identified. However, in general the results are more accurate than those achieved when using the satellite imagery.

In conclusion, the automatic determination of tree heights from satellite imagery depends heavily on the shape and the size of a specific compartment, and most certainly on the magnitude of the encountered parallax difference (i.e. height). The

<sup>41</sup>  $h_{aut1}$  = mean height of all profile lines (see 1. on previous page)

<sup>42</sup>  $h_{aut2}$  = mean height using cut-off value (see 2. on previous page)

<sup>43</sup>  $h_{aut3}$  = mean height using truncation (see 3. on previous page)

aerial photography with a 2m post spacing), the fidelity of the resulting model with the real canopy surface can be just remarkable.

#### 9.2.4 Comparative evaluation of the described methods

The major goal of this investigation was to probe the potential of high resolution satellite imagery for forest inventory purposes and subsequently identify a method that can be considered suitable to bring forth a reliable variable for the estimation of timber volume. Thus it was of interest to examine whether the observed measurements are sufficiently important and accurate for the conduction of further studies.

Results of the different methods of the determination of tree height are presented in Table 9.10.

Based on the presented observations it can be concluded that the manual determination of the tree heights in the satellite imagery is superior to the automatically derived values in terms of accuracy and ease of operation. The calculated accuracy for the manual method amounts to about  $\pm 6\%$  as compared to the terrestrial survey. The outliers concerning compartments A16a and R33 can be explained by the low tree height (i.e. very poor parallax difference) in the first instance and the difficulty of identifying a suitable ground location close to the edge of the stand (i.e. for the proper placement of the floating mark) in the latter instance. The automatically extracted values for compartment A29c are rather unrealistic, thus suggesting that the vertical positioning of the reference plane has been carried out in an incorrect manner.

With respect to the height estimation in the aerial photography more or less the same general statements apply. The accuracies of the manually performed measurements are about the same as obtained in the IRS-1C imagery, which is quite remarkable, if one takes the coarse resolution and the higher inherent elevation error of the spaceborne sensor design into account.

**Table 9.10** Results of the different methods used for the extraction of tree heights from IRS-1C

Compartment	Species	$h_t$ (m)	$h_t$ (%)	$h_{aut1}$ (m)	$h_{aut1}$ (%)	$h_{aut2}$ (m)	$h_{aut2}$ (%)	$h_{aut3}$ (m)	$h_{aut3}$ (%)	$h_m$ (m)	$h_m$ (%)
A15	<i>E. grandis</i>	40.01	100	32.32	80.78	41.69	104.20	48.61	121.49	38.13	95.30
R19d/e	<i>P. elliotii</i>	28.32	100	14.13	49.89	19.62	69.28	21.3	75.21	29.50	104.17
R40a	<i>P. elliotii</i>	28.22	100	20.25	71.76	28.60	101.35	25.34	89.79	29.00	102.76
A62	<i>E. grandis</i>	41.49	100	47.56	114.63	49.86	120.17	48.18	116.12	41.11	99.08
A44a	<i>E. grandis</i>	34.84	100	-	-	-	-	-	-	33.00	94.72
A16a	<i>P. patula</i>	13.34	100	-	-	-	-	-	-	21.83	163.64
R33	<i>P. elliotii</i>	43.38	100	-	-	-	-	-	-	35.08	80.87
A29c	<i>E. grandis</i>	43.88	100	59.03	134.53	93.03	212.01	-	-	41.33	94.19

\* no useful results could be achieved employing the automatic method

- no data

$h_t$  = terrestrial measurement (ground survey)

$h_{aut1}$  = mean height of all profile lines (see 1. on page 155)

$h_{aut2}$  = mean height using cut-off value (see 2. on page 155)

$h_{aut3}$  = mean height using truncation (see 3. on page 155)

$h_m$  = manual measurement (for aerial photography combination of manual and semi-automatic methods)

**Table 9.11** Results of the different methods used for the extraction of tree heights from aerial photographs

Compartment	Species	$h_t$ (m)	$h_t$ (%)	$h_{aut1}$ (m)	$h_{aut1}$ (%)	$h_{aut2}$ (m)	$h_{aut2}$ (%)	$h_{aut3}$ (m)	$h_{aut3}$ (%)	$h_m$ (m)	$h_m$ (%)
A15	<i>E. grandis</i>	40.01	100	38.50	96.23	44.35	110.85	50.52	126.17	38.27	95.65
R19d/e	<i>P. elliotii</i>	28.32	100	21.99	77.65	24.15	85.28	25.58	90.32	24.47	86.41
R40a	<i>P. elliotii</i>	28.22	100	23.35	82.39	26.00	92.13	25.48	90.29	27.69	98.12
A16a	<i>P. patula</i>	13.34	100	-	-	-	-	-	-	13.94	104.50
R33	<i>P. elliotii</i>	43.38	100	27.14	62.56	39.24	90.46	42.43	97.81	40.55	93.48
A29c	<i>E. grandis</i>	43.88	100	-	-	-	-	-	-	44.91	102.35

The determination of tree height from aerial photography and satellite imagery is in many cases not an easy task and sources for possible errors are abundant. The following list of possible influencing factors in conjunction with the extraction of elevation information is by no means complete and comprehensive. It is rather to provide some practical and hands-on information on the difficulties which were encountered during this study.

The occurrence of errors in the determination of tree heights can be attributed to the following factors:

- When extracting terrain data automatically:
  - the improper definition of the reference plane (i.e. ground fill)
  - the existence of image matching errors
  - the coarse spatial resolution of the imagery (e.g. IRS-1C)
  - lack of flexibility of the algorithm used for terrain extraction; improper parameter settings
  - improper definition of the stereomodel (as caused by inaccurate ground points, wrong parameter settings, errors in orientation of the images)
  - poor quality of the images (e.g. due to scanning errors, poor radiometric resolution, adverse weather conditions during acquisition of imagery)
  - incorrect survey /inventory information, when using terrestrial data as reference (same applies to extraction of elevation information from aerial photography)
  - choosing the wrong post spacing.
  
- The semi-automatic method employing an image correlator is very susceptible to image matching errors, thus leading to total mismatches of features.
  
- Manual measurements can be influenced by:
  - the ability to identify treetops (aerial photography)
  - the selection of an inappropriate zooming level (particularly important for satellite imagery)
  - the absence of measurable ground points close to the edge of a stand or sampling plot (important for aerial photography and IRS-1C imagery)
  - the lack of contrast in the imagery

- a poor B/H ratio (i.e. resulting in a small parallax difference)
- the variability of the terrain especially within the area of the sampling plots
- the poor definition of features
- lack of skills and training of the operator
- inappropriate equipment
- heights of the objects to be measured (low objects are very difficult to measure).

Some of the mentioned error sources might be mutually exclusive, but most of them do have a synergetic effect (e.g. the combination of poor B/H ratio and insufficient height of objects) on the deterioration of the quality and thus reliability of the resulting elevation information.

### 9.3 Application of inventory methods

#### 9.3.1 Two (three)-phase sampling

For the determination of the regression estimator (i.e. correlation between dbh ground survey and tree height IRS-1C imagery), the correlation between the height measurements as carried out on the satellite imagery and the mean heights (i.e. average of each sampling plot) from the aerial photography (used as reference) had to be scrutinised first. The results for the compartments A15 and A29c are presented in Figures 9.13 and 9.14 (see also Appendix 11).

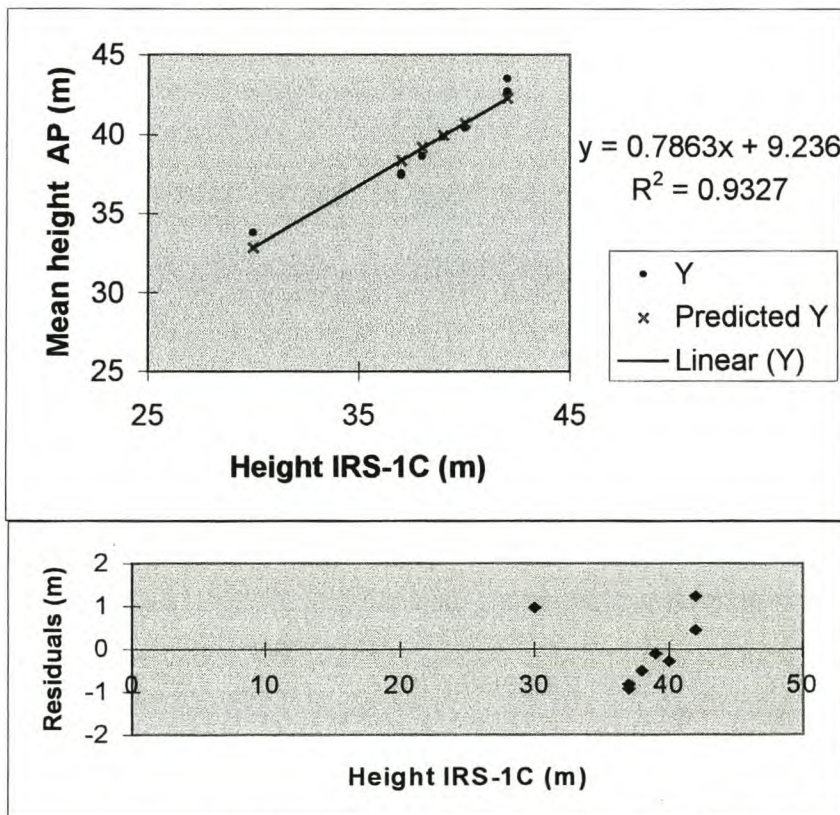


**Figure 9.13** Linear regression showing the relationship between mean height aerial photography (AP) and mean height IRS-1C for compartment A15. The regression equation with the corresponding trend line, as well as the  $R^2$  value are provided on top, the residuals are shown at the bottom.

In compliance with the two (three)-phase sampling procedure the heights obtained from IRS-1C were used as the independent variable, the mean heights from aerial photographs as the dependent variable (i.e. the one to be predicted). The presented results for compartment A15 indicate a close relationship between the heights of the satellite imagery and the aerial photography respectively. The  $R^2$  value (0.93) is very good and the residual plot does not show any large outliers, thus indicating that a higher-order model would be more appropriate.

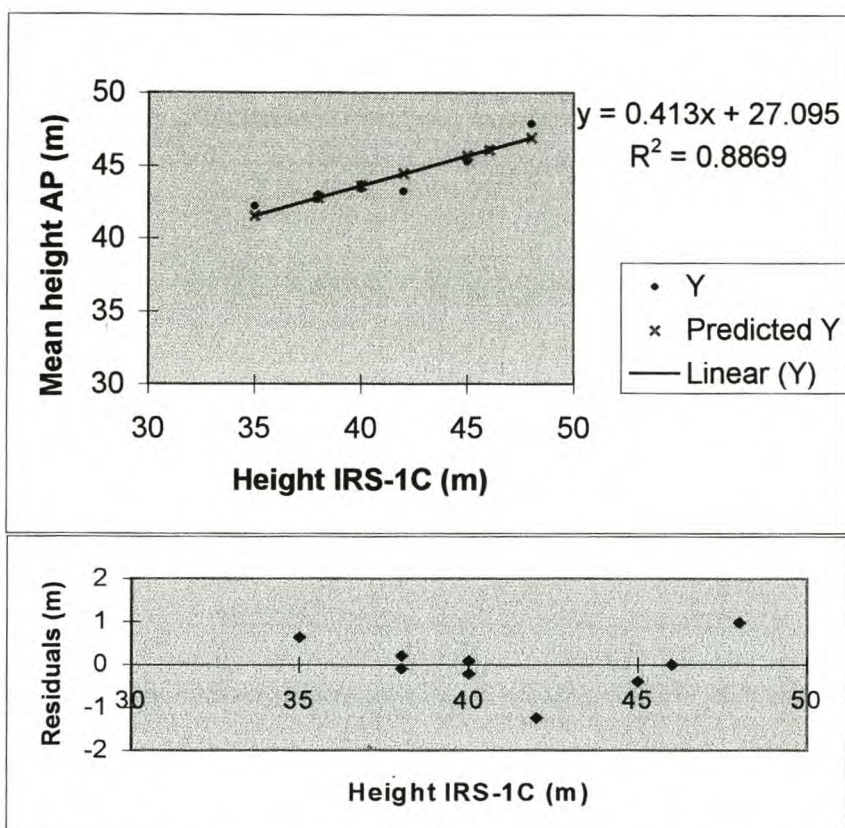


**Figure 9.14** Linear regression showing the relationship between mean height aerial photography (AP) and mean height IRS-1C for compartment A29c. The regression equation with the corresponding trend line, as well as the  $R^2$  value are provided on top, the residuals are shown at the bottom.

A similar trend for compartment A29c showing the relationship between mean height as extracted from the satellite imagery and the corresponding heights from the aerial photography is represented in Figure 9.14. The coefficient of determination ( $R^2$ ) is almost as good as the one obtained for compartment A15. The residual plot reveals that no extreme outliers exist, but the distribution of the points indicates a certain trend. A higher-order model would therefore be more appropriate.

The close relationship between the observations from the IRS-1C imagery and the results of the height measurements from the aerial photography suggest that the estimates for the tree heights from the satellite imagery can be used for the calculation of the regression estimator, if the relationship between the mean tree heights in the reference medium (i.e. aerial photography) and the dbh as determined based on the ground survey is close enough. For the further analysis the relationship between the

mean heights of the aerial photography and the mean heights of the ground survey had to be examined. The results of this assessment are shown in Figure 9.15.

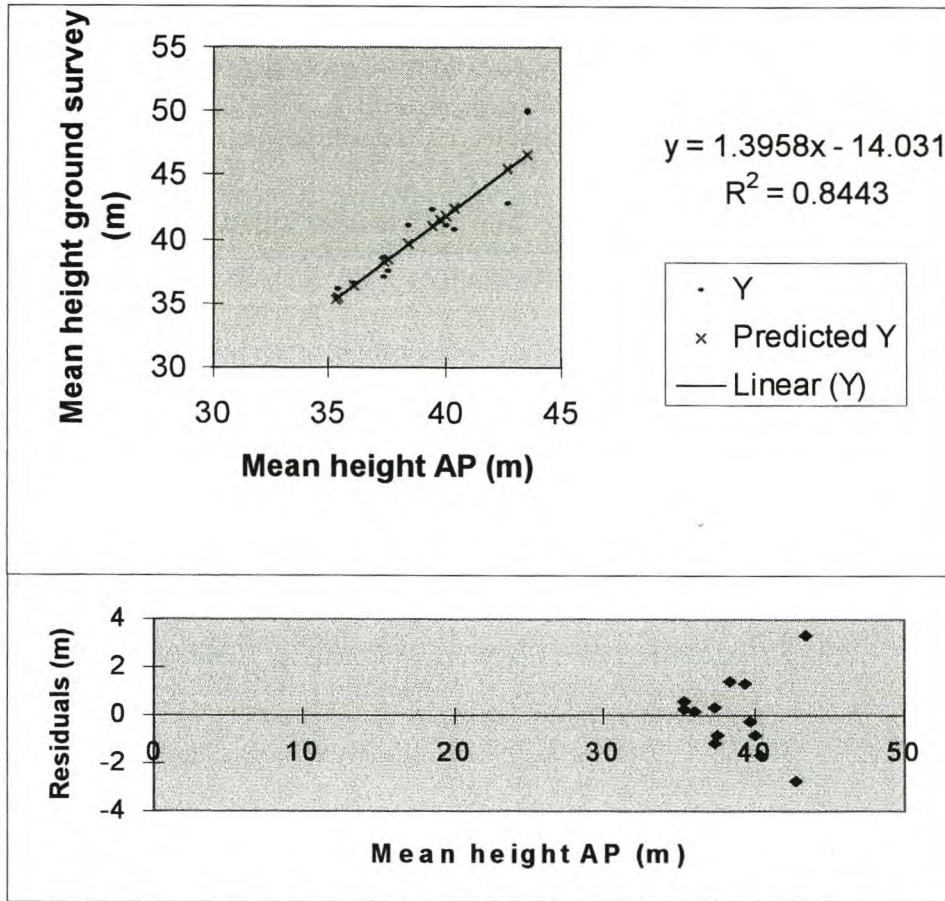


**Figure 9.15** Linear regression showing the relationship between mean from height ground survey and mean height from aerial photography (AP) for compartment A15. The regression equation with the corresponding trend line, as well as the  $R^2$  value are provided on top, the residuals are shown at the bottom.

The regression statistics reveal that there is definitely a close relationship between the independent variable ‘mean height AP’ and the dependent variable ‘mean height ground survey’. The  $R^2$  value of 0.84 is very good and the residual plot indicates only a few outliers (values are  $-2.769$  and  $3.314$ ). However, these are relatively small (i.e.  $< 10\%$  of the total tree height) and do not violate the good fit of the linear model.

Since the close relationship between the ‘mean height AP’ and the ‘mean height ground survey’ has been established, only the correlation between the dbh as resulting from the ground survey and the mean heights from the aerial photography needed to be assessed (see also Kättsch, 1991). If this relationship is close enough, the calculation of the regression estimator could be carried out with confidence. The

results of the regression analysis for compartment A15 are displayed in the following Figure 9.16.

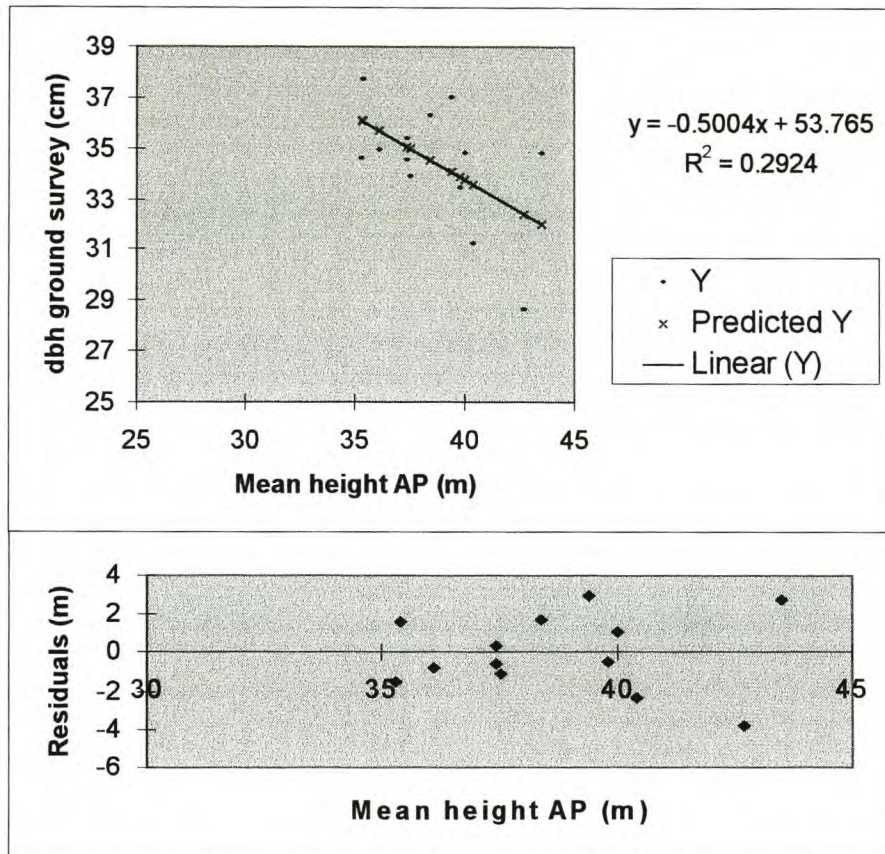


**Figure 9.16** Linear regression showing the relationship between dbh ground survey and mean height aerial photography (AP) for compartment A15. The regression equation with the corresponding trend line, as well as the  $R^2$  value are provided on top, the residuals are shown at the bottom.

The low  $R^2$  value of the regression analysis is a clear indication of the very poor correlation between the X (i.e. mean height AP) and the Y (i.e. dbh ground survey) variable. More importantly, one would have expected a positive slope of the trend line, as opposed to the resulting negative one in the graph above. The residual plot indicates three relatively small outliers with values of 2.95, 2.80 and  $-3.79$ . The values are in the magnitude of about the mean annual height increment for this compartment. For further analysis the three outliers were discarded and the resulting figures scrutinised for possible improvement of the general trend. The regression analysis with the three discarded outliers is shown in the following Figure 9.17.

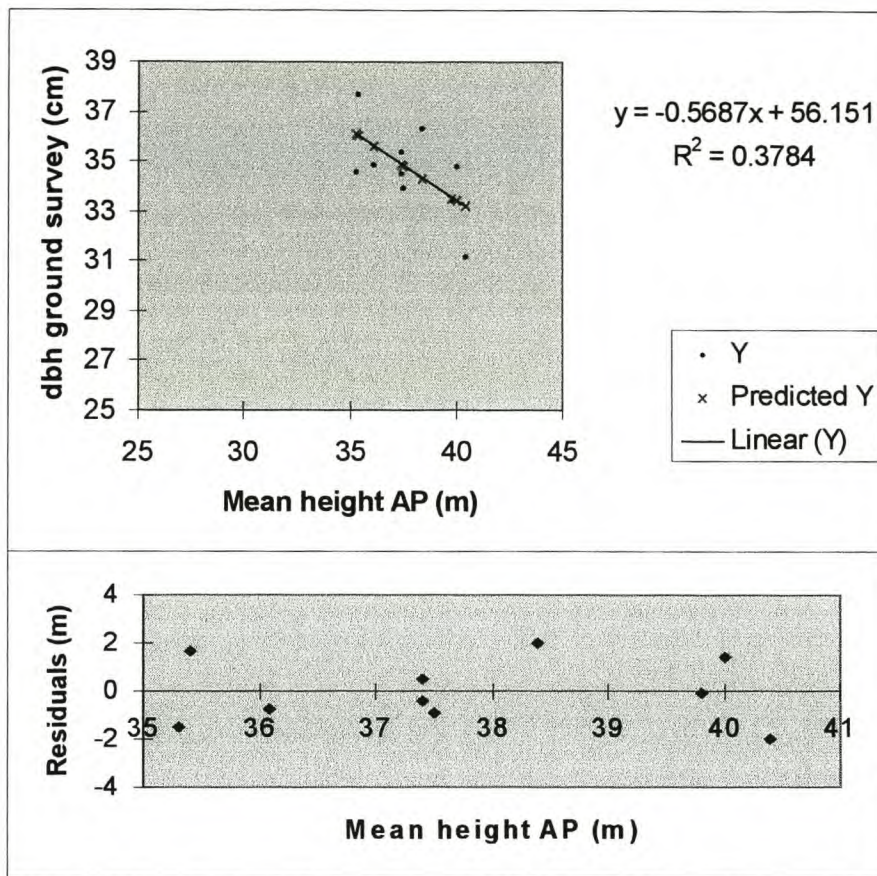


**Figure 9.17** Linear regression showing the relationship between dbh ground survey and mean height aerial photography (AP) for compartment A15. The regression equation with the corresponding trend line, as well as the  $R^2$  value are provided on top, the residuals are shown at the bottom. The outliers 4,5 and 6 were excluded from the calculations.

The figures reveal that the coefficient of determination has improved slightly. However, the value is much too low to further consider the correlation between the 'dbh ground survey' and the 'mean height AP' as a serious candidate for the determination of the regression estimator. The residuals also show some improvement, but some further manipulation of the  $R^2$  value would be at the expense of the sampling size, which is low already. Possible reasons for the poor performance of the correlation are:

1. The sampling size was too small.
2. The height measurements carried out on the aerial photography did not correspond exactly with the location of the trees measured on the ground. This may have resulted in a discrepancy between the height estimations from the two different sources and thus effected the relationship between dbh and tree height (see also Hildebrandt, 1996; Kättsch, 1991; Van Laar and Akça, 1997).
3. Discrepancies in the ground data itself (e.g. improper measurement of tree height and dbh).

- The ground survey was conducted before the delivery of the satellite imagery took place. Therefore it was not possible to establish a sampling design which would have been tailored for the analysis of the IRS-1C imagery.

In summary it can be said that the correlation between dbh ground survey and the tree height as calculated from the aerial photograph data is very poor, thus severely effecting the assumed relationship between tree height as extracted from the IRS-1C imagery and dbh ground survey. In consequence, the regression estimator could not be determined with confidence.

### 9.3.2 The Hugerhoff method

All stands included in this investigation were assessed for the possible suitability of estimating timber volume using the method proposed by Hugerhoff (Akça, 1983; Hugerhoff, 1933; 1939). As an example of all appraised stands, the analysis of stand A15 is presented in detail. The scrutiny was limited to the height values as achieved by the automatic generation of the surface models (i.e. AATE) from the satellite imagery as well as the aerial photography. The shape of a stand profile and possible discrepancies is provided in Figure 9.18.

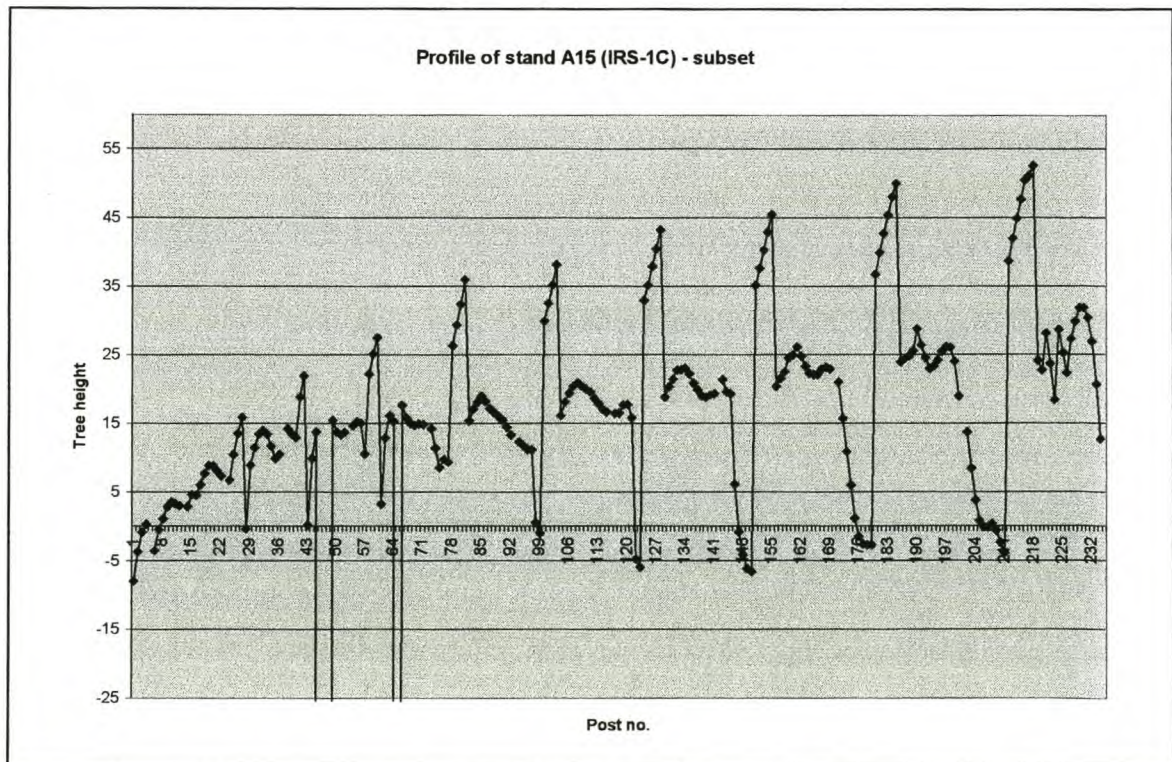


**Figure 9.18** Vertical profile of compartment A15 (IRS-1C) shown as subset with 20m post spacing

At a first glance, the graph seems to reflect a certain repetitive pattern and a useful distribution of height values, which could be subject to further exploitation in terms of timber volume estimation or at least the calculation of mean tree height. However, when on closer inspection a number of substantial blunders in terms of height fluctuations are detected. Some of the height values drop down to 885m below the ground level (see also Appendix 11). Although no logical explanation could be attained so far, it was considered to be rewarding to perform further analysis on the data. For this purpose a Fourier transform was carried out in order to check for possible flaws, inconsistencies and possible repetitive patterns in the data. First of all the elevation values were exported from MS Excel format to the GIS software package ArcView for the generation of a raster layer. Subsequently this grid was further manipulated in the ERDAS Imagine image processing software package. The resulting graphical representation of the Fourier analysis is shown in Figure 9.19.

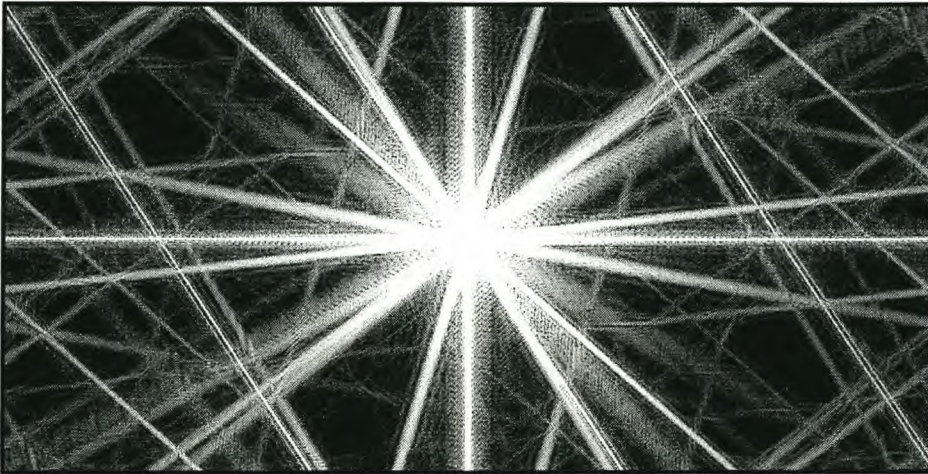


**Figure 9.19** Fourier transform of the IRS-1C representation of tree heights in compartment A15

The results are discouraging. The Fourier transform indicates unequivocally that no distinct homogenous underlying frequency pattern exists. The number of lines and the criss-cross structure indicate that the underlying structure of the data is very complex with many superimposing effects (i.e. modulation) and clear signs of blunders (noise). In consequence, the obtained elevation values as extracted automatically do not represent merely a 'true' elevation, but contain information from different sources, which degrade the terrain information. Thus, no further analysis of the profile data was conducted with the aim of making deductions for the further use as input for the calculation of timber volume. The results of applying a filter to the

An examination of the remaining stands revealed more or less the same characteristics for the frequency patterns as shown in Figures 9.18 and 9.19. Furthermore, the scrutiny of the DSMs of the aerial photographs with a 20m post spacing disclosed similar tendencies. Thus, further evaluations had to be abandoned as well. However, the vertical profiles derived from the DSMs with a 2m post spacing did not indicate any apparent flaws in terms of outliers with high leverage. However, because of technical constraints (i.e. limited data analysis capacity) this analysis has to be subject of future investigations.

### 9.3.3 Eichhorn's law

The two presented inventory methods have proven not to be suitable for the determination of timber volume from the extracted height information. However, a remedy may be at hand. According to Eichhorn's law a relationship between the mean stand height and the total volume production of forest stands exists, regardless of the age of the stands and the site quality (Mitscherlich, 1970; Von Gadow and Bredekamp, 1992). Eichhorn observed this relationship for *Abies alba* in the Black Forest in Germany in 1904. Since then his observations have been confirmed and extended to numerous other tree species such as spruce (*Picea abies*) and beech (*Fagus sylvatica*), and more recently for *Pinus patula*. The relationship between total volume production and mean height is shown for *Pinus patula* in Figure 9.24 on page 175.

Eichhorn's law is based on the assumption that stand density is held constant, since the thinning regime and the espacement in the forest considerably influence the relationship between total volume production and mean height (Mitscherlich, 1970). However, in plantation forestry silvicultural regimes usually remain constant for long periods of time. Thus, it is very easy to estimate total volume production at a given age by merely predicting the stand height for that specific age.

Volume tables can be created with ease, when the relationship between age and height and between height and total volume production is known. Since the increment will also be known, this procedure can be extended to the construction of yield tables.

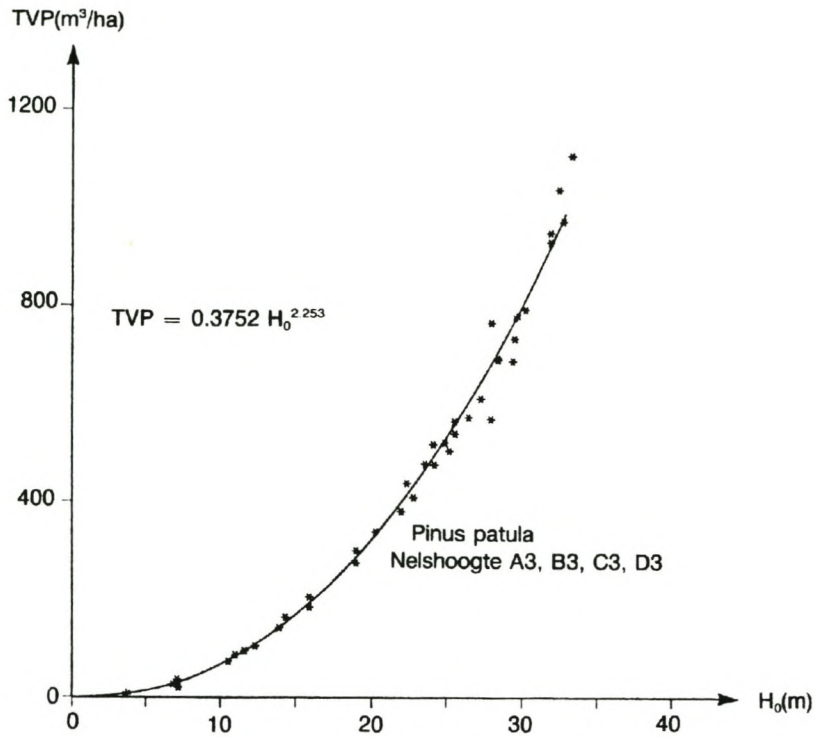


**Figure 9.24** Relationship between total volume production (TVP) and mean height in *Pinus patula* stands (Nelshoogte CCT experiment). Note that stand density is held constant in this case (Von Gadow and Bredenkamp, 1992).

The well-known CCT experiments provide data with which the parameters of Eichhorn's curve can be determined for a wide range of species. However, it is known that Eichhorn's law on its own has been shown to be inadequate for the prediction of volume from height without knowledge of a second variable, preferably age (or site index).

## 10. SUMMARY AND CONCLUSIONS

The aim of the study was to probe the potential of state-of-the-art satellite technology (IRS1-C) in forest inventory by employing digital photogrammetry technology.

The following secondary objectives were defined:

1. Extraction of forest inventory parameters from the imagery (i.e. satellite scenes; aerial photography that was used as reference) such as tree height, canopy closure, crown diameter, with the estimation of stand volume as a derived parameter.
2. Creation of Digital Terrain Models (DTMs) and Digital Surface Models (DSMs).
3. Comparison of the results obtained by the application of the different terrain extraction methods (i.e. manual, semi-automatic and automatic) in terms of performance and accuracy.
4. Exploration of various inventory concepts for the possible integration and application of the obtained satellite information.

The approach used a softcopy photogrammetric workstation, IRS-1C stereo panchromatic satellite imagery and digital aerial imagery. The aerial images were obtained by scanning panchromatic aerial photographs (scale 1:30 000) at a nominal resolution of 15 micrometers. All the tests were carried out on a LH System DPW 770 softcopy workstation<sup>44</sup>. The study was conducted over various sites in the Sabie area (province of Mpumalanga) in South Africa, where extensive man made forests (predominantly pine and eucalypt) are to be found. Eight different compartments with different tree species (*Eucalyptus grandis*, *Pinus patula* and *Pinus elliottii*) and age classes were scrutinised. A ground survey was conducted in September 1997. An IRS-1C subscene (acquired in 1998), representing an area of 70km x 70km was chosen, for which a network of highly accurate (i.e. sub-meter) ground control points had been used as reference. The extraction of stand parameters such as tree/stand height has been performed manually, semi-automatically, as well as automatically in the aerial photography as well as the satellite imagery. In addition, the compartment area was determined using a GIS tool.

Prior to the actual extraction of elevation information, the following factors had to be scrutinised:

---

<sup>44</sup> LH Systems' photogrammetry software is called SOCET SET (Softcopy Exploitation Tools)

1. The overall performance of LH Systems' Adaptive Automatic Terrain Extraction (AATE) tool, which was used for the creation of the digital terrain and surface models.
2. The image matching process.
3. The effect on the stereo model when performing image enhancement.
4. The skills of the operator.
5. The fidelity of the stereo model.

The overall performance of the AATE tool was impressive in terms of modelling even difficult terrain conditions and canopy surfaces when applied to aerial photographs and using a dense post spacing for the creation of the terrain model. However, single trees were not modelled properly, as in some cases they were simply omitted by the extraction algorithm. In contrast, AATE performed very poorly when extracting elevation data from the IRS-1C imagery. In all instances the edges of the compartments were not modelled properly, as these were characterised by a gradual rise of the elevation points instead of a sharp rise. Furthermore, smaller objects such as windbreaks were totally ignored by AATE.

Image matching problems were abundant in the IRS-1C imagery when looking at areas where features had changed (e.g. clearfelled or burnt) between the times when the satellite imagery was acquired (time gap). In these specific areas the matching algorithm failed completely in finding conjugate points in the corresponding images. Furthermore, matching errors were not interpolated properly and the resulting blunders were propagated a fair distance into the neighbouring image areas. For the aerial photography, matching failures were scarce due to the absence of the time gap between the acquisition of the different photographs. This clearly indicates that it is advisable to acquire satellite imagery either featuring an along-track technology or platforms with an extremely high revisit rate (i.e. a few days) to avoid any substantial time gaps.

Severe effects on the fidelity of the stereo model of the IRS-1C imagery were observed when image enhancement techniques such as image sharpening were applied. This amounted to deviations from the 'true' value up to a magnitude of -57m for certain ground control and checkpoints. It can therefore be concluded that image

enhancement should only be performed temporarily, thus only for certain display purposes.

Three different test persons were asked to manually remeasure the same features in the IRS-1C stereo model. The results suggested very clearly that a well-trained and highly skilled operator can achieve a much higher accuracy in the measurements with a high degree of consistency.

The good results for the vertical and planimetric accuracies (average deviation of 2.52m for the Z value) in ground space could not be confirmed for the image space in the IRS-1C stereo model. The calculation of the vertical accuracy yielded a deviation of between one and two pixels from the true value, translating to 5 to 10m (up to 12m). Thus, not only accurate measurements and the correct distribution of the ground control points seem to be crucial for the overall accuracy of the stereo model, but also the B/H ratio of the image acquisition platform.

#### The determination of tree/stand height

Due to the coarse spatial resolution of the IRS-1C imagery and the suboptimal B/H ratio (0.57) of the image geometry only objects exceeding a height of about 20m could be manually measured with confidence. Furthermore, the parallax difference and the contrast were only big enough at the edges of the compartments. A certain height increment of the stand would have been to be taken into consideration because of time delay. However, because of the inherent vertical error in the stereomodel (i.e. 5-12m) the increment factor was considered negligible.

Tree heights were determined in the IRS-1C imagery and aerial photography using manual, semi-automatic and automatic procedures.

The results of the manual extraction of height information was similar to that obtained in a non-digital environment such as an Analytical Plotter (AP) or a mirror stereoscope in combination with a parallax bar. The obtained tree heights in the IRS-1C imagery compared very well to the heights measured in the aerial photography. The difference was about  $\pm 10\%$ , with a clear trend of underestimation. The IRS-1C measurements deviated from the terrestrially gathered information by about  $\pm 5\%$ ,

which is remarkable, bearing the coarse ground resolution and the vertical accuracy of the stereo model of 1-2 pixels in mind.

The semi-automatic determination of tree heights was carried out by means of SOCET SET's autocorrelator, which exploits an image matching technique. This tool was very useful for the proper identification and measurement of treetops in the aerial photography, since parts of the crowns were obscured by shadows. In contrast, the autocorrelator did not work for the satellite imagery, as the coarse structure of the imagery did not allow any identification of single trees. In addition verification by visual inspection was impossible. Tree heights obtained from the aerial photographs yielded an accuracy of about 95% compared to the ground survey data.

The automatic determination of tree height for each compartment comprised the creation of a reference plane (ground fill) to represent the forest floor and the generation of a digital surface model of the stand canopy. The resulting models were visually inspected for blunders and the elevation values exported into a spreadsheet programme for calculation of the tree heights. The satellite imagery and the aerial photography were evaluated by applying the same post spacing (i.e. 20m) for terrain extraction. The obtained ground fills (using a 2<sup>nd</sup> order polynomial) were very satisfactory when these were visually compared to the contour lines on a topographical map. Due to the finer spatial resolution the ground fills from the aerial photography were more accurate than these obtained from the satellite imagery. Once again, the relatively poor performance of AATE resulted in the degradation of the entire terrain and surface models. The automatic terrain extraction algorithm produced a great number of blunders when applied to the satellite imagery, which in turn resulted in tree heights of -885m. This outcome is mainly due to image matching problems (some of them caused by the time gap between the two satellite scenes) and the inevitable sparse post spacing for the terrain extraction process. Some lack of performance by the AATE tool however requires clarification on the part of the software designer<sup>45</sup> (LH Systems).

---

<sup>45</sup> LH Systems has been approached for this purpose

The elevation information for each compartment was exported as vertical height profiles into spreadsheets. When using the height information of all vertical profiles (i.e. including the edges of the stands), an accuracy of between 50% and 115% was achieved for the satellite imagery compared to the ground survey. An underestimate of about 25% for the aerial photographs was achieved compared to terrestrial data. When applying a cut-off value for the profile data (i.e. for all profile lines per compartment all values smaller than half of the total maximum tree height), accuracies were about between 70% and 120% for the IRS-1C imagery and  $\pm 15\%$  for the aerial photography when set against the ground truth data. Using only profile data within the interquartile range (i.e. only 50% of the elevation data per profile after truncation) yielded accuracies of  $\pm 25\%$  for the IRS-1C imagery and an underestimate of between 10% to 25% for the aerial photographs.

In summary, the automatic terrain extraction procedure worked slightly better for the aerial photography than for the satellite imagery. In general it must be concluded that the obtained accuracies for the satellite imagery and the aerial photography using automatic terrain extraction were by no means good enough to be used as an input for the calculation of timber volume. In addition the results revealed that AATE did not generate any useful results for compartments featuring small sizes (i.e. about 5ha) and a poor circumference/area ratio. For these reasons, further analysis of this data was omitted.

The obtained results leave no doubt that a post spacing of 20m is not dense enough to carry enough terrain information to adequately represent the evaluated forest compartments. In addition, the AATE tool seems to be more tuned for the terrain extraction from aerial photographs than from satellite imagery. This has been confirmed particularly for dense post spacing (e.g. 2m) as was used for the creation of a surface model using aerial photographs. The resulting surface models represented the canopy structure of the stands very well. Bearing this in mind, the results have to be seen in the context of a combination of the different factors such as coarse spatial resolution, the design of the terrain extraction algorithm, the sparse post spacing and the quality of the imagery.

The validation of the manually extracted (i.e. more accurate) tree heights comprised the application in two-phase sampling using regression estimators, and the Hugerhoff method.

Since the sampling points on the IRS-1C imagery could not be directly linked to the ground data, aerial photography information had to be used as reference. The correlation between the heights of IRS-1C and aerial photography proved to be very strong ( $R^2 = 0.93$ ) as was the case between the heights from aerial photography and from ground survey ( $R^2 = 0.84$ ). However, due to the extremely weak relationship between dbh from ground survey and from height aerial photography ( $R^2 = 0.29$ ; negative slope), the results of the manual height determination had to be considered unfit for use as a regression estimator and thus for the calculation of timber volume. A possible reason for the poor coefficient of determination is that a number of the trees on the aerial photographs could not be accurately assigned to ground information (i.e. dbh) due to identification problems (Hildebrandt, 1996; Van Laar and Akça, 1997).

For the possible exploitation of the terrain information to be used in the Hugerhoff method a Fourier transform of the automatically extracted elevation data was carried out. The results of the profile analysis showed that the obtained tree heights are affected by a combination of numerous factors such as spatial resolution of the imagery, the post spacing for the terrain extraction, the occurrence of matching errors, the canopy structure, and the tree height itself. In addition, a great number of blunders (i.e. outliers) occurred in the vertical profiles. All these factors degraded the quality of the height information to such an extent that it was decided to discard the Hugerhoff method for the calculation of timber volume.

However, with the highly accurate manually extracted tree height information from the IRS-1C imagery available, an efficient and cost-effective remedy seems to be at hand. Only between eight and ten measurements on the satellite imagery are sufficient enough to calculate a mean height for the stand to compare well with the results achieved for the height determination in aerial photographs. Based on Eichhorn's law (Mitscherlich, 1970; Von Gadow and Bredenlamp, 1992) these results can be used to estimate timber volume. As far as is known research dealing with the

relationship between total volume production and mean height in plantation forestry in South Africa has only been conducted for *Pinus patula*. Nevertheless, the outcomes look promising and the extension to other tree species should be seriously considered.

The prevailing situation in the forestry sector is characterised by the dependence on labour-, and cost-intensive inventory methods. The results are of considerable relevance to those concerned with the inventory of vast, inaccessible forest areas and for those searching for highly efficient, cost-effective schemes.

## **11. RECOMMENDATIONS**

The presented study has shown clearly that using high resolution stereo satellite imagery has large potential for applications in forestry. The softcopy environment offers a user-friendly and efficient means for evaluating IRS-1C imagery and a variety of other types of digital imagery. However, there is still some room for improvement, particularly with respect to the automatic extraction of terrain information from satellite imagery. The occurrence of severe blunders and the sometimes strange performance of the AATE algorithm (i.e. interpolation failures) are of major concern. These issues definitely have to be addressed and resolved by the designers of the SOCET SET software in form of test trials with a range of stereo satellite images (e.g. SPOT, Ikonos2) dealing with varying conditions regarding terrain, image quality, sensor geometry and the like. Furthermore, a more user-friendly graphical interface and a real end-to-end digital photogrammetry solution are desirable. New modules for the automatic identification and extraction of features such as trees should be designed and integrated as well as fully-fledged GIS tools and image processing techniques. An option for the automatic calculation of object heights and volumes will certainly be regarded as a bonus. In addition, the user will without any doubt appreciate the provision of information on the structure of the algorithms used in order to facilitate the scientific analysis of the results.

The manual determination of tree heights in the IRS-1C imagery has proven to be very successful and efficient. Although the outcomes were very encouraging, the

regression analysis in this study revealed that for future investigations it would be advisable to conduct the ground survey after the acquisition and evaluation of the satellite imagery. The ground survey should be carried out with the highest possible (and economically justifiable) accuracy. According to the findings of Howard (1997) and others terrestrial measurements can easily deviate from the true value in the magnitude of about 10% for mean heights and up to 25% for single tree heights and therefore have a severe impact on the calculation of timber volume.

In order to avoid substantial time gaps between the acquisition dates of the satellite stereo imagery preference should be given to platforms either featuring a high revisit rate (i.e. a few days) or an along-track image acquisition mode.

The findings of the study also show that there is still a considerable demand for research concerning the inventory designs employing remote sensing technology. Eichhorn's law seems to be of great benefit for the calculation of timber volume for *Pinus patula*. Thus, an extension of the investigations to other tree species such as *Eucalyptus grandis* and *Pinus elliotti* will definitely contribute to the efficiency of forest inventory. Various other approaches such as the creation of specific volume tables for the exploitation of satellite imagery are to be considered seriously. Furthermore, the integration of other auxiliary variables for regression analysis (i.e. estimators) like image texture parameters and spectral reflectance values is likely to be rewarding and should be subject to future investigations. With the advent of the new satellite generation featuring a spatial resolution of less than one metre, texture analysis and even perhaps the creation of stereograms could offer viable solutions.

## 12. OUTLOOK

Photogrammetry has entered an era in which digital image processing plays a major role in the tasks of extracting information from images, leading to an increased level of automation. The greatest success until now of the DPS has been in the field of digital orthophoto production and in the area of digital elevation data acquisition, where a high degree of automation has already been achieved. It is absolutely certain that the DPW will supersede the AP very soon, though the AP's niche of cost effective map compilation will remain for some time. Project management software, combined with powerful image databases and universal use of the Internet will cause further stimulation of the technology, commencing with digital cameras and the development of high resolution multispectral spaceborne scanners. GPS triangulation, DTM generation, orthophoto mosaicking and feature extraction will be the mainstay, all benefiting from automation. Remote sensing, GIS and photogrammetry may well converge, with all functionalities combined on one computer platform (Walker and Petrie, 1996). Furthermore, it can be foreseen that the cut-throat competition between vendors will lead to a further decline in prices, thus enabling a broader user community to embark on the DPW domain.

A further potential of advancements will certainly lie in the continuous automation of information extraction and integration processes, for example with the integration of expert systems into DPSs. However, the degree of progress will largely depend on the precise understanding of how human operators solve problems. Artificial intelligence and cognitive science will help to analyse these processes. Some other developments will certainly comprise a shift from data-driven, pixel-to-pixel operations to a more symbolic processing (i.e. entity-driven) of abstract presentations, as is already happening in computer vision. The verities of photogrammetry will certainly continue to apply, however, the increased sophistication of the systems will continue to demand high levels of knowledge and expertise on the part of the users.

It can be envisaged that the described technological developments will definitely be to the benefit of the forestry sector. In particular with the advent of high resolution satellite imagery, which will gradually supersede small scale aerial photography,

exciting and rewarding applications are waiting to be discovered, thus leading to a better understanding and management of the forests of our globe.

### 13. REFERENCES

- ACKERMANN, F., and HAHN, M., 1991. Image pyramids for Digital Photogrammetry. In: EBNER, H., FRITSCH, D., and HEIPKE, C., (Eds.). *Digital Photogrammetric Systems*. Verlag Wichmann, Karlsruhe, pp. 43-58.
- ACKERMANN, F., 1996a. Techniques and Strategies for DEM Generation. In: *Digital Photogrammetry: An Addendum to the Manual of Photogrammetry*. American Society for Photogrammetry and Remote Sensing, Bethesda, Maryland, pp. 135-141.
- ACKERMANN, F., 1996b. The Status and Accuracy Performance of GPS Photogrammetry. In: *Digital Photogrammetry: An Addendum to the Manual of Photogrammetry*. American Society for Photogrammetry and Remote Sensing, Bethesda, Maryland, pp. 108-114.
- ACKERMANN, R.J., and ESLAMI RAD, A., 1996. Quality control procedure for photogrammetric digital mapping. *International Archives of Photogrammetry and Remote Sensing*. Vol.XXXI, Part B4: 12-17.
- AGOURIS, P., and STEFANIDIS, A., 1996. Scale difference considerations in conjugate feature matching. *International Archives of Photogrammetry and Remote Sensing*. Vol.XXXI, Part B3: 8-13.
- AKÇA, A., 1983. *Rationalisierung der Bestandeshöhenermittlung in der Forsteinrichtung und bei Großrauminventuren*. *Forstarchiv* 2:103-106.
- AKÇA, A., 1989. *Permanente Luftbildstichprobe*. *Allg. Forst- und Jagdzeitung* 160: 65-69.
- AKÇA, A., HILDEBRANDT, G., HUSS, J., KENNEWEG, H., PEERENBOOM, H.-G., and RHODY, B., 1984. In: J. HUSS (Ed.), *Luftbildmessung und Fernerkundung in der Forstwirtschaft*. Verlag Wichmann, Karlsruhe. 406 pp.
- AKÇA, A., DONG, P.U., and BEISCH, T., 1993. *Zweiphasige Stichprobeninventur zur Holzvorrats-, und Zuwachsschätzung*. *Proceedings of a Symposium on the Application of Remote Sensing in Forestry, Zvolen 1993*, pp. 1625ff.
- AKENO, K., 1996. DEM generation from multisensor stereopairs – AVHRR and MSS. *The International Archives of Photogrammetry and Remote Sensing*. Vol. XXXII, Part 4: 36-44.
- ALLEN, J., and SHEARS, J., 1995. A digital view: softcopy photogrammetry in GIS. *GIS Europe* September 1995.

- AL-ROUSAN, N., CHENG, P., PETRIE, G., TOUTIN, TH., and VALADAN ZOEJ, M.J., 1997. Automated DEM extraction and orthoimage generation from SPOT level 1B imagery. *Photogrammetric Engineering & Remote Sensing*. Vol.LXIII, No.8: 965-974.
- AL-ROUSAN, N., and PETRIE, G., 1998. System calibration, geometric accuracy testing and validation of DEM & orthoimage data extracted from SPOT stereopairs using commercially available image processing systems. *The International Archives of Photogrammetry and Remote Sensing*. Vol. XXXII, Part 4: 8-15.
- ALWAN, R.H., and NAJI, M.A., 1996. Automatic stereo image matching using edge detection technique. *International Archives of Photogrammetry and Remote Sensing*. Vol.XXXI, Part B3: 29-35.
- ARMENAKIS, C., and SAVOPOL, F., 1998. Mapping potential of the IRS-1C Pan satellite imagery. *The International Archives of Photogrammetry and Remote Sensing*. Vol. XXXII, Part 4: 23-26.
- EVERY, T.E., and BURKHART, H., 1988. *Forest Measurements*. McGraw-Hill Series in Forest Resources, New York. 331 pp.
- BACHER, U., 1998. Experimental studies into automated DTM generation on the DPW 770. *The International Archives of Photogrammetry and Remote Sensing*. Vol. XXXII, Part 4: 1-7.
- BÄHR, H.-P., and WIESEL, J., 1991. Cost-benefit analysis of digital orthophoto technology. In: EBNER, H., FRITSCH, D., and HEIPKE, C., (Eds.). *Digital Photogrammetric Systems*. Verlag Wichmann, Karlsruhe, pp. 59-71.
- BAINS, S., and MULLINS, J., 1998. A face in the crowd. *New Scientist* 2147: 37-39.
- BAKER, J.G., 1980. Elements of photogrammetric optics. In: SLAMA, C.C., (Editor-in-chief). *Manual of Photogrammetry*. American Society of Photogrammetry and Remote Sensing, Falls Church, Va. 4<sup>th</sup> Ed. 1056 pp.
- BALTSAVIAS, E.P., 1996. Digital ortho-images – a powerful tool for the extraction of spatial- and geo-information. *ISPRS Journal of Photogrammetry & Remote Sensing* 51: 63-77.
- BALTSAVIAS, E.P., and STALLMANN, D., 1996. Geometric potential of MOMS-02/D2 data for point positioning, DTM and orthoimage generation. *International Archives of Photogrammetry and Remote Sensing*. Vol.XXXI, Part B4: 110-116.
- BALTSAVIAS, E.P., STEFANIDIS, A., LI, H., and SINNING, M., 1996. Automatic DSMs by digital photogrammetry. *Surveying World* January/February: 18-21.

- BALTSAVIAS, E.P., STEFANIDIS, A., LI, H., SINNING, M., and MASON, S., 1996. Comparison of two photogrammetric systems with emphasis on DTM generation: case study glacier measurement. *International Archives of Photogrammetry and Remote Sensing*. Vol.XXXI, Part B4: 104-109.
- BALTSAVIAS, E., and KÄSER, C., 1998. DTM and orthoimage generation - A thorough analysis and comparison of four digital photogrammetric systems. *The International Archives of Photogrammetry and Remote Sensing*. Vol. XXXII, Part 4.
- BARRETT, E.C., and CURTIS, L.F., 1976. *Introduction to Environmental Remote Sensing*. Chapman and Hall, London. 336 pp.
- BELEIT, S., 1994. *Erfassung der Kronendachstruktur mit Hilfe analytischer Photogrammetrie am Beispiel des Buchenaltholzbestandes der Naturwaldzelle Hellberg*. In: *Photogrammetrie & Forst*, Tagungsband.
- BERNHARDBSEN, T., 1992. *Geographic information systems*. Viak IT, Norway. 318 pp.
- BILL, R., and FRITSCH, D., 1996. *Grundlagen der Geo-Informationssysteme*. Verlag Wichmann, Heidelberg. 2 vol.
- BITTERLICH, W., 1984. *The relascope idea*. Commonwealth Agricultural Bureaux, Slough. 242 pp.
- BONIFACE, P.R., 1996. State-of-the-Art in Soft Copy Photogrammetry. In: *Digital Photogrammetry: An Addendum to the Manual of Photogrammetry*. American Society for Photogrammetry and Remote Sensing, Bethesda, Maryland, pp. 227-229.
- BREDENKAMP, B.V., 1994. The volume of standing trees. In: VAN DER SIJDE, H.A., (Ed.). *South African Forestry Handbook*. Southern African Institute of Forestry, Pretoria. 846 pp.
- BUDD, J.T.C., 1991. Remote sensing techniques for monitoring land-cover. In: GOLDSMITH, B., (Ed.). *Monitoring for Conservation and Ecology*. Chapman and Hall, London. 275 pp.
- BUSCH, A., 1996. A common framework for the extraction of lines and edges. *International Archives of Photogrammetry and Remote Sensing*. Vol.XXXI, Part B3: 88-93.
- CAMPBELL, J.B., 1996. *Introduction to Remote Sensing*. The Guildford Press, New York. 551 pp.

- CARSON, W.W., MILLER, S.B., and WALKER, A.S., 1996. Automated forest inventory using a Digital Photogrammetric Workstation. *Proceedings of the 2<sup>nd</sup> International Airborne Remote Sensing Conference*. Vol.111, No.841: 251-257.
- CARSON, W.W., MILLER, S.B., WALKER, A.S., and ZHANG, B., 1997. New algorithm for automated forest inventory on a Digital Photogrammetric Workstation. *Proceedings of the 3<sup>rd</sup> International Airborne Remote Sensing Conference*. Vol.3, No.825: 272-277.
- CATLOW, D.R., 1986. The multi-disciplinary applications of DEMs. *Proceedings AUTO CARTO London, Vol.1*: 447-454.
- CHAPUIS, A., 1995. Developments in Digital Photogrammetry and a description of the flow of data through a digital photogrammetric system. *Digital Photogrammetry and Remote Sensing 1995. Proceedings SPIE*. Vol.2646, No.320: 49-56.
- CHENG, P., and TOUTIN, T., 1998. Unlocking the potential for IRS-1C data. *EOM*. March: 24-26.
- CLARKE R., 1986. *The Handbook of Ecological Monitoring*. Clarendon Press, Oxford.
- COCHRAN, W.G., 1977. *Sampling Techniques*. John Wiley and Sons, New York. 3<sup>rd</sup> Ed. 428 pp.
- COLWELL, R.N., 1980. Remote Sensing of Natural Resources: Its Basic Concepts in Retrospect and Prospect. In: *Proceedings of Remote Sensing for Natural Resources at University of Idaho, Moscow, Idaho*, pp. 48-84.
- COLWELL, R.N., 1986. Land Applications for Remote Sensing from Space. In: McELROY, J.H., (Ed.). *Space Science and Applications*. IEEE Press, New York. 260 pp.
- COMBS, J.E., 1980. Planning and executing the photogrammetric project. In: SLAMA, C.C., (Editor-in-chief). *Manual of Photogrammetry*. American Society of Photogrammetry and Remote Sensing, Falls Church, Va. 4<sup>th</sup> Ed. 1056 pp.
- CONNORS, P.M., and PERRY, L., 1996. An integrated GPS-flight management system. In: *Digital Photogrammetry: An Addendum to the Manual of Photogrammetry*. American Society for Photogrammetry and Remote Sensing, Bethesda, Maryland, pp. 58-63.
- COOPS, N., BI, H., BARNETT, P., and RYAN, P., 1999. Estimating mean and current annual increments of stand volume in a regrowth eucalypt forest using historical Landsat multi spectral scanner imagery. *Journal of Sustainable Forestry*. Vol.9(3/4): 149-168.

- CORBLEY, K.P., 1996. One-Meter-Satellites: Practical Applications by Spatial Data Users - Part Three. *Geo Info Systems* supplement. Space Imaging EOSAT.
- CRACKNELL, A.P., and HAYES, L.W.B., 1988. *Introduction to remote sensing*. Taylor and Francis, London.
- DAM, A., and WALKER, A.S., 1996. Recent developments in digital photogrammetric systems from Leica-Helava. *International Archives of Photogrammetry and Remote Sensing*. Vol.XXXI, Part B2: 66-71.
- DE GIER, A., and STELLINGWERF, D., 1994. Timber volume and increment determination: two-phase aerial photo field regression samples versus simple random field samples. *ITC Journal*. 1994-2: 163-167.
- DEHN, R., TAUBE, D., and SLOBODA, B., 1985. *Schaftvermessung an stehenden Bäumen mit einem eindimensionalen Paßpunktsystem*. *Allg. Forstzeitschrift* 15: 350-353.
- DÖRSTEL, C., and OHLHOF, T., 1996. Processing and display of three-line imagery at a digital photogrammetric workstation. *International Archives of Photogrammetry and Remote Sensing*. Vol. XXXI, Part B2: 72-77.
- DOWMAN, I., 1991. Design of Digital Photogrammetric Workstations. In: EBNER, H., FRITSCH, D., and HEIPKE, C., (Eds.). *Digital Photogrammetric Systems*. Verlag Wichmann, Karlsruhe, pp. 28-38.
- DOWMAN, I.J., EBNER, H., and HEIPKE, C., 1992. Overview of European developments in Digital Photogrammetric Workstations. *Photogrammetric Engineering and Remote Sensing*. Vol.LVIII, No.1: 51-56.
- DREWNIOK, C, and ROHR, K., 1997. Exterior orientation – an automatic approach based on fitting analytic landmark models. *ISPRS Journal of Photogrammetry and Remote Sensing* 52: 132-145.
- DROESEN, W.J., and VAN DEVENTER, A.P., 1996. High resolution landscape monitoring with digital photogrammetry. *Proceedings of a European Conference and Exhibition on Geographical Information at Barcelona, Spain*. 1: 467-476.
- DWIVEDI, R.S., 1990. Future trends in resources sensing from space. In: CRACKNELL, A., HAYES, L., and GEN, H.W., (Eds.). *Remote Sensing Yearbook*. Taylor and Francis, London.
- EASTMAN, R., 1997. IDRISI for Windows – User's Guide. Clark University, Massachusetts, USA.

- EBNER, H., HEIPKE, C., and HOLM, M., 1993. Global image matching and surface reconstruction in object space using aerial images. In: Barrett, E.B., and McKeown, D.M. (Editors). Integrating photogrammetric techniques with scene analysis and machine vision. *Proceedings of SPIE*: 44-57.
- EBNER, H., OHLHOF, T., and PUTZ, E., 1996. Orientation of MOMS- 02/D2 and MOMS-2P imagery. *International Archives of Photogrammetry and Remote Sensing*. Vol.XXXI, Part B3: 158-164.
- ECKSTEIN, W., 1996. Segmentation and texture analysis. *International Archives of Photogrammetry and Remote Sensing*. Vol.XXXI, Part B3: 165-175.
- ELACHI, C., 1987. *Introduction to the Physics and Techniques of Remote Sensing*. John Wiley and Sons, New York. 413 pp.
- FAO, 1985. Forest Resources 1980. Int. Year of the Forest 1985. FAO, Rome.
- FÖRSTNER, W., 1993. Feature extraction in digital photogrammetry. *Photogrammetric Record*. 14(82): 595-611.
- FOA (Forest Owners Association), 1998. Abstract of South African forestry facts for the year 1996/97. Brochure published by the FOA, source: Department of Water Affairs and Forestry, South Africa.
- FRIEDMAN, S.J., 1980. Automation of the photogrammetric process. In: SLAMA, C.C., (Editor-in-chief). *Manual of Photogrammetry*. American Society of Photogrammetry and Remote Sensing, Falls Church, Va. 4<sup>th</sup> Ed. 1056 pp.
- FRITSCH, D., HAHN, M., SCHNEIDER, F., STALLMANN, D., and KIEFNER, M., 1996. Experiences in processing MOMS-02/D2 stereo image data. *International Archives of Photogrammetry and Remote Sensing*. Vol.XXXI, Part B4: 267-272.
- FRITSCH, D., HAHN, M., KIEFNER, M., and STALLMANN, D., 1998. Improvement of the automatic MOMS-2P DTM generation. *The International Archives of Photogrammetry and Remote Sensing*. Vol. XXXII, Part 4: 170-175.
- GOLDSMITH, B., 1991. *Monitoring for conservation and ecology*. Chapman and Hall, London. 275 pp.
- GOPALA KRISHNA, B., KARTIKEYAN, B., IYER, K.V., MITRA, R., and SRIVASTAVA, P.K., 1996. Digital Photogrammetric Workstation for topographic map updation using IRS-1C stereo imagery. *International Archives of Photogrammetry and Remote Sensing*. Vol.XXXI, Part B4: 481-485.

- GRABMEIER, K.A., TEMPFLI, K., and ACKERMANN, R., 1996. Interpretability of scanned aerial photographs. *International Archives of Photogrammetry and Remote Sensing*. Vol.XXXI, Part B4: 305-310.
- GRAHAM, Jr., L.N., ELLISON, Jr., K., and RIDDELL, C.S., 1997. The architecture of a Softcopy Photogrammetry System. *Photogrammetric Engineering and Remote Sensing*. Vol.LXIII, No.8: 1013-1020.
- GRÜN, A., 1985. Adaptive least squares correlation: A powerful image matching technique. *South African Journal of Photogrammetry, Remote Sensing and cartography*. 14(3): 175-219.
- GRÜN, A., and LI, H., 1996. Linear feature extraction with LSB-snakes from multiple images. *International Archives of Photogrammetry and Remote Sensing*. Vol.XXXI, Part B3: 266-272.
- GRUNER, H., 1980. Foundations of photogrammetry. In: SLAMA, C.C., (Editor-in-chief). *Manual of Photogrammetry*. American Society of Photogrammetry and Remote Sensing, Falls Church, Va. 4<sup>th</sup> Ed. 1056 pp.
- GÜLICH, E., 1996. Fundamentals of Softcopy Photogrammetric Workstations. In: *Digital Photogrammetry: An Addendum to the Manual of Photogrammetry*. American Society for Photogrammetry and Remote Sensing, Bethesda, Maryland. pp. 213-226.
- GÜNTHER, K.P., and KLEMP-HÖPFNER, M., 1994. Airborne fluorescence lidar detects stress in plants. *Laser Focus World*. August 1994: 17-18.
- HÄNEL, S., TRÄNKNER, H., and ECKSTEIN, W., 1987. *Automatische Baumkronenentdeckung im Luftbild – der Weg durch den Engpaß*. *Proceedings 2 DFVLR(DLR) Statusseminar Oberpfaffenhofen*, pp. 53-66.
- HALLIDAY, D., and RESNICK, R., 1988. *Fundamentals of physics*. John Wiley and Sons, New York. 3<sup>rd</sup> Ed. (extended). 1202 pp.
- HARRIS, R., 1987. *Satellite Remote Sensing*. Routledge and Kegan Paul, London. 220 pp.
- HAUMANN, D.G., 1995. Digital aerotriangulation on the *Helava* digital scanning workstation DSW 100. *Proceedings SPIE 2646*: 68-76.
- HEIPKE, C., 1995. State-of-the-art of digital photogrammetric workstations for topographic applications. *Photogrammetric Engineering and Remote Sensing*. Vol.61, No.1: 49-56

- HEIPKE, C., 1996a. Automation of interior, relative and absolute orientation. *International Archives of Photogrammetry and Remote Sensing*. Vol.XXXI, Part B3: 297-311.
- HEIPKE, C., 1996b. Overview of image matching techniques. *OEFPE workshop on applications of digital photogrammetric workstations, Lausanne*.
- HEITZINGER, D., and KAGER, H., 1998. High quality DTMs from contour-lines by knowledge-based classification of problem regions. *The International Archives of Photogrammetry and Remote Sensing*. Vol. XXXII, Part 4: 230-237.
- HEITZINGER, D., and PFEIFER, N., 1996. A new approach to modelling 3D-surfaces. *Tutorial on Advanced DTM technology, XVIII<sup>th</sup> ISPRS Congress, Vienna*.
- HILDEBRANDT, G., 1996. *Fernerkundung und Luftbildmessung*. Verlag Wichmann, Heidelberg. 676 pp.
- HOLOPAINEN, M., and LUKKARINEN, E., 1994. *Digitaalisten Ilmakuvien Käyttö Metsävarojen Inventoinnissa* (The use of digital aerial photographs in a forest inventory). *University of Helsinki Dept. of Forest Resource Management Publications* 4: 1-32.
- HOLOPAINEN, M., and WANG, G., 1998. The calibration of digitised aerial photographs for forest stratification. *International Journal of Remote Sensing*. Vol.19, No.4: 677-696.
- HONKAVAARA, E., and HØGHOLEN, A., 1996. Automatic tie point extraction in aerial triangulation. *International Archives of Photogrammetry and Remote Sensing*. Vol.XXXI, Part B3: 337-342.
- HOWARD, J.A., 1991. *Remote Sensing of Forestry resources*. Chapman and Hall, London. 420 pp.
- HOWARD, M.D., 1997. A study of the measurement of bark thickness, diameter at breast height, merchantable height and total tree height. *Unpublished M.Sc. thesis, University of Stellenbosch*.
- HUGERSHOFF, R., 1933. *Die photogrammetrische Vorratsermittlung*. In: *Tharandter forstliches Jahrbuch* 84: 159-166.
- HUGERSHOFF, R., 1939. *Die Bildmessung und ihre forstlichen Anwendungen*. *Der Deutsche Forstwirt* 50: 612-619.
- JACOBSEN, K., 1998a. Self-calibration of IRS-1C PAN-camera. *The International Archives of Photogrammetry and Remote Sensing*. Vol.XXXII, Part4.

- JACOBSEN, K., 1998b. Mapping with IRS-1C images. Paper presented at the ASPRS Annual Convention.
- JACOBSEN, K., KONECNY, G., and WEGMANN, H., 1998. High resolution sensor test comparison with SPOT, KFA 1000, KVR 1000, IRS-1C and DPA in Lower Saxony. *The International Archives of Photogrammetry and Remote Sensing*. Vol. XXXII, Part 4.
- JAMET, O., 1996. *Extraction automatique d'objets sur Stations Photogrammetriques Numeriques*. *International Archives of Photogrammetry and Remote Sensing*. Vol. XXXI, Part B3: 365-376.
- JENSEN, J.R., 1996. Issues Involving the Creation of Digital Elevation Models and Terrain Corrected Orthoimagery Using Soft-Copy Photogrammetry. In: *Digital Photogrammetry: An Addendum to the Manual of Photogrammetry*. American Society for Photogrammetry and Remote Sensing, Bethesda, Maryland, pp. 167-179.
- KÄTSCH, C., 1991a. *Zweiphasige Stichprobenverfahren für Zwecke der Betriebsinventur auf der Basis einfacher Luftbildauswertung*. Diss., Georg-August Universität Göttingen.
- KÄTSCH, C., 1991b. *Rationalisierung von Waldinventuren auf Betriebsebene – welche Möglichkeiten bietet das Luftbild?* *Allgemeine Forst und Jagdzeitung*. Heft 9: 161-165.
- KÄTSCH, C., and VAN LAAR, A., 1994. *Modelle zur Schätzung des Holzvorrates von Waldbeständen aus photogrammetrischen Variablen*. *Allgemeine Forst und Jagdzeitung*. Heft 9: 157-163.
- KÄTSCH, C., and VOGT, H., 1999. Remote sensing from space – present and future applications in forestry, nature conservation and landscape management. *SAFJ*, No. 185: 14-26.
- KÄTSCH, C., and STÖCKER, M., 2000. *Untersuchung zur automatischen Ermittlung von Bestandeshöhen auf Luftbildern mit Hilfe der Digitalen Photogrammetrie*. *Allgemeine Forst und Jagdzeitung*. Heft 171, Jg.4: 74-80.
- KAISER, D., and MILLER, S.B., 1996. Comparison of Softcopy VS. Hardcopy Photogrammetry for DTM Collection, Editing and Quality Control. In: *Digital Photogrammetry: An Addendum to the Manual of Photogrammetry*. American Society for Photogrammetry and Remote Sensing, Bethesda, Maryland, pp. 142-144.
- KERSTEN, T., and O'SULLIVAN, W., 1996. Experiences with the Helava Automated Triangulation System. *International Archives of Photogrammetry and Remote Sensing*. Vol. XXXI, Part B3: 591-596.

- KERSTEN, T.P., and STALLMANN, D., 1995. Experiences with semi- automatic aerotriangulation on Digital Photogrammetric workstations. *Proceedings SPIE* 2646: 77-88.
- KILIAN, J., HAALA, N., and ENGLICH, M., 1996. Capture and evaluation of airborne laser scanner data. *International Archives of Photogrammetry and Remote Sensing*. Vol.XXXI, Part B3: 383-388.
- KILKKI, P., and PÄIVINEN, R., 1987. Reference sample plots to combine field measurements and satellite data in forest inventory. *Univ. Helsinki, Depart. Forest Mensuration and Management. Research Notes* 19: 209-215.
- KLETZLI, R., 1996. GPS Aided Photogrammetry. In: *Digital Photogrammetry: An Addendum to the Manual of Photogrammetry*. American Society for Photogrammetry and Remote Sensing, Bethesda, Maryland, pp. 71-74.
- KÖHL, M., 1991. Vierphasige Stichprobenverfahren zur Holzvorratsschätzung. In: *Fernerkundung in der Forstwirtschaft*. Verlag Wichmann, Karlsruhe, pp. 170-187.
- KÖLBL, O., 1996. Photogrammetric Scanners. In: *Digital Photogrammetry: An Addendum to the Manual of Photogrammetry*. American Society for Photogrammetry and Remote Sensing, Bethesda, Maryland, pp. 3-38.
- KONECNY, G., and SCHIEWE, J., 1996. Mapping from digital satellite image data with special reference to MOMS-02. *ISPRS Journal of Photogrammetry and Remote Sensing*. Vol.51, No.4: 173-181.
- KONECNY, G., and LEHMANN, G., 1984. *Photogrammetrie*. De Gruyter, Berlin. 392 pp.
- KORNUS, W., LEHNER, M., EBNER, H., FRÖBA, H., and OHLHOF, T., 1998. Photogrammetric point determination and DEM generation using MOMS-2P three-line imagery. *The International Archives of Photogrammetry and Remote Sensing*. Vol. XXXII, Part 4.
- KOUKOULAS, S., and BLACKBURN, G.A., 1997. Modelling woodland gap dynamics using high resolution imagery: but when is a gap not a gap? *Proceedings of the 23<sup>rd</sup> Annual Conference and Exhibition of the Remote Sensing Society* : 147-153.
- KRAMER, H., and AKÇA, A., 1996. *Leitfaden zur Waldmeßlehre*. Sauerländer's Verlag, Frankfurt a.M.
- KRAUS, K., 1993. *Photogrammetry*. Vol.1,2. Verlag Dümmler, Bonn. 397 pp.

- KRAUS, K., 1997. *Herausforderungen an die Photogrammetrie und Fernerkundung – Zukünftige Aspekte in der Forschung. Photogrammetrie, Fernerkundung, Geoinformation. Heft 6.*
- KRUMMHEUER, F., 1998. *Auswertung von Luftbildern ausgewählter Buchenbestände mit Fouriertechniken. DGPF 3: 165-176.*
- KRUPNIK, A., and SCHENK, T., 1997. Experiments with matching in the object space for aerotriangulation. *ISPRS Journal of Photogrammetry and Remote Sensing 52: 160-168.*
- KUBIK, K., and HARVEY, P., 1996. Experimental study of optimal digital mapping parameters. *International Archives of Photogrammetry and Remote Sensing. Vol. XXXI, Part B2: 203-206.*
- KUNTZ, S. and SIEGERT, F., 1994. Evaluation of ERS-1 SAR data for forest monitoring in Indonesia. *Proceedings of the First ERS-1 Pilot Project Workshop, Toledo, Spain (ESA SP-365) : 263-271.*
- LAPRADE, G.L., 1980. Stereoscopy. In: SLAMA, C.C., (Editor-in-chief). *Manual of Photogrammetry.* American Society for Photogrammetry and Remote Sensing, Falls Church, Va. 4<sup>th</sup> Ed. 1056 pp.
- LEBERL, F., 1991. The promise of softcopy photogrammetry. In: EBNER, H., FRITSCH, D., and HEIPKE, C., (Eds.). *Digital Photogrammetric Systems.* Verlag Wichmann, Karlsruhe. pp. 3-14.
- LEBERL, F.W., 1996. Practical Concerns in Softcopy Photogrammetry Processing Systems. In: *Digital Photogrammetry: An Addendum to the Manual of Photogrammetry.* American Society for Photogrammetry and Remote Sensing, Bethesda, Maryland. pp. 230-238.
- LEBERL, F.W., GRUBER, M., KELLERER-PIRKLBAUER, W., PINZ, A., and URAY, P., 1996. Surface reconstruction. *International Archives of Photogrammetry and Remote Sensing. Vol. XXXI, Part B3: 421-428.*
- LH SYSTEMS, 1998. User's Manual SOCET SET.
- LIGHT, D.L., 1980. Satellite photogrammetry. In: SLAMA, C.C., (Editor-in-chief). *Manual of Photogrammetry.* American Society for Photogrammetry and Remote Sensing, Falls Church, Va. 4<sup>th</sup> Ed. 1056 pp.
- LILLESAND, T.M., and KIEFER, R.W., 1994. *Remote Sensing and Image Interpretation.* 3<sup>rd</sup> Ed. John Wiley and Sons, Singapore. 750 pp.

- LINDGREN, D.T., 1985. *Land use planning and remote sensing*. Martinus Nijhoff Publishers, Dordrecht. 176 pp.
- LÖTSCH, F., and HALLER, K.E., 1964. *Forest Inventory*. Vol.1. BLV, München. 436 pp.
- LÖTSCH, F., ZÖHRER, F., and HALLER, K.E., 1973. *Forest Inventory*. Vol.2. BLV, München. 469 pp.
- LO, K.-C., 1996. Linear features extraction by string matching for automatic DEM generation. *International Archives of Photogrammetry and Remote Sensing*. Vol.XXXI, Part B3: 472-477.
- LUCAS, J.R., 1996. Covariance propagation in kinematic GPS photogrammetry. In: *Digital Photogrammetry: An Addendum to the Manual of Photogrammetry*. American Society for Photogrammetry and Remote Sensing, Bethesda, Maryland, pp. 124-129.
- LUCAS, J.R., and LAPINE, L.A., 1996. Airborne GPS. In: *Digital Photogrammetry: An Addendum to the Manual of Photogrammetry*. American Society for Photogrammetry and Remote Sensing, Bethesda, Maryland, pp. 39-40.
- LUE, Y., 1996. Towards a higher level of automation for *SoftPlotter*. *International Archives of Photogrammetry and Remote Sensing*. Vol.XXXI, Part B3: 478-483.
- MAAS, H.-G., 1996. Automatic DEM generation by multi-image feature based matching. *International Archives of Photogrammetry and Remote Sensing*. Vol.XXXI, Part B3: 484-489.
- MACDONALD, A., GEMMELL, F., and VARJO, J., 1997. Investigation of spectral vegetation indices for forest information content. *Proceedings of the 23<sup>rd</sup> Annual Conference and Exhibition of the Remote Sensing Society*. Pp: 153-158.
- MADER, G.L., 1996. Kinematic positioning with the Global Positioning System. In: *Digital Photogrammetry: An Addendum to the Manual of Photogrammetry*. American Society for Photogrammetry and Remote Sensing, Bethesda, Maryland, pp. 41-51.
- MAGUIRE, D.J., GOODCHILD, M.F., and RHIND, D.W., (Eds.), 1991. *Geographical information systems: principles and applications*. Longman Scientific and Technical, Harlow, Essex. 2 vol.
- MANZER, G., 1996. Avoiding Digital Orthophoto Problems. In: *Digital Photogrammetry: An Addendum to the Manual of Photogrammetry*. American Society for Photogrammetry and Remote Sensing, Bethesda, Maryland, pp. 158-162.

- MATHER, A.S., 1992. *Global Forest Resources*. Bellhaven Press, London. 341 pp.
- MAUNE, D.F., 1996. Introduction to Digital Elevation Models (DEM). In: *Digital Photogrammetry: An Addendum to the Manual of Photogrammetry*. American Society for Photogrammetry and Remote Sensing, Bethesda, Maryland, pp. 131-134.
- MAYR, W., and REINHARDT, W., 1996. Digital Photogrammetry joins GIS – a powerful combination. *International Archives of Photogrammetry and Remote Sensing*. Vol.XXXI, Part B4: 553-556.
- McCLOY, K.R., 1990. The development of resource monitoring strategies. In: CRACKNELL, A., HAYES, L., and GEN, H.W., (Eds.). *Remote Sensing Yearbook*. Taylor and Francis, London.
- McGLONE, C., 1996. Sensor Modelling in Image Registration. In: *Digital Photogrammetry: An Addendum to the Manual of Photogrammetry*. American Society for Photogrammetry and Remote Sensing, Bethesda, Maryland, pp. 115-123.
- McKEON, D.M., Jr., McGLONE, C., COCHRAN, S.D., HSIEH, Y.C., ROUX, M., and SHUFELT, J.A., 1996. Automatic Cartographic Feature Extraction Using Photogrammetric Principles. In: *Digital Photogrammetry: An Addendum to the Manual of Photogrammetry*. American Society for Photogrammetry and Remote Sensing, Bethesda, Maryland, pp. 195-212.
- MEAS-YEDID, V., and STAMON, G., 1995. Map vegetation areas segmentation based on texture operators. *Proceedings SPIE* 2646: 268-276.
- MEINEL, G., LIPPOLD, R., and NETZBAND, M., 1998. The potential use of new high resolution satellite data for urban and regional planning. *The International Archives of Photogrammetry and Remote Sensing*. Vol. XXXII, Part 4: 375-381.
- MEYER, P., STAENZ, K., and ITTEN, K.I., 1996. Semi-automated procedures for tree species identification in high spatial resolution data from digitised colour infrared aerial photography. *ISPRS Journal of Photogrammetry and Remote Sensing*. Vol.51, No.1: 5-16.
- MILLER, S.B., HELAVA, U.V., and DEVENECIA, K., 1992. Softcopy Photogrammetric Workstations. *Photogrammetric Engineering and Remote Sensing*. Vol.LVIII, No.1: 77-84.
- MITSCHERLICH, G., 1970. *Wald, Wachstum und Umwelt. Vol.1. J.D. Sauerländer's Verlag, Frankfurt am Main. 142 pp.*
- MOFFITT, F.H., 1967. *Photogrammetry*. International Textbook Company, Scranton, Pennsylvania. 540 pp.

- MORGADO, A., and DOWMAN, I., 1997. A procedure for automatic absolute orientation using aerial photographs and a map. *ISPRS Journal of Photogrammetry and Remote Sensing* 52: 169-182.
- NESSET, E., 1997. Determination of mean tree height of forest stands using airborne laser scanner data. *ISPRS Journal of Photogrammetry and Remote Sensing* 52: 49-56.
- NESSET, E., 1999. Point accuracy of combined pseudorange and carrier phase differential GPS under forest canopy. *Can. J. For. Res.* 29: 547-553.
- NAITHANI, K.K., and KOUL, P.N., 1996. Map updation and terrain modelling. *International Archives of Photogrammetry and Remote Sensing*. Vol.XXXI, Part B4: 586-592.
- NEVATIA, R., 1996. Matching in 2-D and 3-D. *International Archives of Photogrammetry and Remote Sensing*. Vol.XXXI, Part B3: 567-574.
- NIELSEN, U., 1971. Tree and Stand Measurements from Aerial Photographs: An annotated Bibliography. *Canadian Forestry Service. Forest Management Inst., Information Report FMR-x-29*. January 1971.
- NILSSON, M., 1996. Estimation of tree heights and stand volume using an airborne Lidar system. *Remote Sens. Environ.* 56: 1-7.
- NOLETTE, C., GAGNON, P.-A., and AGNARD, J.-P., 1992. The DVP: design, operation, and performance. *Photogrammetric Engineering and Remote Sensing*. Vol.LVIII, No.1: 65-70.
- NORVELLE, F.R., 1992. Stereo correlation: window shaping and DEM corrections. *Photogrammetric Engineering and Remote Sensing*. Vol.LVIII, No.1: 111-115.
- NORVELLE, F.R., 1996. Using Iterative Orthophoto Refinements to Generate and Correct Digital Elevation Models (DEMs). In: *Digital Photogrammetry: An Addendum to the Manual of Photogrammetry*. American Society for Photogrammetry and Remote Sensing, Bethesda, Maryland, pp. 151-156.
- NRSA, 1995. *IRS-1C Handbook*. Hyderabad, India.
- NRSA, 1997. *IRS-1D Handbook*. Hyderabad, India
- OLSEN, R.W., 1980. Rectification. In: SLAMA, C.C., (Editor-in-chief). *Manual of Photogrammetry*. American Society for Photogrammetry and Remote Sensing, Falls Church, Va. 4<sup>th</sup> Ed. 1056 pp.

- OTT, R.L., 1993. *An introduction to statistical methods and data analysis*. Duxbury Press, Belmont. 4<sup>th</sup> Ed. 1183 pp.
- PAN, H.-P., 1996. Uniform full-information image matching using complex conjugate wavelet pyramids. *International Archives of Photogrammetry and Remote Sensing*. Vol.XXXI, Part B3: 619-625.
- PETRIE, G., and EL-NIWEIRI, A.E.H., 1994. Comparative testing of space images for small-scale topographic mapping of Sudan. *ITC Journal 1994-2*: 95-112.
- PETRIE, G., and LIWA, E.J., 1995. Comparative tests of small-scale aerial photographs and Spot satellite images for topographic mapping and map revision in eastern, central and southern Africa. *ITC Journal*. No.1995-1: 43-55.
- PETRIE, G., 1995. *Photogrammetry and remote sensing*. In: AGI Source Book, Association for Geographic Information, London, pp. 73-85.
- PETRIE, G., 1997a. The current situation in Africa regarding topographic mapping and map revision from satellite images. *ITC Journal 1997-1*: 49-63.
- PETRIE, G., 1997b. Developments in digital photogrammetric systems for topographic mapping applications. *ITC Journal 1997-2*: 121-135.
- PETRIE, G., AL-ROUSSAN, N., EL-NIWEIRI, A.E.H., LI, Z., and VALADAN ZOEJ, M.J., 1997. Topographic mapping of arid and semi-arid areas in the Red Sea region from stereo space imagery. *EARSel Advances in Remote Sensing Yearbook*: 11-30.
- PETRIE, G., 1998a. Topographic mapping from space imagery: with special reference to Africa and the Middle East. *Festschrift – G.Konecny; Wissenschaftliche Arbeiten der Fachrichtung Vermessungswesen der Universität Hannover*. 227: 229-241.
- PETRIE, G., 1998b. Space imagery for topographic mapping. *Geoinformatics*. Vol.1, No.3: 24-33.
- PHILIP, M.S., 1994. *Measuring Trees and Forests*. 2<sup>nd</sup> Ed. CAB International, Wallingford. 310 pp.
- PIECHULLEK, C., and HEIPKE, C., 1996. DTM refinement using multi image Shape from Shading. *International Archives of Photogrammetry and Remote Sensing*. Vol.XXXI, Part B3: 644-651.
- PRODAN, M., 1965. *Holzmesslehre*. J.D. Sauerländer's Verlag, Frankfurt. 644 pp.

- RAO, D.P., GAUTAM, N.C., NAGARAJA, R., and RAM MOHAN, P., 1996. IRS-1C applications in land use mapping and planning. *Current Science*. 70: 575-581.
- REES, W.G., 1990. *Physical Principles of Remote Sensing*. Cambridge University Press, Cambridge. 247 pp.
- ROSENHOLM, D., 1993. Land use and vegetation mapping by satellite: SSC Satellitbild experiences 1987-1993. *ITC Journal* 3: 251-260.
- ROSENHOLM, D., and ÅKERMAN, D., 1998. Digital orthophotos from IRS - production and utilisation. *The International Archives of Photogrammetry and Remote Sensing*. Vol. XXXII, Part 4: 501-505.
- ROTTENSTEINER, F., 1996. Three dimensional object reconstruction by object space matching. *International Archives of Photogrammetry and Remote Sensing*. Vol. XXXI, Part B3: 692-696.
- ROY, P.S., DUTT, C.B.S., JADHAV, R.N., RANGANATH, B.K., MURTHY, M.S.R., GHARAI, B., UDAYA LAKSHMI, V., KANDAYA, A.K., THAKKER, P.S., 1996. IRS-1C data utilisation for forestry applications. *Current Science*. 70: 606-613.
- RÜTHER, H., and VAN DER VLUGT, G., 1996. Multi-image correlation for Digital Photogrammetric Measurement Systems. *International Archives of Photogrammetry and Remote Sensing*. Vol. XXXI, Part B5: 499-505.
- RÜTHER, H., and VAN DER MERWE, 1996. An image matching scheme using a hybrid feature- and area based approach. *International Archives of Photogrammetry and Remote Sensing*. Vol. XXXI, Part B3: 703-709.
- RYDÉN, A., 1997. Approaches to practical remote sensing for environmental studies: Experiences from a case study in Swaziland and Southern Moçambique. *ITC Journal* 2: 136-145.
- SAGERER, G., KUMMERT, F., and SOCHER, G., 1996. Semantic models and object recognition in computer vision. *International Archives of Photogrammetry and Remote Sensing*. Vol. XXXI, Part B3: 710-723.
- SAR-SIG (SAR Special Interest Group), 1999. FEATURE: SAR from scratch. *Remote Sensing Society Newsletter*. No.99: 28-31.
- SAVOPOL, F., and ARMENAKIS, C., 1998. Modelling of the IRS-1C satellite PAN stereo imagery using the DLT approach. *The International Archives of Photogrammetry and Remote Sensing*. Vol. XXXII, Part 4: 511-514.

- SAYN-WITTGENSTEIN, L., and ALDRED, A.H., 1967. Tree volumes from large scale photos. *Photogrammetry and Engineering* 33: 69-73.
- SCHANDA, E., 1976. Introductory Remarks on Remote Sensing. In: SCHANDA, E., (Ed.). *Remote Sensing for Environmental Sciences*. Springer-Verlag, Berlin. 367 pp.
- SCHARDT, M., 1990. *Verwendbarkeit von Thematic Mapper Daten zur Klassifizierung von Baumarten und natürlichen Altersklassen*. Dissertation, Univ. Freiburg i.Br., Faculty of Forestry.
- SCHEAFFER, R.L., MENDENHALL, W., and OTT, L., 1986. *Elementary survey sampling*. Duxbury Press, Boston. 3<sup>rd</sup> Ed. 324 pp.
- SCHEER, L., AKÇA, A., and FELDKÖTTER, C., 1997. Efficient growing stock estimation from satellite data employing two-phased sampling with regression. *Geo-Information-Systems* 10: 22-25.
- SCHENK, T., 1994. Concepts and algorithms in digital photogrammetry. *ISPRS Journal of Photogrammetry and Remote Sensing*. Vol.49, No.6: 2-8.
- SCHENK, A.F., 1996. Automatic Generation of DEMs. In: *Digital Photogrammetry: An Addendum to the Manual of Photogrammetry*. American Society for Photogrammetry and Remote Sensing, Bethesda, Maryland, pp. 145-150.
- SCHENK, T., 1996. Digital aerial triangulation. *International Archives of Photogrammetry and Remote Sensing*. Vol.XXXI, Part B3: 735-745.
- SCHENK, T., and TOTH, C., 1991. Knowledge-based systems for Digital Photogrammetric Workstations. In: EBNER, H., FRITSCH, D., and HEIPKE, C., (Eds.). *Digital Photogrammetric Systems*. Verlag Wichmann, Karlsruhe, pp. 123-134.
- SCHENK, T., and TOTH, C., 1992. Conceptual issues of Softcopy Photogrammetric Workstations. *Photogrammetric Engineering and Remote Sensing*. Vol.LVIII, No.1: 103-109.
- SCHERZ, J.P., and SCHMIDT, K.K., 1997. Assessment of operational accuracy of DVP softcopy stereoplottter as a tool for GIS capture. *Proceedings of the 3<sup>rd</sup> International Airborne Remote Sensing Conference*. Vol.3, No.825: 305-312.
- SCHIEWE, J., 1996. Mapping using high-resolution and stereoscopic space imagery of MOMS-02. *International Archives of Photogrammetry and Remote Sensing*. Vol.XXXI, Part B4: 742-747.

- SCHIEWE, J., 1998. Effect of lossy data compression techniques on geometry and information content of satellite imagery. *The International Archives of Photogrammetry and Remote Sensing*. Vol. XXXII, Part 4: 540-544.
- SCHNEIDER, C.-T., 1993. *Proceedings SPIE Computer Vision for Industry*. 1989: 370-374.
- SCHULZE, R.E., 1997. South African Atlas of Agrohydrology and Climatology. Part of commission report to DWAf. Dept. of Agricultural Engineering, University of Natal, Pietermaritzburg.
- SHAH, P., 1996. Wavelets and their Applications in Photogrammetry and Remote Sensing Imagery. In: *Digital Photogrammetry: An Addendum to the Manual of Photogrammetry*. American Society for Photogrammetry and Remote Sensing, Bethesda, Maryland, pp. 83-86.
- SHARIF, M., and SALIM, M.J., 1996. DEM optimisation using satellite images. *International Archives of Photogrammetry and Remote Sensing*. Vol.XXXI, Part B4: 774-779.
- SHEARS, J.C., and ALLAN, J.W., 1996. Softcopy Photogrammetry and its uses in GIS. *International Archives of Photogrammetry and Remote Sensing*. Vol.XXXI, Part B4: 70-73.
- SHIVER, B.D., and BORDERS, B.E., 1996. *Sampling techniques for forest resource inventory*. John Wiley and Sons, New York. 356 pp.
- SIMONETT, D.S., 1976. *Remote Sensing of environment*. Addison-Wesley, Reading, Mass. 694 pp.
- ŠKALOUD, J., CRAMER, M., and SCHWARZ, K.P., 1996. Exterior orientation by direct measurement of camera position and attitude. *International Archives of Photogrammetry and Remote Sensing*. Vol.XXXI, Part B3: 125-129.
- SLAMA, C.C., 1980. Aerotriangulation. In: SLAMA, C.C., (Editor-in-chief). *Manual of Photogrammetry*. American Society of Photogrammetry and Remote Sensing, Falls Church, Va. 4<sup>th</sup> Ed. 1056 pp.
- SMIT, J.L., RÜTHER, H., and SIEBRITS, E., 1996. The 3D mapping of a textured surface using Digital Photogrammetry techniques. *International Archives of Photogrammetry and Remote Sensing*. Vol.XXXI, Part B4: 728-733.
- SMITH, M.J., and WALDRAM, D.A., 1996. Automated digital terrain modelling of coastal zones. *International Archives of Photogrammetry and Remote Sensing*. Vol.XXXI, Part B4: 919-924.

- SRIVASTAVA, P.K., and ALURKAR, M.S., 1997. Inflight calibration of IRS-1C imaging geometry for data products. *ISPRS Journal of Photogrammetry and Remote Sensing* 52: 215-221.
- SRIVASTAVA, P.K., RAMAKRISHNAN, R., NANDKUMAR, R., PADMANABHAN, N., GOPALA KRISHNA, B., and MAJUMDER, K.L., 1996. Cartographic potential of IRS-1C data products. *International Archives of Photogrammetry and Remote Sensing*. Vol.XXXI, Part B4: 823-828.
- STÖCKER, M., 1999. *Untersuchungen zum forstlichen Anwendungspotential der digitalen Photogrammetrie, dargestellt am Beispiel von Waldbeständen des Forstamtes Seesen*. Unpublished diploma thesis, Fachhochschule Hildesheim/Holzminde, Göttingen, Faculty of Forestry.
- SWERDLOW, J.L., 1998. Population. *National Geographic* 4: 5-6.
- TANG, L., BRAUN, J., and DEBITSCH, R., 1997. Automatic aerotriangulation – concept, realisation and results. *ISPRS Journal of Photogrammetry and Remote Sensing* 52: 122-131.
- TAYLOR, D.R.F., (Ed.), 1991. *Geographic information systems: the microcomputer and modern cartography*. Pergamon Press, Oxford. 251 pp.
- THEODOSSIOU, E.J., and DOWMAN, I.J., 1990. Height accuracy of SPOT. *Photogrammetric Engineering and Remote Sensing*. Vol.56, No.12: 1643-1649.
- THOMAS, M., EVERARD, D.A., and VAN WYK, G.F., 1997. An evaluation of a two-metre resolution black and white satellite image for woodland remote sensing applications. *Southern African Forestry Journal* 180: 33-36.
- THOMPSON, M., 1997. CSIR/ARC National land-cover database project. *CSIR Report*, Pretoria. 26 pp.
- THOMPSON, M.M., 1980. Foundations of photogrammetry. In: SLAMA, C.C., (Editor-in-chief). *Manual of Photogrammetry*. American Society of Photogrammetry and Remote Sensing, Falls Church, Va. 4<sup>th</sup> Ed. 1056 pp.
- TIWARI, A.K., 1994. Mapping forest biomass through digital processing of IRS-1A data. *Int. Journal of Remote Sensing* 15: 1849-1866.
- TOMPPA, E., 1993. Multi-source National Forest Inventory of Finland. *Proceedings of Ilvessalo Symposium on National Forest Inventories. Finland*. IUFRO S4.02. *The Finnish Forest Research Institute. Research Papers* 444: 52-60.

- TOMPPO, E., and PEKKARINEN, A., 1997. *Methodenerprobung der Finnischen Nationalen Multiquellen-Waldinventur in Nordrhein-Westfalen*. In: *Testlauf zur Landeswaldinventur. Heft 5 der Schriftenreihe der Landesforstverwaltung Nordrhein-Westfalen* : 52-67.
- TOTH, C.K., 1996. Image Compression in Photogrammetric Practice: An Overview. In: *Digital Photogrammetry: An Addendum to the Manual of Photogrammetry*. American Society for Photogrammetry and Remote Sensing, Bethesda, Maryland, pp. 75-82.
- TOTH, C.K., and TEMPLER, A., 1996. Extracting high resolution Digital Elevation Models and features in a softcopy environment. *International Archives of Photogrammetry and Remote Sensing*. Vol.XXXI, Part B3: 863-867.
- TRINDER, J. and DONNELLY, B., 1996. Digital Photogrammetry. *International Journal for Geomatics (GIM)*. 10: 6-8.
- TSENG, Y-H., TZEN, J-J., TANG, K-P., and LIN, S-H., 1997. Image-to-image registration by matching area features using Fourier descriptors and neural networks. *Photogrammetric Engineering and Remote Sensing*. Vol.63, No.8: 975-983.
- TYUKAVKIN, D.V., and BEKLEMISHEV, N.D., 1995. Contour based computer vision system. *Proceedings SPIE* 2646: 261-267.
- TWU, Z.-G., and DOWMAN, I.J., 1996. Automatic height extraction from ERS-1 SAR imagery. *International Archives of Photogrammetry and Remote Sensing*. Vol.XXXI, Part B2: 380-383.
- ULANDER, L.M.H., GUSTAVSSON, A., HELLSTEN, H., and LARSSON, B., 2000. Use of low VHF-band SAR data for biomass mapping and forestry management planning. *Proceedings of the 28<sup>th</sup> International Symposium on Remote Sensing of Environment, Cape Town, South Africa*.
- VALADAN ZOEJ, M.J., and PETRIE, G., 1998. Mathematical modelling and accuracy testing of SPOT level 1B stereopairs. *Photogrammetric Record*. 16(91): 67-82.
- VAN DER MERWE, N., and RÜTHER, H., 1996. An image matching scheme using a hybrid feature- and area based approach. *International Archives of Photogrammetry and Remote Sensing*. Vol.XXXI, Part B3: 703-709.
- VAN DER ZEL, D., 1988. A forest map of Southern Africa with the aid of Landsat imagery. *CSIR Report*, Pretoria, 79pp. 31 maps.
- VAN LAAR, A., 1963. The Aerial Photograph in Forestry. Part I, Reprint *Southern African Forestry Journal* 47.

- VAN LAAR, A., 1964. The Aerial Photograph in Forestry. Part II, Reprint *Southern African Forestry Journal* 48.
- VAN LAAR, A., and AKÇA, A., 1997. *Forest Mensuration*. Cuvillier Verlag, Göttingen. 418 pp.
- VOHRA, K.V., and DOWMAN, I.J., 1996. Automatic extraction of large buildings from high resolution satellite images for registration with a map. *International Archives of Photogrammetry and Remote Sensing*. Vol.XXXI, Part B3: 903-908.
- VON GADOW, K., and BREDENKAMP, B., 1992. *Forest management*. Academia, Pretoria. 151 pp.
- VOSELMAN, G., 1995. Applications of tree search methods in digital photogrammetry. *ISPRS Journal of Photogrammetry and Remote Sensing*. Vol.50, No.4: 29-37.
- WALKER, A.S., 1995. Analogue, analytical and digital photogrammetric workstations: practical investigations of performance. *Photogrammetric Record*, 15(85): 17-25.
- WALKER, A.S., and PETRIE, G., 1996. Digital Photogrammetric Workstations 1992-1996. *International Archives of Photogrammetry and Remote Sensing*. Vol.XXXI, Part B2: 384-395.
- WARNER, W.S., SUNDHEIM, E., and BLANKENBERG, L.E., 1997. Comparing slope maps generated from digital photogrammetry with field measurements. *Proceedings of the 3<sup>rd</sup> International Airborne Remote Sensing Conference*. Vol.3, No.825: 285-292.
- WELCH, R., and REMILLARD, M., 1996. GPS, Photogrammetry and GIS for Resource Mapping Applications. In: *Digital Photogrammetry: An Addendum to the Manual of Photogrammetry*. American Society for Photogrammetry and Remote Sensing, Bethesda, Maryland, pp. 183-194.
- WILD, D., and KRZYSZEK, P., 1996. Automatic breakline detection using an edge preserving filter. *International Archives of Photogrammetry and Remote Sensing*. Vol.XXXI, Part B3: 946-952.
- WIND, M., 1998. Investigation into the automatic generation of heights of different Danish landscape types. *The International Archives of Photogrammetry and Remote Sensing*. Vol. XXXII, Part 4.
- WOLFF, B., 1992. *Betriebs- und bestandesweise Holzvorratsinventur auf der Basis von permanenten terrestrischen und Luftbild-Stichproben*. Diss., University of Göttingen.

- WOLF, P.R., 1974. *Elements of Photogrammetry*. McGraw-Hill Book Company, New York. 562 pp.
- WONG, K.W., 1980. Basic mathematics of photogrammetry. In: SLAMA, C.C., (Editor-in-chief). *Manual of Photogrammetry*. American Society of Photogrammetry and Remote Sensing, Falls Church, Va. 4<sup>th</sup> Ed. 1056 pp.
- WROBEL, B., and KRAUTH, A., 1996. *Ein Ansatz zur Vegetationserkennung aus Luftbildern mit Hilfe von Markov-Zufallsfeldern in Verbindung mit der Oberflächenrekonstruktion*. *International Archives of Photogrammetry and Remote Sensing*. Vol.XXXI, Part B3: 965-970.
- ZENG, B.Q., and ZE, X.G., 1996. A reliable method for assessing the image measurement quality under the influence of image compression. *International Archives of Photogrammetry and Remote Sensing*. Vol.XXXI, Part B1: 160-162.
- ZHANG, J., and KIRBY, R.P., 1997. An evaluation of fuzzy approaches to mapping land cover from aerial photographs. *ISPRS Journal of Photogrammetry and Remote Sensing* 52: 193-201.
- ZHANG, B. and MILLER, S.B., 1997. Adaptive automatic terrain extraction. In: MCKEOWN, D.M., MCGLONE, J.C., and JAMET, O. (Eds.). Integrating photogrammetric techniques with science analysis and machine vision III. *Proceedings of SPIE*. Vol. 3072, 338: 27-36.
- ZHENG, YONG-JIAN, 1993. Digital photogrammetric inversion: theory and application to surface reconstruction. *Photogrammetric Engineering and Remote Sensing*. Vol.LIX, No.4: 489-498.
- ZÖHRER, F., 1980. *Forstinventur*. Verlag Paul Parey, Hamburg und Berlin. 207 pp.

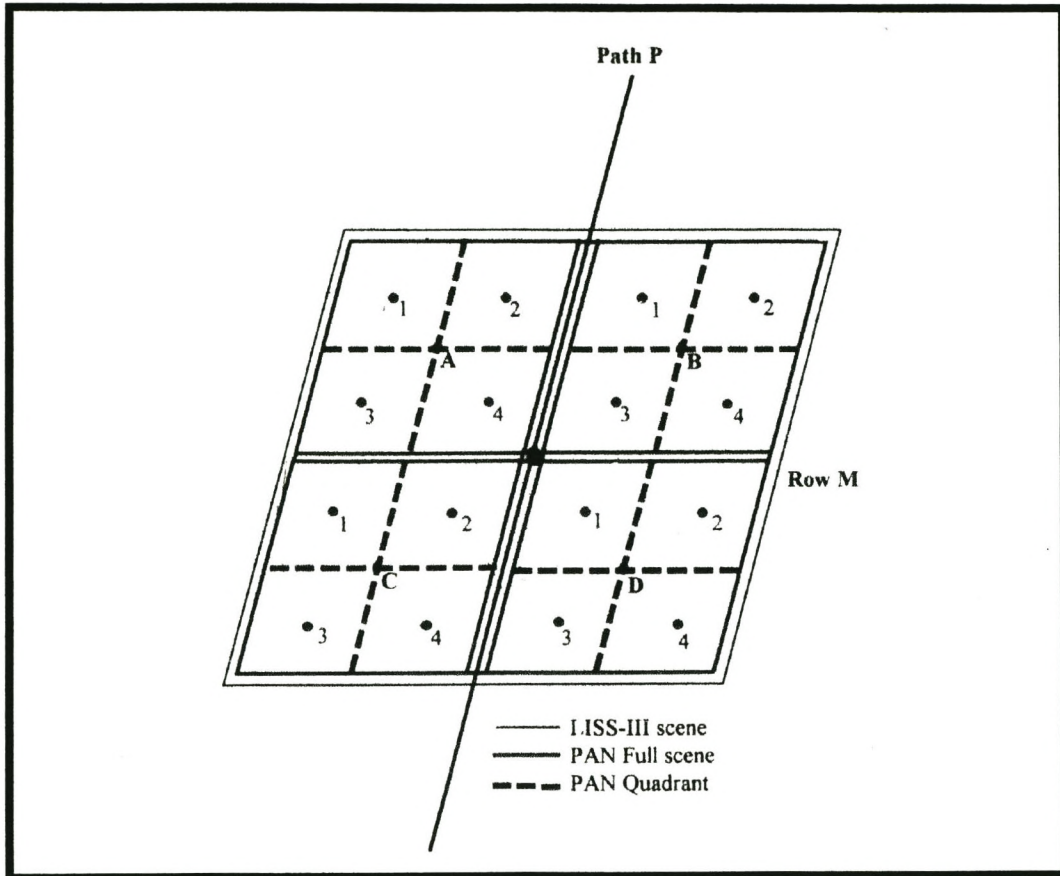


**Figure 5** PAN subscenes (NRSA, 1995)

## APPENDIX 4: ACCURACY REPORT - TRIANGULATION

**Table 1** Accuracy report for IRS-1C stereo pair; the ground residuals of X,Y and Z are given in metres

DPW Solution Accuracy QA Report - SCENE 1							
=====							
Solution Method: Absolute							
Iterations: 3							
Redundancy: 52							
Earth Curvature Used: Yes							
Image ID	Atm. Ref. Used	Lens Dist. Used					
=====							
imp_min1.sup (scene 1)	N/A	N/A					
imp_min2.sup (scene 2)	N/A	N/A					
Image ID: <b>imp_min1.sup</b>	Point ID	Use	Pt Type	Ground Residuals			Image
Residual	Image	sigma		X	Y	Z	line
sample	line	sample		=====			
=====	===	=====		=====			
imp_min1_0	ON		Tie				0.16
0.00	0.50	0.50					
imp_min1_1	ON		Tie				-0.46
-0.01	0.50	0.50					
imp_min1_2	ON		Tie				0.09
0.00	0.50	0.50					
imp_min1_3	ON		Tie				-0.28
-0.01	0.50	0.50					
imp_min1_4	ON		Tie				0.09
0.00	0.50	0.50					
imp_min1_5	ON		Tie				-0.19
-0.00	0.50	0.50					
imp_min1_6	ON		Tie				0.17
0.00	0.50	0.50					
imp_min1_7	ON		Tie				-0.31
-0.01	0.50	0.50					
imp_min1_8	ON		Tie				-0.49
-0.01	0.50	0.50					
1	ON		XYZ Cntrl	-0.26	-4.95	2.72	-0.32
-0.35	0.50	0.50					
2	ON		XYZ Cntrl	8.99	2.44	2.26	-0.30
-0.50	0.50	0.50					
3	ON		XYZ Cntrl	-5.20	6.14	1.25	-0.11
-0.03	0.50	0.50					
4	ON		XYZ Cntrl	0.20	14.95	-0.54	0.28
0.10	0.50	0.50					
6	ON		XYZ Cntrl	10.15	-4.23	-1.59	0.15
-0.04	0.50	0.50					
7	ON		XYZ Cntrl	-9.07	-8.00	-3.45	-0.26
0.63	0.50	0.50					
8	ON		XYZ Cntrl	-5.94	3.35	-4.26	0.69
0.70	0.50	0.50					
9	ON		XYZ Cntrl	1.78	-0.05	-0.95	0.59
0.10	0.50	0.50					

10		ON	XYZ Cntrl	3.81	-2.12	1.57	0.16
-0.29	0.50	0.50					
12		ON	XYZ Cntrl	3.96	1.92	-1.97	0.07
0.17	0.50	0.50					
13		ON	XYZ Cntrl	-1.88	-3.28	0.29	-0.32
-0.01	0.50	0.50					
14		ON	XYZ Cntrl	-6.55	-6.18	4.69	-0.33
-0.47	0.50	0.50					
imp_min1_9		ON	Tie				0.18
0.00	1.00	1.00					
imp_min1_10		ON	Tie				0.08
0.00	0.50	0.50					
imp_min1_11		ON	Tie				0.26
0.00	0.50	0.50					
imp_min1_12		ON	Tie				0.36
0.01	0.50	0.50					
imp_min1_13		ON	Tie				-0.16
-0.00	0.50	0.50					
imp_min1_14		ON	Tie				0.25
0.00	0.50	0.50					
imp_min1_15		ON	Tie				0.04
-0.00	0.50	0.50					
RMS error of control pts				<b>5.834m</b>	<b>6.068m</b>	<b>2.521m</b>	0.30
0.24							
RMS error of check points				0.000	0.000	0.000	

DPW Solution Accuracy QA Report - SCENE 2

Image ID: **imp\_min2.sup**

Point ID	Use	Pt Type	Ground Residuals			Image
Residual	Image	sigma	X	Y	Z	line
sample line	sample					
=====	===	=====	=====	=====	=====	
imp_min1_0	ON	Tie				-0.07
0.02	0.50	0.50				
imp_min1_2	ON	Tie				-0.06
0.00	0.50	0.50				
imp_min1_3	ON	Tie				0.21
-0.02	0.50	0.50				
imp_min1_5	ON	Tie				0.23
0.02	0.50	0.50				
imp_min1_6	ON	Tie				-0.22
-0.04	0.50	0.50				
imp_min1_8	ON	Tie				0.51
0.03	0.50	0.50				
1	ON	XYZ Cntrl	-0.26	-4.95	2.72	0.12
0.32	0.50	0.50				
2	ON	XYZ Cntrl	8.99	2.44	2.26	0.57
-0.06	0.50	0.50				
3	ON	XYZ Cntrl	-5.20	6.14	1.25	0.44
0.43	0.50	0.50				
4	ON	XYZ Cntrl	0.20	14.95	-0.54	0.53
0.03	0.50	0.50				

6		ON	XYZ Cntrl	10.15	-4.23	-1.59	-0.34
-0.67	0.50	0.50					
7		ON	XYZ Cntrl	-9.07	-8.00	-3.45	-0.31
-0.10	0.50	0.50					
8		ON	XYZ Cntrl	-5.94	3.35	-4.26	-0.59
-0.28	0.50	0.50					
9		ON	XYZ Cntrl	1.78	-0.05	-0.95	-0.55
-0.22	0.50	0.50					
10		ON	XYZ Cntrl	3.81	-2.12	1.57	-0.20
0.00	0.50	0.50					
12		ON	XYZ Cntrl	3.96	1.92	-1.97	0.18
-0.34	0.50	0.50					
13		ON	XYZ Cntrl	-1.88	-3.28	0.29	0.06
0.07	0.50	0.50					
14		ON	XYZ Cntrl	-6.55	-6.18	4.69	-0.16
0.72	0.50	0.50					
imp_min1_1		ON	Tie				0.37
-0.02	0.50	0.50					
imp_min1_4		ON	Tie				-0.12
-0.03	0.50	0.50					
imp_min1_7		ON	Tie				0.27
-0.01	0.50	0.50					
imp_min1_9		ON	Tie				-0.16
0.01	1.14	1.14					
imp_min1_10		ON	Tie				-0.11
-0.03	0.50	0.50					
imp_min1_11		ON	Tie				-0.34
-0.04	0.54	0.54					
imp_min1_12		ON	Tie				-0.22
-0.03	0.36	0.36					
imp_min1_13		ON	Tie				0.13
-0.01	0.50	0.50					
imp_min1_14		ON	Tie				-0.20
-0.00	0.50	0.50					
imp_min1_15		ON	Tie				-0.09
-0.03	0.50	0.50					
RMS error of control pts				<b>5.834m</b>	<b>6.068m</b>	<b>2.521m</b>	0.31
0.23							
RMS error of check points				0.000	0.000	0.000	

DPW Solution Accuracy QA Report - SCENES 1 AND 2  
=====

Ground Point Summary  
=====

Pt_ID	Use	Pt_Type	X	Y	Z	NumImages
1	ON	XYZ Cntrl	30:51:49.28E	25:01:41.04S	1314.00	2
2	ON	XYZ Cntrl	30:51:01.98E	25:01:59.51S	1407.00	2
3	ON	XYZ Cntrl	30:49:57.43E	25:03:01.54S	1336.00	2
4	ON	XYZ Cntrl	30:49:48.10E	25:02:17.48S	1310.00	2
6	ON	XYZ Cntrl	30:48:46.88E	25:00:45.32S	1280.00	2
7	ON	XYZ Cntrl	30:48:24.30E	25:03:17.09S	1188.00	2
8	ON	XYZ Cntrl	30:55:25.48E	25:00:18.55S	790.00	2
9	ON	XYZ Cntrl	30:55:59.22E	25:00:42.62S	826.00	2
10	ON	XYZ Cntrl	30:55:46.38E	25:01:23.58S	870.00	2
12	ON	XYZ Cntrl	30:53:21.30E	25:02:30.12S	993.00	2
13	ON	XYZ Cntrl	30:54:30.29E	25:01:57.02S	969.00	2
14	ON	XYZ Cntrl	30:52:09.52E	25:01:08.67S	1273.00	2
imp_min1_0	ON	Tie	30:49:21.18E	25:02:20.20S	1255.84	2
imp_min1_2	ON	Tie	30:52:02.96E	25:09:23.62S	1461.86	2
imp_min1_3	ON	Tie	30:52:06.27E	25:01:24.54S	1337.96	2
imp_min1_5	ON	Tie	30:46:49.17E	25:07:38.21S	1131.18	2
imp_min1_6	ON	Tie	30:59:49.63E	25:03:49.19S	771.51	2
imp_min1_8	ON	Tie	30:58:28.27E	25:08:40.93S	1170.73	2
imp_min1_1	ON	Tie	30:54:39.42E	24:56:59.01S	963.15	2
imp_min1_4	ON	Tie	30:48:37.59E	24:55:34.97S	1474.67	2
imp_min1_7	ON	Tie	31:01:27.23E	24:57:12.18S	856.26	2
imp_min1_9	ON	Tie	30:55:24.90E	25:08:03.34S	1280.52	2
imp_min1_10	ON	Tie	30:53:32.47E	25:05:14.45S	878.63	2
imp_min1_11	ON	Tie	30:54:29.84E	25:02:31.57S	850.91	2
imp_min1_12	ON	Tie	30:56:31.70E	25:00:27.41S	737.05	2
imp_min1_13	ON	Tie	30:55:42.29E	24:57:48.13S	935.21	2
imp_min1_14	ON	Tie	30:47:41.06E	25:04:27.56S	1119.11	2
imp_min1_15	ON	Tie	30:51:02.14E	24:59:41.72S	1011.20	2

Pt_ID	Use	Pt_Type	X res.	Y res.	Z res.	NumImages
1	ON	XYZ Cntrl	-0.26	-4.95	2.72	2
2	ON	XYZ Cntrl	8.99	2.44	2.26	2
3	ON	XYZ Cntrl	-5.20	6.14	1.25	2
4	ON	XYZ Cntrl	0.20	14.95	-0.54	2
6	ON	XYZ Cntrl	10.15	-4.23	-1.59	2
7	ON	XYZ Cntrl	-9.07	-8.00	-3.45	2
8	ON	XYZ Cntrl	-5.94	3.35	-4.26	2
9	ON	XYZ Cntrl	1.78	-0.05	-0.95	2
10	ON	XYZ Cntrl	3.81	-2.12	1.57	2
12	ON	XYZ Cntrl	3.96	1.92	-1.97	2
13	ON	XYZ Cntrl	-1.88	-3.28	0.29	2
14	ON	XYZ Cntrl	-6.55	-6.18	4.69	2

RMS of control points                   **5.834m    6.068m    2.521m**

RMS of check points                   0.000    0.000    0.000

## APPENDIX 5: USEFUL INTERNET WEBSITES ON THE TOPICS OF REMOTE SENSING AND PHOTOGRAMMETRY

### 1. Satellite technology

<http://www.nrsa.gov.in>

<http://202.54.32.164>

<http://www.digitalglobe.com>

<http://www.nasa.gov>

<http://www.jpl.nasa.gov>

<http://www.noaa.gov>

<http://www.esrin.esa.it>

<http://web.ngdc.noaa.gov>

<http://adro.radar1.sp-agency.ca>

<http://spaceimaging.com>

<http://www.laafb.af.mil/SMC/CZ/homepage>

<http://www.spotimage.fr>

<http://www.nasda.go.jp>

NRSA, Hyderabad, India

NRSA (National Remote Sensing  
Administration, India)

Earthwatch

NASA (National Aeronautics and  
Space Administration, USA)

JPL (Jet Propulsion Laboratory)

NOAA (National Oceanic and  
Atmospheric Administration)

ESA (European Space  
Administration)

Defense met. satellite

Radarsat home page

Spaceimaging (Ikonos satellite)

NAVSTAR GPS

SPOT image

National Space Development Agency  
of Japan

### 2. Distributors of satellite imagery

<http://spaceimaging.com>

<http://www.cils.dlr.de>

<http://www.eurimage.com>

<http://ccrs.nrcan.gc.ca>

<http://eosps0.gsfc.nasa.gov>

<http://cen.cenet.com/d2/sate.htm>

<http://www.spotimage.fr>

<http://www.digitalglobe.com>

<http://www.sac.co.za>

Spaceimaging (Ikonos satellite, IRS-  
1 C/D data, Landsat, SPOT)

DLR (German Aerospace Centre)

Eurimage

Geomatics Canada

NASA EOS data centre

Russian satellite data

SPOT image

Earthwatch

Satellite Application Centre, South  
Africa

### 3. Software companies (digital image processing, digital photogrammetry and GIS)

<http://www.erdas.com>

<http://www.esri.com>

<http://www.clarklabs.org>

<http://www.lh-systems.com>

<http://www.mapinfo.com>

<http://www.microimages>

ERDAS (Imagine, etc.)

ESRI (Arc/Info; ArcView, etc.)

Clark Labs (IDRISI)

LH Systems (SOCET SET, etc.)

Mapinfo

Microimages (TNTmips, etc.)

<http://www.rsinc.com>  
<http://www.intergraph.com>

Research Systems (ENVI/IDL)  
Intergraph (ImageSatation SSK)

#### 4. Other useful addresses

<http://ourworld.compuserve.com/homepages/eworks>  
<http://www.the-rss.org>  
<http://iufro.boku.ac.at>  
<http://www.lib.berkeley.edu/EART/abbrev2.html>

<http://cla.sc.edu/geog/rslab/rslab.html>  
<http://www.asprs.org>

<http://www.csiro.au>

<http://www.csir.co.za/mikomtek>

Earthworks  
Remote Sensing Society  
IUFRO  
Dictionary of Remote Sensing  
abbreviations  
Index for Remote Sensing archives  
American Society for  
Photogrammetry and Remote Sensing  
CSIRO, Australia (Industrial and  
Scientific Research)  
CSIR (Council for Scientific and  
Industrial Research, South Africa)

**APPENDIX 7: ABSTRACT OF SOUTH AFRICAN FORESTRY FACTS FOR  
THE YEAR 1996/97**

**APPENDIX 8: POSITION OF FLYING STRIP : MPUMALANGA, SOUTH AFRICA**



**Figure 1** The yellow boxes indicate the area covered by the aerial photographs No. 529, 530, 531 and 532 used in this study against a backdrop of IRS-1C imagery of the same area. The town of Sabie can be detected on the lower left corner of the image. The Klipkraal road runs diagonally through the boxed area.

# ERDAS Imagine File Information

## APPENDIX 9: LAYER INFORMATION OF THE TWO IRS-1C SCENES

### File Information:

File Name: irs\_1c\_06\_05\_98.img  
Last Modified: Tue Nov 03 17:57:42 1998  
Number of Layers: 1

### Layer Information:

Name: Band\_1  
Width: 4320  
Height: 4606  
Type: Continuous  
Block Width: 64  
Block Height: 64  
Pixel Depth: Unsigned 8-bit  
Compression Type: None

### Histogram:

Bin Function: Direct  
Minimum: 2  
Maximum: 254  
Mean: 72.437

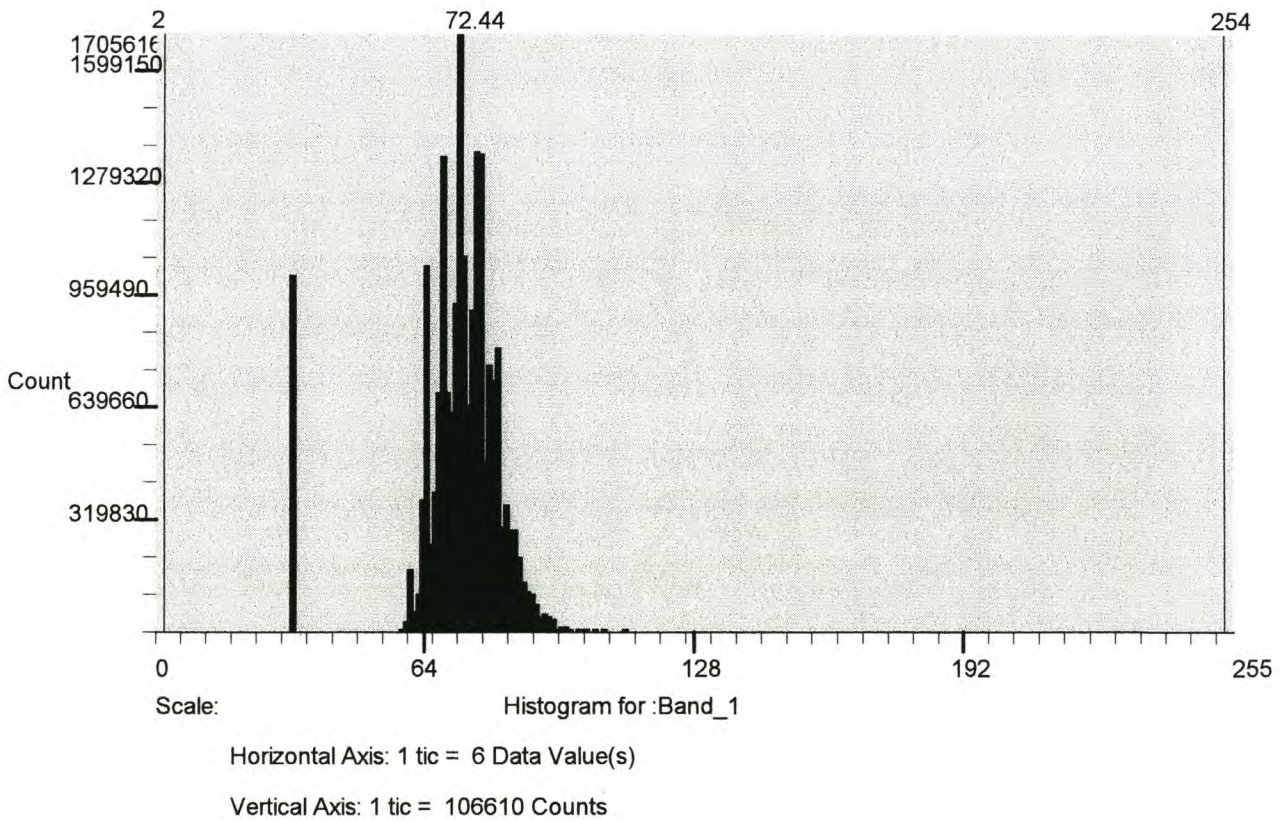


**Figure 1** Histogram for scene 1. The relatively poor contrast is due to the narrow range of the reflectance values.

# ERDAS Imagine File Information

## File Information:

File Name: irs\_1c19\_06\_98.img  
Last Modified: Tue Nov 10 20:38:46 1998  
Number of Layers: 1

## Layer Information:

Name: Band\_1  
Width: 4320  
Height: 4606  
Type: Continuous  
Block Width: 64  
Block Height: 64  
Pixel Depth: Unsigned 8-bit  
Compression Type: None

## Histogram:

Bin Function: Direct  
Minimum: 2  
Maximum: 254  
Mean: 66.2151

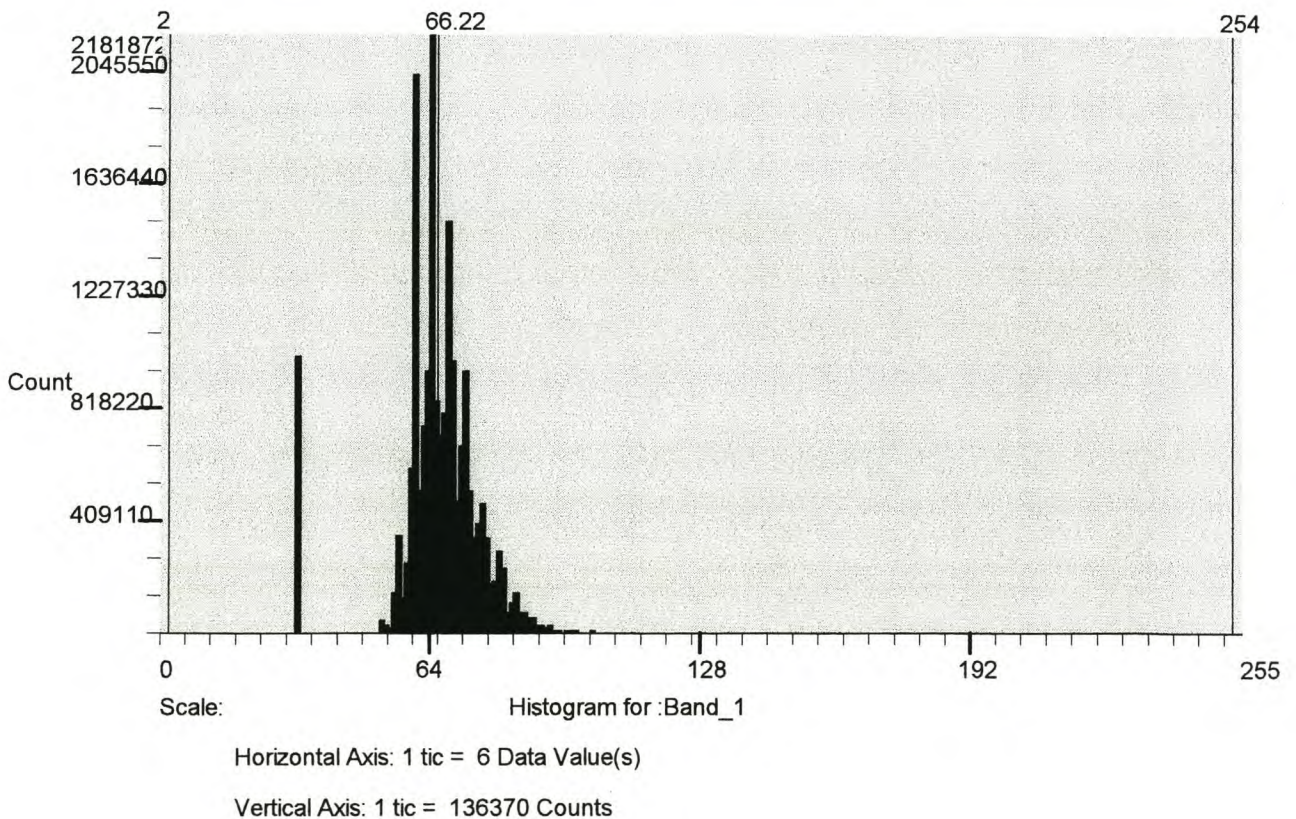


**Figure 2** Histogram for scene 2. The relatively poor contrast is due to the narrow range of the reflectance values.

**APPENDIX 10: LOCATION AND DISTRIBUTION OF GROUND CONTROL POINTS (GCPS) IN THE TEST AREA**



**Figure 3** Location and distribution of used GCPs (indicated with red crosses)

**IRS-1C**

Elevation data for compartment A15

longitude (degrees)	latitude (degrees)	CANOPY (m)	GROUND FILL (m)	TREE HEIGHT (m)	max diff (m)	max diff (m)	
30.89515658	-25.03707929	982.2569	990.2261353	-7.969238281		0.266418	
30.89535474	-25.03707929	985.61554	989.3738403	-3.758300781		3.520996	max diff ignoring small trees
30.89555291	-25.03707929	988.28888	989.1776123	-0.88873291		8.809998	21.87109
30.89575107	-25.03707929	989.44818	989.1817627	0.266418457	0.266418457	15.81653	27.4494
30.89495842	-25.03689874	984.80212	988.3652344			21.87109	35.92957
30.89515658	-25.03689874	987.26654	987.7684326	-3.563110352		27.4494	38.14978
30.89535474	-25.03689874	989.43274	988.3885498	-0.50189209		35.92957	43.18671 50% of red. Pop
30.89555291	-25.03689874	991.13513	988.3387451	1.044189453		38.14978	45.44775 45.44775
30.89575107	-25.03689874	991.8559	988.3348999	2.796386719		43.18671	49.99451 49.99451
30.89594923	-25.03689874	991.45813	988.2032471	3.520996094	3.520996094	45.44775	52.65851 52.65851
30.89614739	-25.03689874	990.42651	987.4404907	3.254882813		49.99451	52.65302 52.65302
30.89634556	-25.03689874	988.95361	986.1184692	2.986022949		52.65851	51.20685 51.20685
30.89495842	-25.0367182	989.0329	984.4423218			52.65302	47.97058 47.97058
30.89515658	-25.0367182	990.7868	986.2661133	2.835144043		51.20685	46.86615 46.86615
30.89535474	-25.0367182	992.73218	986.7045898	4.590576172		47.97058	46.47681 46.47681
30.89555291	-25.0367182	994.6098	986.9338989	4.520690918		46.86615	48.66046 48.66046
30.89575107	-25.0367182	995.75885	986.9488525	6.027587891		46.47681	47.95398 47.95398
30.89594923	-25.0367182	995.42792	986.69104	7.67590332		48.66046	44.82489 44.82489
30.89614739	-25.0367182	994.034	985.9614868	8.809997559	8.809997559	47.95398	42.69806 48.61032
30.89634556	-25.0367182	992.06635	984.7515869	8.736877441		44.82489	38.55554
30.89654372	-25.0367182	989.9021	983.1835938	8.072509766		42.69806	40.17157
30.89674188	-25.0367182	991.79541	981.3847656	7.314758301		38.55554	28.69867
30.89476025	-25.03653765	992.9931	979.4507446			40.17157	24.0033
30.89495842	-25.03653765	993.26373	977.4472046	6.718505859		28.69867	41.68701
30.89515658	-25.03653765	992.6452	992.993103	10.41064453		24.0033	
30.89535474	-25.03653765	994.77179	985.8831177	13.5423584		8.739746	
30.89555291	-25.03653765	997.11359	985.7058716	15.81652832	15.81652832	8.814636	means in red
30.89575107	-25.03653765	998.99615	985.5761719	-0.347900391		7.979675	
30.89594923	-25.03653765	999.30487	985.3654175	8.888671875		7.992432	
30.89614739	-25.03653765	998.34692	984.9393921	11.40771484		32.32302	
30.89634556	-25.03653765	995.80615	984.1703491	13.41998291			

Elevation data for compartment A15

<b>longitude</b> (degrees)	<b>latitude</b> (degrees)	<b>CANOPY</b> (m)	<b>GROUND FILL</b> (m)	<b>TREE HEIGHT</b> (m)
30.89515658	-25.03455161	977.4389038	938.3701172	29.32421875
30.89535474	-25.03455161	979.5773315	937.3381348	11.29974365
30.89555291	-25.03455161	981.9399414	936.4787598	5.066955566
30.89614739	-25.03455161	982.1737061	934.203125	7.934265137
30.89634556	-25.03455161	974.9945068	961.5599976	6.32434082
30.89654372	-25.03455161	969.2851563	961.1818237	3.973999023
30.89674188	-25.03455161	959.0442505	960.4220581	1.601745605
30.89694005	-25.03455161	963.2820435	959.6708984	-0.783691406
30.89713821	-25.03455161	943.6741333	959.0996704	-2.940307617
30.89733637	-25.03455161	959.2501221	958.6880493	-4.85559082
30.89753453	-25.03455161	943.6239624	958.3560791	-6.484802246
30.8977327	-25.03455161	970.6899414	958.0302124	37.30285645
30.89793086	-25.03455161	961.1462402	957.6612549	39.06878662
30.89812902	-25.03455161	970.1643677	957.2232666	42.23919678
30.89832718	-25.03455161	100.3682556	956.7073364	45.46118164
30.89852535	-25.03455161	100.7450195	956.1148071	48.61694336
30.89872351	-25.03455161	100.432428	955.4519653	48.6605835
30.89892167	-25.03455161	989.7529907	954.7263794	47.97058105
30.89911984	-25.03455161	995.8654175	953.9446411	13.43450928
30.899318	-25.03455161	977.4299927	953.1121826	8.10333252
30.89951616	-25.03455161	977.331604	952.2333984	-1.377807617
30.89991249	-25.03455161	958.2507324	950.3529053	-15.42553711
30.90011065	-25.03455161	959.9793091	949.3599243	0.562072754
30.90030881	-25.03455161	959.9145508	948.3383789	-14.7321167
30.90050697	-25.03455161	956.8881226	947.2935181	12.659729
30.90070514	-25.03455161	952.7205811	946.2303467	3.484985352
30.9009033	-25.03455161	948.6664429	945.1533813	12.94110107
30.90110146	-25.03455161	944.8234253	944.065979	-856.3390808 Note these blunders
30.90129963	-25.03455161	941.383728	942.9701538	-855.3697876
30.90149779	-25.03455161	938.5609131	941.8665161	-855.0195374
30.90169595	-25.03455161	935.6677246	940.756958	35.02661133

## **APPENDIX 12: RESULTS OF THE REGRESSION ANALYSIS**

**compartment A15**

Plot no.	Tree height		Difference	Diff. in %
	IRS-1C	Tree height AP*		
1		33.8	-3.8	-11.24
2		37.5	-0.5	-1.33
3		37.4	-0.8	-2.14
4		39.8	-0.8	-2.01
5		42.7	-0.7	-1.64
6		43.5	-1.5	-3.45
7		38.6	-0.6	-1.55
8		40.4	-0.4	-0.99
Mean	38.13	39.21	-1.14	-3.04
St.dev.	3.83	2.92	1.13	

\* Tree heights: comparison IRS-1C and AP manual measurement

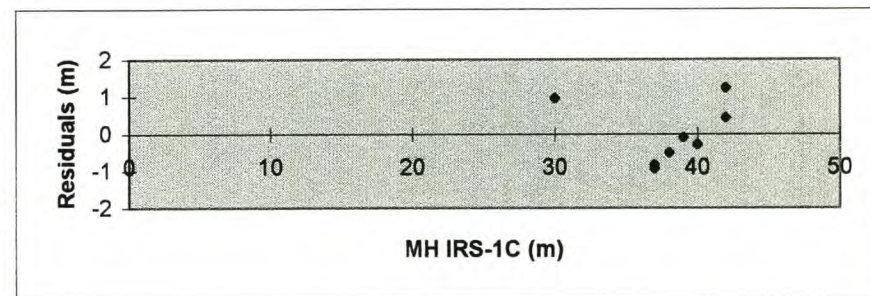
SUMMARY OUTPUT

A15 IRS/AP

Regression Statistics	
Multiple R	0.965762024
R Square	0.932696288
Adjusted R Square	0.921479002
Standard Error	0.874581425
Observations	8

MH = mean height  
 AP = aerial photograph

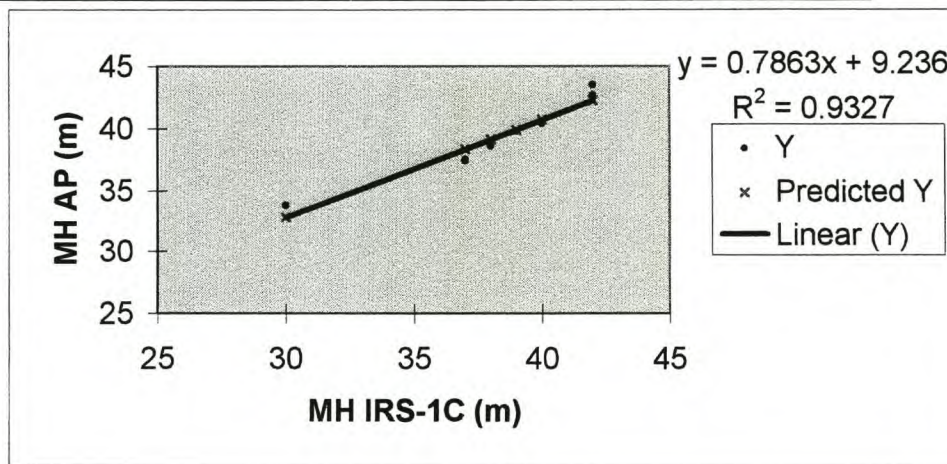
ANOVA					
	df	SS	MS	F	Significance F
Regression	1	63.59939399	63.599	83.14813	9.77788E-05
Residual	6	4.589356015	0.7649		
Total	7	68.18875			



	Coefficients	Standard Error	t Stat	P-value	Lower 95%	Upper 95%	Lower 95.0%	Upper 95.0%
Intercept	9.235965978	3.301929901	2.7971	0.031282	1.156428663	17.31550329	1.156428663	17.31550329
X Variable 1	0.786269745	0.086227407	9.1186	9.78E-05	0.575278727	0.997260763	0.575278727	0.997260763

RESIDUAL OUTPUT

Observation	Predicted Y	Residuals
1	32.82405832	0.975941677
2	38.32794654	-0.827946537
3	38.32794654	-0.927946537
4	39.90048603	-0.100486027
5	42.25929526	0.440704739
6	42.25929526	1.240704739
7	39.11421628	-0.514216282
8	40.68675577	-0.286755772



**compartment A29c**

Plot no.	Tree height		Difference	Diff. in %
	IRS-1C	Tree height AP*		
1	42	43.2	-1.2	-2.78
2	38	42.7	-4.7	-11
3	40	43.4	-3.4	-7.83
4	35	42.2	-7.2	-17.06
5	40	43.7	-3.7	-8.47
6	46	46.1	-0.1	-0.22
7	45	45.3	-0.3	-0.66
8	48	47.9	0.1	0.21
9	38	43	5	11.63
Mean	41.33	44.17	-1.72	-4.02
St.dev.	4.27	1.87	3.52	
Diff. average IRS-1C/ AP			-2.84	-6.43%
AP* = aerial photograph				

Tree heights: comparison IRS-1C and AP manual measurement

SUMMARY OUTPUT

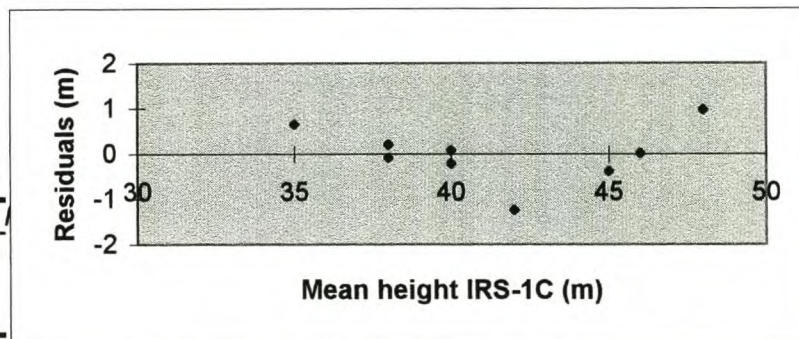
A29c IRS / AP

Regression Statistics	
Multiple R	0.94176454
R Square	0.88692044
Adjusted R Square	0.87076622
Standard Error	0.67350617
Observations	9

MH = mean height

AP = aerial photograph

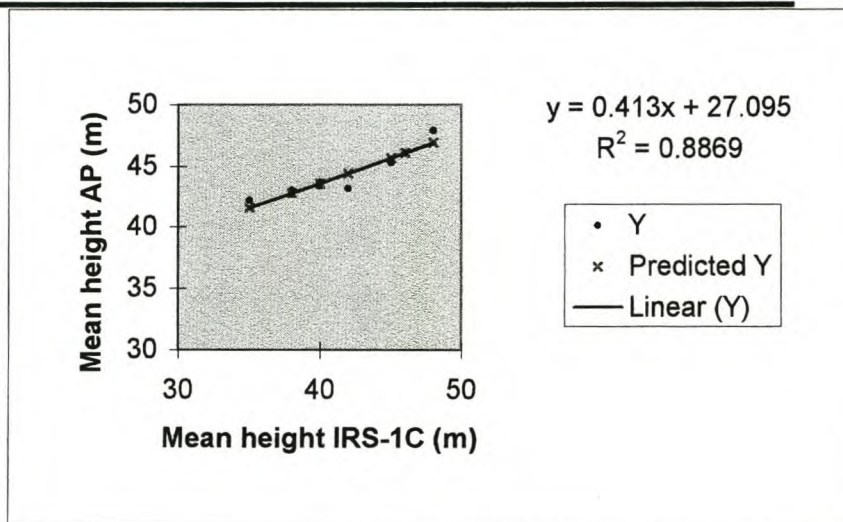
ANOVA					
	df	SS	MS	F	Significance
Regression	1	24.90472603	24.90473	54.90332	0.000148
Residual	7	3.175273973	0.453611		
Total	8	28.08			



	Coefficients	Standard Error	t Stat	P-value	Lower 95%	Upper 95%	Lower 95.0%	Upper 95.0%
Intercept	27.0954338	2.314822733	11.70519	7.51E-06	21.62175	32.56912	21.62175	32.56912
X Variable 1	0.4130137	0.055739768	7.409677	0.000148	0.28121	0.544817	0.28121	0.544817

RESIDUAL OUTPUT

Observation	Predicted Y	Residuals
1	44.4420091	-1.24200913
2	42.7899543	-0.08995434
3	43.6159817	-0.21598174
4	41.5509132	0.649086758
5	43.6159817	0.084018265
6	46.0940639	0.005936073
7	45.6810502	-0.38105023
8	46.9200913	0.979908676
9	42.7899543	0.210045662



**compartment A15**

Plot no.	Tree height AP*	Tree height ground survey	Difference	Diff. in %
1	40	41	-1	-2.44
2	39.8	41.3	-1.5	-3.63
3	40.4	40.7	-0.3	-0.74
4	39.4	42.3	-2.9	-6.86
5	43.5	50	-6.5	-13
6	42.7	42.8	-0.1	-0.23
7	37.4	37	0.4	1.08
8	36.1	36.5	-0.4	-1.1
9	35.4	36	-0.6	-1.67
10	37.5	37.5	0	0
11	35.3	35.5	-0.2	-0.56
12	37.4	38.5	-0.9	-2.86
13	38.4	41	-2.6	-6.34
Mean	38.72	40.01	-1.28	-2.95
St.dev.	2.57	3.91	1.85	3.84

comparison AP - terrestrial survey for manual determination of tree height /semi-automatic method

SUMMARY OUTPUT

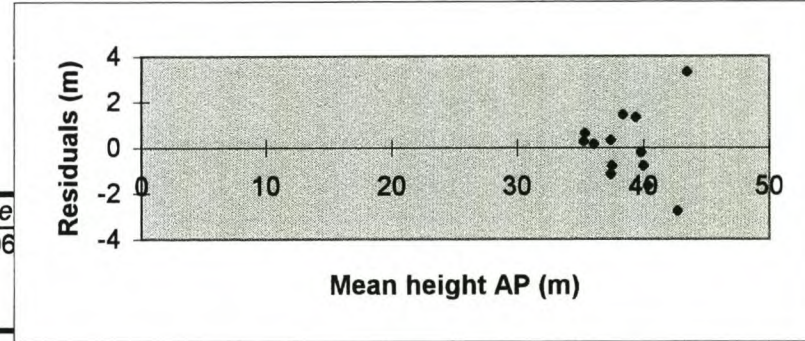
A15 AP/survey ground

T = terrestrial

Regression Statistics	
Multiple R	0.918848
R Square	0.844282
Adjusted R Square	0.830126
Standard Error	1.610887
Observations	13

ANOVA

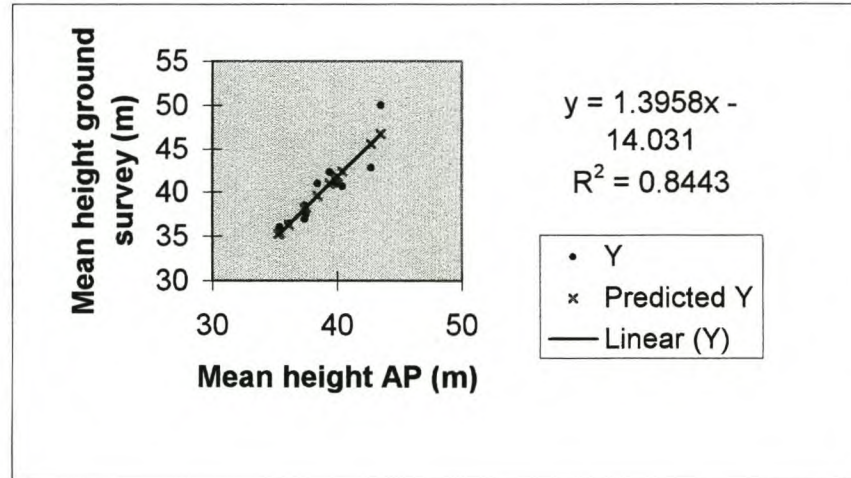
	df	SS	MS	F	ignificance
Regression	1	154.7647	154.7647	59.64061	9.12E-06
Residual	11	28.54451	2.594955		
Total	12	183.3092			



	Coefficients	Standard Error	t Stat	P-value	Lower 95%	Upper 95%	Lower 95.0%	Upper 95.0%
Intercept	-14.0314	7.011659	-2.00116	0.070664	-29.464	1.401126	-29.464	1.401126
X Variable 1	1.395805	0.18074	7.722733	9.12E-06	0.997999	1.793611	0.997999	1.793611

RESIDUAL OUTPUT

Observation	Predicted Y	Residuals
1	41.80076	-0.80076
2	41.5216	-0.2216
3	42.35909	-1.65909
4	40.96328	1.336718
5	46.68608	3.313917
6	45.56944	-2.76944
7	38.17167	-1.17167
8	36.35713	0.142875
9	35.38006	0.619938
10	38.31125	-0.81125
11	35.24048	0.259519
12	38.17167	0.328328
13	39.56748	1.432523



Compartment  
A15

E.GRAND Age  
11

				without outliers	
tree height ground	dbh	Tree height AP*		dbh	Tree height AP*
41	34.8	40	1	34.8	40
41.3	33.4	39.8	2	33.4	39.8
40.7	31.2	40.4	3	31.2	40.4
42.3	37	39.4	4	37	39.4
50	34.8	43.5	5	34.8	43.5
42.8	28.6	42.7	6	28.6	42.7
37	34.5	37.4	7	34.5	37.4
36.5	34.9	36.1	8	34.9	36.1
36	37.7	35.4	9	37.7	35.4
37.5	33.9	37.5	10	33.9	37.5
35.5	34.6	35.3	11	34.6	35.3
38.5	35.4	37.4	12	35.4	37.4
41	36.3	38.4	13	36.3	38.4
mean	40.008	34.392			

		without outliers	
	dbh	Tree height AP*	outliers 4, 5 and 6 discarded
1	34.8	40	
2	33.4	39.8	
3	31.2	40.4	
7	34.5	37.4	
8	34.9	36.1	
9	37.7	35.4	
10	33.9	37.5	
11	34.6	35.3	
12	35.4	37.4	
13	36.3	38.4	

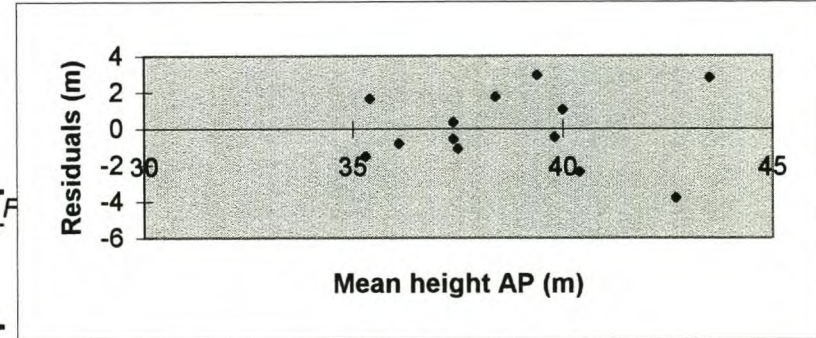
		without outliers	
		Tree height AP*	outliers 4, 5 and 6 discarded
subsample	33.4	39.8	
random:	34.6	35.3	
	34.5	37.4	
	36.3	38.4	

SUMMARY OUTPUT

A15 dbh terrestrial / mean height AP

Regression Statistics	
Multiple R	0.540785683
R Square	0.292449155
Adjusted R Square	0.228126351
Standard Error	2.09154116
Observations	13

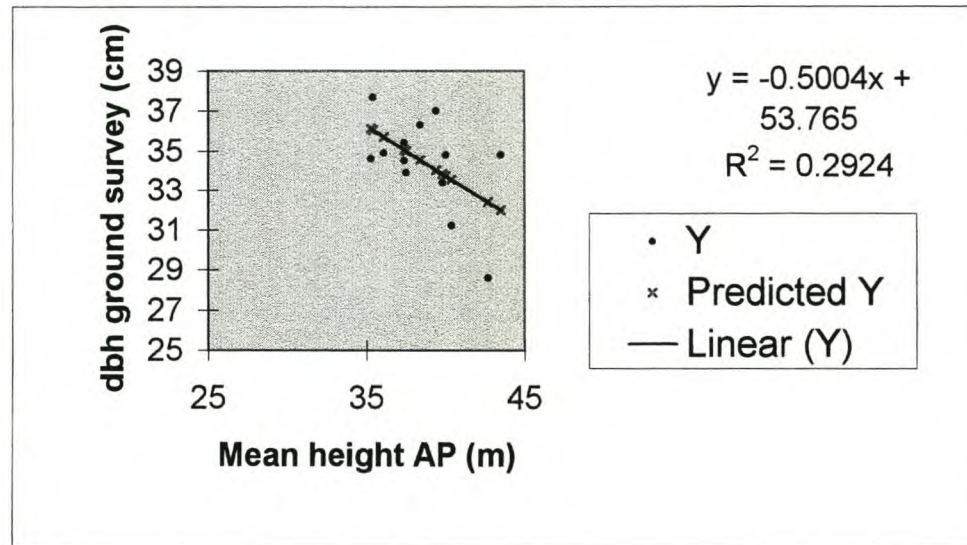
ANOVA					
	df	SS	MS	F	Significance F
Regression	1	19.88924	19.88924	4.546586	0.056357
Residual	11	48.11999	4.374544		
Total	12	68.00923			



	Coefficients	Standard Error	t Stat	P-value	Lower 95%	Upper 95%	Lower 95.0%	Upper 95.0%
Intercept	53.76462118	9.10379	5.90574	0.000102	33.7273	73.80194	33.7273	73.80194
X Variable 1	-0.500377658	0.234669	-2.13227	0.056357	-1.01688	0.016125	-1.01688	0.016125

RESIDUAL OUTPUT

Observation	Predicted Y	Residuals
1	33.74951485	1.050485
2	33.84959039	-0.44959
3	33.54936379	-2.34936
4	34.04974145	2.950259
5	31.99819305	2.801807
6	32.39849518	-3.7985
7	35.05049677	-0.5505
8	35.70098772	-0.80099
9	36.05125208	1.648748
10	35.000459	-1.10046
11	36.10128985	-1.50129
12	35.05049677	0.349503
13	34.55011911	1.749881



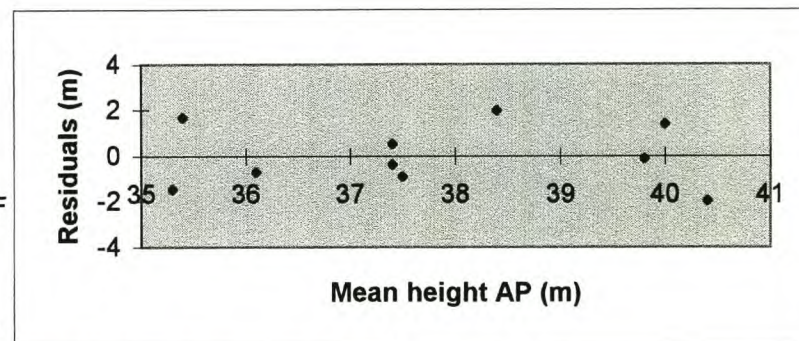
SUMMARY OUTPUT

A15 dbh terrestrial / mean height AP without outliers 4,5,6

Regression Statistics	
Multiple R	0.6151479
R Square	0.37840693
Adjusted R Square	0.3007078
Standard Error	1.44090199
Observations	10

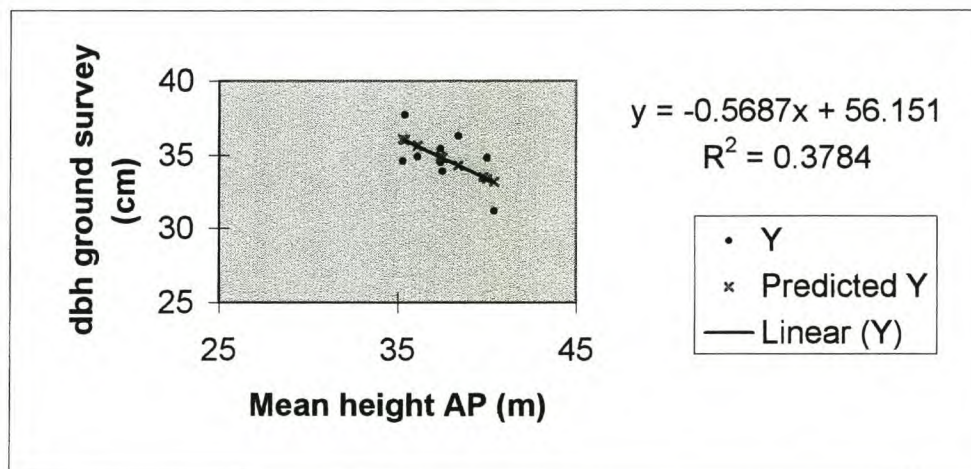
ANOVA					
	df	SS	MS	F	Significance F
Regression	1	10.1114117	10.11141	4.870156	0.058368
Residual	8	16.6095883	2.076199		
Total	9	26.721			

	Coefficients	Standard Error	t Stat	P-value	Lower 95%	Upper 95%	Lower 95.0%	Upper 95.0%
Intercept	56.1508493	9.74440473	5.762368	0.000423	33.6802	78.6215	33.6802	78.6215
X Variable 1	-0.5687278	0.25771103	-2.20684	0.058368	-1.16301	0.025555	-1.16301	0.025555



RESIDUAL OUTPUT

Observation	Predicted Y	Residuals
1	33.401737	1.39826301
2	33.5154826	-0.1154826
3	33.1742459	-1.9742459
4	34.8804293	-0.3804293
5	35.6197754	-0.7197754
6	36.0178849	1.6821151
7	34.8235565	-0.9235565
8	36.0747577	-1.4747577
9	34.8804293	0.51957071
10	34.3117015	1.98829852



## **APPENDIX 13: SAMPLING DESIGNS USED IN FOREST INVENTORY**

As described by Van Laar and Akça (1997): “The objective of forest inventories is to obtain qualitative and quantitative information about forest resources and their physical environments, at a specified point in time and at reasonable cost.” This definition entails the reporting of the status quo of a forest with factors such as area, volume and volume distribution in terms of size classes, but also the potential of the forest for wildlife and recreation, and expected changes in growth, vitality and mortality.

The manifold tasks of a forest inventory depend largely on the degree of development of the forest economy and infrastructure (Lötsch and Haller, 1964). In many developing countries the major goal is the exploitation of the existing resources, thus forest inventory has to assess the possibilities to obtain timber of certain species, volume and quality. At a higher level of development, which is characterised by the introduction of planned and sustained management, continuous forest inventory is required for the periodic control and review of management activities.

Depending on the purpose and scale of a forest inventory, certain classes can be distinguished:

- National and regional forest inventories, which provide the basis for forest policy decisions and long-term planning of the forest industry.
- Management inventories, which support managers in the decision making process.
- Surveys required for planning harvesting and silviculture operations.
- Multi-resource inventories for wildlife, landuse and recreation management.
- Inventories to scrutinise and quantify the impact of pollution and other stress inducing factors on growth and health status of trees and forests (Van Laar and Akça, 1997).

Each of these categories has its specific requirements concerning the quality and accuracy of the information. So for instance the assessment of the timber value would require the accurate measurement of the growing stock, whereas the focus of the evaluation of the forestry potential of a specific area would be on the productivity potential of certain sites.

In many business inventories, all items are counted and listed. In contrast, a forest inventory deals with the assessment of vast areas being home to a great diversity of biological organisms (e.g. trees, animals) which are not identical and therefore would require individual measurement rather than being merely counted. Because of the magnitude of such an operation a 100% inventory is not practically and economically feasible. The alternative to such a full inventory is a sample, which is defined as process of making inferences about a population by examining only a subset of the whole (Cochran, 1977; Lötsch and Haller, 1964; Schaeffer *et al.*, 1990; Van Laar and Akça, 1997). The sample itself consists of  $n$  sampling units on which tree, stand or site characteristics are measured. Reasons for sampling in forest inventories are not just the existing constraints in terms of time and costs that do not allow a 100% inventory, but sampling is also useful when destructive sampling techniques are involved which cannot be carried out on a large scale. Furthermore, sampling makes it possible to obtain a greater variety and more reliable information for selected sampling units and in many cases sampling is the only means of obtaining information about certain populations, which could otherwise not be collected (Cochran, 1977; Van Laar and Akça, 1997).

In the early days of forest inventory, sampling was carried out in a rather subjective manner. These enumerations have proven to produce overestimates of the timber volume, and therefore subjective sampling was gradually superseded by probability sampling. Furthermore, because of the time and cost constraints most inventories are faced with, scientific sampling methods were developed to obtain information with highest possible accuracy, in combination with negligible bias, and with the optimum cost-benefit ratio. In most instances the total cost are specified prior to sampling, since the decision as to which sampling method should be applied is usually based on the expected accuracy of the target variable at lowest possible cost. Unfortunately the inventory cost per unit varies considerably and thus the following influencing factors have to be considered carefully:

- The type of information required (e.g. volume, increment, and density).
- The variability of the subject variable.
- The size of the population.
- The shape of the forest tract to be inventoried.
- The constraints in terms of available time, trained staff, and money.

- The accessibility of the forest, as well as topographic features.
- The specified maximum error of the estimates (Van Laar and Akça, 1997).

Other aspects such as the shape and size of the sampling plots and the layout of the sampling design also have severe impacts on the possible success or failure of a forest inventory. As a matter of fact, the variability of the volume estimates increases with decreasing plot size. However, in relatively homogenous plantation forests, the plot size has a less severely effect on the coefficient of variation than it has in natural forests (Van Laar and Akça, 1997).

Most forest inventories are based on the assumption that all observations made and measurements taken on each sampling plot (be it on the ground, on an aerial photograph, or on a satellite image) to obtain the individual target variables are determined free from error. However, such an assumption cannot be justified in practice, since a variety of possible errors is inherent to all measurements and observations. Reasons for these errors (i.e. systematic and random errors) are manifold and can be due to the following circumstances:

- Inaccuracy of the measuring device (i.e. instrument not being calibrated).
- Peculiarities of the object to be measured (e.g. the cross section of a tree always deviates from a perfect circle).
- Uncertainties and inconsistencies of the measuring procedure (e.g. rounding errors or improper handling of the measuring devices).
- Physical or topographical influences (e.g. adverse weather conditions can impede proper measurements, or steep terrain can influence trigonometric determination of tree height).
- Imperfection of human senses (e.g. defective eyesight) (Hildebrandt, 1996; Lötsch *et al.*, 1973; Prodan, 1965).

Some of these errors can be accounted and compensated for, whereas others will remain and thus cause a degradation of the obtained results.

## SAMPLING METHODS

Selective, random and systematic sampling

Before the advent of statistically sound sampling methods the subjective selection of sampling plots was widely used in forestry. This sampling method, sometimes also

referred to as *selective sampling*, yielded good results only if the cruiser was highly skilled and experienced. The major drawback of this method is, that no valid variance, and thus no confidence interval could be calculated. In addition, the variability of the sampled areas were smaller than the true variability in the stand due to the fact that only areas were selected that appeared to be representative of the average stand condition (Shiver and Borders, 1996).

All statistically sound sampling procedures are based on *random* or *systematic* sampling or are a combination of both. The most basic probability sampling method, the simple *random* sampling, does not allow for any subjectivity and is based on the idea that every sample size of  $n$  sampling units has an equal probability of being selected. An important aspect of this sampling method is reflected in the fact that the estimators are unbiased and consistent. The selection of a random sample from a population requires the development of a frame (i.e. a list of sampling units), which is usually established by using aerial photographs or maps in order to identify the location of the sampling units. The next step would be then to randomly select (without replacement) sampling units to be in the sample by drawing random numbers and allocating the sampling units accordingly.

Problems associated with this sampling method are the sometimes difficult location and identification of the sampling units in the field, and the likely chance of obtaining a non-representative sample when sampling units clump together in one area of the tract (Cochran, 1977; Lötsch and Haller, 1964; Prodan, 1965; Schaeffer *et al.*, 1990; Shiver and Borders, 1996; Van Laar and Akça, 1997).

In contrast to the random selection of sampling units the *systematic* sampling exploits a predictable, systematic pattern of sampling units. Most commonly the sampling plots are laid out on a square or rectangular grid across the stand, where the first unit (i.e. starting point) is drawn randomly and every  $k$ th unit thereafter in a systematic manner using the same intervals (e.g. distances, angles, or number of points on a grid). The main disadvantage of this sampling method lies in the fact that the sampling units are not selected randomly, and therefore it is not possible to estimate the variance of the sample. However, this problem can be circumvented for most populations in the practice of forest inventory as proposed by Schaeffer *et al.* (1990).

The advantages and conveniences of the systematic sampling method refer to the fact that it eliminates the need to develop a frame prior to sampling, and that the establishment of the sampling plots is less time consuming and more cost efficient than with random selection. In addition, the complete coverage of the stand is ensured as there is no risk of sampling plots clumping together (Cochran, 1977; Schaeffer *et al.*, 1990; Shiver and Borders, 1996). Detailed information on the calculation of the required sample size, the sampling error, the size of the sampling plot, etc. are exhaustively dealt with in references such as Cochran (1977), Lötsch and Haller (1964), Ott (1993), Philip, 1994; Prodan (1965), Schaeffer *et al.* (1990), Shiver and Borders (1996), and Van Laar and Akça (1997).

### **Point sampling (angle count sampling)**

This sampling technique, being unique to forestry, was developed by the Austrian forester Walter Bitterlich in 1948 (Lötsch *et al.*, 1973; Prodan, 1965; Shiver and borders, 1996; Van Laar and Akça, 1997). The invention, also referred to as plotless sampling, angle count sampling, prism cruising, relascope sampling and Bitterlich sampling, was originally designed to estimate basal area per hectare. It was later extended by Grosenbaugh and re-defined as PPS sampling (Probability Proportional to Size), based on the observation that the larger sampling units (trees) have a higher probability of selection. The probability of selection is proportional to tree basal area. The rationale behind this method is that larger trees have more volume and typically more value than smaller trees. As a higher proportion of the higher-volume trees is included in the sample, less time is spent on the smaller trees, and thus efficiency of the sampling is increased. Bitterlich's deliberations resulted in the proof of the universal validity of the angle count principle: counting from a random point the trees whose breast height cross section exceeds a certain critical angle, produces an unbiased estimate of the basal area/ha. Although large trees seem to be favoured in this method, the effect is reversed by the fact that large trees account for fewer trees per hectare, thus resulting in an unbiased estimator. The possibilities for relationship of angle to tree size in point sampling are illustrated in the following figure.

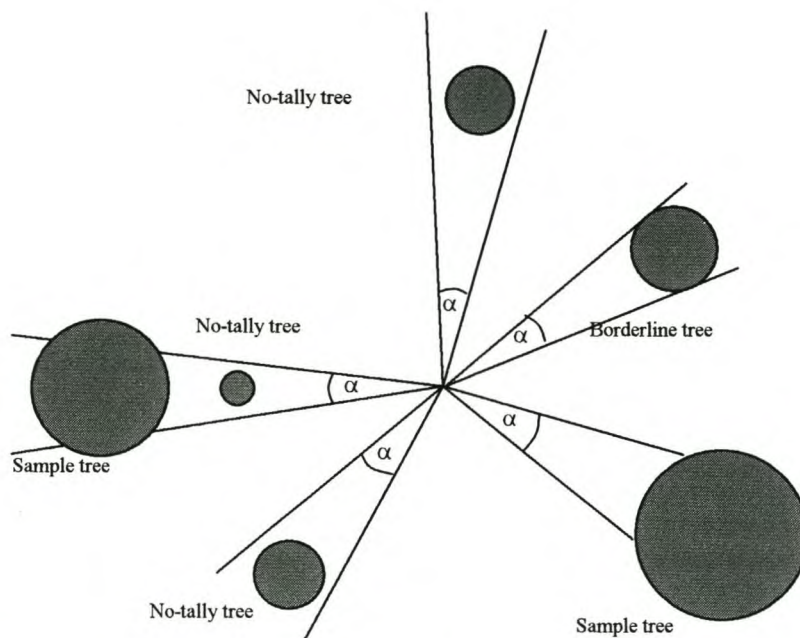


**Figure 1** The qualification of individual trees as sample trees is determined by a means of a constant critical angle ( $\alpha$ ) the vertex of which lies in the sample point (graph in analogy with Shiver and Borders, 1996)

The critical angle defines the ratio between the diameter of a tree and its distance from the sampling point. The use of different critical angles results in different Basal Area Factors (BAF) to calculate basal area per unit area. Basal area per hectare can then be simply determined by applying the following formula:

$$G = BAF \times N$$

where  $G$  = basal area per hectare

$BAF$  = Basal Area Factor (i.e.  $2500/\text{plot radius factor}^2$ )

$N$  = total number of trees counted 'in' (Van Laar and Akça, 1997).

Subsequently the estimation of stand volume is done by the multiplication of the stand basal area with the stand form height (as obtained from a subsample by means of the so-called 'form height/diameter' measurements) or with the point sampling factor (as expressed as the ratio volume/basal area).

A great number of methods have been devised to account for the boundary or edge effect bias (Lötsch and Haller, 1964; Prodan, 1965; Shiver and Borders, 1996; Van Laar and Akça, 1997). In addition, in order to avoid sampling errors, factors such as the calibration of the instruments, the correct sampling position, the correction of slope, and the neglect of hidden trees have to be taken into account.

Almost anything can be used to conduct a point sample, ranging from simple devices such as coins or blades simply held at arm's length or using a stick, to sophisticated instruments like the Bitterlich's mirror relascope. It has become very common to use commercially made angle gauges, which are patterns cut into metal at the appropriate width. Another commonly used device is the wedge prism, which is a ground and calibrated prism that bends light at a specific angle. A third instrument for projecting angles is the already mentioned Bitterlich relascope. It projects a choice of several different angles and automatically corrects for slope. Furthermore, it also allows for the determination of upper stem diameters and tree heights.

#### Stratified sampling

Locating sampling plots in a random or systematic fashion over the entire area is only efficient if the area is relatively uniform. In rather heterogeneous areas it is advisable to divide the population into homogenous subpopulations, referred to as strata. The different strata are then sampled separately to obtain the target variable such as site quality, age, stand treatment, species composition, etc. However, the most important prerequisite is that the variables have to be closely related to the quantity being measured. When a random sample gets selected from each stratum the procedure is called stratified sampling.

In many instances aerial photographs are used as a basis for stratification and a careful perusal of the area to be investigated is essential. If no up-to-date aerial photography is available, a decision has to be made as to whether to delay the inventory until a new flying mission was carried out, or rather use a combination of satellite imagery and old photography. When remote sensing imagery is employed, the boundaries of the strata usually follow natural features or forest types (Hildebrandt, 1996; Howard, 1991). In some cases only insufficient or poor quality information (e.g. poor aerial photography) is available prior to the inventory, so the population will then be poststratified on the basis of the data gathered in the field.

The purpose of stratifying is to firstly reduce the variation within the strata, and secondly to increase the variation between the strata. Furthermore, as holds true for all goals in designing surveys is to maximise the information obtained for a fixed expenditure. Therefore the main reasons for using stratified sampling are:

- Stratification may produce a gain in precision in the estimates of characteristics of the entire population.
- The cost per observation may be reduced by stratification.
- The estimation of population parameters may be desired for subgroups of the population (Cochran, 1977; Schaeffer *et al.*, 1990; Shiver and Borders, 1996).

However, several potential disadvantages may be associated with stratified sampling. First, each sampling unit must be assigned to only one stratum, thus not allowing any overlaps. In certain situations such as plantations the definition of strata might be fairly easy, whereas in natural or extremely heterogeneous manmade forests with many tree species the identification of potential strata might be almost impossible. Another problem might occur in conjunction with stratified sampling, when the stratum size cannot be estimated accurately. This size must be known in order to obtain sample estimates of population parameters and their associated variance or standard error.

In stratified sampling the values of the sample sizes of the respective strata can be chosen in various fashions. The simplest rule would be to allocate the sampling units proportional to the size of the strata. Other methods include the equal allocation of sampling units and the so-called Neyman allocation, in which the differences in stratum variability and the stratum size are taken into account (Shiver and Borders, 1996). Very often the cost of sampling is a major consideration in the determination of the sample size to employ for a forest inventory. An allocation scheme referred to as optimal allocation has been designed to keep the number of expensive plots to a minimum, while still meeting the desired bound on the population parameter of interest such as tract volume or product class. The proportion of sample plots allocated to a given stratum is given below:

$$W_h = \frac{N_h S_{y_h} / \sqrt{C_h}}{\sum_{h=1}^L N_h S_{y_h} / \sqrt{C_h}}$$

where:  $C_h$  = cost of a sample unit in stratum  $h$

$N_h$  = stratum size

$S_{y_h}$  = stratum variability (Shiver and Borders, 1996).

The underlying idea behind the stratification of sampling is that the estimates from different strata can be combined to obtain overall population estimates of the mean and total. One of the most important observations is that the variance within the strata is less than variation among strata. The practical implication of this would be that stratified sampling would produce an estimate as precise as simple random or systematic sampling, but using fewer sample plots.

### Cluster sampling

According to Schaeffer *et al.* (1990) “a *cluster sample* is a simple random sample in which each sampling unit is a collection, or cluster, of elements”. Cluster sampling is also referred to as single-stage cluster sampling, where once a primary unit is selected, all elements (i.e. secondary sampling units) within the primary are measured for the characteristic of interest (e.g. timber volume). A good example for this method is the cruising using fixed-area plots, where the plots are chosen as primaries and subsequently every secondary (i.e. the individual tree) within each plot is measured (Shiver and Borders, 1996).

A very popular design is known as satellite design, which has been applied successfully in the USA, Sweden, Finland, Austria and Thailand (Lötsch and Haller, 1964; Van Laar and Akça, 1997). It is based on the idea that once a randomly selected centre square (tract) is chosen to serve as the camp centre, a great number of sampling areas are then located around the periphery of each square to form the cluster.

Cluster sampling is less costly than stratified or simple random sampling if the cost of obtaining observations increases with increasing distance of the elements or if the cost of compiling a frame containing all population elements is very high. This sampling design is particularly suited for vast forest areas with difficult access, when the relocation of plot centres (as for example achieved by random selection) in the field is cumbersome and travelling times are considerably high.

A very popular variation of the cluster sampling is the so-called two-stage cluster sampling. This design, however, will be discussed in the subsequent chapter.

### Multistage sampling

Another method of performing sub-sampling is designated as ‘multistage sampling’ or ‘multistage cluster sampling’ (Schaeffer *et al.* 1990; Shiver and Borders, 1996). In multistage sampling, the sampling units are selected in an hierarchical order, where the population is partitioned into primary units, and subsequently these are broken down into secondary units, tertiary units and so forth. A very common variation of this method is two-stage sampling. The sample is obtained by “first selecting a simple random sample of clusters and then selecting a simple random sample of elements from each sampled cluster” (Schaeffer *et al.*, 1990). The underlying principle is to assign a value to each cluster by measuring only a portion of the elements in the cluster.

The most common application of two-stage sampling in forest inventory is the estimation of timber characteristics for large forest areas, where it may not be possible to perform an inventory of every single stand. This may be due to monetary constraints, time limitation, or other factors. The proposed method clearly helps to reduce cost and time, however, the final estimate may be more variable than if an adequate cruise was carried out in each stand.

The availability of satellite imagery has stimulated interest in subsampling methods. A possible design of multi (three) -phase and multi (three) stage sampling employing imagery acquired by spaceborne sensor systems is shown as Figure 2.

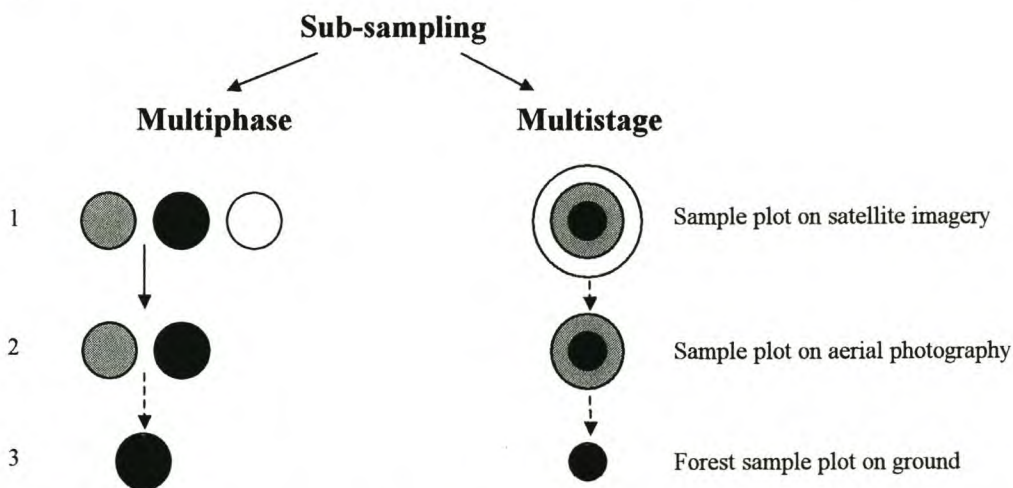


**Figure 2** Multiphase and multistage sub-sampling consisting of three steps; plot size is preserved in multiphase sampling; in multistage sampling the population is divided into primary units, then each primary unit is broken down into secondary units, and in turn, each secondary unit is divided into tertiary units and so forth (graph in analogy with Howard, 1991)

In multistage sampling the subsamples in the field form a part of each photo plot, whereas in multiphase sampling the size of the individual photo plots is retained, but only a percentage of the plots is sampled in the field.

Successful applications of this strategy for the estimation of timber volume are described by Hildebrandt (1996), Howard (1991), Köhl (1991), and Scheer *et al.* (1997).

## APPENDIX 14: IMAGE MINIFICATION

Main applications for this technique are associated with image matching, image analysis, digital surface modelling, and data storage. When working with digital images, a major problem is the enormous amount of data to be stored. In the usual quantisation with 256 grey levels (8bit), an aerial photograph scanned with a pixel size of 20 $\mu$ m amounts to a *data storage* of about 100Mb. Similar problems can be encountered with regard to *data transfer* rates when image processing hardware is integrated into a network of computers. Because of the immense size of digital imagery, transfer times range from a few minutes for local transfers, and up to many hours or even days for a transmission via telephone modem. In many instances it is not even necessary to store or transfer the original image, since only either sections of the image or low zooming levels are requested. The multi-resolution representation of an image as an efficient encoding process (i.e. data compression algorithm) has been developed to offer a viable solution to the above mentioned problems. With the production of hardware chips for image compression and decompression and the introduction of real time disks, image pyramids can be displayed almost in real time (Ackermann and Hahn, 1991).

Minification creates an image pyramid from a digitised image in order to facilitate the entire process of zooming in and out of the image and to considerably reduce computational costs. The hierarchical architecture of the pyramid is suited to represent iconic as well as symbolic image information.

For practical reasons, image minification is usually run:

- After an image is imported.
- After an image is rectified.
- After an orthophoto is generated.
- Or after having created any new image file (LH Systems, 1998).

The generation of image pyramids is governed by the principle of the image information being represented by a series of images with decreasing geometrical resolution. The original image is then called the 1:1, and the minified images correspondingly 2:1, 4:1, and so forth (LH Systems, 1998). The principle is demonstrated in Figure 1.

One of the prime applications within the *image analysis* environment is the extraction of features (such as roads, buildings, etc.) for the purpose of image segmentation, i.e. the separation of an image into meaningful regions. Segmentation can be obtained through the definition of the region by edge extraction. The procedure itself is based on the extraction of a series of edge maps beginning on a coarse level of an image pyramid, and the subsequent tracking of these features by matching through the pyramid down to the lowest level. The basic idea behind this technique is for only the strong information to be detected and the noisy edges to be eliminated (Ackermann and Hahn, 1991).

These days most *matching* algorithms are based on image pyramids. A common procedure is to start matching at a low-resolution level, with successive computations being performed on each level of the hierarchy using the outcome of the higher level as prior information. Matching techniques such as interest operators, edge detection, multi-level correlation, Vertical Line Locus, and least squares matching through scale space are exhaustively being dealt with in Ackermann and Hahn (1991) and Kraus (1993).

Most of the previously mentioned methods can in an analogous manner be applied to the reconstruction of digital surfaces. Since the multigrid representation of surface models has many features in common with image pyramids, they can be seen as DEM pyramids. So for instance tasks like the manipulation of breaklines in a DEM pyramid are very similar to the problem of how to present and track edges in an image pyramid. As for the multigrid representation of digital surface models, the reconstruction process derives height rasters resolved in a certain number of levels by progressively refining the grid space. Because of the small difference between image and DEM pyramids, elementary image processing algorithms for the transformation, enhancement, segmentation, encoding or visualisation of DEMs can be used in a similar fashion (Ackermann and Hahn, 1991).

## APPENDIX 15: PERFORMANCE OF VARIOUS SOFTCOPY SYSTEMS

The process of gradual evolution from analogue to analysis of spatial information in a purely digital environment is happening without great difficulties. There is a fair amount of enthusiasm since softcopy systems have become fully operational, and the potential benefits are apparent. For the generation of DEMs, a great number of studies have elucidated the ease and accuracy of the (automatic) extraction of elevation data performed on a softcopy platform (Petrie, 1998b; Petrie *et al.*, 1997; Smith and Waldram, 1996; Toth and Templer, 1996; Wind, 1998). Many traditional suppliers of photogrammetric as well as image processing systems have entered the highly competitive softcopy market scene. The variety of products ranges from simple add-on modules for the generation of DEMs to fully-fledged high-performance softcopy systems. Not surprisingly, the specifications and the price tags vary greatly. With this in mind, it is intriguing to have a closer look at the performance of some of the systems.

Most of the investigations dealing with the evaluation of digital photogrammetric systems have focused on the analysis of scanned aerial photographs, using scanned topographic maps, GPS measurements, and/or existing DEMs as reference data. A comprehensive test has been conducted by Baltsavias and Käser (1998), when evaluating four commonly used systems, namely PHODIS by Zeiss, DPW 770 by LH Systems, the Autometric Softplotter, and INPHO's Match-T (PHODIS and Match-T use identical software, but the user interface and the matching parameters settings differ, so yielding different results). The conclusions are:

- The efficient use of these systems requires a considerable amount of relevant knowledge.
- The systems are so called 'black boxes' and not open and flexible enough: The content of many algorithms is not known; the user is bound to standard streamlined processing flow.
- The differences between the systems are significant; the results heavily depend on the choice of many and not well explained matching parameters.
- In all cases, blunders remain in the results, thus requiring time consuming manual editing.

- Methods with dense measurements lead to lower mean and RMSE with breaklines.
- Large errors specifically occurred at or close to surface discontinuities, perspective differences, low texture and edges parallel to epipolar lines.
- The contours of some systems are too smooth, hence many details get lost.
- Although all systems provide accuracy and blunder indicators, the quality criteria are not reliable, and therefore the entire dataset has to be checked.
- Feature based matching algorithms perform better at discontinuities than area based ones.
- Fast, complete, and easy-to-use pre- and post-editing tools are scarce.
- Poor filtering of trees and buildings is a common feature.
- The problems encountered become worse with larger image scales and/or steeper terrain.
- Fully-fledged systems like the DPW 770 are complicated to handle and require significant training.

Although the DPW 770 didn't render the best DEM results (only the ATE module within the SOCET SET suite was used, the adaptive method was not tested), the overall excellent performance of this system is indisputable. In a similar case study, when comparing the DPW 770 with the VirtuoZo<sup>46</sup> system, the authors conclude that the accuracy of the resulting DEM is equal to that of manual measurements, once the big blunders are eliminated. In comparison, both systems feature very small RMS errors in the resulting DEMs, but the DPW 770 has more functions, on the other hand it is also more expensive and less easy to use (Baltsavias, *et al.*, 1996).

An interesting evaluation has been undertaken by Bacher (1998). In his investigation he tested both SOCET SET's (on LH Systems' DPW 770) non-adaptive and the new adaptive method under varying conditions. The resulting DEMs values suggest that the adaptive method (AATE) is superior to the non-adaptive one as far as accuracy and user friendliness are concerned. Both automatic extraction methods seem to yield best results in flat and open, well-textured terrain, where elevation accuracies of better than one metre can be achieved. Nonetheless, the performance deteriorates quickly

---

<sup>46</sup> Developed by the Wuhan Technical University of Surveying and Mapping, China and Geonautics Pty Ltd, Australia

when little texture, steep terrain and particular edges to forest regions and built-up areas are involved.

Stereo imagery acquired by spaceborne systems has been accessible to users for many years, although not being used excessively. This imagery can be exploited in a traditional manner by employing analytical plotters, where hardcopies have to be produced first. However, recent studies have shown that the softcopy option offers some significant advantages over the traditional system such as the potential of the automation of certain procedures (e.g. orientation, feature extraction, image matching) and the application of image processing techniques (Baltsavias, 1996; Petrie, 1995). A limited number of software modules that are able to handle SPOT and other spaceborne stereo imagery are currently available, of which most of them are in use with big mapping and survey agencies and military services. In this context it is interesting to note that there have been very few independent studies to assess the quality of elevation data as generated by commercially available image processing systems (Petrie *et al.*, 1997b). A rewarding and comprehensive example for such a study is the accuracy test and validation of DEM data extracted from SPOT stereopairs that has been conducted by Al-Rousan and Petrie (1998). None of the initially five packages would run properly with the SPOT test data when evaluated for this study. After a few modifications, only three systems were considered fit for the tests, others failed completely to produce any kind of sensible answer or systems were simply not available. Most software packages for the generation of DEMs (e.g. EASI/PACE, OrthoMax, SOCET SET) employ a solution based on the initial modelling of the orbital track based on the ephemeris data provided in the header file of the satellite image. The photogrammetric solution then employs classical analytical methods based on the use of 3D collinearity equations. By contrast, DMS first uses a 2D polynomial procedure to rectify and fit the individual SPOT images to the GCPs, and subsequently measures and computes the terrain elevation values employing simple parallax heighting formulae.

The overall impression has been that the final results from this validation were surprisingly good, but only after extensive use of filtering techniques to remove the artefacts. With regard to the height accuracy, the tested systems EASI/PACE (PCI), OrthoMax (ERDAS) and DMS (R-WEL), produced RMSE values in the range of  $\pm 5$

to 7m (better than one metre for OrthoMax) at both the control points and check points, thus comparing even favourably with the best published figures for tests using analytical plotters. Regarding the overall performance, the figures obtained by the EASI/PACE system were consistently the best, but those obtained by the other two packages were only slightly less good. However, it has to be taken into consideration that all the tests were performed in a terrain that was really suited for the application of image matching techniques. Thus, with large areas of vegetation or steep slopes, severe matching problems are likely to be encountered.

## **APPENDIX 16: GENERATION OF DTMS FROM NON-PHOTOGRAPHIC SENSORS SUCH AS SPOT, MOMS-02 AND SAR**

### **1. SPOT**

Due to the monoscopic nature of most space imagery and its relatively low ground resolution, photogrammetrists have shown little real interest in the utilisation of space borne sensor systems. This situation changed somewhat with the availability of SPOT imagery featuring stereo coverage in an across-track mode. The coverage of large areas on a systematic basis has prompted a few mapping agencies to investigate the possibilities of small-scale mapping from SPOT stereo imagery, mainly in the arid and semi-arid areas around the Red Sea. This resulted in the mapping for part of the Yemen and Djibouti at the end of the 1980s. Since then, a small number of institutions have embarked on similar projects such as the Ethiopian Mapping Authority (EMA), the Saudi Military Survey Department (MSD), and most recently, the National Cartographic Institute (INC) in Algeria (Petrie 1997a; 1998a; 1998b). Other mapping projects using SPOT stereo scenes have been conducted in Cameroon and Jordan, or are under way, as is the case in Morocco. Evidence for the production of topographic maps based on the monoscopic analysis of SPOT imagery provides the SPOT Image marketing literature for Guinea and Moçambique. In addition, successful map revision campaigns employing SPOT imagery are reported for countries such as Ivory Coast, Nigeria, Uganda, Canada, and the Baltic States, whereas announcements for similar undertakings exist for Mexico, Bolivia, Macedonia, and Vietnam (Petrie 1998a; 1998b). The typical end products of the mapping process would then be topographic maps (i.e. hard copies), generated at scales of 1:50 000 for the more densely populated areas. Scales of 1:100 000 and 1:200 000 were considered adequate and efficient enough for the rural and unpopulated areas. Unfortunately the use and exploitation of satellite stereo images requires the availability of expensive high-tech solutions and systems and the availability of well trained personnel. The general and chronic lack of these resources explains why, as it seems, only two institutions in Sub-Saharan Africa, namely the Ethiopian and the Zimbabwean mapping authorities, are equipped with analytical plotters (Petrie, 1997a). Digital photogrammetry workstations are conspicuous by

their total absence in this part of the world with the exception of South Africa (e.g. at University of Cape Town).

A large number of accuracy tests have been carried out in a number of countries, usually involving just one or two stereo models. Most of the investigations carried out in Africa and Asia refer to map accuracy and content specifications as being established by the former colonial powers. However, they are not dissimilar to those used in highly developed countries. The specifications for the three basic map scales are shown in the following table (accuracies indicated as RMSE values).

**Table 1** Topographic map specifications (according to Petrie 1995 and 1997a)

<i>Scale</i>	<i>Plan resolution (at 0.1mm)</i>	<i>Plan accuracy (± 0.3mm)</i>	<i>Spot height accuracy</i>	<i>Contour interval* (m)</i>
1:50 000	5m	± 15m	3m	10 to 20
1:100 000	10m	± 30m	5m	20 +
1:200 000	20m	± 60m	8m	25 to 40

\* At 90% of the points shown by a contour to lie within half the contour line interval

Extensive tests carried out in Sudan, France, Japan, Cyprus, Jordan, and Nepal yielded planimetric accuracies (RMSE) of about ±15-18m, and elevation accuracies of ± 8-12m, thus pointing to a minimum contour interval of 25 to 30m (Al-Rousan *et al.*, 1997; Al-Rousan and Petrie, 1998; Naithani and Koul, 1996; Petrie, 1995, 1997a, 1998a and 1998b; Petrie *et al.* 1997; Petrie and El-Niweiri, 1994; Petrie and Liwa, 1995; Sharif and Salim, 1996; Theodossiou and Dowman, 1990; Valadan Zoej and Petrie, 1998). SPOT (stereo) imagery appears to be suitable for the revision of 1:50 000 maps to some extent, but certainly serious consideration must be given to the question as to whether topographic mapping programmes at a scale of 1:100 000 should be carried on a basis of small-scale aerial photography or space imagery, even with slightly relaxed specifications. The results also clearly indicate, that the level of accuracy largely depends on factors such as the geometric and radiometric quality of the imagery, its interpretability, the B/H ratio of the stereo pair, the topographical conditions on the ground, the skills of the operator, the accuracy of the GCPs, and most unequivocally on the performance of the software used for the creation of the 3-D model (e.g. the image matching process).

Sources of error in the height measurement of satellite stereo imagery are manifold. One of the main concerns, which could be identified during the conduction of above-mentioned projects, was directly related to the quality of the image. Not only the resolution and the radiometric quality of the image impose some substantial limitations on the analysis of the scenes, but the illumination condition as a result of the sun angle and the attitude of the satellite with respect to the sun also plays a vital role in the identification and measurement of features. Due to the lack of image texture as well as the presence of very dark (e.g. in rough or steep parts of the terrain) or strongly lit areas (e.g. sand plumes, snow), operators encounter difficulties in finding the ground, i.e. it is arduous to set the floating mark accurately on surfaces. Another problem seems to be directly associated with atmospheric conditions. Natural phenomena such as haze and clouds usually result in either the obstruction of features in the scene or in very poor contrast, thus promoting the occurrence of gross measurement errors. High vegetation such as forests can have a significant negative effect on the interpretability of particular areas in the image. In aerial photographs the operator can clearly perceive the height variation of the trees, whereas in SPOT images, the vegetation can convey the impression of a "cloud covering the area" (Theodossiou and Dowman, 1990). However, one of the major difficulties experienced in height measurements with SPOT imagery is caused by changes in vegetation, hydrology, etc. The main reason for this are the seasonal weather conditions over the time interval that may elapse between the acquisition of the individual images comprising the stereo pair (Petrie, 1997a). The very different appearance of vegetation, cultivated areas, and water bodies in the corresponding images result in dilemmas with orientation and stereo viewing (Al-Roussan *et al.*, 1997).

The majority of commercially available satellite imagery is used for the compilation and revision of topographic maps, where the focus lies on the detection, interpretation, measurement and plotting of specific features. In general, the extraction of features requires good spatial resolution and good contrast in the images. Unfortunately, the shortfall in the coarse ground resolution of satellite imagery contributes a lot to the problem related to the detection of certain objects on the ground. The resulting map detail is then seriously deficient or incomplete. In particular, the results concerning the identification of man-made features such as minor roads and tracks, power lines,

communication networks, and individual buildings are not satisfactory when looking at the outcomes of certain projects. In many cases towns were difficult to delineate, and villages could not be discerned with adequate confidence. Regarding large area land cover and vegetation, thicker woodlands, plantations, large fields, and forests could be identified with ease, whereas shrubland and bush country could not. In order to overcome this major problem, the location of the missing features would have to be carried out during a thorough field completion process (Petrie 1997a; 1997b). Despite the prevailing shortfalls inherent to SPOT imagery, the use of (stereo) space imagery can produce useful results provided that users are aware of the limitations in accuracy of elevation and planimetry (Petrie *et al.*, 1997).

## 2. MOMS-02 and other along-track satellite systems

The MOMS-02 along-track scanner system with its outstanding three-line geometry (B/H ratio of 0.8 and resolution of 13.5m for the stereo sensors) has until now been largely experimental. Unfortunately the image data acquisition system on board the Russian Mir space station is doomed due to the well-documented incidents on the platform in terms of attitude control and power supply. Accuracy tests performed in Australia, Sudan, and Ethiopia demonstrate that with elevation accuracies of  $\pm 5$  to 15m (similar to SPOT), the map requirements for 1:100 000 scale maps can be met with ease and that MOMS imagery is quite capable of supplying the required contour and elevation data (Ebner *et al.*, 1996; Konecny and Schiewe, 1996; Petrie *et al.*, 1997;). Recent investigations give rise to the hope that accuracies in compliance with map specifications of a 1:25 000 scale can be achieved when employing digital photogrammetry technology (Baltsavias and Stallmann, 1996; Dörstel and Ohlhof, 1996; Fritsch *et al.*, 1996; Fritsch *et al.*, 1998; Kornus *et al.*, 1998; Schiewe, 1996).

Another scanning system using along-track stereo technology is taking a ride on board the Japanese JERS-1. Due to the coarse ground resolution (18x24m pixel) of its OPS sensor and the poor B/H ratio (0.3), the imagery has not found much favour with the mapping community (Petrie, 1998a).

### 3. SAR<sup>47</sup> and LIDAR<sup>48</sup>

The community of SAR users soon realised that this technology was not the magic bullet that some had professed it to be. Well-known shortcomings such as the relatively poor resolution of satellite SAR images (e.g. Radarsat, ERS-2), the speckle present on the imagery, the extreme variability in the detection of ground features, or the foreshortening and shadowing in rough terrain, impose a substantial constraint on the possible application and adoption to topographic mapping for instance (Kuntz and Siegert, 1994; Petrie, 1997). However, the success of the shuttle-carried SIR-C/X-SAR and the ERS-1 have shown that now it is possible to perform quantitative measurements of specific features with great precision on a routine basis. According to Twu and Dowman (1996) DEMs with a height accuracy of about 17m are obtainable when extracting elevation information from stereo ERS<sup>49</sup>-1 SAR imagery. In particular the introduction of new techniques such as interferometric polarimetry are paving the way for SAR to obtain structural information, like the structure of forest stands (SAR-SIG, 1999).

A number of new technologies such as Lidar, employing laser scanning devices, have recently evolved. Although most of these have proven their ability to serve as a useful tool in forest inventory (Næsset, 1997; Nilsson, 1996) and in the creation of DEMs, as far as is known only airborne systems have been tested.

The procedure of combining different types of sensors to gain a maximum of information has been practised in the user community for decades. However, the generation of DEMs from multisensor stereopairs has only recently become a real option with the appearance of new techniques (in particular image matching techniques) on the market. For instance Akeno (1996) combined imagery of Landsat's MSS and NOAA's AVHRR for the creation of a DEM, demonstrating a vertical accuracy of about 320m. Albeit its high errors, this method has the potential to produce DEMs which are able to fill data gaps in blank regions at a very small

---

<sup>47</sup> Synthetic Aperture Radar

<sup>48</sup> Light Detection and Ranging

<sup>49</sup> European Radar Satellite

scale (e.g. world maps). Further refinements and improvements of this method can be expected for the future.

## INDEX

### 3

3-D display, 105

### A

AATE, 84, 97, 108, 109, 110, 111, 121, 123, 124, 125, 128, 129, 130, 131, 137, 138, 139, 141, 151, 152, 154, 157, 158, 168, 175, 177, 178, 180, 253, 270, 278

absolute orientation, 23, 68, 96

absorption, 11, 13

aerial photographs, 1, 32, 34, 36, 37, 38, 42, 43, 44, 45, 48, 49, 50, 51, 53, 54, 58, 59, 80, 81, 86, 88, 117, 120, 121, 122, 123, 126, 127, 130, 146, 149, 155, 156, 160, 163, 172, 174, 175, 177, 178, 179, 190, 191, 197, 198, 205, 222, 241, 244, 252, 258, 269, 272, 273, 274, 277

angle count sampling, 85, 242

ATE, 97, 108, 109, 111, 114, 120, 128, 253

atmosphere, 9, 10, 11, 12, 17, 27, 28, 110, 269, 271, 277

auto correlator, 128, 133, 143, 146, 148, 273

automatic extraction, 128, 204, 270

### B

B/H ratio, 30, 79, 107, 119, 142, 162, 176, 257, 259

block adjustment, 69, 83, 84, 119

blunder, 123, 130, 137, 156, 157, 169, 175, 177, 179, 180, 252, 253, 274

BSQ, 77, 80, 89, 93

### C

calibration, 17, 23, 71, 77, 92, 94, 102, 185, 191, 202, 243

CIR, 38, 46, 52, 53, 58

classification, 3, 9, 19, 33, 38, 39, 49, 55, 56, 57, 59, 98, 106, 123, 191

conjugate points, 101, 102, 109, 115, 139, 175

contour lines, 29, 69, 98, 123, 124, 130, 137, 138, 139, 141, 150, 151, 152, 177, 210, 273, 274

crown parameters, 43, 46, 269, 277

### D

dbh, 43, 46, 47, 48, 85, 86, 87, 132, 133, 134, 163, 164, 165, 166, 167, 168, 179, 275

digital photogrammetry, 1, 5, 83, 125

displacement, 11, 21, 22, 25, 29, 39, 40, 44, 49, 92, 102, 157, 271

DPS, 61, 62, 63, 182, 269, 272, 277

DPW, 62, 63, 66, 67, 68, 71, 82, 83, 87, 89, 174, 182, 185, 213, 214, 215, 252, 253, 269, 277

DPW770, 3, 82, 83, 88, 108, 113, 270, 272, 278

DSMs, 1, 83, 87, 138, 150, 172, 174, 185, 270, 278

DTM, 36, 48, 63, 69, 71, 83, 84, 97, 98, 99, 100, 101, 108, 110, 111, 112, 113, 114, 115, 120, 129, 141, 182, 185, 186, 189, 191, 192, 198, 270, 272, 278

DTMs, 1, 23, 25, 36, 63, 68, 83, 88, 96, 97, 99, 100, 102, 106, 114, 116, 123, 138, 150, 174, 191, 270, 278

## E

Eichhorn's law, 172, 173, 179, 181, 270, 278  
electromagnetic radiation, 8, 9  
elevation information, 1, 87, 97, 98, 124, 125, 126, 131, 153, 161, 162, 170, 174, 177, 260, 270  
energy, 5, 6, 8, 9, 10, 11, 12, 13, 15, 17, 32, 271  
export, 83, 84, 89, 115  
exterior orientation, 24, 68

## F

feature extraction, 67, 69, 71, 72, 84, 85, 92, 94, 99, 100, 103, 116  
fiducial marks, 23, 65, 94  
filters, 19, 67, 94, 114, 170, 275  
flying mission, 12, 23, 27, 80, 87, 93, 244  
FOM, 115  
forest inventory, 2, 50, 51, 88, 121, 131, 181, 238  
Fourier transform, 45, 136, 153, 169, 170, 171, 179, 220, 275  
frame photography, 92

## G

geometry, 6, 18, 22, 23, 27, 28, 30, 41, 43, 68, 77, 81, 92, 94, 102, 107, 109, 110, 158, 176, 180, 201, 202, 259  
GIS, 3, 5, 36, 45, 61, 62, 63, 69, 70, 71, 83, 85, 96, 97, 105, 116, 127, 169, 174, 180, 182, 184, 196, 200, 201, 204, 217  
GLONASS, 98  
GPS, 27, 28, 62, 69, 70, 71, 84, 93  
greyscale, 65, 92  
ground control points, 23, 24, 27, 29, 67, 68, 78, 95, 118, 174, 176  
ground survey, 126, 133, 134, 145, 148, 154, 155, 160, 163, 164, 165, 166, 167, 168, 174, 177, 178, 179, 180, 275  
ground truthing, 28, 49, 57, 87

## H

HATS, 84, 95, 96  
Hugershoff method, 88, 131, 134, 154, 168, 178, 179, 270, 278

## I

image enhancement, 19, 84, 94, 121, 123, 124, 140, 141, 175  
image matching, 69, 71, 88, 94, 97, 100, 101, 102, 103, 108, 111, 121, 123, 128, 139, 157, 161, 175, 177, 185, 189, 190, 191, 198, 199, 203, 249, 254, 255, 257, 260  
image minification, 96, 97, 111, 249  
import, 84, 87, 88, 89, 92, 93, 115  
increment, 3, 33, 35, 46, 48, 87, 166, 172, 176, 188, 239, 269, 277  
infrared, 6, 7, 8, 11, 13, 14, 15, 16, 52, 55, 57, 58, 196  
Interactive Terrain Edit, 114, 130, 270, 278  
interior orientation, 94

**INTERNET, 217**

interpolation, 99, 101, 103, 105, 111, 114, 120, 123, 130, 140, 157, 180, 250, 273

inventory, 1, 2, 3, 33, 34, 35, 36, 37, 41, 48, 49, 50, 51, 54, 55, 57, 59, 73, 80, 85, 88, 120, 121, 122, 131, 134, 159, 161, 163, 172, 174, 180, 181, 187, 191, 193, 201, 238, 239, 240, 241, 244, 245, 247, 260, 269, 270, 272, 273, 277, 278

IRS-1C, 3, 18, 60, 68, 73, 75, 76, 78, 79, 80, 82, 84, 88, 89, 93, 94, 97, 106, 107, 116, 117, 118, 119, 120, 121, 123, 124, 126, 130, 133, 134, 136, 138, 139, 140, 141, 143, 144, 145, 146, 147, 150, 151, 152, 154, 155, 156, 157, 158, 159, 160, 161, 163, 164, 168, 169, 174, 175, 176, 178, 179, 180, 185, 187, 189, 191, 192, 197, 199, 202, 207, 208, 211, 212, 213, 222, 223, 226, 270, 271, 272, 273, 274, 275, 278

**L**

Landsat, 2, 7, 18, 55, 56, 57, 58, 60, 84, 89, 187, 203, 217, 260, 271

LIDAR, 18, 260, 278

**M**

manual extraction, 125, 144, 270, 278

map specifications, 257, 259, 276

matching errors, 137, 138, 156, 157, 175, 179, 274

mean height, 47, 86, 87, 126, 127, 134, 135, 145, 148, 154, 155, 160, 163, 164, 165, 166, 167, 172, 173, 179, 274, 275

MOMS-02, 185, 189, 193, 200, 256, 259, 278

MOMS-02P, 3

multispectral, 3, 14, 15, 35, 54, 55, 59, 62, 71, 75, 84, 108, 182, 271, 272

**N**

NAVSTAR, 98, 217

near infrared, 13, 15, 16

**O**

ocular estimation, 41

operator, 68, 69, 72, 88, 94, 95, 96, 97, 100, 101, 105, 108, 112, 121, 125, 127, 128, 142, 147, 162, 175, 176, 257, 258, 270, 273

orientation, 12, 16, 21, 22, 23, 24, 25, 31, 34, 49, 62, 65, 68, 71, 72, 78, 83, 84, 87, 88, 92, 93, 94, 95, 104, 110, 111, 115, 117, 161, 188, 191, 197, 201, 254, 258, 269, 270, 271, 277, 278

orthophotos, 36, 63, 68, 71, 84, 96, 97, 98, 105, 115, 117, 199

overlap, 23, 24, 79, 80, 95, 117, 119, 131

**P**

panchromatic, 3, 52, 81, 84, 93, 106, 174

parallax, 23, 25, 26, 30, 39, 40, 96, 103, 109, 110, 112, 124, 125, 126, 127, 133, 144, 146, 155, 159, 162, 176, 254

perimeter delineation, 130

photogrammetry, 1, 3, 4, 5, 6, 7, 21, 27, 29, 36, 45, 61, 62, 64, 70, 71, 83, 84, 93, 97, 98, 100, 102, 103, 111, 123, 124, 128, 131, 133, 135, 174, 180, 182, 184, 185, 188, 189, 190, 194, 195, 200, 202, 204, 205, 217, 256, 259, 269, 277

planefill, 114, 130

principal point, 21, 22, 23, 25, 40, 92, 94

processing, 1, 4, 7, 32, 36, 38, 45, 59, 66, 93, 96, 110, 123, 127, 169  
projects, 89, 259  
pushbroom, 18, 31, 63, 64, 77, 271, 272

## R

radiation, 4, 8, 9, 10, 11, 12, 13, 14, 17, 28, 46, 55, 57, 269, 277  
rectification, 120, 197, 270, 278  
regression, 47, 49, 50, 88, 120, 130, 132, 133, 135, 136, 163, 164, 165, 166, 167, 168,  
178, 179, 180, 181, 188, 200, 274, 275  
relative orientation, 23, 25, 94, 95  
remote sensing, 2, 3, 4, 5, 6, 7, 8, 9, 10, 11, 14, 15, 27, 32, 34, 54, 55, 56, 57, 58, 59,  
64, 68, 75, 76, 85, 120, 123, 131, 134, 181, 182, 186, 188, 192, 195, 198, 199, 202,  
244, 269, 271, 272, 277  
resolution, 2, 7, 17, 29, 43, 55, 56, 57, 58, 60, 64, 65, 66, 70, 75, 76, 79, 81, 82, 101,  
102, 106, 108, 119, 120, 121, 133, 136, 138, 140, 142, 144, 146, 150, 152, 158,  
159, 161, 174, 176, 177, 178, 179, 180, 181, 182, 188, 192, 193, 196, 200, 202,  
203, 204, 249, 250, 251, 256, 257, 258, 259, 260, 272, 275

## S

sampling, 36, 42, 44, 46, 48, 49, 50, 85, 86, 88, 110, 126, 127, 131, 132, 133, 134,  
148, 161, 162, 163, 167, 168, 178, 179, 200, 239, 240, 241, 242, 243, 244, 245,  
246, 247, 248, 250, 270, 278  
sampling plot, 85, 134, 242  
SAR, 55, 60, 194, 199, 203, 256, 260, 278  
satellite images, 57, 180  
scanner, 3, 30, 31, 63, 65, 71, 81, 89, 117, 187, 193, 197, 259, 272  
scanners, 18, 31, 62, 63, 64, 65, 81, 182  
scattering, 10, 11, 12  
semi-automatic, 128, 146, 270, 278  
semi-automatic determination, 128, 270  
sensor, 3, 4, 7, 9, 11, 18, 19, 24, 29, 30, 54, 56, 58, 60, 62, 63, 64, 73, 77, 78, 79, 81,  
85, 93, 94, 95, 96, 97, 102, 106, 107, 110, 111, 117, 119, 121, 140, 144, 158, 159,  
175, 180, 192, 247, 256, 259, 273  
shadow method, 39  
sidelap, 79, 80  
signal power, 103, 109, 131  
SOCET SET, 66, 83, 84, 85, 88, 89, 92, 93, 94, 95, 96, 99, 108, 111, 112, 114, 115,  
116, 117, 119, 125, 127, 128, 130, 133, 137, 141, 142, 147, 149, 150, 157, 174,  
177, 180, 194, 217, 253, 254  
softcopy, 18, 23, 61, 62, 63, 69, 70, 71, 72, 80, 81, 87, 97, 100, 101, 102, 105, 120,  
124, 174, 180, 184, 194, 200, 203, 252, 254, 278  
South Africa, 2, 56, 60, 73, 74, 174, 179, 189, 203, 218, 257, 272  
spectral signature, 9, 13, 37  
SPOT, 7, 18, 55, 58, 60, 64, 68, 75, 76, 84, 89, 93, 94, 95, 106, 107, 108, 123, 180,  
185, 192, 202, 203, 217, 254, 256, 257, 258, 259, 271, 272, 278  
stand height, 38, 39, 41, 49, 88, 120, 127, 129, 130, 134, 135, 144, 145, 146, 172, 174,  
176, 269, 277  
stand profile, 134, 135, 168, 273

stereo, 1, 3, 18, 22, 23, 36, 59, 62, 64, 66, 67, 70, 71, 75, 78, 79, 82, 87, 88, 96, 97, 100, 102, 104, 106, 108, 111, 115, 120, 121, 123, 124, 125, 130, 139, 140, 143, 146, 174, 175, 176, 177, 180, 181, 185, 189, 198, 199, 212, 213, 254, 256, 257, 258, 259, 260, 270, 273, 278  
stereomodel, 22, 26, 101, 161, 176  
stereoplotters, 26, 36  
Stereoscopy, 25, 194, 269, 277  
SUNSAT, 2, 60  
surface fitting, 88, 97, 101, 105  
surface models, 87, 128, 151, 155, 157, 158, 168, 175, 177, 178, 251, 274

## T

terrain extraction, 1, 88, 92, 96, 97, 100, 108, 111, 112, 113, 115, 116, 117, 121, 123, 129, 138, 140, 141, 152, 153, 161, 174, 177, 178, 179, 205, 270, 272, 273, 278  
test area, 3, 73, 76, 78, 80, 85, 117, 118, 123, 130, 140, 269, 272, 277  
texture, 37, 38, 46, 56, 70, 102, 105, 124, 128, 140, 142, 144, 181, 189, 196, 253, 254, 258  
tie point, 95, 191  
tie points, 24, 69, 84, 94, 95, 96, 102, 110, 118, 119, 273  
timber volume, 35, 42, 43, 46, 47, 50, 57, 88, 120, 144, 156, 159, 168, 169, 172, 178, 179, 181, 239, 246, 248  
transmittance, 14  
tree canopy, 128, 129, 158  
tree height, 1, 38, 39, 40, 41, 47, 50, 85, 86, 87, 120, 121, 126, 127, 128, 129, 131, 132, 133, 134, 144, 145, 148, 153, 154, 159, 161, 163, 165, 167, 168, 169, 174, 177, 178, 179, 191, 197, 240, 262, 269, 270, 273, 277, 278  
triangulation, 23, 24, 63, 68, 69, 71, 72, 83, 84, 87, 88, 92, 93, 95, 111, 117, 118, 119, 137, 182, 191, 200  
two-phase sampling, 131, 132

## V

video, 31, 63, 66, 272  
VITec, 66, 89

## W

wavelength, 8, 9, 10, 11, 13, 14  
whiskbroom, 18, 63, 271